# APPLICATIONS OF WERNER COMPLEXES AS CHIRAL SOLVATING AGENTS AND CATALYSTS IN ENANTIOSELECTIVE SYNTHESIS

A Dissertation

by

QUANG HUYNH LUU

Submitted to the Office of Graduate and Professional Studies of
Texas A&M University
in partial fulfillment of the requirements for the degree of

DOCTOR OF PHILOSOPHY

Chair of Committee, John A. Gladysz
Committee Members, David C. Powers
François P. Gabbaï
Perla B. Balbuena

Head of Department, Simon W. North

August 2020

Major Subject: Chemistry

ABSTRACT

When NMR spectra of chiral racemic organic molecules containing a Lewis basic functional group are recorded in the presence of air and water stable salts of the cobalt(III) trication $[Co((S,S)\text{-}NH_2CHArCHArNH_2)_3]^{3+}$ ($(S,S)$-$\mathbf{2}^{3+}$ for Ar = Ph), separate signals are usually observed for the enantiomers (28 diverse examples, >12 functional groups). Several chiral molecules can be simultaneously analyzed, and enantiotopic groups in prochiral molecules differentiated (16 examples). Particularly effective are the mixed bis(halide)/tetraarylborate salts Λ-$(S,S)$-$\mathbf{2}^{3+}$ $2X^-BAr_f^-$ (X = Cl, I; $BAr_f$ = $B(3,5\text{-}C_6H_3(CF_3)_2)_4$), which are applied in $CD_2Cl_2$ or $CDCl_3$ at 1-100 mol% (avg 34 and 14 mol%). Job plots establish 1:1 binding for Λ-$(S,S)$-$\mathbf{2}^{3+}$ $2Cl^-BAr_f^-$ and 1-phenylethyl acetate or 1-phenylethanol, and ca. 1:2 binding with DMSO ($CD_2Cl_2$). Selected binding constants are determined, which range from 7.60-2.73 $M^{-1}$ for the enantiomers of 1-phenylethanol to 28.1-22.6 $M^{-1}$ for the enantiomers of 1-phenylethyl acetate. The NH moieties of the $C_2$ faces of the trication are believed to hydrogen bond to the Lewis basic functional groups, as seen in the crystal structure of a hexakis(DMSO) solvate of Λ-$(S,S)$-$\mathbf{2}^{3+}$ $3I^-$. These salts rank with the most broadly applicable chirality sensing agents discovered to date.

The chiral enantiopure cobalt(III) complex Δ-$(S,S)$-$\mathbf{2}^{3+}$ $2Cl^-B(C_6F_5)_4^-$ is an effective catalyst, together with pyridine (10 mol% each), for enantioselective additions of substituted cyanoacetate esters $NCCH(R)CO_2R'$ to acetylenic esters $R''C{\equiv}CCO_2R'''$. In the resulting adducts, which feature quaternary carbon stereocenters, $NC(R'O_2C)C\text{-}(R)CR''C{=}CHCO_2R'''$, C=C isomers in which the $CO_2R'''$ moiety is *trans* to the new carbon-carbon bond dominate (avg. ratio 98:2). These are obtained in 70-98% ee (avg. 86%; data for optimum R' and R'''), as determined by $^1H$ NMR with the chiral solvating agent Λ-$(S,S)$-$\mathbf{2}^{3+}$ $2I^-BAr_f^-$. NMR experiments show that the cyanoacetate and acetylenic

esters and pyridine can hydrogen bond to certain NH groups of the catalyst. Rates are zero order in the cyanoacetate and acetylenic esters as well as the catalyst, and implications are discussed.

Exploratory studies were conducted with three additional reactions. First, the reaction of methyl 2-oxocyclopentanecarboxylate with *N*-fluorobenzenesulfonimide in the presence of Λ-(*S*,*S*)-$\mathbf{2}^{3+}$ $2Cl^{-}BAr_f^{-}$ (10 mol%) gave the monofluorinated product methyl 1-fluoro-2-oxocyclopentanecarboxylate in >99% yield and 79% ee. Second, the Neber reaction of 3-((tosyloxy)imino)butanoate catalyzed by 10 mol% Λ-(*S*,*S*)-$\mathbf{2}^{3+}$ $2Cl^{-}BAr_f^{-}$ in the presence of 2.0 equiv of $Et_3N$ gave 3-methyl-2*H*-azirine-2-carboxylate in >99% yield and 97% ee. Third, intramolecular hydride transfer and cyclization of dimethyl 2-(2-(dialkylamino)benzylidene)malonate gave tetrahydroquinoline products in 50% to >99% yields and 0-82% ee using 10 mol% of the catalyst Λ-$[Co((S,S)\text{-}NH_2CHArCHArNH_2)_3]^{3+}$ $2Cl^{-}BAr_f^{-}$ (Λ-(*S*,*S*)-$\mathbf{3b}^{3+}$ $2Cl^{-}BAr_f^{-}$ for Ar = 1-naphthyl) at 50-80 °C. Extension of these promising results to other substrates will be studied and communicated in the future.

When the complex Λ-(*S*,*S*)-$\mathbf{2}^{3+}$ $3Cl^{-}$ was treated with AgF, a new salt Λ-(*S*,*S*)-$\mathbf{2}^{3+}$ $3F^{-}$ was obtained in 98% yield. This could be used as the catalyst in the trifluoromethylation of aromatic aldehydes to give trimethylsilyl-1-aryl-2,2,2-trifluoroethanols in 20-70% isolated yields and 54-99% ee. Extension to other aldehydes gave low yields and ee values. The chloride anions in Λ-(*S*,*S*)-$\mathbf{2}^{3+}$ $2Cl^{-}BAr_f^{-}$ were exchanged in situ with anions of the enantiomers of proline to generate the catalyst Λ-(*S*,*S*)-$\mathbf{2}^{3+}$ $2(\text{prolinate})^{-}BAr_f^{-}$. The catalyst was used in the addition of acetone to *trans*-β-nitrostyrene to give the adduct 5-nitro-4-phenylpentan-2-one in 90% yield and 58% ee. Without the proline anions or the cation Λ-(*S*,*S*)-$\mathbf{2}^{3+}$, lower ee values were obtained.

# DEDICATION

*To my late grandmother who told me to go learn as much as possible and bring them all back home for her. She never stopped seeking knowledge, even at the age of 96. I really miss you grandma!*

ACKNOWLEDGEMENTS

I express my sincere appreciation to my advisor, Dr. John A. Gladysz, for providing ultimate supports throughout my doctoral study. I have received invaluable lessons from you, and they will stand useful far beyond graduate school. Thank you for maintaining a perfect balance between freedom and guidance, which allowed my creativity to develop. Special thanks go to my committee members, Dr. François P. Gabbaï, Dr. David C. Powers, and Dr. Perla B. Balbuena for helpful advices and discussions.

I am humble and honored to have known and worked with many past and present members of the Gladysz group. I appreciate all scientific and non-scientific rendezvous that we had. My Ph.D. experience would not be the same without them. Between sleepless NMR nights and early teaching classes, I managed to meet amazing people I dearly call friends. The earth would be a strange place without any one of them.

No words can describe my gratitude toward my parents, sisters, and brother. My beloved family have always been a safe place for me to fall back into whenever I stumble, and I know they will forever be. Mom and Dad, no trophies or degrees will ever be able to recognize the sacrifice you have made for my education. Thank you for making me a better person every day and for always believing in me. Your courage and intellect are my endless inspiration.

CONTRIBUTORS AND FUNDING SOURCES

**Contributors**

This work was supervised by a dissertation committee consisting of Professor John A. Gladysz (advisor), Professor David C. Powers, and Professor François P. Gabbaï of the Department of Chemistry, as well as Professor Perla B. Balbuena of the Department of Chemical Engineering.

The data used in Chapter 2 were obtained by the student in collaboration with Dr. Kyle G. Lewis (fellow graduate student) and Anik Banerjee (undergraduate student) of the Department of Chemistry.

The data used in chapter 4 were obtained by the student in collaboration with Teresa Faber (undergraduate visiting student) of Maastricht University, Netherlands.

All crystal structures were determined by Dr. Nattamai Bhuvanesh (staff member), although all crystallographic data were interpreted by the student.

All other work conducted for the dissertation was completed by the student independently.

**Funding Sources**

This work was made possible in part by the Welch Foundation under Grant Number A-1656.

TABLE OF CONTENTS

LIST OF FIGURES

LIST OF TABLES

LIST OF SCHEMES

# 1. INTRODUCTION

## 1.1. Hydrogen bond donors in asymmetric organocatalysis

"Organocatalysis", the use of small organic molecules to catalyze reactions, had been documented even before the term itself was envisioned. The earliest reaction was reported by Liebig in 1860, in which acetaldehyde was described as a necessary component for the formation of the oxamide product from cynogen and water but was fully recovered after work-up (Figure 1.1).[1]

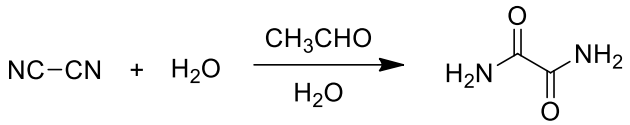


**Figure 1.1.** Oxamide synthesis from cyanogen reported by Liebig using acetaldehyde as the catalyst.

In the early 2000s, the term was officially introduced in peer-reviewed papers.[2] Since then, organocatalysis has become a major field of research. One of the main playgrounds for researchers in this field involves designing chiral small molecules serving as the catalysts for synthesizing enantiopure products in pharmaceutical and agricultural chemistry.[3] Due to the abundance of types of organic stereocenters, the term "organocatalysts" was originally believed to be exclusive for metal-free organic molecules.[3]

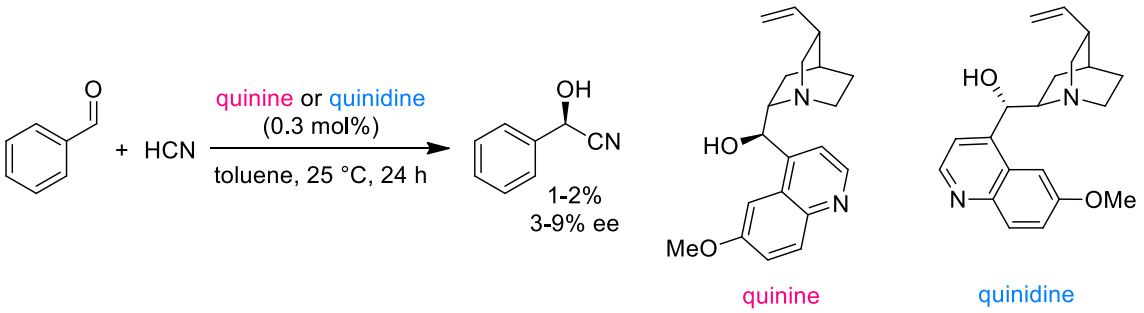


**Figure 1.2.** Quinine and quinidine as the catalysts for hydrocyanation of benzaldehyde.

A more recent definition has expanded the scope to include other species in which inorganic elements are present but are "not part of the active principle".[6] A notable example is the "planar-chiral" derivatives of DMAP developed by Fu and coworkers.[7] The catalyst contains a metal core which only transfers the chiral information and does not actively participate in the catalysis. This renders it, in the eyes of many, as an organocatalyst. One application of the iron-containing catalyst in the Staudinger reaction is shown in Figure 1.3.

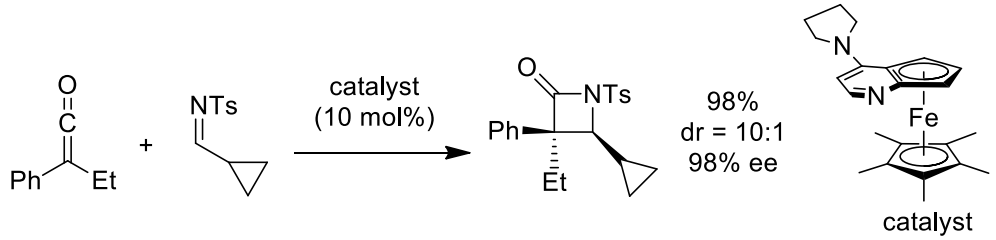


**Figure 1.3.** Metal-containing organocatalyst for Staudinger synthesis of a lactam.

Regardless of how organocatalysts are defined, they can be divided into two principle categories: (1) catalysts that activate substrates through covalent bonds and (2) those that activate substrates through non-covalent bonds. The former category usually consists of amine catalysts that can form iminium or enamine intermediates whereas hydrogen bond donating catalysts constitute a major part of the latter.[6] The first use of a hydrogen bond donor as the catalyst was reported in 1942 by Wassermann. The work features phenol as the catalyst, which activates benzoquinone through hydrogen bonding for a Diels-Alder reaction with cyclopentadiene (Figure 1.4).[8]

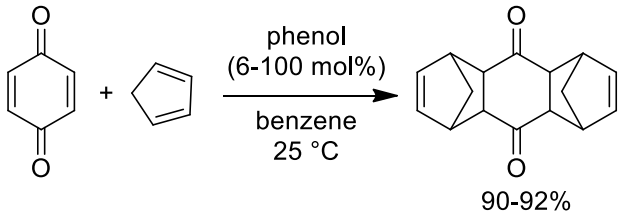


**Figure 1.4.** Diels-Alder reaction between benzoquinone and cyclopentadiene catalyzed by phenol.

Since then many chiral hydrogen bond donor catalysts have been developed and applied in asymmetric catalysis.[6b,9] The next subsections are centered around these catalysts. Subsection 1.1.1 discusses current catalysts that do not have metals in the molecules. Subsection 1.1.2 introduces chiral-at-metal hydrogen bond donors.

### 1.1.1. Hydrogen bond donors without metals in the molecules

Wynberg is recognized as the first to suggest hydrogen bonding between reactants and a chiral catalyst (Figure 1.5).[9a,b,10] In that work, addition of 4-*t*-butylthiophenol to 5,5-dimethyl cyclohexen-1-one was accomplished using 1 mol% of cinchonidine as the catalyst. The exact yield for each substrate was not reported individually (range 80-98%) and the highest ee reached was 75% (for the substrate in Figure 1.5).

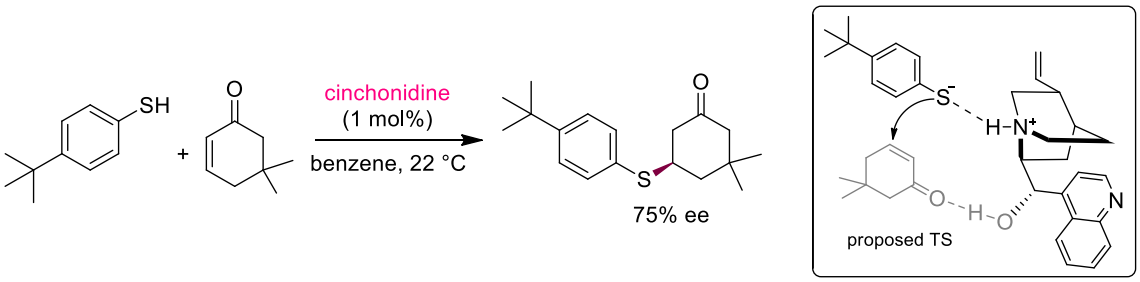


**Figure 1.5.** Asymmetric addition of 4-*t*-butylthiophenol to 5,5-dimethyl cyclohexen-1-one using cinchonidine as the hydrogen bond donating catalyst.

Since then, other designs have been brought into play to utilize this mode of activation for catalysis with high enantioselectivity.[9] Almost all of these approaches are based on two factors: (1) enantiopurity of the catalyst, and (2) the acidity ($pK_a$) of the X-H bonds in the molecule (X = O/N). A majority of the catalysts reported in the literature contain carbon stereocenters, with some occasional exceptions of sulfur stereocenters in sulfonamide.[11] A variety of NH and OH bonds have been used as the hydrogen bond donors. The acidity ($pK_a$, Figure 1.6)[9b] of these NH and OH bonds affects the reaction outcomes. For example, in the Strecker reaction between N-allylbenzylidene and HCN,

reported by Jacobsen (Figure 1.7),[12] a urea catalyst ($pK_a$ 27, Figure 1.6) gave only a 45% ee of the product while a thiourea catalyst ($pK_a$ 21, Figure 1.6) gave an 80% ee.

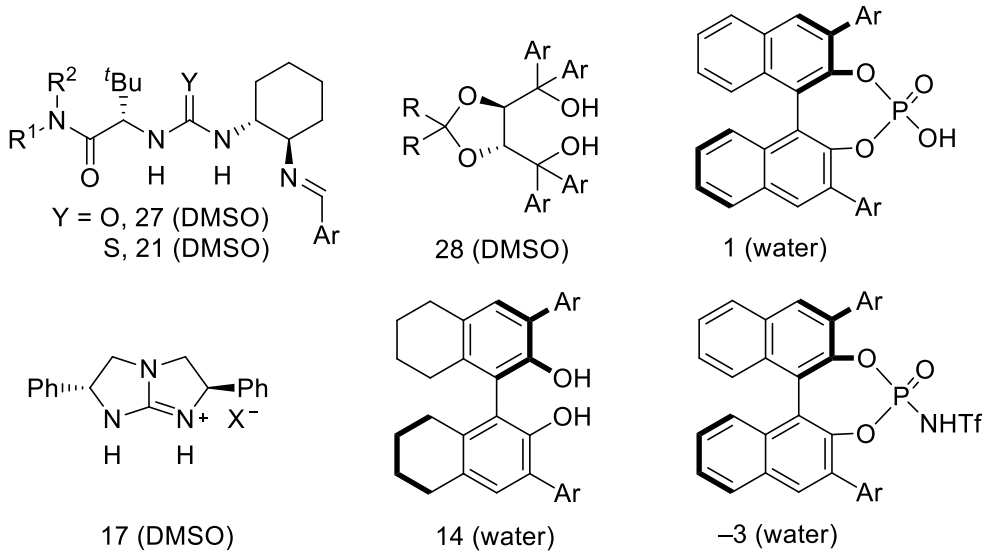


**Figure 1.6.** Representatives of chiral hydrogen bond donors in asymmetric catalysis with their $pK_a$ values in DMSO or water.

The reaction depicted in Figure 1.7 also marked the introduction of the well-known chiral thiourea catalysts.[9d,9f] Since then, thiourea catalysts have been further developed to perform a new mode of activation through anion binding.[13] Figure 1.8 shows one of the first applications of this new approach in the Pictet-Spengler reaction.[13b]

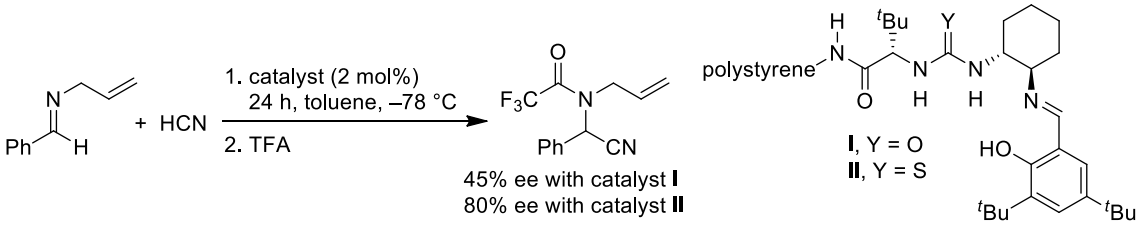


**Figure 1.7.** Enantioselective Strecker reaction catalyzed by urea and thiourea hydrogen bond donors.

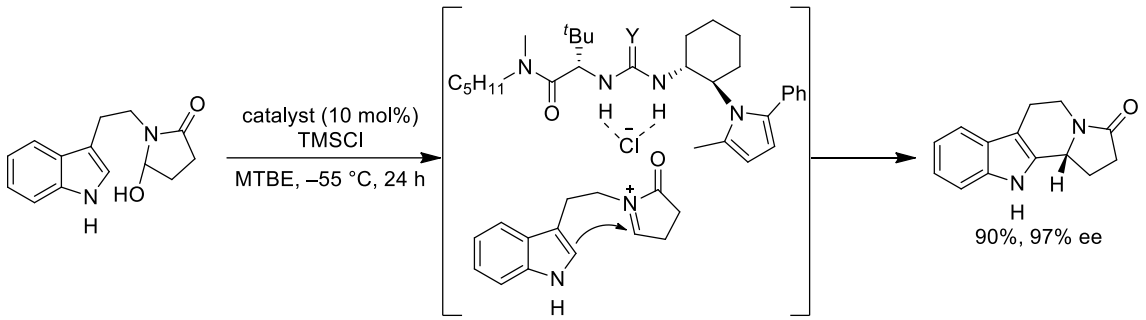


**Figure 1.8.** An example of hydrogen bond donor catalysis by anion binding.

One of the newest members of organic hydrogen bond donors are squaramides/thiosquaramides (Figure 1.9), which were introduced by Rawal in 2008.[14] These feature comparable $pK_a$ values[15] and geometrical characteristics[9g,16] to ureas/thioureas, also summarized in Figure 1.9. Some even exhibit stronger hydrogen bonds to substrates with common Lewis basic functional groups such as $NO_2$, C=O, and CN,[9g] and are effective in many reactions.[9f]

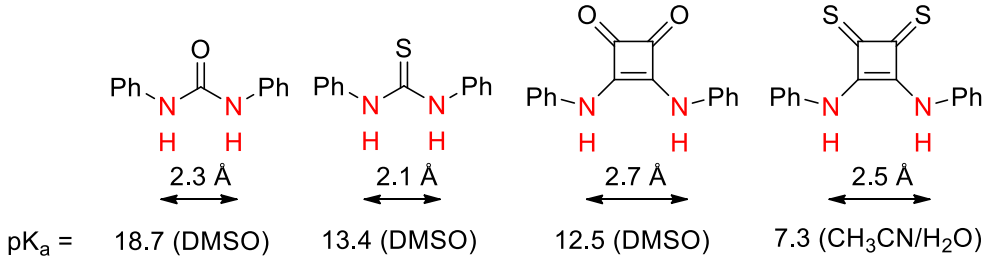


**Figure 1.9.** Representatives of (thio)ureas and (thio)squaramides.

### 1.1.2. Chiral-at-Metal Hydrogen-Bond Donors

This group of catalysts also have two features: (1) metal and/or ligand based stereocenter(s), and (2) X-H bonds for hydrogen bonding. These catalysts exhibit hydrogen bonding through second coordination sphere interaction. In other word, the ligands in these metal complexes bear X-H units (X = N or O) which act as the hydrogen bond donors. It is necessary to note that hydrogen bonding in the second coordination sphere has been observed and widely exploited in other applications.[17]

The metals in these catalysts do not directly activate the reactants. Although enantiomers of metal complexes can be found with many geometries (Figure 1.10),[18-21] tetrahedral and octahedral hydrogen bond donors are the most commonly seen.

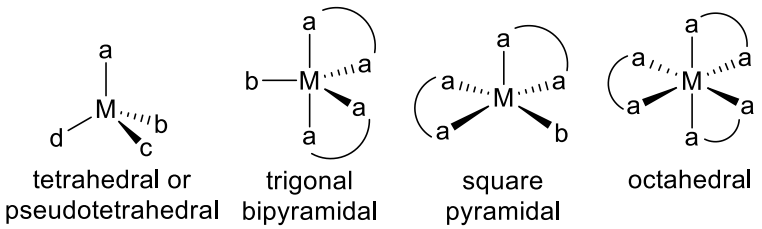


**Figure 1.10.** Representatives of chirality in metal complexes with different geometries (only one enantiomer is shown in each case).

Several groups have reported chiral-at-metal tetrahedral hydrogen bond donating catalysts.[22,23] Most notable examples include the 2-guanidinobenzimidazole based cyclopentadienyl ruthenium complexes reported by the Gladysz group.[22] Especially, the bifunctional catalyst $S_{Ru}R_CR_C$-**1**$^+$ $PF_6^-$ (Figure 1.11) gave high enantioselectivities in the addition of malonates to *trans*-β-nitrostyrene.[22a] Recent mechanistic studies confirmed that the substrates are activated through hydrogen bonding with the NH units of the 2-guanidinobenzimidazole containing ligand.[22b,22c]

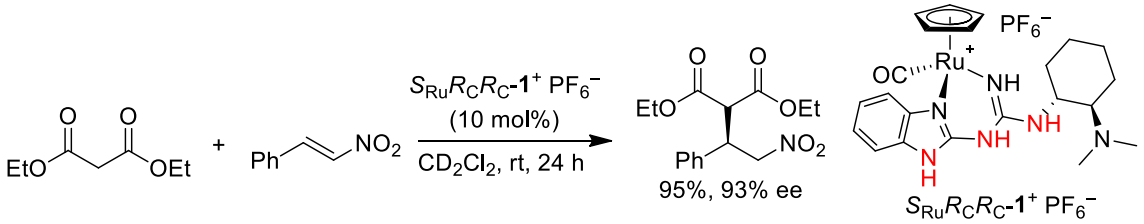


**Figure 1.11.** Enantioselective reaction catalyzed by chiral tetrahedral ruthenium complex.

Another species of organometallic ruthenium compound has also been reported to activate reactants through the OH moiety in the ligand (Figure 1.12).[23] The OH unit is directly bound to the ruthenium center, enhancing its acidity. Consequently, a complete

proton transfer to the imine substrates instead of hydrogen bonding was observed, leading to no enantioselectivity in the investigated Aza-Diels–Alder reaction (Figure 1.12).[23]

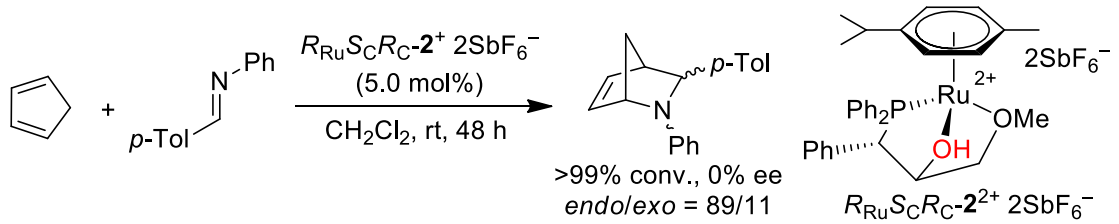


**Figure 1.12.** Aza-Diels–Alder reaction catalyzed by chiral pseudotetrahedral ruthenium complex.

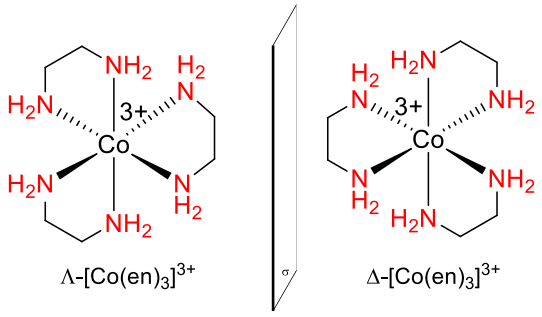


**Figure 1.13.** Two enantiomers of the trication cobalt(III) tris(ethylenediamine).

Enantioselective catalysis involving octahedral complexes started with the pioneering report from the Gladysz group in 2008 with the chiral cation $[Co(en)_3]^{3+}$ (en = ethylenediamine).[24] Two enantiomers of this cation is shown in Figure 1.13. The coordinated NH units have comparable $pK_a$ (ca. 15)[25] to those of the organic hydrogen bond donors (Figure 1.6 and 1.9). The addition of dimethyl malonate to cyclopentenone was catalyzed by the enantiopure lipophilic catalyst Δ-$[Co(en)_3]^{3+}$ $3BAr_f^-$ ($BAr_f^-$ = $(B(3,5\text{-}C_6H_3(CF_3)_2)_4^-)$ to give the 3-substituted cyclopentanone adduct in 33% ee (Figure 1.14).

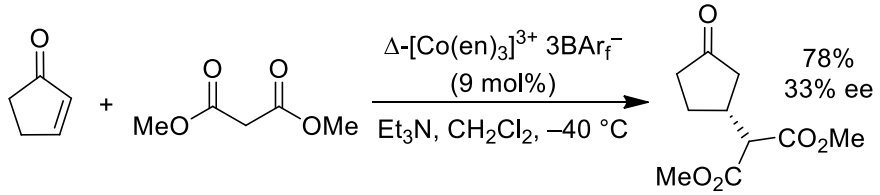


**Figure 1.14.** Enantioselective Michael addition catalyzed by the Werner complex Δ-$[Co(en)_3]^{3+}$ $3BAr_f^-$.

From this initial report, members of the Gladysz group, especially Carola Ganzman, Kyle Lewis, and Subrata Ghosh, have contributed significantly to the development of Werner type complexes in enantioselective catalysis. The catalysts have encompassed many different metals[26] and nitrogen donor ligands,[27-29] which resulted in multiple studies and applications in enantioselective catalysis over the past decade (Figure 1.15).[30]

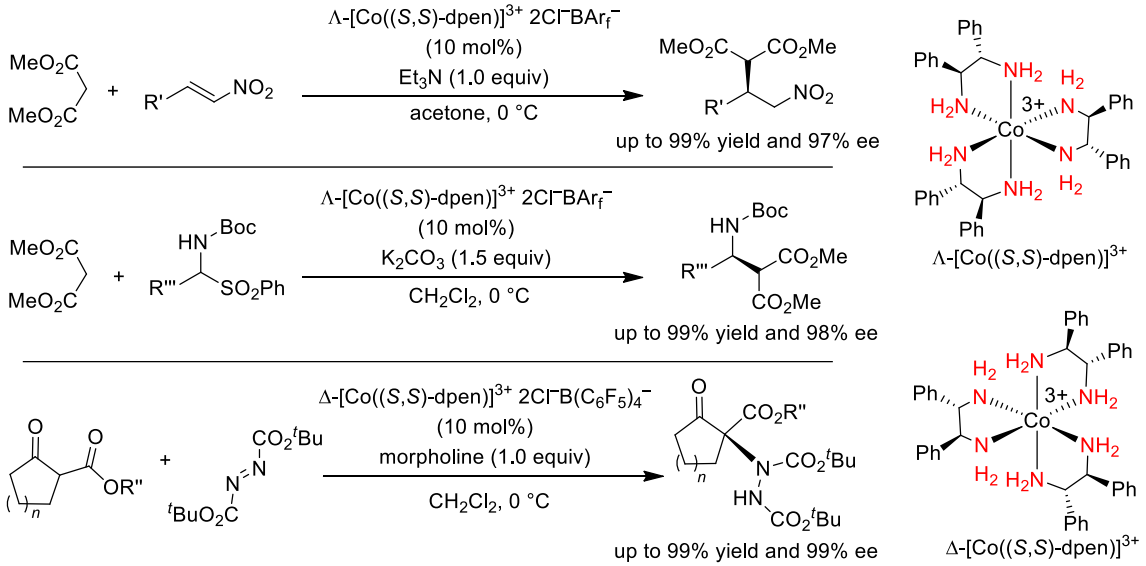


**Figure 1.15.** Representatives of enantioselective reactions catalyzed by Werner type complexes.

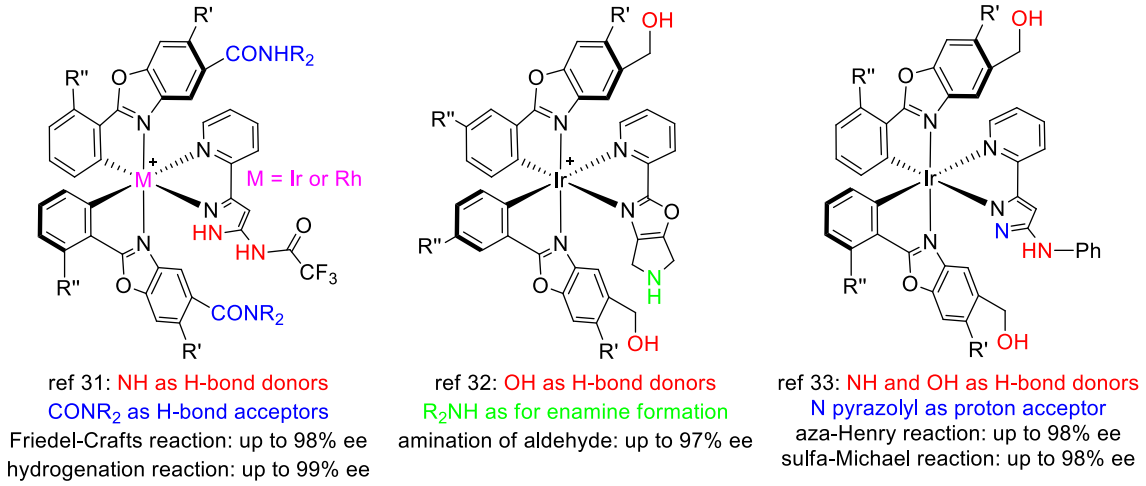


**Figure 1.16.** Representatives of the cations in Meggers' catalysts.

Other groups have also reported chiral-at-metal octahedral hydrogen bond donating catalysts. For example, Meggers and coworkers have developed octahedral iridium(III) and rhodium(III) complexes in which NH and OH groups of the ligands act as hydrogen bond donors (Figure 1.16).[31-33]

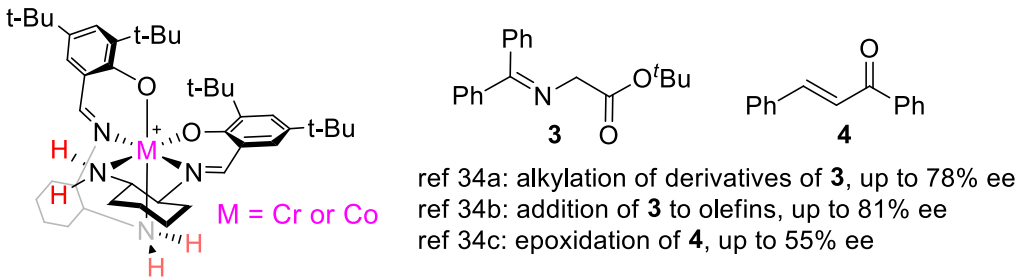


**Figure 1.17.** A representative of the cations in Belokon's catalysts.

The Belokon group has also demonstrated some successes in synthesizing octahedral cobalt(III) and chromium(III) complexes from a Schiff base ligand bearing a chiral diamine (Figure 1.17).[34] The NH units in these complexes are reported to activate substrates and/or reagents in several reactions through hydrogen bonding.

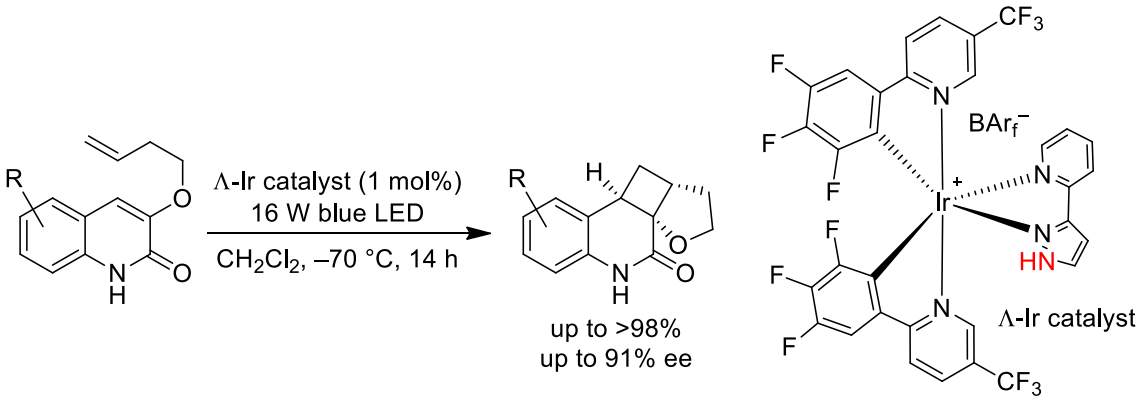


**Figure 1.18.** A reaction involving Yoon's photocatalyst.

Iridium complexes have also been used as chiral photocatalysts. By integrating a NH unit to one of the ligands, the Yoon group has achieved high yields and enantioselectivities in an intramolecular [2+2] cycloaddition (Figure 1.18).[35] It was

speculated that the pyrazolyl NH unit kept the substrates close to the iridium chiral center through hydrogen bonding and thus is responsible for the high enantioselectivity.

**1.2. Expanding applications of Werner complexes in enantioselective synthesis**

The cobalt(III) cations in Figures 1.13 and 1.15 have six $NH_2$ groups with two diastereotopic hydrogen atoms on each nitrogen atom. Consequently, there are a total of 12 NH moieties in the molecule available for hydrogen bonding to substrates, as opposed to two or three in the other hydrogen bond donor catalysts described in sections 1.1.1 and 1.1.2. Therefore, it is hypothesized that this new class of catalysts can exhibit unique activities and applications in organic synthesis.

Coexisting with the cations in Werner complexes are the anions. Beside the role of bringing the cations into organic solvents ($BAr_f^-$ and $B(C_6F_5)_4^-$),[24,27] the anions (such as $Cl^-$, $BF_4^-$, and $PF_6^-$, and chiral phosphates) have also shown some effects in the enantioselectivities of several reactions (Figure 1.15).[30,36] In this study, it is speculated that when the chlorides in these catalysts are metathesized to other anions, which can actively participate in a reaction as catalysts or activators in cooperation with the chiral cation, more interesting activities can be observed.

In this dissertation, the application of the complexes of the type Λ-[Co((*S*,*S*)-$NH_2CHPhCHPhNH_2)_3]^{3+}$ $2X^-X'^-$ as chiral solvating agents will be reported in chapter 2. Chapters 3 and 4 will discuss several enantioselective reactions catalyzed by Λ- and Δ-[Co((*S*,*S*)-$NH_2CHPhCHPhNH_2)_3]^{3+}$ $2X^-X'^-$. Chapter 5 will present data of some asymmetric transformations, in which X and X' of Λ-[Co((*S*,*S*)-$NH_2CHPhCHPhNH_2)_3]^{3+}$ $2X^-X'^-$ also participate in the transformations.

## 1.3. References

(1) (a) von Liebig, J. Ueber die Bildung des Oxamids aus Cyan. *Justus Liebigs Ann. Chem.* **1860**, *113*, 246-247. (b) Langenbeck, W. Über organische Katalysatoren. III. Die Bildung von Oxamid aus Dicyan bei Gegenwart von Aldehyden. *Justus Liebigs Ann. Chem.* **1929**, *469*, 16-25.

(2) (a) MacMillan, D. C. The advent and development of organocatalysis. *Nature* **2008**, *455*, 304-308. (b) Ahrendt, K. A.; Borths, C. J.; MacMillan, D. W. C. New Strategies for Organic Catalysis: The First Highly Enantioselective Organocatalytic Diels-Alder Reaction. *J. Am. Chem. Soc.* **2000**,

(3) Berkessel, A.; Groeger, H. *Asymmetric Organocatalysis: from Biomimetic Concepts to Applications in Asymmetric Synthesis*; Wiley-VCH: Weinheim, 2005.

(4) Fiske, P. S.; Bredig, G. Durch Katalysatoren bewirkte asymmetrische Synthese. *Biochem. Z.* **1912**, *687*, 7-23. (b) List, B.; Grossman, O. *Synfacts* **2019**, *15*, 554.

(5) *Cinchona Alkaloids in Synthesis and Catalysis: Ligands, Immobilization and Organocatalysis*; Song, C. E., Ed.; Wiley-VCH: Weinheim, 2009.

(6) (a) Thematic issue: List, B. *Chem. Rev.* **2007**, *107*, 5413-5415. (b) *Asymmetric Organocatalysis*; List, B., Ed.; Topics in Current Chemistry Series Vol 291; Springer: Heidelberg, 2010.

(7) (a) Ruble, J. C.; Fu, G. C. Chiral π-Complexes of Heterocycles with Transition Metals: A Versatile New Family of Nucleophile Catalysts. *J. Org. Chem.* **1996**, *61*, 7230-7231. (b) Garrett, C. E.; Fu, G. C. Nucleophilic Catalysis with π-Bound Nitrogen Heterocycles: Synthesis of the First Ruthenium Catalysts and Comparison of the Reactivity and the Enantioselectivity of Ruthenium and Iron Complexes. *J Am. Chem. Soc.* **1998**, *120*, 7479-7483. (c) Fu, G. C. Enantioselective Nucleophilic Catalysis with "Planar-Chiral" Heterocycles. *Acc. Chem. Res.* **2000**, *33*, 412-420. (d) Fu, G. C.

Asymmetric Catalysis with "Planar-Chiral" Derivatives of 4-(Dimethylamino)pyridine. *Acc. Chem. Res.* **2004**, *37*, 542-547.

(8) (a) Wassermann, A. Homogenenous Catalysis of Diene Syntheses. A New Type of Third-order Reaction. *J. Chem. Soc.* **1942**, 618-621. (b) Rubin, W.; Steiner, H.; Wassermann, A. Catalysis of Diels-Alder Diene Associations. Part V. Proton- and Electron-transfer Processes. *J. Chem. Soc.* **1949**, 3046-3057.

(9) For reviews of hydrogen-bond donating catalysts, see: (a) Taylor, M. S.; Jacobsen, E. N. Asymmetric Catalysis by Chiral Hydrogen-Bond Donors. *Angew. Chem., Int. Ed.* **2006***, 45,* 1520-1543; Asymmetrische Katalyse durch chirale Wasserstoffbrückendonoren. *Angew. Chem.* **2006**, *118*, 1550-1573. (b) Doyle, A. G.; Jacobsen, E. N. Small-Molecule H-Bond Donors in Asymmetric Catalysis. *Chem. Rev.* **2007**, *107*, 5713-5743. (c) Yu, X.; Wang, W. Hydrogen-Bond-Mediated Asymmetric Catalysis. *Chem. Asian J.* **2008**, *3*, 516-532. (d) Takemoto, Y. Recognition and Activation by Ureas and Thioureas: Stereoselective Reactions using Ureas and Thioureas as Hydrogen-Bonding Donors. *Org. Biomol. Chem.* **2005**, ***3***, 4299-4306. (e) Miyabe, H.; Takemoto, Y. Discovery and Application of Asymmetric Reaction by Multi-Functional Thioureas. *Bull. Chem. Soc. Jpn.* **2008**, *81*, 785-795. (f) Held, F. E.; Tsogoeva, S. B. Asymmetric Cycloaddition Reactions Catalyzed by Bifunctional Thiourea and Squaramide Organocatalysts: Recent Advances. *Catal. Sci. Technol.* **2016**, *6*, 645-667. (g) Zhao, B.-L.; Li, J.-H.; Du, D.-M. Squaramide-Catalyzed Asymmetric Reactions. *Chem. Rec.* **2017**, *17*, 994-1018.

(10) Hiemstra, H.; Wynberg, H. Addition of Aromatic Thiols to Conjugated Cycloalkenones, Catalyzed by Chiral -Hydroxy Amines. A Mechanistic Study on Homogeneous Catalytic Asymmetric Synthesis. *J. Am. Chem. Soc.* **1981**, *103*, 417-430.

(11) Tan, K. L.; Jacobsen, E. N. Indium-Mediated Asymmetric Allylation of Acylhydrazones Using a Chiral Urea Catalyst. *Angew. Chem., Int. Ed.* **2007**, *46*, 1315-1317. *Angew. Chem.* **2007**, *119*, 1337-1339.

(12) Sigman, M.; Jacobsen, E. N. Schiff base catalysts for the asymmetric Strecker reaction identified and optimized from parallel synthetic libraries. *J. Am. Chem. Soc.* **1998**, *120*, 4901-4902.

(13) (a) Taylor, M. S.; Jacobsen, E. N. Highly Enantioselective Catalytic Acyl-Pictet–Spengler Reactions. *J. Am. Chem. Soc.* **2004**, *126*, 10558-10559. (b) Raheem, I. T.; Thiara, P. S.; Peterson, E. A.; Jacobsen, E. N. Enantioselective Pictet–Spengler-Type Cyclizations of Hydroxylactams: H-Bond Donor Catalysis by Anion Binding. *J. Am. Chem. Soc.* **2007**, *129*, 13404-13405.

(14) Malerich, J. P.; Hagihara, K.; Rawal, V. H. Chiral Squaramide Derivatives are Excellent Hydrogen Bond Donor Catalysts. *J. Am. Chem. Soc.* **2008**, *130*, 14416-14417.

(15) (a) Jakab, G.; Tancon, C.; Zhang, Z.; Lippert, K. M. Schreiner, P. R. (Thio)urea Organocatalyst Equilibrium Acidities in DMSO. *Org. Lett.* **2012**, *14*, 1724-1727. (b) Ni, X.; Li, X.; Wang, Z.; Cheng, J-.P. Squaramide Equilibrium Acidities in DMSO. *Org. Lett.* **2014**, *16*, 1786-1789.

(16) Storer, R. I.; Aciro, C.; Jones, L. H. Squaramides: physical properties, synthesis and applications. *Chem. Soc. Rev.* **2011**, *40*, 2330-2346.

(17) (a) Mercer, D. J.; Loeb, S. J. Metal-based anion receptors: an application of second-sphere coordination. *Chem. Soc. Rev.* **2010**, *39*, 3612-3620. (b) Reedijk, K. Coordination chemistry beyond Werner: interplay between hydrogen bonding and coordination. *Chem. Soc. Rev.* **2013**, *42*, 1776-1783. (c) Ghosh, S. K.; Ehnbom, A.; Lewis, K. G.; Gladysz, J. A. Hydrogen bonding motifs in structurally characterized salts of the

tris(ethylenediamine) cobalt trication, $[Co(en)_3]^{3+}$; An interpretive review, including implications for catalysis. *Coord. Chem. Rev.* **2017**, *350*, 30-48.

(18) For a general review of all geometries, see: Knof, U.; von Zelewsky, A. Predetermined Chirality at Metal Centers. *Angew. Chem., Int. Ed.* **1999**, *38*, 302-332. Prädeterminierte Chiralität an Metallzentren. *Angew. Chem.* **1999**, *111*, 312-333.

(19) For reviews of tetrahedral chiral complexes, see: (a) Brunner, H. Optically Active Organometallic Compounds of Transition Elements with Chiral Metal Atoms. *Angew. Chem., Int. Ed.* **1999**, *38*, 1194-1208. Optisch aktive metallorganische Verbindungen der Übergangselemente mit chiralen Metallatomen. *Angew. Chem.* **1999**, *111*, 1248-1263. (b) Ganter, C. Chiral Organometallic half-sandwich complexes with defined metal configuration. *Chem. Soc. Rev.* **2003**, *32*, 130-138. (c) Bauer, E. Chiral-at-metal complexes and their catalytic applications in organic synthesis. *Chem. Soc. Rev.* **2012**, *41*, 3153-3167.

(20) For examples of trigonal bipyramidal and square pyramidal chiral complexes, see: (a) Lennartson, A.; Håkansson, M. Total Spontaneous Resolution of Five-Coordinate Complexes. *Angew. Chem., Int. Ed.* **2009**, *48*, 5869-5871. *Angew. Chem.* **2009**, *121*, 5983-5985. (b) Lennartson, A.; Håkansson, M. A missing link between chiral four- and five-coordinate complexes. *New. J. Chem.* **2015**, *39*, 3353-3356. (c) Lennartson, A.; Håkansson, M. Absolute asymmetric synthesis of five-coordinate complexes. *New. J. Chem.* **2015**, *39*, 5936-5943.

(21) For reviews of octahedral complexes, see: (a) Pierre, J.-L. Enantioslective creation of helical chirality in octahedral (OC-6) complexes. Recent advances. *Coord. Chem. Rev.* **1998**, *178-180*, 1183-1192. (b) Knight, P. D.; Scott, P. Predetermination of chirality at octahedral centres with tetradentate ligands: prospects for enantioselective catalysis. *Coord. Chem. Rev.* **2003**, *242*, 125-143. (c) Meggers, E. Asymmetric Synthesis

of Octahedral Coordination Complexes. *Eur. J. Inorg. Chem.* **2011**, 2911-2926. (d) Ehnbom, A.; Gosh, S. K.; Lewis, K. G.; Gladysz, J. A. Octahedral Werner complexes with substituted ethylenediamine ligands: a stereochemical primer for a historic series of compounds now emerging as a modern family of catalysts. *Chem. Soc. Rev.* **2016**, *45*, 6799-6811.

(22) (a) Mukherjee, T.; Ganzmann, C.; Bhuvanesh, N.; Gladysz, J. A. Syntheses of Enantiopure Bifunctional 2-Guanidinobenzimidazole Cyclopentadienyl Ruthenium Complexes: Highly Enantioselective Organometallic Hydrogen Bond Donor Catalysts for Carbon-Carbon Bond Forming Reactions. *Organometallics* **2014**, *33*, 6723-6737. (b) Wititsuwannakul, T.; Mukherjee, T.; Hall, M. B.; Gladysz, J. A. Computational Investigations of Enantioselection in Carbon-Carbon Bond Forming Reactions of Ruthenium Guanidinobenzimidazole Second Coordination Sphere Hydrogen Bond Donor Catalysts. *Organometallics* **2020**, *39*, 1149-1162. (c) Mukherjee, T.; Ghosh, S. K.; Wititsuwannakul, T.; Bhuvanesh, N.; Gladysz, J. A. Chiral-at-Metal Ruthenium Complexes with Guanidinobenzimidazole and Pentaphenylcyclopentadienyl Ligands: Synthesis, Resolution, and Preliminary Screening as Enantioselective Second Coordination Sphere Hydrogen Bond Donor Catalysts. *Organometallics* **2020**, *39*, 1163-1175.

(23) Pardo, P.; Carmona, D.; Lamata, P.; Rodríguez, R.; Lahoz, F. J.; García-Orduña, P.; Oro, L. A. Reactivity of the Chiral Metallic Brønsted Acid [($\eta^6$-*p*-$MeC_6H_4$*i*Pr)Ru($\kappa^3$*P*,*O*,*O'*-POH)][$SbF_6$]$_2$ (POH = $S_{C1}$,$R_{C2}$)-$Ph_2PC(Ph)HC(OH)HCH_2$-OMe) toward Aldimines. *Organometallics* **2014**, *33*, 6927-6936.

(24) Ganzmann, C.; Gladysz, J. A. Phase Transfer of Enantiopure Werner Cations into Organic Solvents: An Overlooked Family of Chiral Hydrogen Bond Donors for Enantioselective Catalysis. *Chem. Eur. J.* **2008**, *14*, 5397-5400.

(25) Goodall, D. M.; Hardy, M. J. Conjugate Bases of Tris (ethylenediamine)cobalt(III) and Nitropenta-ammine-cobalt(III) in Aqueous Hydroxide-Dimethyl Sulphoxide Mixtures. *J. Chem. Soc., Chem. Commun.* **1975**, *72*, 919-921.

(26) Maximuck, W. J.; Ganzmann, C.; Alvi, S.; Hooda, K. R.; Gladysz, J. A. Rendering Classical Hydrophilic Enantiopure Werner Salts $[M(en)_3]^{n+}$ $nX^-$ Lipophilic (M/*n* = Cr/3, Co/3, Rh/3, Ir/3, Pt/4); New Chiral Hydrogen Bond Donor Catalysts and Enantioselectivities as a Function of Metal and Charge. *Dalton Trans*. **2020**, *49*, 3680-3691.

(27) Ghosh, S. K.; Lewis, K. G.; Kumar, A.; Gladysz, J. A. Syntheses of Families of Enantiopure and Diastereopure Cobalt Catalysts Derived from Trications of the Formula $[Co(NH_2CHArCHArNH_2)_3]^{3+}$. *Inorg. Chem.* **2017**, 56, 2304-2320.

(28) Ghosh, S. K.; Ganzmann, C.; Bhuvanesh, N.; Gladysz, J. A. Werner Complexes with ω-Dimethylaminoalkyl Substituted Ethylenediamine Ligands: Bifunctional Hydrogen-Bond-Donor Catalysts for Highly Enantioselective Michael Additions. *Angew. Chem., Int. Ed.* **2016**, *55*, 4356-4360; Werner-Komplexe mit ω-Dimethylaminoalkyl-substitutierten Ethylendiaminliganden: bifunktionale H-Brückendonor-Katalysatoren für hoch enantioselektive Michael-Additionen. *Angew. Chem.* **2016**, *128*, 4429-4433.

(29) Maximuck, W. J.; Gladysz, J. A. Lipophilic Chiral Cobalt(III) Complexes of Hexaamine Ligands; Efficacies as Enantioselective Hydrogen Bond Donor Catalysts. *Mol. Catal.* **2019**, *473*, 110360 (this journal has replaced conventional pagination by article numbers).

(30) (a) Lewis, K. G.; Ghosh, S. K.; Bhuvanesh, N.; Gladysz, J. A. Cobalt(III) Werner Complexes with 1,2-Diphenylethylenediamine Ligands: Readily Available, Inexpensive, and Modular Chiral Hydrogen Bond Donor Catalysts for Enantioselective

Organic Synthesis. *ACS Cent. Sci.* **2015**, *1*, 50-56. (b) Kumar, A.; Ghosh, S. K.; Gladysz, J. A. Tris(1,2-diphenylethylenediamine)cobalt(III) Complexes: Chiral Hydrogen Bond Donor Catalysts for Enantioselective *α*-Aminations of 1,3-Dicarbonyl Compounds. *Org. Lett.* **2016**, *18*, 760-763. (c) Joshi, H.; Ghosh, S. K.; Gladysz, J. A. Enantioselective Additions of Stabilized Carbanions to Imines Generated from α-Amido Sulfones By Using Lipophilic Salts of Chiral Tris(1,2-diphenylethylenediamine) Cobalt(III) Trications as Hydrogen Bond Donor Catalysts. *Synthesis* **2017**, *49*, 3905-3915.

(31) (a) Chen, L.-A.; Tang, X.; Xi, J.; Xu, W.; Gong, L.; Meggers, E. Chiral-at-Metal Octahedral Iridium Catalyst for the Asymmetric Construction of an All-Carbon Quaternary Stereocenter. *Angew. Chem., Int. Ed.* **2013**, *52*, 14021-14025 and *Angew. Chem.* **2013**, *125*, 14271-14275. (b) Xu, W.; Shen, X.; Ma, Q.; Gong, L.; Meggers, E. Restricted Conformation of a Hydrogen Bond Mediated Catalyst Enables the Highly Efficient Enantioselective Construction of an All-Carbon Quaternary Stereocenter. *ACS Catal.* **2016**, *6*, 7641-7646. (c) Xu, W.; Arieno, M.; Löw, H.; Huang, K.; Xie, X.; Cruchter, T.; Ma, Q.; Xi, J.; Huang, B.; Wiest, O.; Gong, L.; Meggers, E. Metal-Templated Design: Enantioselective Hydrogen-Bond-Driven Catalysis Requiring Only Parts-per-Million Catalyst Loading. *J. Am. Chem. Soc.* **2016,** *138*, 8774-8780.

(32) Huo, H.; Fu, C.; Wang, C.; Harms, K.; Meggers, E. Metal-templated Enantioselective Enamine/H-bonding Dual Activation Catalysis. *Chem. Commun*. **2014**, *50*, 10409-10411.

(33) (a) Hu, Y.; Zhou, Z.; Gong, L.; Meggers, E. Asymmetric aza-Henry reaction to provide oxindoles with quaternary carbon stereocenter catalyzed by a metal-templated chiral Brønsted base. *Org. Chem. Front.* **2015**, *2*, 968-972. (b) Ding, X.; Lin, H.; Gong, L.; Meggers, E. Enantioselective Sulfa-Michael Addition to α,β-Unsaturated γ-Oxoesters Catalyzed by a Metal-Templated Chiral Brønsted Base. *Asian J. Org. Chem.* **2015**, *4*, 434-

437. (c) Ding, X.; Tian, C.; Hu, Y.; Gong, L.; Meggers, E. Tuning the Basicity of a Metal-Templated Brønsted Base to Facilitate the Enantioselective Sulfa-Michael Addition of Aliphatic Thiols to α,β-Unsaturated *N*-Acylpyrazoles. *Eur. J. Org. Chem.* **2016**, *2016*, 887-890.

(34) (a) Belokon, Y. N.; Maleev, V. I.; North, M.; Larionov, V. A.; Savel´yeva, T. F.; Nijland, A.; Nelyubina, Y. V. Chiral Octahedral Complexes of CoIII As a Family of Asymmetric Catalysts Operating under Phase Transfer Conditions. *ACS Catal.* **2013**, *3*, 1951-1955. (b) Maleev, V. I.; North, M.; Larionov, V. A.; Fedyanin, I. V.; Savel´yeva, T. F.; Moscalenko, M. A.; Smolyakov, A. F.; Belokon, Y. N. Chiral Octahedral Complexes of Cobalt(III) as "Organic Catalysts in Disguise" for the Asymmetric Addition of a Glycine Schiff Base Ester to Activated Olefins. *Adv. Synth. Catal.* **2014**, *356*, 1803-1810. (c) Larionov, V. A.; Markelova, E. P.; Smol´yakov, A. F.; Savel´yeva, T. F.; Maleev, V. I.; Belokon, Y. N. Chiral octahedral complexes of Co(III) as catalysts for asymmetric epoxidation of chalcones under phase transfer conditions. *RSC Adv.* **2015**, *5*, 72764-72771.

(35) Skubi, K. L.; Kidd, J. B.; Jung, H.; Guzei, I. A.; Baik, M.-H.; Yoon, T. P. Enantioselective Excited-State Photoreactions Controlled by a Chiral Hydrogen-Bonding Iridium Sensitizer. *J. Am. Chem. Soc.* **2017**, *139*, 17186-17192.

(36) Kabes, C. Q.; Maximuck, W. J.; Ghosh, S. K.; Kumar, A.; Bhuvanesh, N.; Gladysz, J. A. Chiral Tricationic tris(1,2-diphenylethylenediamine) Cobalt(III) Hydrogen Bond Donor Catalysts with Defined Carbon/ Metal Configurations; Matched/Mismatched Effects upon Enantioselectivities with Enantiomeric Chiral Counter Anions. *ACS Catal.* **2020**, *10*, 3249-3263.

# 2. THE ROBUST, READILY AVAILABLE COBALT(III) TRICATION $[Co(NH_2PhCHCHPhNH_2)_3]^{3+}$ IS A PROGENITOR OF BROADLY APPLICABLE CHIRALITY AND PROCHIRALITY SENSING AGENTS*

## 2.1. Introduction

Ever since the recognition of molecular chirality, chemists have sought to quantify enantiomer ratios in non-racemic samples.[1] For more than a century, the dominant method was polarimetry, despite many intrinsic limitations.[2,3] Today, nearly every analytical technique is being brought to bear on the problem, often in a quest for high throughput screening.[4,5] Two broad classes of assays see the most use: "chiral" chromatography[6,7] and NMR spectroscopy.[8-13]

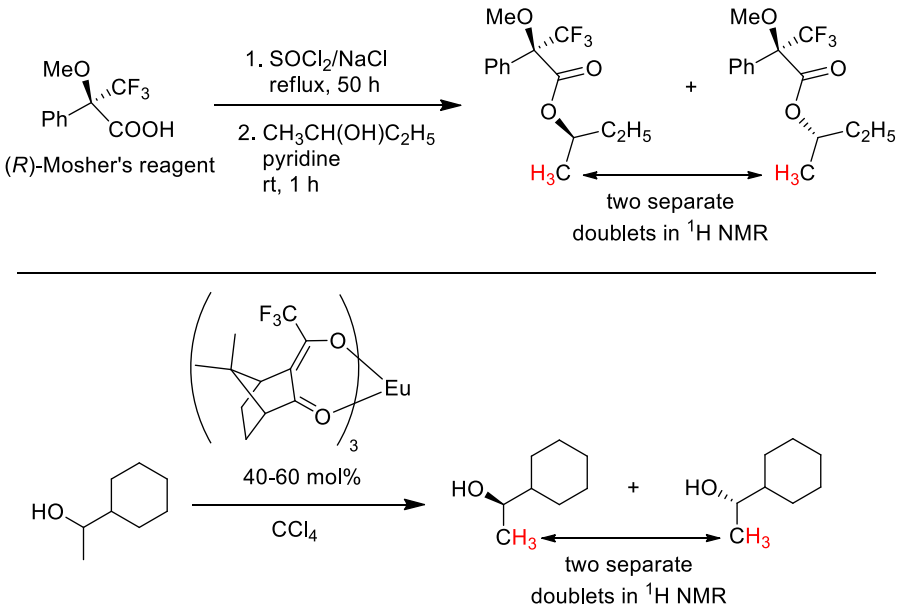


**Figure 2.1.** Examples of a chiral derivatizing agent (CDA, Mosher's reagent) and its application (top), and a chiral lanthanide shift reagent (CLSR, tris(3-trifluoroacetyl-*d*-nopinato)europium(III)) and its application (bottom).

NMR methods can be divided into three principal categories: chiral derivatizing agents (CDAs, Figure 2.1, top),[8-12,14,15] paramagnetic chiral lanthanide shift reagents (CLSRs, Figure 2.1, bottom),[16] and chiral solvating agents (CSAs, see below).[8,10-13] Over



*Adapted with permission from Luu, Q. H.; Lewis, K. G.; Banerjee, A.; Bhuvanesh, N.; Gladysz, J. A. *Chem. Sci.* **2018**, *9*, 5087-5099.-Published by the Royal Society of Chemistry.

the past few years, the last approach has attracted increasing attention.[17-30] Many but not all of the CSAs are hydrogen bond donors, often with two-four NH or OH groups.[17,21,22,25-28,30] Some of these have been tailored to recognize a specific functional group,[19,23,24,26-28] while others have wider applicability.[17,20-22,25,29,30]

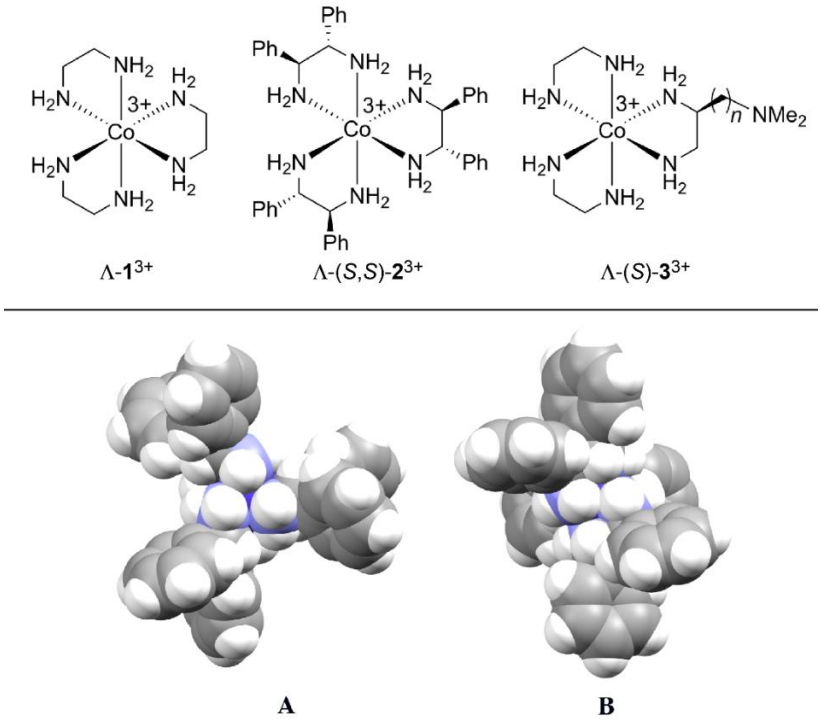


**Figure 2.2.** Top: chiral hydrogen bond donor catalysts based upon cobalt(III) tris(ethylenediamine) trications. Bottom: space filling representations of the trication of Λ-(*S*,*S*)-**2**$^{3+}$ $3Cl^{-}\cdot 2H_2O\cdot 2CH_3OH$; A, view down the idealized $C_3$ axis; B, view down one of three idealized $C_2$ axes.[42]

The first chiral inorganic compounds to be isolated in enantiomerically pure form were reported by Werner some 110 years ago, and included salts of the trication $[Co(en)_3]^{3+}$ (**1**$^{3+}$; en = ethylenediamine).[31-35] The Gladysz group has recently found that lipophilic salts of this trication[36] and the related species $[Co((S,S)\text{-}NH_2CHArCHArNH_2)_3]^{3+}$ ((*S*,*S*)-**2**$^{3+}$ for Ar = Ph)[37-40] and $[Co(en)_2((S)\text{-}NH_2\text{-}CH_2CH((CH_2)_nN(CH_3)_2)NH_2)]^{3+}$ ((*S*)-**3**$^{3+}$)[41] – all of which are depicted in Figure 2.2 – serve as hydrogen bond donor catalysts for a variety of organic transformations. The

trication $\mathbf{1}^{3+}$ features only metal centered chirality, for which the absolute configurations are traditionally designated Λ and Δ.[42] In the trications $\mathbf{2}^{3+}$ and $\mathbf{3}^{3+}$, the three ethylenediamine ligands are substituted with six aryl groups[43] or a single $(CH_2)_nN(CH_3)_2$ moiety, respectively.[44] The latter constitutes a bifunctional catalyst.[41] Both enantiomers of the $NH_2CHPhCHPhNH_2$ (dpen) ligand in $\mathbf{2}^{3+}$ are commercially available at modest prices.[45]

Although the mechanisms of these transformations are still under investigation, their effectiveness is thought to be rooted in the large number of NH groups (twelve). Those of one diastereomer of $\mathbf{2}^{3+}$ are depicted in Figure 2.2 (bottom). As many as five to six might play a role in transition state assemblies,[46] as opposed to a maximum of two with most literature catalysts such as thioureas.[47] As such, they might possess unique capabilities as CSAs. Indeed, in the course of screening catalytic reactions by NMR, marked differentiation of enantiomers and enantiotopic (prochiral) groups were noted.

In this chapter, I report a detailed study of chirality and prochirality sensing by the preceding complexes, and in particular the commercially available[48] bis(chloride)/tetraarylborate mixed salt Λ-(*S*,*S*)-$\mathbf{2}^{3+}$ $2Cl^-BAr_f^-$ ($BAr_f$ = $B(3,5\text{-}C_6H_3(CF_3)_2)_4$) and the bis(iodide) analog Λ-(*S*,*S*)-$\mathbf{2}^{3+}$ $2I^-BAr_f^-$. These robust, air and water stable substances are remarkable in affording baseline NMR signal separations at loadings as low as 1 mol%. The scope of functional group applicability ranks with the most versatile existing CSAs, and they appear unsurpassed in differentiating enantiotopic groups in achiral molecules.[49-56]

## 2.2. Results

### 2.2.1. Syntheses of cobalt(III) CSAs.

Enantiopure Λ-$\mathbf{1}^{3+}$ $3BAr_f^-$ and diastereopure Λ-(*S*,*S*)-$\mathbf{2}^{3+}$ $2Cl^-BAr_f^-$, Λ-(*S*,*S*)-$\mathbf{2}^{3+}$ $2Cl^-B(C_6F_5)_4^-$, Λ-(*S*,*S*)-$\mathbf{2}^{3+}$ $3BAr_f^-$, and Δ-(*S*,*S*)-$\mathbf{2}^{3+}$ $2Cl^-BAr_f^-$ were prepared according

to previously reported procedures.[36,43] Those for the $BAr_f^-$ salts of Λ-(*S*,*S*)-**2**$^{3+}$ are summarized in Scheme 2.1. The key precursor Λ-(*S*,*S*)-**2**$^{3+}$ 3Cl$^-$ is easily synthesized from $CoCl_2$ or $Co(OAc)_2$, $O_2$, and (*S*,*S*)-dpen.[43]

The new triiodide salt Λ-(*S*,*S*)-**2**$^{3+}$ 3I$^-$ was isolated in 97% yield from the reaction of Λ-(*S*,*S*)-**2**$^{3+}$ 3Cl$^-$ and KI in acetone.[57] Addition of 1.0 equiv of $Na^+$ $BAr_f^-$ afforded the mixed bis(iodide)/tetraarylborate salt Λ-(*S*,*S*)-**2**$^{3+}$ 2I$^-$$BAr_f^-$ in 99% yield after workup. This complex could also be isolated in >99% yield from the reaction of excess NaI and Λ-(*S*,*S*)-**2**$^{3+}$ 2Cl$^-$$BAr_f^-$. It possessed the advantage of being – unlike the other salts – soluble in the inexpensive deuterated solvent $CDCl_3$.

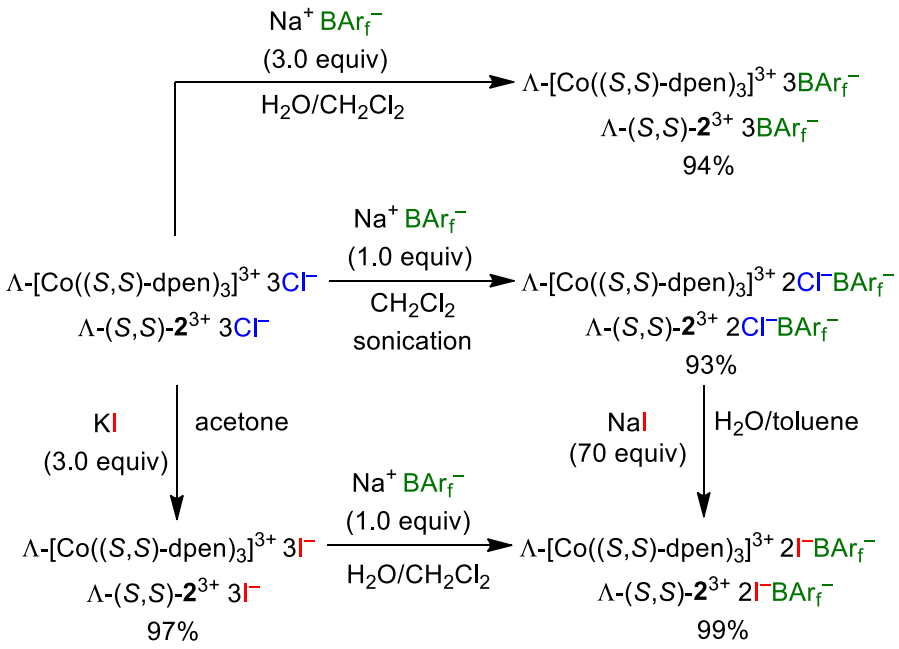


**Scheme 2.1.** Syntheses of cobalt(III) CSAs (all reactions at room temperature, 5 min to 6 h).*

### 2.2.2. Screening of cobalt(III) CSAs.

The efficacies of the preceding complexes as CSAs were screened with racemic 1-phenylethyl acetate (**4**). As presented in Table 2.1, 0.0071 M solutions of the CSAs in various solvents were combined with neat **4** (1.0 equiv). In favorable cases, the chemical

shifts of all of the aliphatic NMR signals of the enantiomers differed, as detailed in Table A-1 of appendix A. In all of these cases, the methine (PhC***H***($CH_3$)O(C=O)$CH_3$) protons were the most strongly differentiated (Δδ, Table 2.1). However, Λ-**1**$^{3+}$ 3BAr$_f^-$ (entry 1) was ineffective in all assays, including additional analytes such as 1-phenethyl amine (**5**), phenyl methyl sulfoxide (**6**), and 2-carbomethoxycyclopentanone (**7**).

**Table 2.1.** Separation of the methine proton $^1$H NMR signals (Δδ, ppm) of the enantiomers of racemic 1-phenylethyl acetate (**4**) as a function of CSA (1.0 equiv) and solvent.[a]*

| Entry | CSA | Solvent | Δδ |
|---|---|---|---|
| 1 | Λ-**1**$^{3+}$ 3BAr$_f^-$ | $CD_2Cl_2$ | —[b] |
| 2 | Λ-(*S*,*S*)-**2**$^{3+}$ 2Cl$^-$BAr$_f^-$ | $CD_2Cl_2$ | 1.32 |
| 3 | Δ-(*S*,*S*)-**2**$^{3+}$ 2Cl$^-$BAr$_f^-$ | $CD_2Cl_2$ | 0.15 |
| 4 | Λ-(*S*,*S*)-**2**$^{3+}$ 2Cl$^-$B($C_6F_5$)$_4^-$ | $CD_2Cl_2$ | 1.37 |
| 5 | Λ-(*S*,*S*)-**2**$^{3+}$ 3BAr$_f^-$ | $CD_2Cl_2$ | 0.34 |
| 6 | Λ-(*S*,*S*)-**2**$^{3+}$ 2I$^-$BAr$_f^-$ | $CD_2Cl_2$ | 1.30 |
| 7 | Λ-(*S*,*S*)-**2**$^{3+}$ 2I$^-$BAr$_f^-$ | $CDCl_3$ | 1.75 |
| 8 | Λ-(*S*,*S*)-**2**$^{3+}$ 2I$^-$BAr$_f^-$ | acetone-$d_6$ | —[b] |
| 9 | Λ-(*S*,*S*)-**2**$^{3+}$ 2I$^-$BAr$_f^-$ | $CD_3CN$ | —[b] |
| 10 | Λ-(*S*,*S*)-**2**$^{3+}$ 2I$^-$BAr$_f^-$ | DMSO-$d_6$ | —[b] |
| 11 | Λ-(*S*,*S*)-**2**$^{3+}$ 2Cl$^-$BAr$_f^-$ | acetone-$d_6$ | —[b] |
| 12 | Λ-(*S*,*S*)-**2**$^{3+}$ 2Cl$^-$BAr$_f^-$ | $CD_3CN$ | —[b] |
| 13 | Λ-(*S*,*S*)-**2**$^{3+}$ 2Cl$^-$BAr$_f^-$ | DMSO-$d_6$ | —[b] |

[a]Samples were prepared in 5 mm NMR tubes as described in the experimental section. [b]Separate signals for the enantiomers were not observed, although line widths increased from 0.6-0.9 to 1.0-2.0 Hz.

In contrast, the bis(chloride) tetraarylborate salts Λ-(*S*,*S*)-**2**$^{3+}$ 2Cl$^{-}$BAr$_f^{-}$ and Λ-(*S*,*S*)-**2**$^{3+}$ 2Cl$^{-}$B(C$_6$F$_5$)$_4^{-}$ gave widely separated methine proton signals in CD$_2$Cl$_2$ (entries 2 and 4; Δδ 1.37-1.32 ppm). The opposite diastereomer of the former, Δ-(*S*,*S*)-**2**$^{3+}$ 2Cl$^{-}$BAr$_f^{-}$, was much less effective (entry 3, Δδ 0.15 ppm). Interestingly, the corresponding tris(tetraarylborate) salt Λ-(*S*,*S*)-**2**$^{3+}$ 3BAr$_f^{-}$ was also less effective (entry 5; Δδ 0.34 ppm), despite the removal of all counter anions that can hydrogen bond to the NH groups of the trication.[43]

The bis(iodide) salt Λ-(*S*,*S*)-**2**$^{3+}$ 2I$^{-}$BAr$_f^{-}$ gave a high Δδ value (entry 6; 1.30 ppm), comparable to that of Λ-(*S*,*S*)-**2**$^{3+}$ 2Cl$^{-}$BAr$_f^{-}$. Happily, when Λ-(*S*,*S*)-**2**$^{3+}$ 2I$^{-}$BAr$_f^{-}$ was applied in the less polar and coordinating solvent CDCl$_3$, the Δδ value increased by 33% (entry 7, 1.75 ppm). Finally, when either Λ-(*S*,*S*)-**2**$^{3+}$ 2Cl$^{-}$BAr$_f^{-}$ or Λ-(*S*,*S*)-**2**$^{3+}$ 2I$^{-}$BAr$_f^{-}$ were employed in the more polar and coordinating solvents acetone-d$_6$, CD$_3$CN, or DMSO-d$_6$, the enantiomers of **4** were no longer differentiated (entries 8-13).

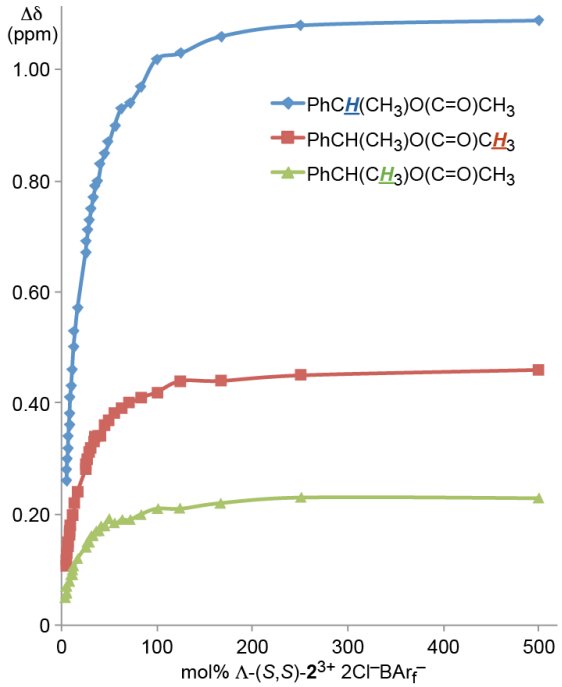


**Figure 2.3.** Dependence of the separation of the aliphatic $^1$H NMR signals of the enantiomers of **4** (Δδ, CD$_2$Cl$_2$) upon the mol% of the CSA Λ-(*S*,*S*)-**2**$^{3+}$ 2Cl$^{-}$BAr$_f^{-}$.*

It was sought to establish the minimum CSA loading needed to resolve the NMR signals of the enantiomers. Accordingly, an NMR tube was charged with a 0.036 M $CD_2Cl_2$ solution of Λ-(*S*,*S*)-**2**$^{3+}$ 2Cl$^-$BAr$_f^-$ (0.70 mL, 0.025 mmol). Then neat **4** was added in increments (0.00050 mL; ca. 0.0012 g, 0.0050 mmol). As shown in Figure 2.3, the Δδ values for all three aliphatic signals were plotted against the mol% of the CSA, which is in great excess at the start. The data spanned a range of 500 mol% down to 5 mol% (total volume of liquids: 0.7005 to 0.7500 mL, or less than a 7% concentration change). Although the Δδ values monotonically decreased, all signals maintained baseline separations.

The concentration dependence of the efficacies of the CSAs was also probed. For this purpose, an NMR tube was charged with a $CD_2Cl_2$ solution that was 0.040 M in **4** (0.020 mmol) and 0.010 M in Λ-(*S*,*S*)-**2**$^{3+}$ 2Cl$^-$BAr$_f^-$ (0.0050 mmol), or a CSA loading of 25 mol%. Then increments of $CD_2Cl_2$ were added, giving more dilute solutions. As shown in Figure 2.4, there was little change in the Δδ values over a twofold dilution. However, up to a 30% decrease could be seen at the lower concentration ranges investigated.

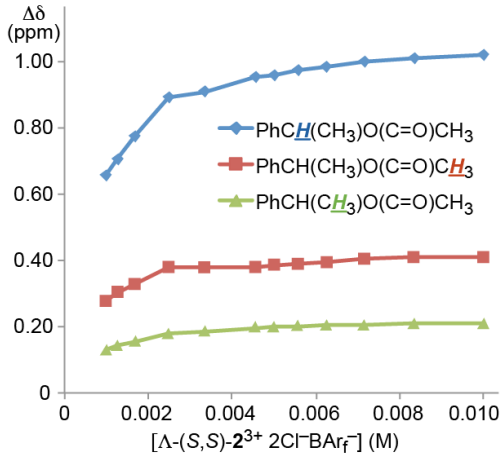


**Figure 2.4.** Dependence of the separation of the aliphatic $^1$H NMR signals of the enantiomers of **4** (Δδ, $CD_2Cl_2$) upon concentration using the CSA Λ-(*S*,*S*)-**2**$^{3+}$ 2Cl$^-$BAr$_f^-$ (constant at 25 mol%).*

### 2.2.3. Functional group scope, chirality sensing.

As summarized in Table 2.2, racemic chiral organic compounds with a variety of Lewis basic functionalities (**4**-**31**) were treated with the most effective CSAs, Λ-(*S*,*S*)-$\mathbf{2}^{3+}$ $2I^{-}BAr_f^{-}$ ($CDCl_3$ solution) and Λ-(*S*,*S*)-$\mathbf{2}^{3+}$ $2Cl^{-}BAr_f^{-}$ ($CD_2Cl_2$ solution). The former could differentiate the $^1H$ NMR signals of the enantiomers in every case, and the latter failed with only three analytes. The signals employed are denoted in red in Table 2.2. With fluorine (**15**) or phosphorus (**19**, **20**) containing analytes, $^{19}F\{^1H\}$ or $^{31}P\{^1H\}$ NMR was used instead. In cases where signals have been assigned to specific enantiomers, the samples were spiked with 0.50 equiv of an authentic sample of one of the enantiomers.

With Λ-(*S*,*S*)-$\mathbf{2}^{3+}$ $2Cl^{-}BAr_f^{-}$, the loadings required for baseline to near-baseline signal separations ranged from 1 to 100 mol%, with an average of 34 mol%. With Λ-(*S*,*S*)-$\mathbf{2}^{3+}$ $2I^{-}BAr_f^{-}$, the loading range was identical, but the average decreased to 14 mol%. When a chiral arene lacking a Lewis basic functional group, *sec*-butyl benzene ($PhCH(CH_3)CH_2CH_3$), was similarly investigated (Λ-(*S*,*S*)-$\mathbf{2}^{3+}$ $2I^{-}BAr_f^{-}$, $CDCl_3$), only a single set of (broadened) NMR signals was observed. Other analytes that gave only one set of signals included the benzylic chloride 1-phenyl-1-chloroethane, BINOL and its diacetate, and (surprisingly) the amide 5-hydroxymethyl-2-pyrrolidinone. However, the enantiomers of alkyl halides that contained additional Lewis basic functional groups, such as **29** and **30** (Table 2.2), were easily differentiated.

**Table 2.2.** Separation of key NMR signals of the enantiomers of various analytes in the presence of the CSAs Λ-(*S*,*S*)-**2**$^{3+}$ 2I$^-$BAr$_f^-$ ($CDCl_3$) or Λ-(*S*,*S*)-**2**$^{3+}$ 2Cl$^-$BAr$_f^-$ ($CD_2Cl_2$).[a]*

| Analyte / NMR signals[b] | Δδ[c] mol% | Δδ[d] mol% | Analyte / NMR signals[b] | Δδ[c] mol% | Δδ[d] mol% |
|---|---|---|---|---|---|
| 4 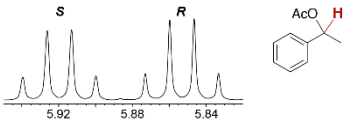 | 0.07 / 1.0 | 0.29 / 5.0 | 5 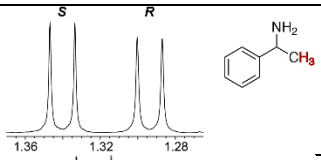 | 0.05 / 10 | 0.01 / 10 |
| 6 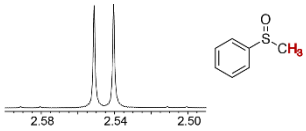 | 0.01 / 4.0 | 0.05 / 10 | 7 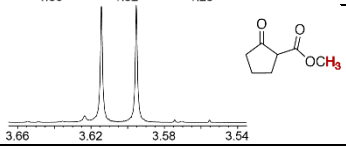 | 0.01 / 3.0 | 0.05 / 10 |
| 8 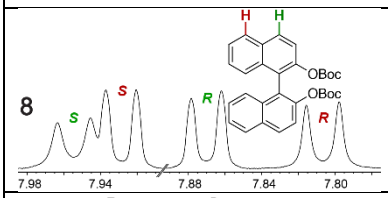 | 0.08 / 100 | 0.04 / 20 | 9 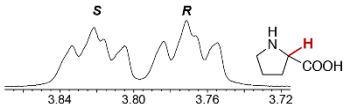 | 0.05 / 20 | 0.04 / 50 |
| 10 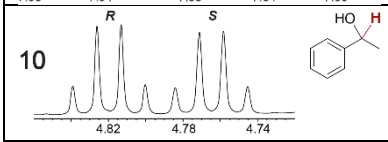 | 0.06 / 3.0 | 0.07 / 50 | 11 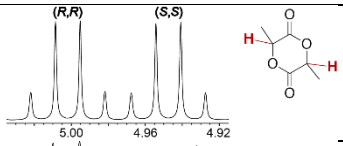 | 0.05 / 3.0 | 0.06 / 30 |
| 12 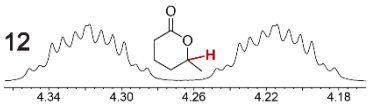 | 0.10 / 1.0 | 0.43 / 100 | 13 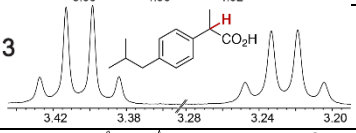 | 0.18 / 30 | 0.06 / 100 |
| 14 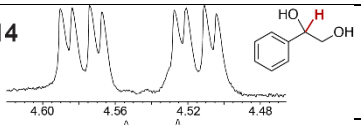 | 0.06 / 30 | 0.32 / 100 | 15 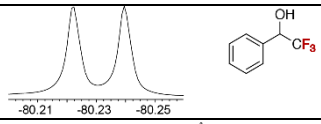 | 0.02[e] / 30 | 0.04[e] / 100 |
| 16 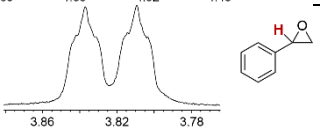 | 0.03 / 10 | 0.04 / 4.0 | 17 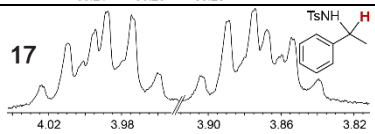 | 0.12 / 30 | 0.28 / 100 |
| 18 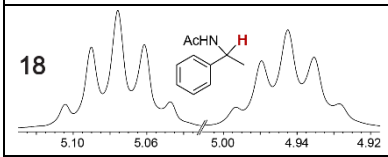 | 0.11 / 1.0 | 0.09 / 1.0 | 19 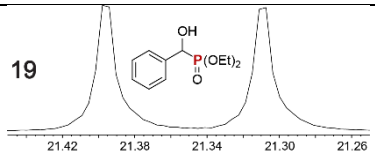 | 0.09[f] / 11 | 0.07[f] / 10 |

[a]Samples were prepared in 5 mm NMR tubes as described in the experimental section. [b]The spectra depicted ($^1$H unless noted) were obtained with Λ-(*S*,*S*)-**2**$^{3+}$ 2I$^-$BAr$_f^-$ in $CDCl_3$. [c]Signal separation (ppm)/mol% using Λ-(*S*,*S*)-**2**$^{3+}$ 2I$^-$BAr$_f^-$. [d]Signal separation (ppm)/mol% using Λ-(*S*,*S*)-**2**$^{3+}$ 2Cl$^-$BAr$_f^-$. [e] $^{19}$F{$^1$H} NMR spectra were utilized. [f] $^{31}$P{$^1$H} NMR spectra were utilized. [g]Separate signals for the enantiomers were not observed.

**Table 2.2.** Continued.[a]*

| Analyte / NMR signals[b] | Δδ[c] mol% | Δδ[d] mol% | Analyte / NMR signals[b] | Δδ[c] mol% | Δδ[d] mol% |
|---|---|---|---|---|---|
| **20** 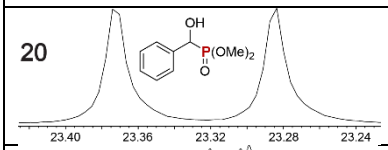 | 0.09[f] / 3.0 | 0.10[f] / 2.0 | **21** 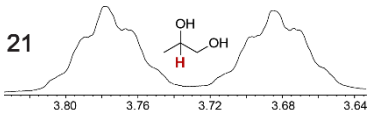 | 0.09 / 5.0 | 0.09 / 12 |
| **22** 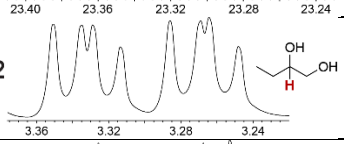 | 0.06 / 5.0 | 0.06 / 4.0 | **23** 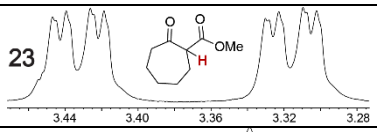 | 0.11 / 7.0 | 0.16 / 50 |
| **24** 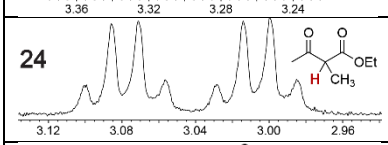 | 0.07 / 33 | —[g] | **25** 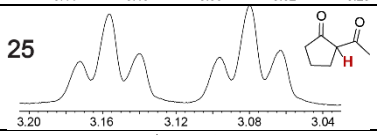 | 0.08 / 6.0 | 0.05 / 33 |
| **26** 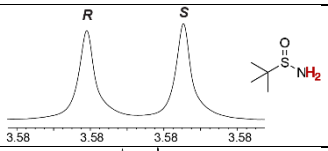 | 0.05 / 2.0 | 0.06 / 3.0 | **27** 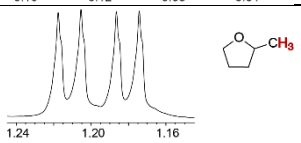 | 0.03 / 3.0 | —[g] |
| **28** 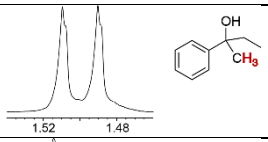 | 0.02 / 22 | —[g] | **29** 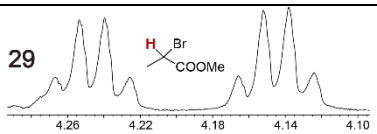 | 0.10 / 11 | 0.07 / 25 |
| **30** 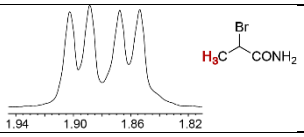 | 0.04 / 2.0 | 0.04 / 2.0 | **31** 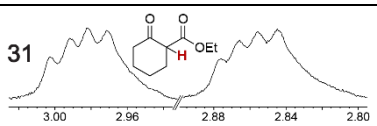 | 0.12 / 18 | 0.06 / 18 |

[a]Samples were prepared in 5 mm NMR tubes as described in the experimental section. [b]The spectra depicted ($^1$H unless noted) were obtained with Λ-(*S*,*S*)-**2**$^{3+}$ 2I$^-$BAr$_f^-$ in $CDCl_3$. [c]Signal separation (ppm)/mol% using Λ-(*S*,*S*)-**2**$^{3+}$ 2I$^-$BAr$_f^-$. [d]Signal separation (ppm)/mol% using Λ-(*S*,*S*)-**2**$^{3+}$ 2Cl$^-$BAr$_f^-$. [e] $^{19}$F{$^1$H} NMR spectra were utilized. [f]$^{31}$P{$^1$H} NMR spectra were utilized. [g]Separate signals for the enantiomers were not observed.

It was sought to verify that reliable quantitative data could be obtained from this new class of CSAs. Thus, scalemic samples of **4** were prepared and the ee values assayed using both Λ-(*S*,*S*)-**2**$^{3+}$ 2Cl$^-$BAr$_f^-$ and chiral HPLC, as described in the experimental section. As depicted in Table 2.3 and Figure 2.5, the two methods were essentially in perfect agreement.

**Table 2.3.** Tabular comparison of ee values of scalemic 4 obtained by NMR and HPLC.*

| Sample | (*R*)-**4** (mL)[a] | (*S*)-**4** (mL)[a] | Theoretical ee (%) | HPLC ee (%)[b] | NMR ee (%)[b] |
|---|---|---|---|---|---|
| 1 | 0.940 | 0.060 | +88 | +88 | +88 |
| 2 | 0.800 | 0.200 | +60 | +60 | +60 |
| 3 | 0.660 | 0.340 | +32 | +32 | +32 |
| 4 | 0.220 | 0.780 | –56 | –56 | –56 |
| 5 | 0.050 | 0.950 | –90 | –90 | –90 |

[a]Per the experimental procedure, the volumes represent the ratios of the enantiomers in the samples assayed. [b]The original traces and spectra are depicted in Figures A-1 to A-5 (appendix A).

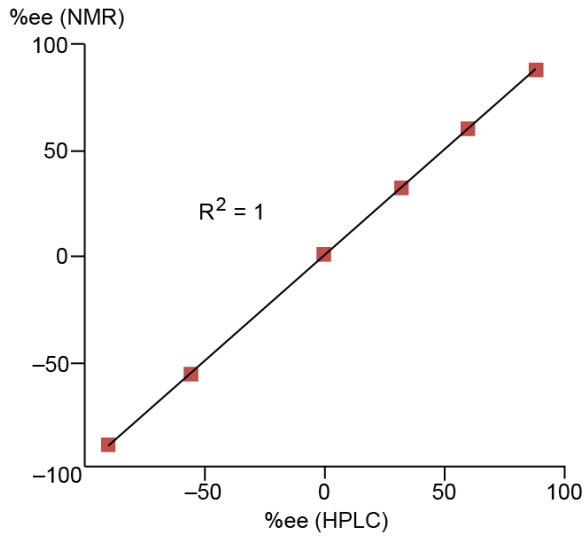


**Figure 2.5.** Graphical comparison of ee values of scalemic **4** obtained by NMR and HPLC.*

### 2.2.4. Prochirality sensing

The types of experiments in the previous section were repeated with achiral molecules using a CSA loading of 100 mol% (1.0 equiv). As summarized in Table 2.4, in many cases different signals were observed for enantiotopic groups. Enantiotopic geminal or vicinal hydrogen atoms also became coupled to each other. Achiral molecules in which enantiotopic groups were not differentiated include nitroethane, propionitrile, propionic acid, methyl isovalerate, tetrahydrofuran, and diethyl phosphite.

**Table 2.4.** Separation of $^1$H NMR signals of enantiotopic groups of various achiral analytes in the presence of 100 mol % (1.0 equiv) of the CSAs Λ-(*S*,*S*)-**2**$^{3+}$ 2I$^-$BAr$_f^-$ ($CDCl_3$) or Λ-(*S*,*S*)-**2**$^{3+}$ 2Cl$^-$BAr$_f^-$ ($CD_2Cl_2$).[a]*

| Analyte / NMR signals[b] | Δδ[c] | Δδ[d] | Analyte / NMR signals[b] | Δδ[c] | Δδ[d] |
|---|---|---|---|---|---|
| 32 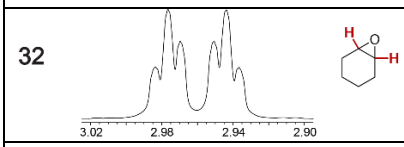 | 0.03 | 0.04 | 33 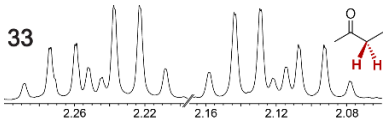 | 0.12 | 0.10 |
| 34 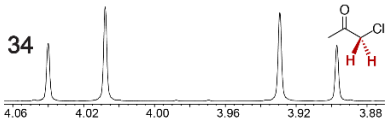 | 0.12 | 0.23 | 35 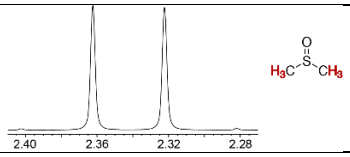 | 0.04 | 0.12 |
| 36 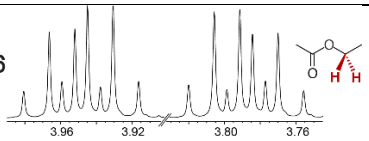 | 0.16 | 0.15 | 37 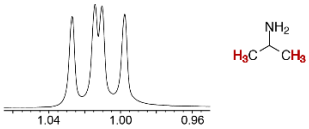 | 0.02 | 0.02 |
| 38 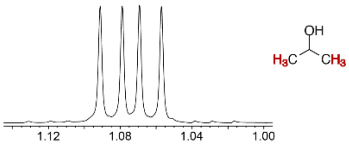 | 0.03 | 0.02 | 39 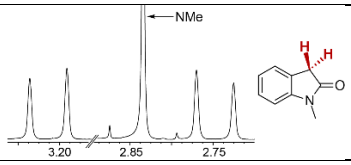 | 0.46 | 0.66 |
| 40 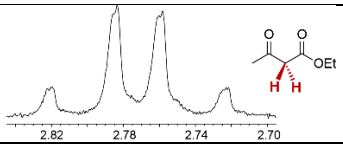 | 0.05 | 0.04 | 41 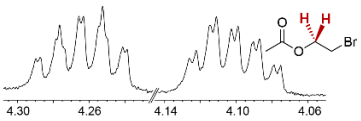 | 0.16 | 0.09 |
| 42  | 0.17 | 0.11 | 43 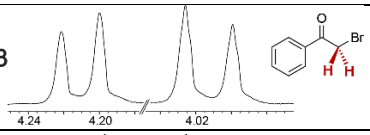 | 0.20 | 0.09 |
| 44 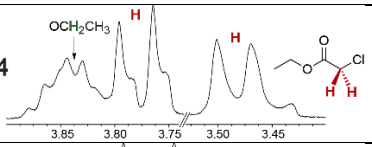 | 0.30 | 0.18 | 45 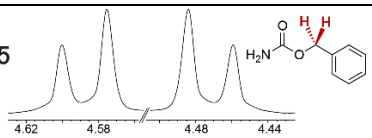 | 0.12 | 0.11 |
| 46 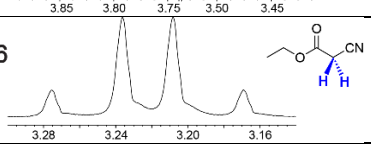 | —[e] | 0.07 | 47 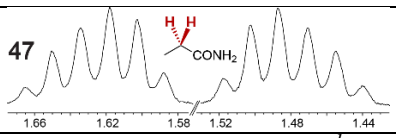 | 0.15 | 0.10 |

[a]Samples were prepared in 5 mm NMR tubes as described in the experimental section. [b]The spectra depicted were obtained with Λ-(*S*,*S*)-**2**$^{3+}$ 2I$^-$BAr$_f^-$ in $CDCl_3$. [c]Signal separation (ppm) using Λ-(*S*,*S*)-**2**$^{3+}$ 2I$^-$BAr$_f^-$. [d]Signal separation (ppm) using Λ-(*S*,*S*)-**2**$^{3+}$ 2Cl$^-$BAr$_f^-$. [e]Separate signals for the enantiomers were not observed in the presence of 100-500 mol% of Λ-(*S*,*S*)-**2**$^{3+}$ 2I$^-$BAr$_f^-$.

### 2.2.5. Enhanced throughput sensing

Higher throughput variants of the above methodology would be desirable. Thus, it was tested whether the enantiomeric purities of two or more analytes could be simultaneously determined. A $CDCl_3$ solution of racemic **4**, 2-carbomethoxycyclopentanone (**7**), 1-phenylethanol (**10**), and two hydroxyphenylmethyl dialkyl phosphonates (**19**, **20**) was prepared (2.0:2.0:2.0:1.0:2.0 mol ratio). Then Λ-**2**$^{3+}$ $2I^-BAr_f^-$ was added (100 mol% with respect to **19**; 50 mol% with respect to the other analytes; average loading per analyte 11 mol%). As shown in Figure 2.6, the enantiomers of all five analytes were differentiated by NMR.

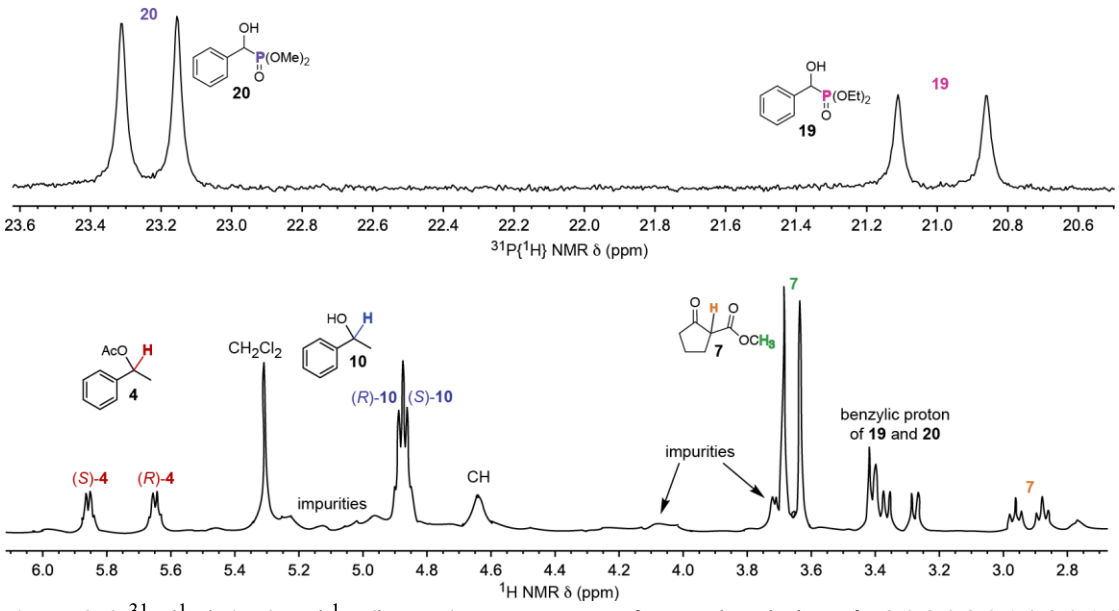


**Figure 2.6.** $^{31}P\{^1H\}$ (top) and $^1H$ (bottom) NMR spectra of a $CDCl_3$ solution of a 2.0:2.0:2.0:1.0:2.0:1.0 mixture of **4**, **7**, **10**, **19**, **20** and the CSA Λ-(*S*,*S*)-**2**$^{3+}$ $2I^-BAr_f^-$ (50 mol% vs. **4**, **7**, **10**, and **20**; 100 mol% vs. **19**).*

Such experiments are potentially complicated by overlapping signals, but this is sidestepped in Figure 2.6 by using a second nucleus, $^{31}P$, to assay the phosphonates **19** and **20**. Some practical uses of simultaneous enantiomeric purity assays would include kinetic resolutions,[58-60] for example the acetylation of **10** to **4** or vice-versa,[58-61] and

enantioselective reactions that afford two or more diastereomers. To date, the closest approximation to this capability seems to involve covalent adducts of CDAs where all analytes contain a common functional group (e.g., a primary amine, Figure 2.7).[62]

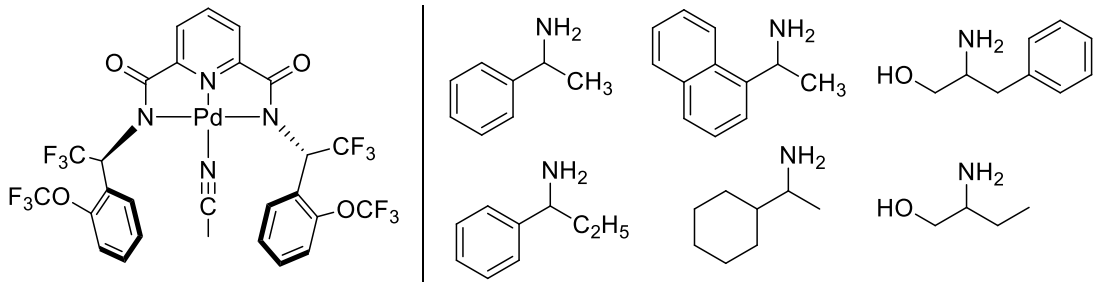


**Figure 2.7.** A palladium based chiral derivatizing agent (left) and the amine analytes for which the enantiomers can be simultaneously discriminated by $^{19}$F NMR (right).[62]

### 2.2.6. Mechanism of chirality and prochirality sensing

Some insight has been previously acquired regarding hydrogen bonding between the twelve NH protons of the trications $\mathbf{1}^{3+}$ and (*S*,*S*)-$\mathbf{2}^{3+}$ and various counter anions.[37,43,46] For example, data for Λ-(*S*,*S*)-$\mathbf{2}^{3+}$ $2Cl^{-}BAr_f^{-}$ indicate that the two chloride anions strongly bind to the two $C_3$ faces (Figure 2.2, bottom left), shifting the $^1$H NMR signals of six NH protons markedly downfield (ca. δ 8 ppm). The other six NH protons, which occupy the three $C_2$ faces (Figure 2.2, bottom right), have only the solvent or the very poorly coordinating $BAr_f^{-}$ anion to interact with. Accordingly, their $^1$H NMR signals remain upfield (ca. δ 4 ppm).[37] These trends are illustrated in the bottom spectrum in Figure 2.8, although it deserves emphasis that the signal separation is both concentration and temperature dependent.[43]

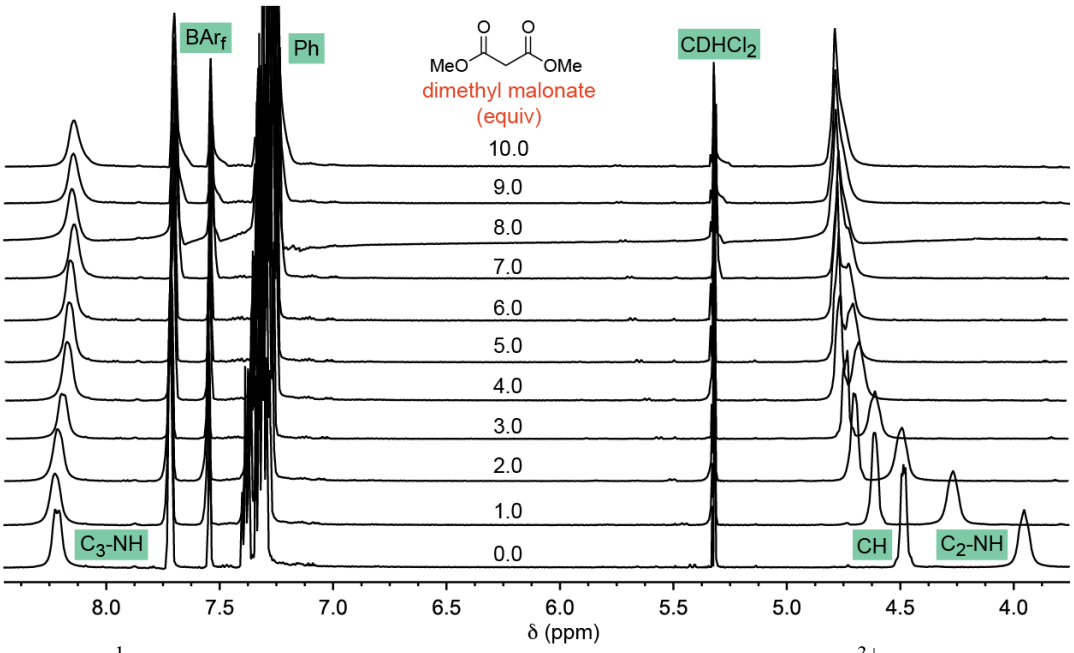


**Figure 2.8.** $^1$H NMR spectra: titration of a 0.019 M $CD_2Cl_2$ solution of Λ-(*S*,*S*)-**2**$^{3+}$ 2Cl$^-$BAr$_f^-$ (0.0076 mmol; bottom spectrum) with dimethyl malonate in 0.0080 mL (0.0073 mmol) increments (ten ascending spectra).*

As exemplified by the other spectra in Figure 2.8, $CD_2Cl_2$ solutions of Λ-(*S*,*S*)-**2**$^{3+}$ 2Cl$^-$BAr$_f^-$ have been titrated with various analytes, such as dimethyl malonate, *trans*-ß-nitrostyrene, methyl ethyl ketone, and both enantiomers of **4**. In proceeding from one to 10 equivalents, appreciable downfield shifts of the upfield $C_2$ NH signals are observed. The downfield $C_3$ NH signals are much less affected. Often there is virtually no shift, as seen with dimethyl malonate (Figure 2.8, $\Delta\delta$ = 0.07 ppm), *trans*-ß-nitrostyrene, and methyl ethyl ketone; with the enantiomers of **4**, there is a modest upfield trend (0.13-0.33 ppm). Although these shifts may reflect a combination of phenomena, it seems assured that the donor functionalities in the analytes hydrogen bond to the $C_2$ faces.

Next, Job plots[63] were constructed using $^1$H NMR data ($CD_2Cl_2$) for Λ-(*S*,*S*)-**2**$^{3+}$ 2Cl$^-$BAr$_f^-$ and the enantiopure analytes (*S*)-**4** and (*S*)-**10** as described in the experimental section. As shown in Figure 2.9, both exhibited maxima when the mol fraction of both components was 0.50, indicative of 1:1 adducts. Analogous experiments with the prochiral

analyte DMSO showed a maximum when the mol fraction of the CSA was 0.3, indicative of a ca. 2:1 DMSO/Λ-(*S*,*S*)-**2**$^{3+}$ 2Cl$^{-}$BAr$_f^{-}$ adduct.

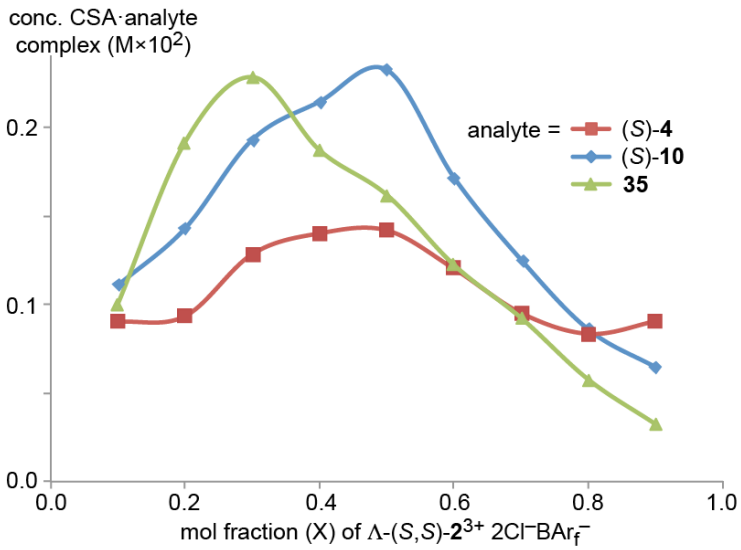


**Figure 2.9.** Job plots for mixtures of Λ-(*S*,*S*)-**2**$^{3+}$ 2Cl$^{-}$BAr$_f^{-}$ and (*S*)-1-phenylethyl acetate ((*S*)-**4**), (*S*)-1-phenylethanol ((*S*)-**10**), and DMSO (**35**) in $CD_2Cl_2$ at ambient temperature.*

In an established protocol for obtaining binding constants (*K*),[63] 0.0050 M $CD_2Cl_2$ solutions of Λ-(*S*,*S*)-**2**$^{3+}$ 2Cl$^{-}$BAr$_f^{-}$ and Λ-(*S*,*S*)-**2**$^{3+}$ 2I$^{-}$BAr$_f^{-}$ were titrated with (*S*)-**4**, (*R*)-**4**, (*S*)-**10**, and (*R*)-**10**. The concentrations of the analytes were plotted versus the change in chemical shift of the $C_2$ NH protons. The *K* values were calculated by nonlinear least-square curve fitting using the 1:1 stoichiometry established from the Job plots and standard equations and software (appendix A and Figure A-7).

As can be seen in Table 2.5, the alcohol **10** exhibited the lowest *K* values (7.60-2.73 M$^{-1}$), while those of the corresponding acetate **4** were somewhat higher (124-22.6 M$^{-1}$). Whereas (*R*)-**4** gave somewhat higher *K* values than (*S*)-**4**, (*S*)-**10** (which has the same relative configuration as (*S*)-**4**) gave higher *K* values than (*R*)-**10**. The *K* values for Λ-(*S*,*S*)-**2**$^{3+}$ 2I$^{-}$BAr$_f^{-}$ and either enantiomer of **4** were considerably higher than those with

Λ-(*S*,*S*)-**2**$^{3+}$ 2Cl$^{-}$BAr$_f^{-}$. However, they were much more comparable for the other analytes.

**Table 2.5.** Binding constants (*K*) for CSAs and representative analytes in $CD_2Cl_2$ at 23 °C.*

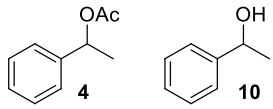


| Entry | CSA | analyte | $K$ (M$^{-1}$)$^a$ |
|---|---|---|---|
| 1 | Λ-(*S*,*S*)-**2**$^{3+}$ 2Cl$^{-}$BAr$_f^{-}$ | (*S*)-**4** | 22.6 |
| 2 | Λ-(*S*,*S*)-**2**$^{3+}$ 2Cl$^{-}$BAr$_f^{-}$ | (*R*)-**4** | 28.1 |
| 3 | Λ-(*S*,*S*)-**2**$^{3+}$ 2I$^{-}$BAr$_f^{-}$ | (*S*)-**4** | 104 |
| 4 | Λ-(*S*,*S*)-**2**$^{3+}$ 2I$^{-}$BAr$_f^{-}$ | (*R*)-**4** | 124 |
| 5 | Λ-(*S*,*S*)-**2**$^{3+}$ 2Cl$^{-}$BAr$_f^{-}$ | (*S*)-**10** | 7.60 |
| 6 | Λ-(*S*,*S*)-**2**$^{3+}$ 2Cl$^{-}$BAr$_f^{-}$ | (*R*)-**10** | 2.73 |
| 7 | Λ-(*S*,*S*)-**2**$^{3+}$ 2I$^{-}$BAr$_f^{-}$ | (*S*)-**10** | 5.60 |
| 8 | Λ-(*S*,*S*)-**2**$^{3+}$ 2I$^{-}$BAr$_f^{-}$ | (*R*)-**10** | 4.28 |

$^a$See experimental section including appendix A for details.

### 2.2.7. Crystal structure of a DMSO adduct

Efforts were made to cocrystallize salts of (*S*,*S*)-**2**$^{3+}$ with analytes from Tables 2.2 and 2.4. This proved to be much more challenging than anticipated. Finally, diethyl ether was allowed to vapor diffuse into a DMSO solution of Λ-(*S*,*S*)-**2**$^{3+}$ 3I$^{-}$. This gave yellow blocks of the hexakis(DMSO) solvate Λ-(*S*,*S*)-**2**$^{3+}$ 3I$^{-}$·6DMSO. X-ray data were acquired and the structure was solved as outlined in Table A-2 (appendix A) and the experimental section. The unit cell contained two independent molecules. Their structures were quite similar, so only one is depicted in Figure 2.10.

Although there was no crystallographic symmetry, the trication exhibited an idealized $C_3$ axis. This lies perpendicular to the plane of the paper in the left view in Figure 2.10. Furthermore, three idealized $C_2$ axes lie in the plane of the paper. The right view in Figure 2.10 is oriented so that one $C_2$ axis runs perpendicular to the plane of the paper. Since the CHPh-CHPh bonds of each chelate are parallel to the $C_3$ axis (Figure 2.10, left), the trication is said to exhibit a $lel_3$ orientation,[42] as previously found in the crystal structure of Λ-(*S*,*S*)-**2**$^{3+}$ 3Cl$^-$ (Figure 2.2, bottom).

As depicted in Figure 2.10 (left), the oxygen atoms of all six DMSO molecules make a single hydrogen bond to a different NH group associated with the three $C_2$ faces. The O···HN and O···N distances (1.975-2.290 Å (avg 2.132 Å)[64-66] and 2.869-3.006 Å (avg 2.929 Å) are close to those found in other crystallographically characterized adducts of DMSO with NH hydrogen bond donors (for five typical examples[67-71] 1.81-2.10 Å (avg 1.97 Å) and 2.65-2.85 Å (avg 2.77 Å)). For further validation, the sums of the relevant van der Waals radii can be considered (oxygen/hydrogen, 1.52 + 1.20-1.10 Å; oxygen/nitrogen, 1.52 + 1.55 Å).[72-74] The closer contacts in Λ-(*S*,*S*)-**2**$^{3+}$ 3I$^-$·6DMSO confirm bonding interactions by both classical[75] and modern[76] criteria.

As illustrated in Figure 2.11, two of the three iodide anions hydrogen bond to the three NH groups on opposite $C_3$ faces, consistent with the rationale for the downfield NH $^1$H NMR signals in Figure 2.8. The I···HN and I···N distances (2.725-2.835 Å (avg 2.767 Å)[64-66] and 3.612-3.712 Å (avg 3.648 Å)) are in typical ranges.[77] The closest contacts for the third iodide anion (see Figures A-7 and A-8) involve the hydrogen atoms of DMSO molecules (2.996-4.043 Å; avg 3.330 Å) and phenyl rings of adjacent trications (3.027-3.285 Å; avg 3.121 Å).[64-66]

Over 150 crystal structures of salts of the trication $[Co(en)_3]^{3+}$ have been determined, and the diverse types of NH/anion hydrogen bonding interactions observed

have been reviewed and classified.[46] The bonding motifs exhibited by the two proximal iodide anions in Λ-(*S*,*S*)-**2**$^{3+}$ 3I$^{-}$·6DMSO are quite common and have been given the designation [$C_3$,$C_3$,$C_3$][1]. Those for the DMSO molecules would be abbreviated [$C_2$][1].

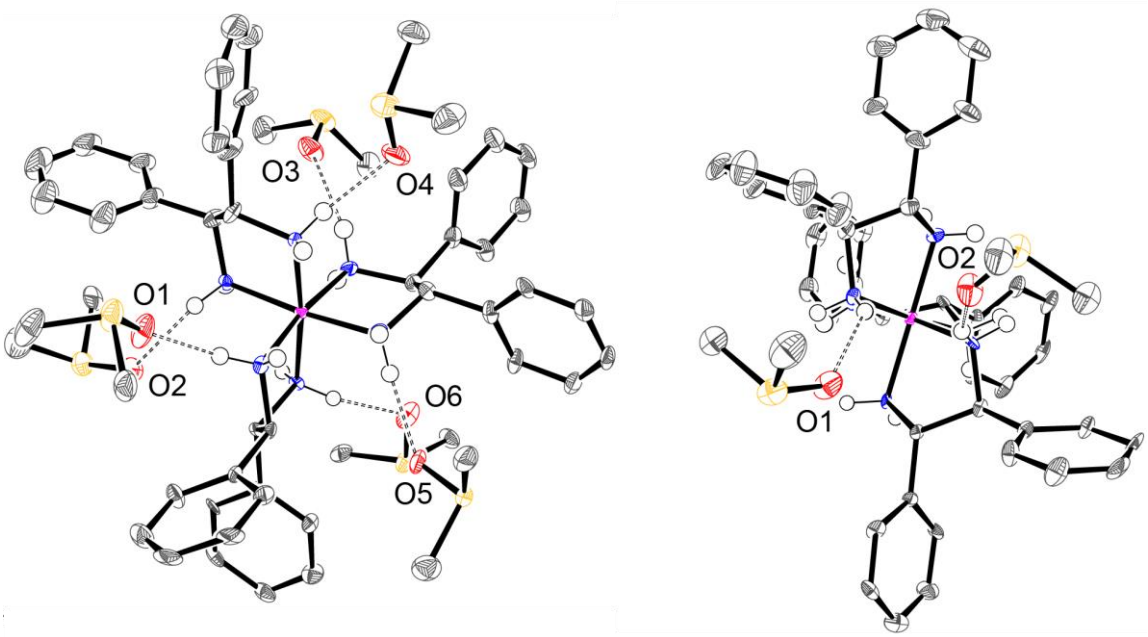


| O atom | O···HN ($C_2$) | O···N | O···H-N |
|---|---|---|---|
| O1 | 2.026<br>2.039[a] | 2.893<br>2.882 | 159.1<br>153.6 |
| O2 | 2.265<br>2.141[a] | 2.923<br>2.965 | 147.6<br>150.2 |
| O3 | 2.290<br>2.256[a] | 3.006<br>3.011 | 135.5<br>140.1 |
| O4 | 1.975<br>2.013[a] | 2.869<br>2.859 | 167.0<br>154.1 |
| O5 | 2.085<br>2.074[a] | 2.870<br>2.897 | 143.9<br>149.8 |
| O6 | 2.197<br>2.219[a] | 2.999<br>2.969 | 146.7<br>139.2 |

[a]The second set of values is for the other independent molecule in the unit cell, which is geometrically similar.

**Figure 2.10.** Thermal ellipsoid diagram (50% probability level) of the trication of Λ-(*S*,*S*)-**2**$^{3+}$ 3I$^{-}$ ·6DMSO viewed along the idealized $C_3$ axis (left) with all six DMSO molecules, and along one of three idealized $C_2$ axes (right) with two DMSO molecules.*

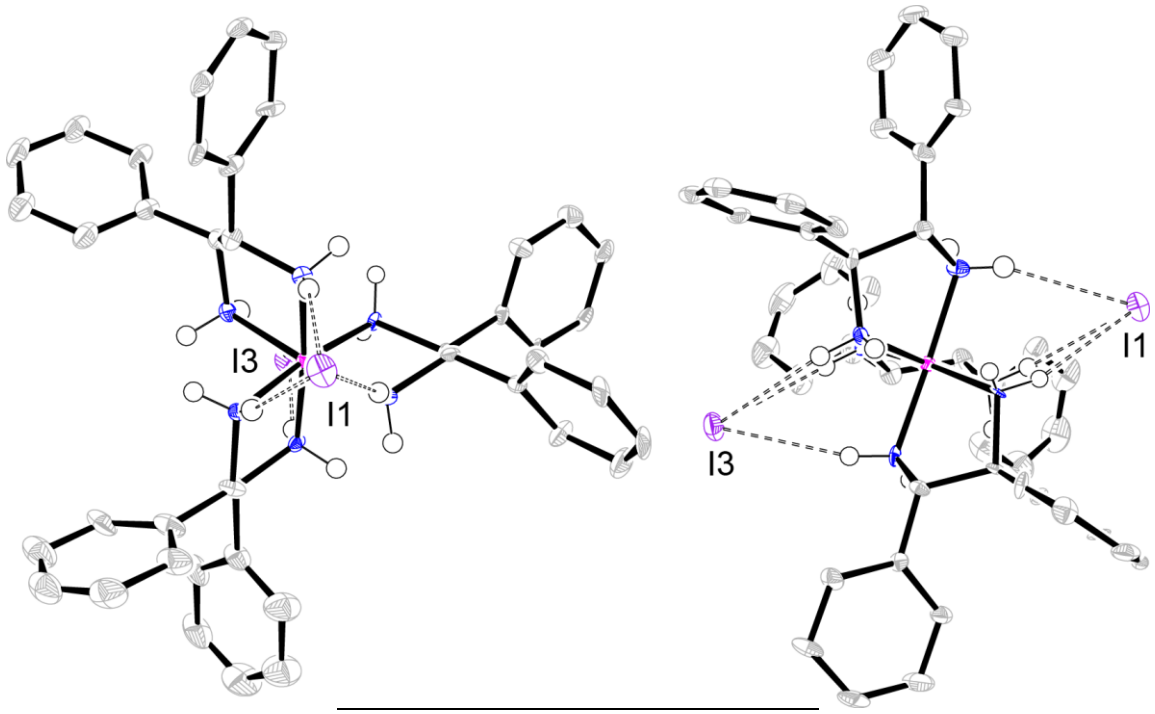


| iodide | I···HN ($C_3$) | I···N | I···H-N |
|---|---|---|---|
| I1 | 2.826<br>2.799[a] | 3.712<br>3.675 | 164.7<br>166.6 |
| I1 | 2.794<br>2.820[a] | 3.681<br>3.700 | 165.2<br>163.0 |
| I1 | 2.771<br>2.693[a] | 3.664<br>3.585 | 167.3<br>166.6 |
| I3 | 2.835<br>2.783[a] | 3.687<br>3.652 | 156.4<br>160.5 |
| I3 | 2.725<br>2.609[a] | 3.612<br>3.506 | 165.5<br>168.6 |
| I3 | 2.760<br>2.798[a] | 3.633<br>3.672 | 161.3<br>161.5 |

[a]The second set of values is for the other independent molecule in the unit cell, which is geometrically similar.

**Figure 2.11** Thermal ellipsoid diagrams (50% probability level) showing interactions of two iodide anions with the trication of Λ-(*S*,*S*)-**2**$^{3+}$ 3I$^{-}$·6DMSO (*lel*$_3$) viewed along the idealized $C_3$ axis (left) and one idealized $C_2$ axis (right). The other independent molecule is similar.*

## 2.3. Discussion

### 2.3.1. New CSAs vs. literature systems

The preceding data document an impressive efficacy of Λ-(*S*,*S*)-**2**$^{3+}$ 2Cl$^{-}$BAr$_f^{-}$ and Λ-(*S*,*S*)-**2**$^{3+}$ 2I$^{-}$BAr$_f^{-}$ as CSAs. The former has the advantage of being commercially available, whereas the latter (easily synthesized from the former) exhibits superior performance characteristics apparently connected to its solubility in $CDCl_3$. The data for Λ-(*S*,*S*)-**2**$^{3+}$ 2Cl$^{-}$B($C_6F_5$)$_4^{-}$ in Table 2.1 suggest that salts with related tetraarylborate anions may be comparably effective. The mechanism of action (following section) clearly involves hydrogen bonding between the $C_2$ NH donor groups of the CSAs and the analytes.

Most of the other CSAs described in the literature also feature hydrogen bond donor groups,[17,19-21,23-30] although many possess acceptor groups as well.[17,20,21,23,29] Typical donor groups include ureas or chalcogenoureas,[25,26,30] squaramides,[27] secondary amines,[24] amides of primary amines,[17,23,29] sulfonamides,[19] and BINOL derivatives.[20] However, many of these have only been applied to one or two functional groups.

The most broadly applicable CSAs for chirality sensing reported to date have been developed by Ema, Sakai, and coworkers.[17] Their lead system, **48** (Figure 2.12, top), was applied to ten functional groups, three of which were not assayed with Λ-(*S*,*S*)-**2**$^{3+}$ 2X$^{-}$ BAr$_f^{-}$ (oxazolidinone, sulfoximine, isocyanate). Their typical loadings were 100-200 mol%, although a chiral sulfoxide was found to require only 5 mol%. Conversely, Tables 2.2 and 2.3 contain several functional groups that they did not study (ester/ß-ketoester, amine, amide/sulfonamide, hydroxyphosphonate, ketone/ 1,3-diketone, ether). Furthermore, with my lead CSA, Λ-(*S*,*S*)-**2**$^{3+}$ 2I$^{-}$BAr$_f^{-}$, the average loading is 14% (range 1-100%).

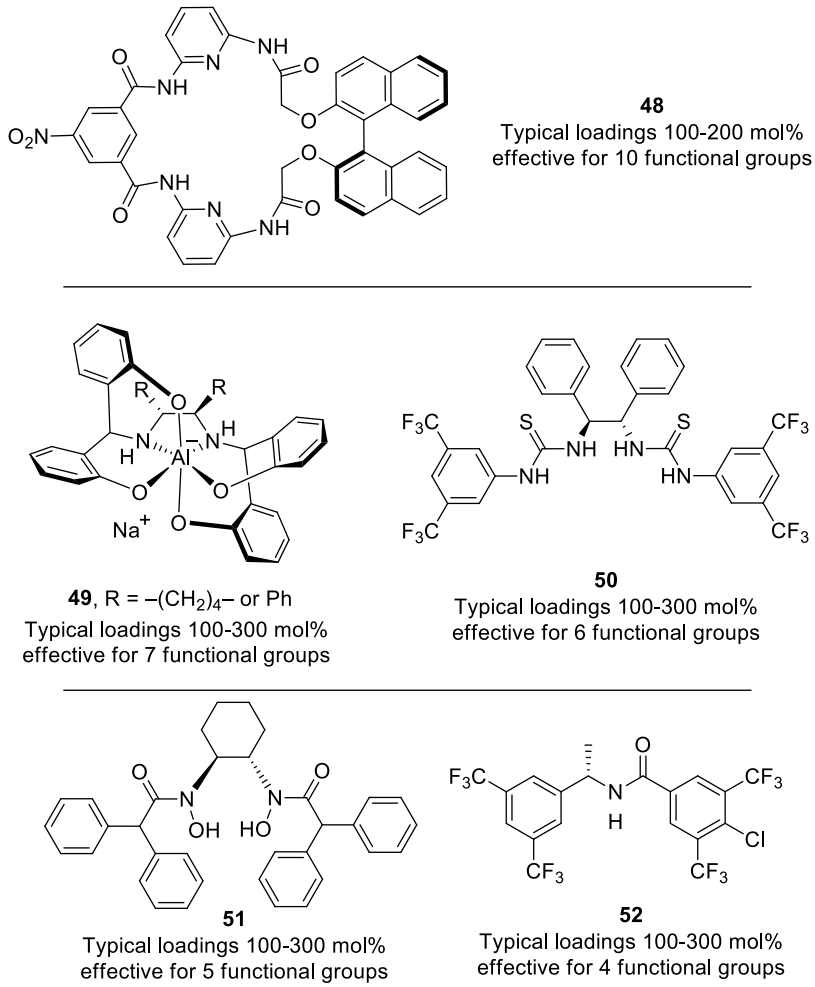


**Figure 2.12.** Some relevant previously reported CSAs.

There is a wider selection of CSAs that have been applied to four-seven functional groups (Figure 2.12, middle and bottom, **49**-**52**).[21,22,25,29] These generally require loadings of 100-300 mol%, although with one analyte the CSA **49** (Figure 2.12, middle) was shown to be effective at 60 mol%. None of these CSAs are commercially available. However, another group has assembled a library of 32 commercial CSAs, and developed high throughput protocols for identifying optimal partners for specific analytes.[78] Far fewer CSAs have been applied to prochirality sensing, and the eight functional groups represented in Table 2.4 exceed the sum of all those in the literature I have been able to locate.[49-55]

To my knowledge, the above salts of Λ-(*S*,*S*)-**2**$^{3+}$ represent the first CSAs that are based upon transition metals. However, transition metals are well represented among chiral derivatizing agents (CDAs).[62,79,80] The ionic CSA **49**[22] in Figure 2.12 is based upon a main group metal, aluminum, and displays several conceptual similarities with my cobalt(III) systems. First, both metals are octahedral and constitute stereocenters. Second, the anion of **49** has $C_2$ symmetry, versus $D_3$ symmetry for the trication **2**$^{3+}$. Third, **49** has two Al-NH groups that can serve as hydrogen bond donors (as well as four Al-O groups that can serve as hydrogen bond acceptors).

### 2.3.2. Analyte binding to Λ-(*S*,*S*)-2$^{3+}$

There is a variety of evidence that the enthalpy of hydrogen bonding to a $C_3$ face of Λ-(*S*,*S*)-**2**$^{3+}$ (**A**, Figure 2.2) is much greater than that to a $C_2$ face (**B**, Figure 2.2). For example, the solid state structures of the diastereomeric trichloride salts Λ- and Δ-(*S*,*S*)-**2**$^{3+}$ 3Cl$^-$ show the three chloride ions to be distributed over two $C_3$ faces and one $C_2$ face (as opposed to, for example, three $C_2$ faces).[37] Scheme 2.1 shows that one chloride ion – presumably that associated with the $C_2$ face – can more easily be replaced by the very poor hydrogen bond acceptor BAr$_f^-$ than the other two.[37,43] As illustrated by the bottom trace in Figure 2.8, the $^1$H NMR spectra of mixed salts Λ-(*S*,*S*)-**2**$^{3+}$ 2X$^-$BAr$_f^-$ always show two NH signals of equal area (6H/6H), with the downfield signal moving upfield as X$^-$ becomes a poorer hydrogen bond acceptor (e.g., BF$_4^-$, PF$_6^-$).[37,43] These observations are consistent with two "occupied" $C_3$ faces and three "free" $C_2$ faces.

When Λ-(*S*,*S*)-**2**$^{3+}$ 2Cl$^-$BAr$_f^-$ is titrated with suitable substrates, such as dimethyl malonate in Figure 2.8, the upfield NH groups shift markedly downfield, but the downfield NH groups are much less affected.[37,43] This indicates dominant analyte binding at the $C_2$ faces. In accord with the Job plots (Figure 2.9), I presume that the binding constants for the first one ((*S*)-**4**, (*S*)-**10**) or two (**35**) analyte molecules are much greater than those for

additional molecules. This may seem at odds with the crystal structure in Figure 2.10, in which the three $C_2$ faces engage in hydrogen bonding with six DMSO molecules (one per NH group). However, interactions that may be very weak in solution are often expressed in the solid state. Also, such six-fold binding gives a more symmetrical species that may be better disposed towards crystallization.

The binding constants ($K$) in Table 2.5 track the order found for the hydrogen bond donor *p*-fluorophenol and the analytes ethyl acetate and benzyl alcohol ($CCl_4$, 25 °C; 11.7 and 7.24 $M^{-1}$).[81] Those for the acetate **4** (22-124 $M^{-1}$) are in the range of values measured for other CSAs and cyclic esters,[17,19] and those for the benzylic alcohol **10** (2.7-7.6 $M^{-1}$) likewise compare well with values obtained with other benzylic alcohols.[26]

The loss of efficacy of Λ-(*S*,*S*)-$\mathbf{2}^{3+}$ $2Cl^-BAr_f^-$ and Λ-(*S*,*S*)-$\mathbf{2}^{3+}$ $2I^-BAr_f^-$ in coordinating solvents (entries 8-13, Table 2.1) presumably reflects the saturation of the $C_2$ faces, obstructing access by the analytes. The halide free salt Λ-(*S*,*S*)-$\mathbf{2}^{3+}$ $3BAr_f^-$, with three very poorly hydrogen bond accepting anions, gives much lower Δδ values (entry 5, Table 2.1). I speculate that the analyte now preferentially binds to an "unoccupied" $C_3$ face, which for some reason gives diminished chiral recognition. Naturally, the cocrystallization of additional analytes with all of the preceding cobalt(III) complexes remains a goal. Crystal structures have been reported for analyte adducts of only a few other CSAs.[22,24] Alternatively, insight can be gained by computational studies,[22,23,26-28] and a series of DFT investigations are currently underway.

**2.4. Conclusion**

The new cobalt based CSAs described in chapter 2 offer unparalleled functional group applicability, effectiveness at significantly lower loadings and in the presence of multiple analytes, extended stability to air and water, and ready availability from inexpensive building blocks. Their success reflects the generality of second coordination

sphere hydrogen bonding between the NH donor groups and Lewis basic functional groups in the analytes. Given the many "best in class" characteristics, and recent commercial availability, they appear primed for wide adoption. In the interval since this work was published, I have also aided in the preparation and investigation of an additional CSA Λ-(*S*,*S*)-**2**$^{3+}$ 2I$^{-}$B($C_6F_5$)$_4^{-}$. In several cases, the data for Λ-(*S*,*S*)-**2**$^{3+}$ 2I$^{-}$B($C_6F_5$)$_4^{-}$ are better than those in Table 2.2. This finding will be communicated in a future date.

**2.5. Experimental**

**General.** The CSAs Λ-(*S*,*S*)-**2**$^{3+}$ 2Cl$^{-}$BAr$_f^{-}$, Λ-(*S*,*S*)-**2**$^{3+}$ 2Cl$^{-}$B($C_6F_5$)$_4^{-}$, Λ-(*S*,*S*)-**2**$^{3+}$ 3BAr$_f^{-}$, and Δ-(*S*,*S*)-**2**$^{3+}$ 2Cl$^{-}$BAr$_f^{-}$ were synthesized as reported earlier,[43] and Λ-**1**$^{3+}$ 3BAr$_f^{-}$ was prepared as described for the enantiomer;[36] Λ-(*S*,*S*)-**2**$^{3+}$ 2Cl$^{-}$BAr$_f^{-}$ is also commercially available.[48] All abbreviations are defined in the introduction. All reactions and workups were conducted in air.

**Λ-(*S*,*S*)-2$^{3+}$ 3I$^{-}$.** A round bottom flask was charged with a suspension of Λ-(*S*,*S*)-**2**$^{3+}$ 3Cl$^{-}$·3$H_2O$ (0.170 g, 0.199 mmol) in acetone (20 mL) and KI (0.099 g, 0.597 mmol) was added with vigorous stirring. A suspension of white particles in an orange solution formed. After 1 h, the mixture was filtered. The solvent was removed from the filtrate by rotary evaporation and oil pump vacuum (20 h, rt) to give Λ-(*S*,*S*)-**2**$^{3+}$ 3I$^{-}$·3$H_2O$ (0.219 g, 0.194 mmol, 97%) as an orange solid, mp 200-202 °C dec (open capillary). Anal. Calcd. for $C_{42}H_{48}CoI_3N_6$·3$H_2O$ (1130.07): C 44.62, H 4.81, N 7.43; found C 44.81, H 4.91, N 7.02.

NMR ($CD_3OD$/acetone-$d_6$, δ in ppm): $^1$H (500 MHz) 7.51-7.49 (m, 12H, *o*-Ph), 7.38-7.37 (m, 18H, *m*-, *p*-Ph), 6.75 (br s, 6H, N**H**H'), 5.95 (br s, 6H, NH**H'**), 5.26 (s, 6H, C**H**Ph), 2.83 (br s, 7H, **H**$_2$O); $^{13}$C{$^1$H} (125 MHz) 136.4 (s, *i*-Ph), 130.1 (s, *p*-Ph), 129.9 and 129.7 (2 s, *o*- and *m*-Ph), 62.8 (s, **C**HPh). IR (powder film, cm$^{-1}$): 3032 (m, $\nu_{NH}$), 1683 (m, $\delta_{NH}$), 1041 (vs, $\delta_{CCN}$).

**Alternative syntheses of Λ-(*S*,*S*)-$\mathbf{2}^{3+}$ 3I⁻** (directly from cobalt(II) precursors. (bypassing Λ-(*S*,*S*)-$\mathbf{2}^{3+}$ 3Cl⁻ in Scheme 2.1). **A.** A gas circulating flask[43] was charged with a solution of $CoI_2$ (0.156 g, 0.50 mmol) in $CH_3OH$ (50 mL). Activated charcoal (0.05 g) and (*S*,*S*)-dpen (0.356 g, 1.68 mmol, 3.36 equiv) were added with vigorous stirring. Air was passed through the suspension. After 17 h, the mixture was filtered through Celite and aqueous HI (0.377 g, 57 wt%, 1.68 mmol) was added. The solvent was removed by rotary evaporation to give an orange solid. A portion was dissolved in acetone-$d_6$. The diastereomers exhibit diagnostic **C**HPh $^{13}C$ NMR chemical shift trends.[43] $^{13}C\{^1H\}$ NMR (acetone-$d_6$, δ in ppm, partial): 62.2 and 64.7 (2s, ca. 2:1, **C**HPh for Λ and Δ-(*S*,*S*)-$\mathbf{2}^{3+}$ 3I⁻ ).The solid was dissolved in 95:5 v/v $CH_2Cl_2/CH_3OH$ (1 mL). The solution was loaded on a silica gel column (2 × 15 cm) packed in $CH_2Cl_2$, which was eluted with $CH_2Cl_2/CH_3OH$ (100:0 v/v, 200 mL; 98:2 v/v, 500 mL; 97:3 v/v as needed). The orange band was collected. Solvents were removed by rotary evaporation. The residue was dried by oil pump vacuum at room temperature (20 h) to give Λ-(*S*,*S*)-$\mathbf{2}^{3+}$ 3I⁻·$H_2O$ (0.208 g, 0.190 mmol, 38%) as an orange solid. **B**. A solution of $Co(OAc)_2 \cdot 4H_2O$ (0.296 g, 1.19 mmol) in $CH_3OH$ (50 mL), activated charcoal (0.1 g), (*S*,*S*)-dpen (0.849 g, 4.00 mmol, 3.36 equiv), air, Celite, and aqueous HI (0.898 g, 57 wt%, 4.00 mmol) were combined in a procedure analogous to that in A. A similar workup (3 mL 95:5 v/v $CH_2Cl_2/CH_3OH$) gave Λ-(*S*,*S*)-$\mathbf{2}^{3+}$ 3I⁻·$H_2O$ (0.611 g, 0.559 mmol, 47%) as an orange solid, mp 200-201 °C dec (open capillary). Anal. Calcd. for $C_{42}H_{48}CoI_3N_6 \cdot H_2O$ (1094.05): C 46.09, H 4.60, N 7.68; found C 46.16, H 4.75, N 7.46.

NMR (acetone-$d_6$, δ in ppm): $^1H$ (500 MHz) 7.57-7.54 (m, 12H, *o*-Ph), 7.53 (br s, 6H, N**H**H', partial overlap with *o*-Ph), 7.32-7.22 (m, 18H, *m*-, *p*-Ph), 5.63 (br s, 6H, NH**H'**), 5.25 (s, 6H, C**H**Ph), 2.83 (br s, 7H, $\mathbf{H_2}O$); $^{13}C\{^1H\}$ (125 MHz) 130.3 (s, *i*-Ph), 130.0 (s, *p*-Ph), 129.6 and 128.8 (2 s, *o*- and *m*-Ph), 63.2 (s, **C**HPh).

**Λ-(*S*,*S*)-2$^{3+}$ 2I$^{-}$BAr$_f^{-}$. A.** A round bottom flask was charged with Λ-(*S*,*S*)-**2**$^{3+}$ 3I$^{-}$ ·3H$_2$O (0.117 g, 0.104 mmol), CH$_2$Cl$_2$ (20 mL), H$_2$O (20 mL), and Na$^{+}$ BAr$_f^{-}$ (0.092 g, 0.104 mmol). The mixture was vigorously stirred until the orange color had entirely transferred to the CH$_2$Cl$_2$ layer (30 min), which was separated. The solvent was removed by passive evaporation (fume hood) and oil pump vacuum (20 h, rt) to give Λ-(*S*,*S*)-**2**$^{3+}$ 2I$^{-}$BAr$_f^{-}$·0.5H$_2$O (0.188 g, 0.103 mmol, 99%) as a red solid, mp 107-110 °C dec (black liquid, open capillary). Anal. Calcd. for C$_{74}$H$_{60}$BCoF$_{24}$I$_2$N$_6$·0.5H$_2$O (1821.20): C 48.79, H 3.37, N 4.61; found C 48.88, H 3.61, N 4.62. **B.** A round bottom flask was charged with aqueous NaI (15.0 mL, 10 wt%, 10.5 mmol), toluene (15.0 mL), and Λ-(*S*,*S*)-**2**$^{3+}$ 2Cl$^{-}$ BAr$_f^{-}$·2H$_2$O (0.259 g, 0.152 mmol). The mixture was vigorously stirred, and after 6 h transferred to a separatory funnel. The clear aqueous layer was discarded, and the red toluene layer was washed with water (2 × 10 mL). The solvent was removed from the toluene layer by rotary evaporation. The residue was dissolved in CH$_3$OH (10 mL) and the solution was stirred for 20 min.[82] The solvent was removed again by rotary evaporation and oil pump vacuum (10 h, rt) to give Λ-(*S*,*S*)-**2**$^{3+}$ 2I$^{-}$BAr$_f^{-}$·0.5 H$_2$O (0.277 g, 0.152 mmol, >99%) as a red solid, mp 108-110 °C dec (black liquid, open capillary). Anal. Calcd., see above; found C 49.17, H 3.50, N 4.46.

Data for Λ-(*S*,*S*)-**2**$^{3+}$ 2I$^{-}$BAr$_f^{-}$·0.5H$_2$O: NMR (δ in ppm): $^1$H (500 MHz, CDCl$_3$ or CD$_2$Cl$_2$) BAr$_f^{-}$ at 7.69 or 7.71 (s, 8H, *o*), 7.49 or 7.55 (s, 4H, *p*); (*S*,*S*)-dpen at 7.37-7.27 or 7.29-7.44 (m, 30H, Ar**H**), 6.98 or 7.88 (br s, 6H, N**H**H'), 4.86 or 4.21 (br s, 6H, NH**H'**), 4.60 (s, 6H, C**H**Ph); 2.22 or 1.78 (br s, 5H or 2H, **H**$_2$O).[83] $^{13}$C{$^1$H} (126 MHz, CD$_2$Cl$_2$) BAr$_f^{-}$ at 162.3 (q, $^1J_{BC}$ = 49.8 Hz, *i*), 135.4 (s, *o*), 129.4 (q, $^2J_{CF}$ = 31.5 Hz, *m*), 125.2 (q, $^1J_{CF}$ = 272.3 Hz, CF$_3$), 118.1 (s, *p*); (*S*,*S*)-dpen ligand at 134.6 (s, *i*-Ph), 130.8 (s, *p*-Ph), 130.3 (s, *o*-Ph), 128.7 (s, *m*-Ph), 62.7 (s, **C**HPh). IR (powder film, cm$^{-1}$): 3064 (m, $\nu_{NH}$), 1608 (m, $\delta_{NH}$), 1354 (s, $\nu_{Ar\text{-}CF_3}$), 1275 (vs, $\nu_{CF}$), 1117 (vs, $\delta_{CCN}$).

**Dependence of Δδ upon CSA and solvent (Table 2.1).** A 5 mm NMR tube was charged with a 0.0071 M solution of a CSA (0.70 mL, 0.0049 mmol) in the indicated solvent. Neat 1-phenylethyl acetate (**4**; 0.00050 mL, 0.0012 g, 0.0050 mmol) was added and a $^1$H NMR spectrum was recorded.

**Dependence of Δδ upon mol% of CSA (Figure 2.3).** A 5 mm NMR tube was charged with a $CD_2Cl_2$ solution of Λ-(*S*,*S*)-**2**$^{3+}$ 2Cl$^-$BAr$_f^-$·2H$_2$O (0.70 mL, 0.036 M, 0.025 mmol). Neat **4** was then added in 0.00050 mL increments (ca. 0.0012 g, 0.0050 mmol). A $^1$H NMR spectrum was acquired after each addition. The total volume of **4** added from the first data point (500 mol%) to the final data point (5 mol%) was 0.050 mL).

**Dependence of Δδ upon concentration (Figure 2.4).** A 5 mm NMR tube was charged with a $CD_2Cl_2$ solution (0.50 mL) that was 0.040 M in **4** (0.020 mmol) and 0.010 M in Λ-(*S*,*S*)-**2**$^{3+}$ 2Cl$^-$BAr$_f^-$·2H$_2$O (0.0050 mmol, 25 mol%). A $^1$H NMR spectrum was recorded. Then $CD_2Cl_2$ was added in increments so as to attain total volumes of 0.60, 0.70, 0.80, 0.90, 1.00, 1.10, 1.50, 2.00, 3.00, 4.00, and 5.00 mL. After each addition, a $^1$H NMR spectrum was recorded.

**Chirality sensing (Table 2.2). A** (liquid analytes **4-7**, **10, 14-18**, **21-25**, **27-29**, **31**). 5 mm NMR tubes were charged with $CD_2Cl_2$ solutions of Λ-(*S*,*S*)-**2**$^{3+}$ 2Cl$^-$BAr$_f^-$·2H$_2$O or $CDCl_3$ solutions of Λ-(*S*,*S*)-**2**$^{3+}$ 2I$^-$BAr$_f^-$·0.5H$_2$O (0.70 mL, 0.0071 M, 0.0049 mmol). The samples were titrated with neat liquid analytes in increments of 0.0050 mmol (1.0 equiv) and monitored by $^1$H NMR. Experiments were halted when separate signals for the enantiomers were no longer observed. The total volume of liquids added usually ranged from 0.72 to 0.80 mL. **B** (solid analytes **8**, **9**, **11-13**, **19-20**, **26**, **30**). Procedure A was repeated, but with the analytes added as 10.0 M $CD_2Cl_2$ or $CDCl_3$ solutions in increments of 0.00050 mL (0.0050 mmol).

**Comparison of ee values obtained by NMR and HPLC (Table 2.3 and Figure 2.5).** Standard solutions of (*R*)- and (*S*)-**4** were prepared in hexanes/isopropanol (99:1 v/v, 0.0010 g/mL). These were mixed at different ratios into five separate volumetric flasks so that the total volume was always 1.00 mL (Table 2.3). Each was assayed by HPLC (Chiralcel OD-H column, hexane/isopropanol 99:1 v/v, 0.5 mL/min, 254 nm). The HPLC samples were concentrated by rotary evaporation, redissolved in $CD_2Cl_2$ (0.70 mL), and transferred to 5 mm NMR tubes. Then Λ-(*S*,*S*)-$\mathbf{2}^{3+}$ $2Cl^-BAr_f^-\cdot 2H_2O$ (0.0085 g, 0.0050 mmol) was added and $^1$H NMR spectra were recorded.

**Enhanced throughput sensing (Figure 2.6).** A 5 mm NMR tube was charged with a $CDCl_3$ solution (0.70 mL) that was 0.029 M in **4**, **7**, **10**, and **20** (0.020 mmol each), and 0.014 M in **19** (0.010 mmol). Then Λ-(*S*,*S*)-$\mathbf{2}^{3+}$ $2I^-BAr_f^-\cdot 0.5H_2O$ (0.018 g, 0.010 mmol) was added, and $^1$H and $^{31}P\{^1H\}$ NMR spectra were recorded.

**Prochirality sensing (Table 2.4).** A 5 mm NMR tube was charged with a $CD_2Cl_2$ solution of Λ-(*S*,*S*)-$\mathbf{2}^{3+}$ $2Cl^-BAr_f^-\cdot 2H_2O$ or a $CDCl_3$ solution of Λ-(*S*,*S*)-$\mathbf{2}^{3+}$ $2I^-BAr_f^-\cdot 0.5H_2O$ (0.70 mL, 0.0071 M, 0.0049 mmol). The analyte (1.0 equiv) was added as a neat liquid (**32**-**38**, **40**-**42**, **44**, **46**) or solid (**39**, **43**, **45**, **47**) and $^1$H NMR spectra were recorded.

**Titration of a CSA with dimethyl malonate (Figure 2.8).** A 5 mm NMR tube was charged with a 0.019 M $CD_2Cl_2$ solution (0.40 mL) of Λ-(*S*,*S*)-$\mathbf{2}^{3+}$ $2Cl^-BAr_f^-\cdot 2H_2O$ (0.0076 mmol). A reference $^1$H NMR spectrum were recorded. A 0.91 M $CD_2Cl_2$ solution of dimethyl malonates was added in 0.0080 mL increments (0.0073 mmol). A $^1$H NMR spectrum was recorded after each addition.

**Job plots (Figure 2.9).**[63] 0.010 M $CD_2Cl_2$ solutions of Λ-(*S*,*S*)-$\mathbf{2}^{3+}$ $2Cl^-BAr_f^-\cdot 2H_2O$ and (*S*)-**4** were prepared and mixed at nine volume ratios (mL/mL: 0.050/0.45, 0.10/0.40, 0.15/0.35, 0.20/ 0.30, 0.25/0.25, 0.30/0.20, 0.35/0.15, 0.40/0.10, 0.45/0.050).

$^1$H NMR spectra were recorded (500 MHz) and the concentration of the adduct CSA·(*S*)-**4** calculated from the equation[84,85]

$$[\text{CSA}\cdot(S)\text{-}\mathbf{4}] = [(\delta_{obs} - \delta_0)/(\delta_c - \delta_0)] \times [\text{CSA}]$$

where [CSA] is the concentration of Λ-(*S*,*S*)-$\mathbf{2}^{3+}$ 2Cl$^-$BAr$_f^-$ in the sample, $\delta_{obs}$ is the chemical shift of the $C_2$ NH protons in the sample (always upfield from the $C_3$ NH protons),[43] $\delta_0$ is the chemical shift of the $C_2$ NH protons of Λ-(*S*,*S*)-$\mathbf{2}^{3+}$ 2Cl$^-$BAr$_f^-$ in otherwise identical samples that lack (*S*)-**4**, and $\delta_c$ is the chemical shift of the $C_2$ NH protons in the complex CSA·(*S*)-**4**. The values for [CSA·(*S*)-**4**] were then plotted versus the mol fraction (X) of Λ-(*S*,*S*)-$\mathbf{2}^{3+}$ 2Cl$^-$BAr$_f^-$ per Figure 2.8. This procedure was repeated with 0.010 M $CD_2Cl_2$ solutions of Λ-(*S*,*S*)-$\mathbf{2}^{3+}$ 2Cl$^-$BAr$_f^-$ and (*S*)-**10** or **35**.

**Binding constants (Table 2.5).**[63] 0.0050 M $CD_2Cl_2$ solutions of Λ-(*S*,*S*)-$\mathbf{2}^{3+}$ 2Cl$^-$BAr$_f^-$·2$H_2O$ and Λ-(*S*,*S*)-$\mathbf{2}^{3+}$ 2I$^-$BAr$_f^-$·0.5$H_2O$ were prepared. One 5 mm NMR tube was charged with 1.0 mL of one solution, and another tube with 1.0 mL of the other. Reference $^1$H NMR spectra were recorded. Analytes were then added in 0.0050 mmol increments (1.0 equiv) using a microsyringe, and a $^1$H NMR spectrum was recorded after each addition. The concentrations of the analytes were plotted versus the change in chemical shift of the $C_2$ NH protons ($\Delta\delta = \delta_{obs} - \delta_0$) as in Figure A-7. The binding constants *K* were calculated by nonlinear least-square curve fitting using Origin Pro 8.0,[86] the 1:1 stoichiometry established from the Job plots, and the equation[87]

$$[\text{Analyte}] = (1/K) \times [x/(1 - x)]$$

where $x = (\delta_{obs} - \delta_0)/(\delta_c - \delta_0)$.

**Crystallography.** A solution of Λ-(*S*,*S*)-$\mathbf{2}^{3+}$ 3I$^-$·3$H_2O$ (0.011 g, 0.010 mmol) in DMSO (0.50 mL) in an open vial was placed inside a 20 mL closed vial containing diethyl ether (7.0 mL). After 4 d, yellow blocks were collected. Data were obtained as outlined in Table A-3. Cell parameters were determined from 45 data frames using a 1° scan.

Integrated intensity information for each reflection was obtained by reduction of the data frames with the program APEX3.[88] Data were corrected for Lorentz, polarization, and crystal decay effects. SADABS[89] was employed for absorption corrections, and the structure was solved using XT/XS in APEX3.[88,90-93] The unit cell contained two independent molecules of Λ-(*S*,*S*)-**2**$^{3+}$ 3I$^{-}$, each associated with six molecules of DMSO. Hydrogen atoms were placed in idealized positions and refined using a riding model. All non-hydrogen atoms were refined with anisotropic thermal parameters. Five of the DMSO molecules were disordered over two positions (occupancy ratios: C1S/3A, C1R/4A, O2/2A, S2/2A, 72:28; C1T/6A, C1U/5A, O3/3A, S3/3A, 79:21; C1V/8A, C1W/7A, O4/4A, S4/4A, 78:22; C1X/10A, C1Y/9A, O5/5A, S5/5A, 72:28; C2C/2E, C1AA/2CA, O12/12A, S12/12A, 52:48). Restraints were applied to keep the metrical parameters meaningful. The data were refined by weighted least squares refinement on $F^2$ to convergence.[90-94] PLATON (ADDSYM)[95] was used to verify the absence of additional symmetry and voids. Flack's parameter (Table A-3) confirmed the absolute stereochemistry.[96]

## 2.6. References

(1) Schreier, P.; Bernreuther, A.; Huffer, M. *Analysis of Chiral Organic Molecules: Methodology and Applications*; Walter de Gruyter & Co.: Berlin, Germany, 1995.

(2) Lyle, G. G.; Lyle, R. E. Polarimetry. In *Asymmetric Synthesis*; Morrison, J. D., Ed.; Academic Press, Inc.: New York, NY, 1983; Vol. 1, pp 13-27.

(3) Schurig, V. Gas Chromatographic Methods. In *Asymmetric Synthesis*; Morrison, J. D., Ed.; Academic Press, Inc.: New York, NY, 1983; Vol. 1, pp 59-60.

(4) Leung, D.; Kang, S. O.; Anslyn, E. V. Rapid determination of enantiomeric excess: a focus on optical approaches. *Chem. Soc. Rev.* **2012**, *41*, 448-479, and references 4 and 6-10 therein.

(5) Jo, H. H.; Lin, C.-Y.; Anslyn, E. V. Rapid Optical Methods for Enantiomeric Excess Analysis: From Enantioselective Indicator Displacement Assays to Exciton-Coupled Circular Dichroism. *Acc. Chem. Res.* **2014**, *47*, 2212-2221 and reference 12 therein.

(6) Schurig, V. Separation of enantiomers by gas chromatography. *J. Chromatogr. A* **2001**, *906*, 275-299.

(7) Okamoto, Y.; Ikai, T. Chiral HPLC for efficient resolution of enantiomers. *Chem. Soc. Rev.* **2008**, *37*, 2593-2608.

(8) Wenzel, T. J. *Discrimination of Chiral Compounds Using NMR Spectroscopy*; John Wiley & Sons: Hoboken, NJ, 2007.

(9) Wenzel, T. J. Chiral Derivatizing Agents, Macrocycles, Metal Complexes, and Liquid Crystals for Enantiomer Differentiation in NMR Spectroscopy. In *Differentiation of Enantiomers II*; Schurig, V., Ed.; Top. Curr. Chem., Vol 341; Springer-Verlag: Berlin, Germany, 2013; pp 1-68.

(10) Wenzel, T. J.; Chisholm, C. D. Assignment of Absolute Configuration Using Chiral Reagents and NMR Spectroscopy. *Chirality* **2011**, *23*, 190-214.

(11) Wenzel, T. J.; Chisholm, C. D. Using NMR spectroscopic methods to determine enantiomeric purity and assign absolute stereochemistry. *Prog. Nucl. Magn. Reson. Spectrosc.* **2011**, *59*, 1-63.

(12) Silva, M. S. Recent Advances in Multinuclear NMR Spectroscopy for Chiral Recognition of Organic Compounds. *Molecules* **2017**, *22*, 247.

(13) Uccello-Barretta, G.; Balzano, F. Chiral NMR Solvating Additives for Differentiation of Enantiomers. In *Differentiation of Enantiomers II*; Schurig, V., Ed.; Top. Curr. Chem., Vol 341; Springer-Verlag: Berlin, Germany, 2013; pp 69-132.

(14) Raban, M.; Mislow, K. The Determination of Optical Purity by Nuclear Magnetic Resonance Spectroscopy. *Tetrahedron Lett.* **1965**, *6*, 4249-4253.

(15) Dale, J. A.; Dull, D. L.; Mosher, H. S. α-Methoxy-α-trifluoromethylphenylacetic Acid, a Versatile Reagent for the Determination of Enantiomeric Composition of Alcohols and Amines. *J. Org. Chem.* **1969**, *34*, 2543-2549.

(16) Aizawa, S.-I.; Okano, M.; Kidani, T. Enantiomeric NMR signal separation behavior and mechanism of samarium(III) and neodymium(III) complexes with (*S*,*S*)-ethylenediamine-*N*,*N'*-disuccinate. *Chirality* **2017**, *29*, 273-281 and references 1-29 therein.

(17) Ema, T.; Tanida, D.; Sakai, T. Versatile and Practical Macrocyclic Reagent with Multiple Hydrogen-Bonding Sites for Chiral Discrimination in NMR. *J. Am. Chem. Soc.* **2007**, *129*, 10591-10596.

(18) Representative papers that have appeared since 2014 and describe new CSAs are given in references 19-30. For a complete bibliography for this period, see the additional references s14-s29 (appendix A).

(19) Couffin, A.; Boullay, O. T. d.; Vedrenne, M.; Navarro, C.; Martin-Vaca, B.; Bourissou, D. Enantiodifferentiation of O-heterocycles using a binol-derived disulfonimide as a chiral solvating agent. *Chem. Commun.* **2014**, *50*, 5997-6000.

(20) Pal, I.; Chaudhari, S. R.; Suryaprakash, N. A versatile ternary ionic complex for chiral discrimination of molecules with diverse functionalities using $^{1}$H NMR. *New J. Chem.* **2014**, *38*, 4908-4912.

(21) Lakshmipriya, A.; Chaudhari, S. R.; Suryaprakash, N. Enantiodifferentiation of molecules with diverse functionalities using a single probe. *Chem. Commun.* **2015**, *51*, 13492-13495.

(22) Seo, M.-S.; Kim, H. $^{1}$H NMR Chiral Analysis of Charged Molecules via Ion Pairing with Aluminum Complexes. *J. Am. Chem. Soc.* **2015**, *137*, 14190-14195.

(23) Huang, H.; Bian, G.; Zong, H.; Wang, Y.; Yang, S.; Yue, H.; Song, L.; Fan, H. Chiral Sensor for Enantiodiscrimination of Varied Acids. *Org. Lett.* **2016**, *18*, 2524-2527.

(24) Gupta, R.; Gonnade, R. G.; Bedekar, A. V. Application of Roof-Shape Amines as Chiral Solvating Agents for Discrimination of Optically Active Acids by NMR Spectroscopy: Study of Match−Mismatch Effect and Crystal Structure of the Diastereomeric Salts. *J. Org. Chem.* **2016**, *81*, 7384-7392.

(25) Bian, G.; Yang, S.; Huang, H.; Zong, H.; Song, L. A bisthiourea-based $^{1}$H NMR chiral sensor for chiral discrimination of a variety of chiral compounds. *Sens. Actuators B Chem.* **2016**, *231*, 129-134.

(26) Bian, G.; Yang, S.; Huang, H.; Zong, H.; Song, L.; Fan, H.; Sun, X. Chirality sensing of tertiary alcohols by a novel strong hydrogen-bonding donor – selenourea. *Chem. Sci.* **2016**, *7*, 932-938.

(27) Li, Y.; Yang, G.-H.; He, C. Q.; Li, X.; Houk, K. N.; Cheng, J.-P. Chirality

Sensing of α-Hydroxyphosphonates by *N-tert*-Butyl Sulfinyl Squaramide. *Org. Lett.* **2017**, *19*, 4191-4194.

(28) Lv, C.; Feng, L.; Zhao, Hongmei; Wang, G.; Stavropoulos, P.; Ai, L. Chiral discrimination of α-hydroxy acids and *N*-Ts-α-amino acids induced by tetraaza macrocyclic chiral solvating agents by using $^{1}$H NMR spectroscopy. *Org. Biomol. Chem.* **2017**, *15*, 1642-1650.

(29) Jain, N.; Khanvilkar, A. N.; Sahoo, S.; Bedekar, A. Modification of Kagan's amide for improved activity as Chiral Solvating Agent in enantiodiscrimination during NMR analysis. *Tetrahedron* **2018**, *74*, 68-76.

(30) Ito, S.; Okuno, M.; Asami, M. Differentiation of enantiomeric anions by NMR spectroscopy with chiral bisurea receptors. *Org. Biomol. Chem.* **2018**, *16*, 213-222.

(31) Werner, A. Zur Kenntnis des asymmetrischen Kobaltatoms. V. *Chem. Ber.* **1912**, *45*, 121-130.

(32) Werner, A. Zur Kenntnis des asymmetrischen Kobaltatoms. IV. *Chem. Ber.* **1911**, *44*, 3279-3284.

(33) Werner, A. Zur Kenntnis des asymmetrischen Kobaltatoms. III. *Chem. Ber.* **1911**, *44*, 3272-3278.

(34) Werner, A. Zur Kenntnis des asymmetrischen Kobaltatoms. II. *Chem. Ber.* **1911**, *44*, 2445-2455.

(35) Werner, A. Zur Kenntnis des asymmetrischen Kobaltatoms. I. *Chem. Ber.* **1911**, *44*, 1887-1898. King, V. L. is listed as an author for the experimental section.

(36) Ganzmann, C.; Gladysz, J. A. Phase Transfer of Enantiopure Werner Cations into Organic Solvents: An Overlooked Family of Chiral Hydrogen Bond Donors for Enantioselective Catalysis. *Chem. Eur. J.* **2008**, *14*, 5397-5400.

(37) Lewis, K. G.; Ghosh, S. K.; Bhuvanesh, N.; Gladysz, J. A. Cobalt(III) Werner

Complexes with 1,2-Diphenylethylenediamine Ligands: Readily Available, Inexpensive, and Modular Chiral Hydrogen Bond Donor Catalysts for Enantioselective Organic Synthesis. *ACS Cent. Sci.* **2015**, *1*, 50-56.

(38) Kumar, A.; Ghosh, S. K.; Gladysz, J. A. Tris(1,2-diphenylethylenediamine)cobalt(III) Complexes: Chiral Hydrogen Bond Donor Catalysts for Enantioselective *α*-Aminations of 1,3-Dicarbonyl Compounds. *Org. Lett.* **2016**, *18*, 760-763.

(39) Joshi, H.; Ghosh, S. K.; Gladysz, J. A. Enantioselective Additions of Stabilized Carbanions to Imines Generated from α-Amido Sulfones By Using Lipophilic Salts of Chiral Tris(1,2-diphenylethylenediamine) Cobalt(III) Trications as Hydrogen Bond Donor Catalysts. *Synthesis* **2017**, *49*, 3905-3915.

(40) Luu, Q. H.; Gladysz, J. A. An Air and Water Stable Hydrogen Bond Donor Catalyst for the Enantioselective Generation of Quaternary Carbon Stereocenters by Additions of Substituted Cyanoacetate Esters to Acetylenic Esters. *Chem. Eur. J.* **2020**, *26*, accepted. DOI:10.1002/chem.202001639.

(41) Ghosh, S. K.; Ganzmann, C.; Bhuvanesh, N.; Gladysz, J. A. Werner Complexes with ω-Dimethylaminoalkyl Substituted Ethylenediamine Ligands: Bifunctional Hydrogen-Bond-Donor Catalysts for Highly Enantioselective Michael Additions. *Angew. Chem., Int. Ed.* **2013**, *55*, 4356-4360; Werner-Komplexe mit ω-Dimethylaminoalkyl-substitutierten Ethylendiaminliganden: bifunktionale H-Brückendonor-Katalysatoren für hoch enantioselektive Michael-Additionen. *Angew. Chem.* **2016**, *128*, 4429-4433.

(42) Review of stereoisomerism in salts of the trication $[Co(en)_3]^{3+}$, and homologs with substituted 1,2-diamine ligands: Ehnbom, A.; Ghosh, S. K.; Lewis, K. G.; Gladysz, J. A. Octahedral Werner complexes with substituted ethylenediamine ligands: a

stereochemical primer for a historic series of compounds now emerging as a modern family of catalysts. *Chem. Soc. Rev.* **2016**, *45*, 6799-6811.

(43) Ghosh, S. K.; Lewis, K. G.; Kumar, A.; Gladysz, J. A. Syntheses of Families of Enantiopure and Diastereopure Cobalt Catalysts Derived from Trications of the Formula $[Co(NH_2CHArCHArNH_2)_3]^{3+}$. *Inorg. Chem.* **2017**, 56, 2304-2320.

(44) Ghosh, S. K.; Ganzmann, C.; Gladysz, J. A. Synthesis of a series of ω-dimethylaminoalkyl substituted ethylenediamine ligands for use in enantioselective catalysis. *Tetrahedron: Asymmetry* **2015**, *26*, 1273-1280.

(45) The best prices in effect as of the submission date of this manuscript are from Oakwood Chemical (http://www.oakwoodchemical.com) (*R*,*R*-dpen; $359/100 g) and Ark Pharm (http://www.arkpharminc.com) (*S*,*S*-dpen; $420/100 g). Accessed May 2, 2020.

(46) Ghosh, S. K.; Ehnbom, A.; Lewis, K. G.; Gladysz, J. A. Hydrogen bonding motifs in structurally characterized salts of the tris (ethylenediamine) cobalt trication, $[Co(en)_3]^{3+}$; An interpretive review, including implications for catalysis. *Coord. Chem. Rev.* **2017**, *350*, 30-48.

(47) Miyabe, H.; Takemoto, Y. Discovery and Application of Asymmetric Reaction by Multi-Functional Thioureas. *Bull. Chem. Soc. Jpn.* **2008**, *81*, 785-795.

(48) https://secure.strem.com/catalog/v/27-4010/16/cobalt_1542135-29-4 (accessed May 2, 2020).

(49) For a brief review of the differentiation of enantiotopic (prochiral) groups by NMR, see pp 339-341 of reference 8. For prochirality sensing using CSAs, see references 50-55. For prochirality sensing using CLSAs and CDAs, see references s28 and s29 (appendix A). For prochirality sensing using chiral liquid crystals and other chiral media see references 56 and s30-s33 (appendix A).

(50) Harger, M. J. P. The Proton Magnetic Resonance Spectra of Chiral Phosphinate Esters. Chemical Shift Non-equivalence of Enantiomers induced by Optically Active Phosphinothioic Acids. *J. Chem. Soc., Perkin Trans. 2* **1980**, 1505-1511.

(51) Anet, F. A. L.; Park, J. Proton Chemical Shift Assignments in Citrate and Trimethyl Citrate in Chiral Media. *J. Am. Chem. Soc.* **1992**, *114*, 411-416.

(52) Reetz, M. T.; Rudolph, J.; Mynott, R. Enantiotopic Group Recognition: Direct Evidence for Selective Complexation of Enantiotopic Groups by a Chiral Host. *J. Am. Chem. Soc.* **1996**, *118*, 4494-4495.

(53) Bilz, A.; Stork, T.; Helmchen, G. New chiral solvating agents for carboxylic acids: discrimination of enantiotopic nuclei and binding properties. *Tetrahedron: Asymmetry* **1997**, *8*, 3999-4002.

(54) Kobayashi, Y.; Hayashi, N.; Kishi, Y. Toward the Creation of NMR Databases in Chiral Solvents: Bidentate Chiral NMR Solvents for Assignment of the Absolute Configuration of Acyclic Secondary Alcohols. *Org. Lett.* **2002**, *4*, 411-414.

(55) Seri, N.; Simaan, S.; Botoshansky, M.; Kaftory, M.; Biali, S. A Conformationally Flexible Tetrahydroxycalix[4]arene Adopting the Unusual 1,3-Alternate Conformation. *J. Org. Chem.* **2003**, *68*, 7140-7142.

(56) Lesot, P.; Aroulanda, C.; Zimmermann, H.; Luz, Z. Enantiotopic discrimination in the NMR spectrum of prochiral solutes in chiral liquid crystals. *Chem. Soc. Rev.* **2015**, *44*, 2330-2375.

(57) All cobalt(III) complexes are isolated as hydrates, consistent with the appreciable hydrogen bond donor strengths of the NH groups. To aid readability, these are not specified in the formulae in the main text or graphics, but are given in the experimental section. The additional mass is taken into account in the stoichiometries and yield calculations. For additional related remarks, see reference 23 in reference 43.

(58) Keith, J. M.; Larrow, J. F.; Jacobsen, E. N. Practical Synthesis of a Soluble Schiff Base Catalyst for the Asymmetric Strecker Reaction. *Adv. Synth. Catal.*, 2001, **343**, 5-26.

(59) Vedejs, E.; Jure, M. Efficiency in Nonenzymatic Kinetic Resolution. *Angew. Chem., Int. Ed.*, 2005, **44**, 3974-4001.Effizienz in der nichtenzymatischen kinetischen Racematspaltung. *Angew. Chem.*, 2005, **117**, 4040-4069.

(60) Pellissier, H. Catalytic Non-Enzymatic Kinetic Resolution. *Adv. Synth. Catal.*, 2011, **353**, 1613-1666.

(61) Müller, C. E.; Schreiner, P. R. Organocatalytic Enantioselective Acyl Transfer onto Racemic as well as *meso* Alcohols, Amines, and Thiols. *Angew. Chem., Int. Ed.*, 2011, **50**, 6012-6042. Organokatalytischer, enantioselektiver Acyltransfer auf racemische sowie *meso*-Alkohole, -Amine und -Thiole. *Angew. Chem.*, 2011, **123**, 6136-6167.

(62) Zhao, Y.; Swager, T. M. Simultaneous Chirality Sensing of Multiple Amines by $^{19}$F NMR. *J. Am. Chem. Soc.* **2015**, *137*, 3221-3224.

(63) Connors, K. A. Binding Constants. *Binding Constants: the Measurement of Molecular Complex Stability*; John Wiley & Son: New York, NY, 1987; pp 21-101.

(64) The C-H and N-H bond lengths determined from X-ray crystal structures are usually ca. 10% too short. See, *inter alia*, references 59 and 60.

(65) Allen, F. H. A Systematic Pairwise Comparison of Geometric Parameters Obtained by X-ray and Neutron Diffraction. *Acta Cryst.* **1986**, *B42*, 515-522.

(66) Dittrich, B.; Lübben, J.; Mebs, S.; Wagner, A.; Luger, P.; Flaig, R. Accurate Bond Lengths to Hydrogen Atoms from Single-Crystal X-ray Diffraction by Including Estimated Hydrogen ADPs and Comparison to Neutron And QM/MM Benchmarks. *Chem. Eur. J.* **2017**, *23*, 4605-4614.

(67) Mizuguchi, J. Structures of Complexes of 2,3,3a,5,6,6a-Hexahydro-3,6-diphenyl-1*H*, 4*H*-pyrrolo-[3,4-*c*]pyrrole-1,4-dithione with *N*-Methyl-2-pyrrolidone and Dimethyl Sulfoxide. *Acta Cryst.* **1992**, *C48*, 1279-1283.

(68) Nagel, N.; Näther, C; Bock, H. *N*,*N'*-Ditosyl-*p*-phenylenediamine Bis(dimethyl sulfoxide), $C_{20}H_{20}N_2O_4S_2 \cdot 2C_2H_6OS$. *Acta Cryst.* **1995**, *C51*, 1935-1937.

(69) Wijaya, K.; Moers, O.; Blaschette, A.; Jones, P. G. Polysulfonylamines. CVI. 1,4,7,10,13,16-Hexaoxacyclooctadecane-Dimethyl Sulfoxide-Bis(4-fluorophenylsulfonyl)amine (1/2/2). *Acta Cryst.* **1998**, *C54*, 1707-1710.

(70) Gilardi, R. D.; Butcher, R. J. 2,6-Diamino-3,5-dinitro-1,4-pyrazine dimethyl sulfoxide solvate. *Acta Cryst.* **2001**, *E57*, o757-o759.

(71) Bond, A. D. A 1:2 complex of pyromellitic diimide and dimethyl sulfoxide. *Acta Cryst.* **2002**, *E58*, o194-o195.

(72) Bondi, A. van der Waals Volumes and Radii. *J. Phys. Chem*. **1964**, *68*, 441-451.

(73) Mantina, M.; Chamberlin, A. C.; Valero, R.; Cramer, C. J.; Truhlar, D. G. Consistent van der Waals Radii for the Whole Main Group. *J. Phys. Chem. A* **2009**, *113*, 5806-5812.

(74) Rowland, R. S.; Taylor, R. Intermolecular Nonbonded Contact Distances in Organic Crystal Structures: Comparison with Distances Expected from van der Waals Radii. *J. Phys. Chem.* **1996**, *100*, 7384-7391.

(75) Hamilton, W. C.; Ibers, J. A. *Hydrogen bonding in solids: methods of molecular structure determination*; W. A. Benjamin: New York, 1968, pp 14-16.

(76) Steiner, T. The Hydrogen Bond in the Solid State. *Angew. Chem., Int. Ed.* **2002**, *41*, 48-76. Die Wasserstoffbrücke im Festkörper. *Angew. Chem.* **2002**, *114*, 50-80. See reference 21 therein for a critique of classical van der Waals criteria.

(77) Steiner, T. Hydrogen-Bond Distances to Halide Ions in Organic and Organometallic Crystal Structures: Up-to-date Database Study. *Acta Cryst.* **1998**, *B54*, 456-463.

(78) Yang, L.; Wenzel, T.; Williamson, R. T.; Christensen, M.; Schafer, W.; Welch, C. J. Expedited Selection of NMR Chiral Solvating Agents for Determination of Enantiopurity. *ACS Cent. Sci.* **2016**, *2*, 332-340.

(79) See pp 365-398 of reference 8.

(80) Storch, G.; Siebert, M.; Rominger, F.; Trapp, O. 5,5'-Diamino-BIPHEP ligands bearing small selector units for non-covalent binding of chiral analytes in solution. *Chem. Commun.* **2015**, *51*, 15665-15668.

(81) Laurence, C.; Gal, J.-F. Thermodynamic and Spectroscopic Scales of Hydrogen-Bond Basicity and Affinity. In *Lewis Basicity and Affinity Scales: Data and Measurement*; John Wiley & Sons: Chichester, UK, 2010; pp 142, 147, and 151.

(82) When the $CH_3OH$ treatment was omitted, the toluene solvate Λ-(*S*,*S*)-**2**$^{3+}$ $2I^-$ $BAr_f^-$·$0.8C_7H_8$ was isolated, mp 110-112 °C dec (black liquid, open capillary). Anal. Calcd. for $C_{74}H_{60}BCoF_{24}I_2N_6$·$0.8C_7H_8$ (1885.85): C 50.68, H 3.55, N 4.45; found C 50.09, H 3.63, N 4.38. $^1$H NMR (500 MHz, $CD_2Cl_2$, δ in ppm) $BAr_f^-$ at 7.71 (s, 8H, *o*), 7.54 (s, 4H, *p*); (*S*,*S*)-dpen at 7.29-7.45 (m, 30H, Ar**H**), 5.31 (br s, 6H, N**H**H'; partial overlap with $CDHCl_2$), 4.88 (br s, 6H, NH**H'**), 4.69 (s, 6H, C**H**Ph); 2.01 (br s, 18H, $\mathbf{H}_2O$);[83] toluene at 7.15-7.23 (m, 4H, $C_6\mathbf{H}_5CH_3$), 2.33 (s, 2.4H, $C_6H_5C\mathbf{H}_3$).

(83) The increased level of water over that derived from the microanalysis is believed to originate from the solvent.

(84) See pp 24-28 of reference 63.

(85) Thordarson, P. Determining association constants from titration experiments in supramolecular chemistry. *Chem. Soc. Rev.* **2011**, *40*, 1305-1323.

(86) http://www.originlab.com/

(87) See pp 189-194 of reference 57.

(88) APEX3 “Program for Data Collection on Area Detectors” BRUKER AXS Inc., 5465 East Cheryl Parkway, Madison, WI 53711-5373 USA.

(89) SADABS, Sheldrick, G. M. “Program for Absorption Correction of Area Detector Frames”, BRUKER AXS Inc., 5465 East Cheryl Parkway, Madison, WI 53711-5373 USA.

(90) Sheldrick, G. M. A short history of SHELX. *Acta Cryst.* **2008**, *A64*, 112-122.

(91) Sheldrick, G. M. SHELXT – Integrated space-group and crystal-structure determination. *Acta Cryst.* **2015**, *A71*, 3-8.

(92) Sheldrick, G. M. Crystal structure refinement with SHELXL. *Acta Cryst.* **2015**, *C71*, 3-8.

(93) XT, XS, BRUKER AXS Inc., 5465 East Cheryl Parkway, Madison, WI 53711-5373 USA.

(94) Dolomanov, O. V.; Bourhis, L. J.; Gildea, R. J.; Howard, J. A. K.; Puschmann, H. *OLEX2*: a complete structure solution, refinement and analysis program. *J. Appl. Cryst.* **2009**, *42*, 339-341.

(95) Spek, A. L. Single-crystal structure validation with the program *PLATON*. *J. Appl. Cryst.* **2003**, *36*, 7-13.

(96) Flack, H. D. On Enantiomorph-Polarity Estimation. *Acta Cryst.* **1983**, *A39*, 876-881. Theory for correct and inverted structures: 0 and 1.

# 3. AN AIR AND WATER STABLE HYDROGEN BOND DONOR CATALYST FOR THE ENANTIOSELECTIVE GENERATION OF QUARTERNARY CARBON STEREOCENTERS BY ADDITION OF SUBSTITUTED CYANOACETATE ESTERS TO ACETYLENIC ESTERS*

## 3.1. Introduction

The efficient enantioselective synthesis of compounds with quaternary carbon stereocenters has been a subject of immense interest over the last 25 years, as reflected by an extensive review literature that emphasizes catalytic methods.[1] There has been a particular focus upon conjugate additions. In this context, racemic "active methylene compounds" with a single carbon-hydrogen bond and three unlike carbon substituents represent attractive building blocks. One obvious choice would be substituted cyanoacetate esters NCCH(R)$CO_2$R', large numbers of which are commercially available or easily prepared. However, many types of acceptors (e.g., conjugated cycloalkenones, Scheme 3.1, top) would yield a second carbon stereocenter, such that diastereoselectivity also becomes an issue.

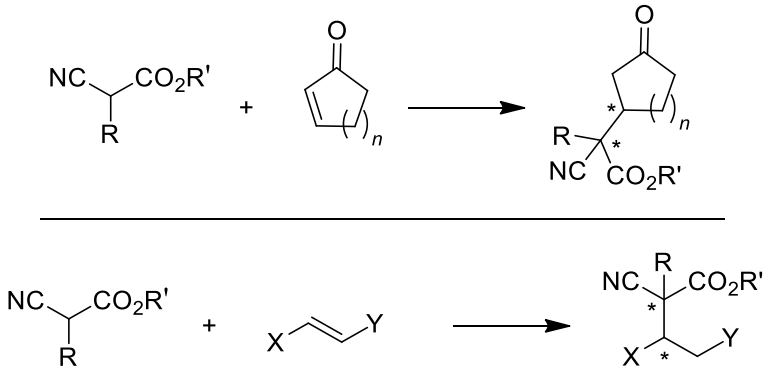


**Scheme 3.1.** Examples of additions of cyanoacetate esters to alkene acceptors.

Given the new family of catalysts that I was interested in applying to this problem (*vide infra*), I sought to evaluate their efficacies one stereocenter at a time. One way to



*Adapted with permission from Luu, Q. H.; Gladysz, J. A. *Chem. Eur. J.* **2020**, *26*, accepted. DOI:10.1002/chem.202001639-Published by John Wiley and Sons.

avoid generating a second stereocenter in additions of substituted cyanoacetate esters would be to employ an acetylenic acceptor, as generalized in Figure 3.1 (top). Of course, there would be the possibility of *cis*/*trans* or *Z*/*E* isomers about the resulting C=C linkage. However, this was seen as a more tractable complication.

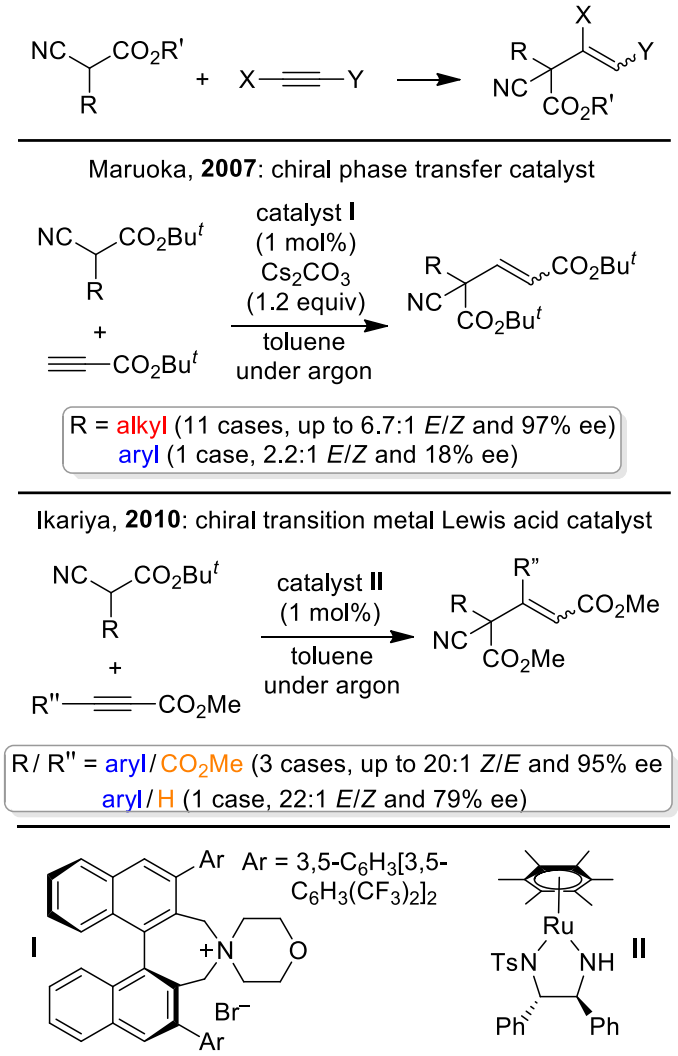


**Figure 3.1.** Enantioselective catalysts for additions of substituted cyanoacetate esters to acetylenic esters developed to date.*

Others have recognized the attractiveness of substituted cyanoacetate esters as building blocks.[2] Of particular value is the attendant installation of multiple functional groups that can be elaborated under different conditions.[3] However, there have only been

scattered reports dealing with acetylenic acceptors, and the best literature methods are summarized in Figure 3.1. One of these, developed by Maruoka, used an enantiopure phase transfer catalyst (**I**).[2a] In this work, only cyanoacetate esters with aliphatic substituents gave high enantioselectivities. Another, developed by Ikariya, used an enantiopure ruthenium Lewis acid catalyst.[2b] However, only cyanoacetate esters with aryl substituents were reported. I saw these divergent strengths and weaknesses as opportunities that might be addressed with new types of catalysts.

In parallel with the review literature cited,[1] there has been extensive recent development of chiral organic hydrogen bond donor catalysts.[4] Some of these are quite effective for the enantioselective construction of quaternary carbon centers from other combinations of reactants.[1f,5] The Gladysz group,[6-9] together with several others,[10-12] has been interested in developing chiral transition metal containing hydrogen bond donors. One impetus has been the application of an untapped region of the chiral pool, believed to provide binding motifs and modes of action that significantly differ from organic counterparts.[13]

The Gladysz group's main catalyst family was inspired by Werner's reports of the first enantiopure chiral inorganic compounds over a century ago.[14,15] One of these, $[Co(en)_3]^{3+}$ $3Cl^-$ (**1**$^{3+}$ $3Cl^-$; en = ethylenediamine),[14e] can be prepared by undergraduate students in an afternoon.[16] The configurations of such "chiral at metal" species are conventionally designated Λ and Δ[17] as depicted in Figure 3.2 (top). The former exhibits a left handed helical array of chelate rings, and the latter a right handed array. However, tris(1,2-diamine) cobalt(III) complexes are substitution inert,[18,19] which precludes direct activation of substrates by the metal. But tellingly, crystal structures reveal extensive NH hydrogen bonding interactions with counter anions.[20]

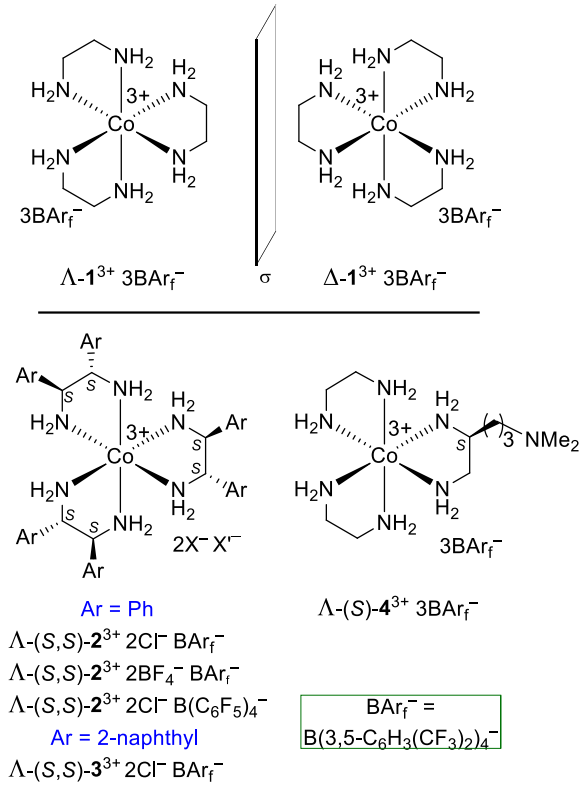


**Figure 3.2.** Catalysts screened in this study.*

Accordingly, the Gladysz group has prepared various tris(1,2-diamine) cobalt salts with one or more tetraarylborate anions of the formula $B(3,5\text{-}C_6H_3(CF_3)_2)_4^-$ ($BAr_f^-$) or $B(C_6F_5)_4^-$.[6-8,21] These anions are very poor hydrogen bond acceptors[22] and help to solubilize the trications in standard organic solvents. In aqueous solution, water would presumably compete for the substrate binding sites, and many educts would be insoluble. In any case, the complexes in Figure 3.2 have been applied to several types of carbon-carbon and carbon-nitrogen bond forming reactions known to be catalyzed by hydrogen bond donors.[6-8]

The Gladysz group has found that tris(adducts) of 1,2-diphenyl ethylenediamine (dpen), $[Co(dpen)_3]^{3+}$ $2X^-X'^-$ ($\mathbf{2}^{3+}$ $2X^-X'^-$), are often particularly enantioselective catalysts. The *S*,*S* and *R*,*R* enantiomers of this ligand are commercially available at surprisingly modest prices.[23] With the former, two sets of diastereomers are possible, the

salts Λ-(*S*,*S*)-**2**$^{3+}$ 2X$^{-}$X'$^{-}$ depicted in Figure 3.3, and the cobalt epimers Δ-(*S*,*S*)-**2**$^{3+}$ 2X$^{-}$ X'$^{-}$. The enantiomeric catalysts derived from (*R*,*R*)-dpen would be expected to give identical ee values (but opposite product configurations).

Analogous complexes have been prepared with a wide variety of aryl groups in place of the dpen phenyl groups.[21] Thus, a catalyst with 2-naphthyl substituents, Λ-(*S*,*S*)-**3**$^{3+}$ 2Cl$^{-}$BAr$_f^{-}$ (Figure 3.2), has been included in this study. In addition, a bifunctional catalyst with an internal tertiary amine, Λ-(*S*)-**4**$^{3+}$ 3BAr$_f^{-}$ (Figure 3.2), which obviates the need for an external base and has given highly enantioselective reactions,[8] has also been examined in screening reactions below.

Accordingly, in this chapter I compare the efficacies of the complexes in Figure 3.2 and selected diasteromers as catalysts for enantioselective additions of substituted cyanoacetate esters to acetylenic esters (Figure 3.1, top). From the standpoints of isolated yields, ee values, and substrate generality, Λ-(*S*,*S*)-**2**$^{3+}$ 2Cl$^{-}$B(C$_6$F$_5$)$_4^{-}$ clearly emerges as the best of a limited number of other catalysts (Figure 3.1) that have previously been reported to effect this transformation.

## 3.2. Results

### 3.2.1. Catalyst Screening.

In initial scout experiments, commercial dimethyl acetylenedicarboxylate (**4a**) and ethyl phenylcyanoacetate (**5a**) were combined in a 1.1:1.0 mol ratio in $CH_2Cl_2$ at a temperature specified in Table 3.1. Then the indicated catalyst (10 mol%) and base were added. The latter was applied in both stoichiometric (100 mol%) and catalytic (10 mol%) quantities. When TLC indicated that the reaction was complete, the solvent was removed and the residue taken up in $CDCl_3$. The *Z*/*E* ratio of the crude addition product **6<u>a</u>a** was then assayed by $^1$H NMR (structure and data: Table 3.1; *Z*/*E* =CH 5.88-5.89/7.07-7.08 ppm, s). Chromatographic workups gave pure **6<u>a</u>a** in 99-95% yields. The ee values were

determined by $^1$H NMR using the chiral solvating agent Λ-(*S*,*S*)-**2**$^{3+}$ 2I$^-$BAr$_f^-$.[24] These and all other reactions and workups were carried out in air.

Table 3.1 shows that useful levels of enantioselectivities were found only with the catalyst Δ-(*S*,*S*)-**2**$^{3+}$ 2Cl$^-$B(C$_6$F$_5$)$_4^-$ and the base pyridine at –36 °C (entry 22). None of the other catalysts were effective (entries 2-8). Interestingly pyridine was best used in catalytic quantities (entry 21 vs. 22). Furthermore, these conditions gave the most favorable *Z*/*E* product ratio (91:9). As with the other catalysts, the enantiomeric purity of the minor *E* isomer was poor (10% ee), but that of the major *Z* isomer was excellent (99% ee). However, the ee dropped to 59% when the catalyst loading was decreased to 5%.

Although Δ-(*S*,*S*)-**2**$^{3+}$ 2Cl$^-$B(C$_6$F$_5$)$_4^-$ readily dissolves in $CH_2Cl_2$ solutions of the substrates, per the conditions employed in Table 3.1, it is only sparingly soluble in the absence of substrates.

**3.2.2. Reaction scope.**

The conditions in entry 22 of Table 3.1 were then applied to a variety of substrates as illustrated in Figure 3.3. When ethyl phenylacetate was replaced by ethyl benzylcyanoacetate (**5b**), the *Z*/*E* ratio of the product remained high (**6<u>a</u>b**; 99:1) but the enantiomeric purity fell to 44% ee. However, *t*-butyl benzylcyanoacetate (**5c**), which features a bulkier ester alkyl group, gave the corresponding adduct **6<u>a</u>c** as a >99:<1 *Z*/*E* mixture in 88% ee. Thus, *t*-butyl esters were used for the remaining reactions.

**Table 3.1.** Screening of catalysts for the addition of ethyl phenylcyanoacetate (**5a**) to dimethyl acetylenedicarboxylate (**4a**).[a]*

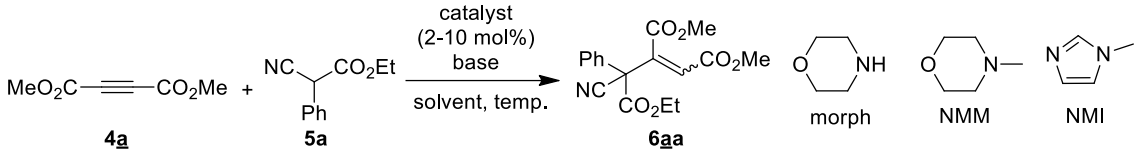


| Entry | Catalyst | Loading (mol%) | Solvent | Base (mol%) | Time (h) | Temp (°C) | Yield (%)[b] | *Z*/*E*[c] | ee (%)[d] |
|---|---|---|---|---|---|---|---|---|---|
| 1 | - | - | $CH_2Cl_2$ | $Et_3N$ (100) | 12 | 23 | 99 | 78/22 | 0/0 |
| 2 | Λ-**1**$^{3+}$ 3$BAr_f^-$ | 10 | $CH_2Cl_2$ | $Et_3N$ (100) | 0.20 | 23 | 99 | 61/39 | 0/0 |
| 3 | Λ-(*S*,*S*)-**2**$^{3+}$ 2$BF_4^-$$BAr_f^-$ | 10 | $CH_2Cl_2$ | $Et_3N$ (100) | 12 | 23 | 99 | 75/25 | 10/4 |
| 4 | Λ-(*S*,*S*)-**2**$^{3+}$ 2$BF_4^-$$BAr_f^-$ | 10 | $CH_2Cl_2$ | $Et_3N$ (10) | 24 | 23 | 28 | 78/22 | 12/4 |
| 5 | Λ-(*S*,*S*)-**2**$^{3+}$ 2$Cl^-$$BAr_f^-$ | 10 | $CH_2Cl_2$ | $Et_3N$ (100) | 12 | 23 | 99 | 78/22 | 0/0 |
| 6 | Λ-(*S*,*S*)-**3**$^{3+}$ 2$Cl^-$$BAr_f^-$ | 10 | $CH_2Cl_2$ | $Et_3N$ (100) | 12 | 23 | 99 | 83/17 | 16/0 |
| 7 | Λ-(*S*)-**4**$^{3+}$ 3$BAr_f^-$ | 10 | $CH_2Cl_2$ | - | 12 | 23 | 99 | 69/31 | 18/40 |
| 8 | Λ-(*S*,*S*)-**2**$^{3+}$ 2$Cl^-$$B(C_6F_5)_4^-$ | 10 | $CH_2Cl_2$ | $Et_3N$ (100) | 12 | 23 | 99 | 79/21 | 0/0 |
| 9 | Δ-(*S*,*S*)-**2**$^{3+}$ 2$Cl^-$$B(C_6F_5)_4^-$ | 10 | $CH_2Cl_2$ | $Et_3N$ (100) | 11 | 23 | 99 | 85/15 | 36/2 |
| 10 | Δ-(*S*,*S*)-**2**$^{3+}$ 2$Cl^-$$B(C_6F_5)_4^-$ | 10 | $CH_2Cl_2$ | NMM (100) | 12 | 23 | 99 | 90/10 | 32/12 |
| 11 | Δ-(*S*,*S*)-**2**$^{3+}$ 2$Cl^-$$B(C_6F_5)_4^-$ | 10 | $CH_2Cl_2$ | NMI (100) | 12 | 23 | 99 | 93/7 | 36/9 |
| 12 | Δ-(*S*,*S*)-**2**$^{3+}$ 2$Cl^-$$B(C_6F_5)_4^-$ | 10 | $CH_2Cl_2$ | morph (100) | 12 | 23 | 5 | - | - |
| 13 | Δ-(*S*,*S*)-**2**$^{3+}$ 2$Cl^-$$B(C_6F_5)_4^-$ | 10 | $CH_2Cl_2$ | pyridine (100) | 12 | 23 | 99 | 95/5 | 14/13 |
| 14 | Δ-(*S*,*S*)-**2**$^{3+}$ 2$Cl^-$$B(C_6F_5)_4^-$ | 10 | acetone | pyridine (100) | 12 | 23 | 99 | 90/10 | 4/2 |

[a]A vial was charged with a stir bar, **4a** (0.0078 g, 0.055 mmol, 0.0068 mL), **5a** (0.0095 g, 0.050 mmol, 0.0087 mL), and 0.50 mL of a solvent. The sample was brought to the indicated temperature, and a catalyst (0.0050 mmol, 10 mol%) and a base were added with stirring. The reaction was monitored by TLC and was worked up as described in the experimental section. [b]Isolated yields after chromatography. [c]Determined by $^1$H NMR. [d]Determined by $^1$H NMR using 10 mol% of the CSA Λ-(*S*,*S*)-**2**$^{3+}$ 2$I^-$$BAr_f^-$.

**Table 3.1.** Continued.[a]*

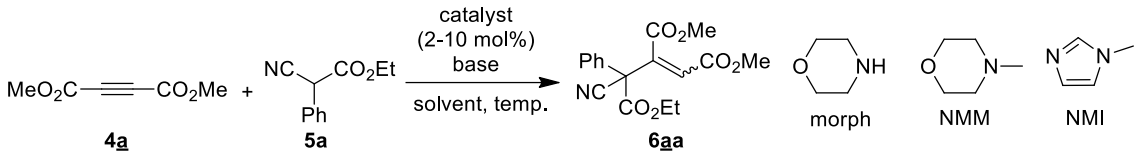


| Entry | Catalyst | Loading (mol%) | Solvent | Base (mol%) | Time (h) | Temp (°C) | Yield (%)[b] | *Z*/*E*[c] | ee (%)[d] |
|---|---|---|---|---|---|---|---|---|---|
| 15 | Δ-(*S*,*S*)-**2**$^{3+}$ 2Cl$^{-}$B(C$_6$F$_5$)$_4^{-}$ | 10 | $CH_3CN$ | pyridine (100) | 12 | 23 | 99 | 87/13 | 12/6 |
| 16 | Δ-(*S*,*S*)-**2**$^{3+}$ 2Cl$^{-}$B(C$_6$F$_5$)$_4^{-}$ | 10 | toluene | pyridine (100) | 12 | 23 | 99 | 88/12 | 8/14 |
| 17 | Δ-(*S*,*S*)-**2**$^{3+}$ 2Cl$^{-}$B(C$_6$F$_5$)$_4^{-}$ | 10 | $CH_2Cl_2$ | $Et_3N$ (10) | 12 | 23 | 99 | 87/13 | 30/11 |
| 18 | Δ-(*S*,*S*)-**2**$^{3+}$ 2Cl$^{-}$B(C$_6$F$_5$)$_4^{-}$ | 10 | $CH_2Cl_2$ | - | 24 | 23 | <1 | - | - |
| 19 | Δ-(*S*,*S*)-**2**$^{3+}$ 2Cl$^{-}$B(C$_6$F$_5$)$_4^{-}$ | 10 | $CH_2Cl_2$ | $Et_3N$ (100) | 12 | 0 | 99 | 86/14 | 36/6 |
| 20 | Δ-(*S*,*S*)-**2**$^{3+}$ 2Cl$^{-}$B(C$_6$F$_5$)$_4^{-}$ | 10 | $CH_2Cl_2$ | $Et_3N$ (10) | 15 | –36 | 99 | 88/12 | 54/13 |
| 21 | Δ-(*S*,*S*)-**2**$^{3+}$ 2Cl$^{-}$B(C$_6$F$_5$)$_4^{-}$ | 10 | $CH_2Cl_2$ | pyridine (100) | 17 | –36 | 99 | 95/5 | 44/22 |
| 22 | Δ-(*S*,*S*)-**2**$^{3+}$ 2Cl$^{-}$B(C$_6$F$_5$)$_4^{-}$ | 10 | $CH_2Cl_2$ | pyridine (10) | 17 | –36 | 95 | 91/9 | 99/10 |
| 23 | Δ-(*S*,*S*)-**2**$^{3+}$ 2Cl$^{-}$B(C$_6$F$_5$)$_4^{-}$ | 5 | $CD_2Cl_2$ | pyridine (10) | 17 | –36 | 95 | 91/9 | 59/10 |
| 24 | Δ-(*S*,*S*)-**2**$^{3+}$ 2Cl$^{-}$B(C$_6$F$_5$)$_4^{-}$ | 2 | $CD_2Cl_2$ | pyridine (10) | 17 | –36 | 94 | 91/9 | 38/7 |
| 25 | Δ-(*S*,*S*)-**2**$^{3+}$ 2Cl$^{-}$B(C$_6$F$_5$)$_4^{-}$ | 10 | $CH_2Cl_2$ | pyridine (20) | 16 | –36 | 99 | 94/6 | 52/6 |
| 26 | Δ-(*S*,*S*)-**2**$^{3+}$ 2Cl$^{-}$B(C$_6$F$_5$)$_4^{-}$ | 10 | $CH_2Cl_2$ | pyridine (10) | 72 | –50 | <1 | - | - |
| 27 | Δ-(*S*,*S*)-**2**$^{3+}$ 2Cl$^{-}$B(C$_6$F$_5$)$_4^{-}$ | 10 | $CH_2Cl_2$ | pyridine (10) | 72 | –60 | <1 | - | - |
| 28 | Δ-(*S*,*S*)-**2**$^{3+}$ 2Cl$^{-}$B(C$_6$F$_5$)$_4^{-}$ | 10 | $CH_2Cl_2$ | pyridine (10) | 72 | –70 | <1 | - | - |

[a]A vial was charged with a stir bar, **4a** (0.0078 g, 0.055 mmol, 0.0068 mL), **5a** (0.0095 g, 0.050 mmol, 0.0087 mL), and 0.50 mL of a solvent. The sample was brought to the indicated temperature, and a catalyst (0.0050 mmol, 10 mol%) and a base were added with stirring. The reaction was monitored by TLC and was worked up as described in the experimental section. [b]Isolated yields after chromatography. [c]Determined by $^1$H NMR. [d]Determined by $^1$H NMR using 10 mol% of the CSA Λ-(*S*,*S*)-**2**$^{3+}$ 2I$^{-}$BAr$_f^{-}$.

Next, the benzyl group in the preceding reaction was replaced by allyl, homoallyl, and related alkyl substituents. As shown for the adducts **6ad-g** in Figure 3.3, only *Z* isomers were obtained (88->99% yields), and with ee values of 70-98%. A series of four substrates with $CH_2$aryl substituents gave similar results (**6ah-k**, 70-99% yields, 85-91% ee). When di*ethyl* acetylenedicarboxylate (**4b**) and **5c** were similarly reacted, the enantiomeric purity of the product **6bc** was close to that obtained with **4a** (83% vs, 88% ee).

Other alkyne substrates were briefly investigated. When unsymmetrically substituted *t*-butyl propiolate (**4c**) and **5c** were analogously combined, a slower reaction took place. After 72 h at 23 °C, the addition product **6cc** (Figure 3.3) was isolated in 53% yield as a <1:>99 *Z*/*E* mixture with an enantiomeric purity of 94% ee. Note that despite the inverted *Z*/*E* ratio, the quarternary carbon atom remains *trans* to the carboalkoxy C=C substituent, exactly as in the other products. When di(*t*-butyl) acetylenedicarboxylate (**4d**) and **5c** were similarly combined, no reaction occurred, even after 72 h at 23 °C, presumably for steric reasons.

In view of evidence for catalyst/pyridine binding presented below, the reaction of **4a** and **6c** was also investigated with the more hindered Brønsted bases 2,6-dimethylpyridine (2,6-lutidine) and 2,6-di(*t*-butyl) pyridine (10 mol%). After 19 h, workups gave **6aa** in 99% and 22% yields, respectively. Much starting material remained in the second reaction. However, the enantioselectivities were essentially unaffected (89% and 86% ee), so these more costly bases offer no advantages.

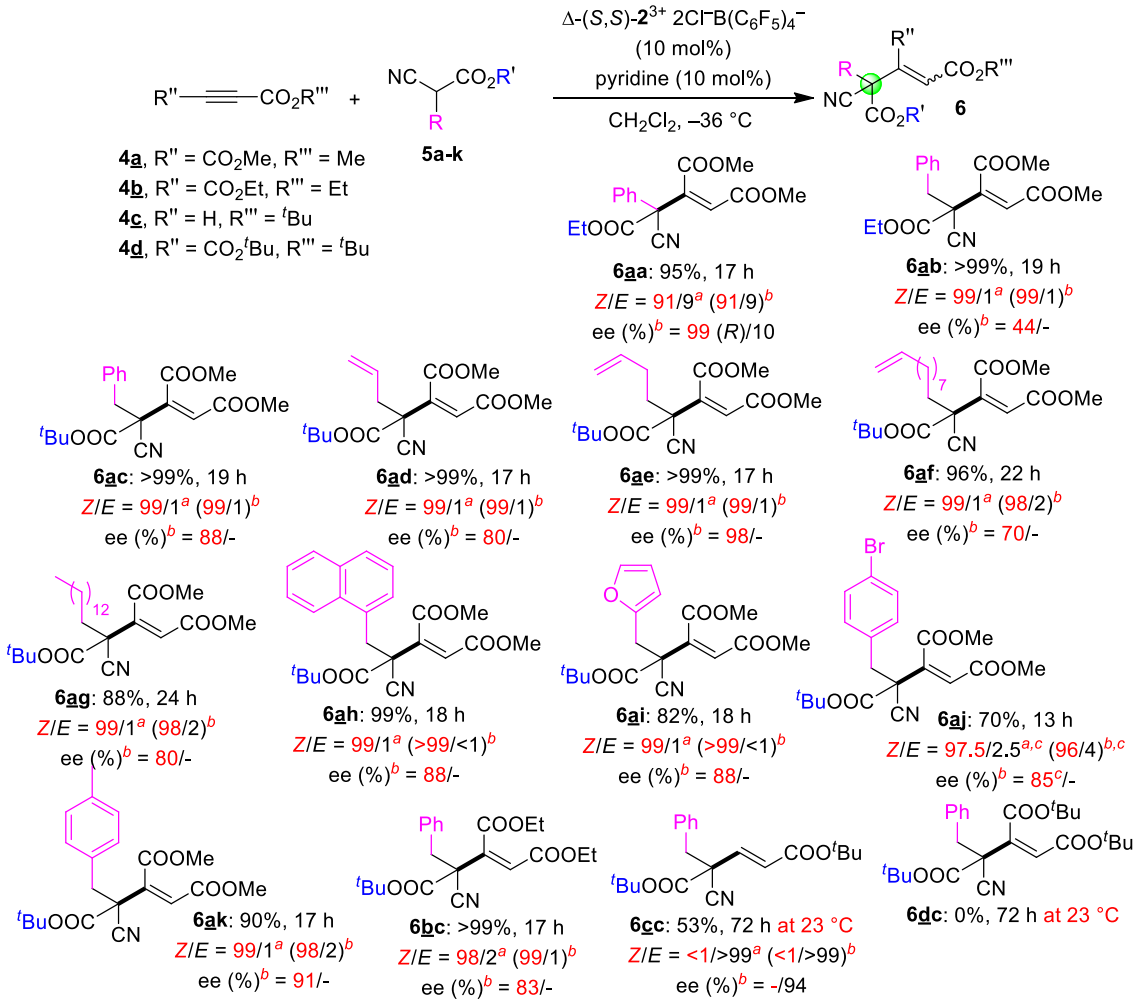


**Figure 3.3**. Substrate scope of the title reaction. [a]Determined by a $^1$H NMR spectrum of the crude mixture. [b]Determined by $^1$H NMR analysis of the purified product. [c]Average of six runs.*

Of all the products in Figure 3.3, only **6aa** has been previously reported in the literature. The others were characterized by NMR ($^1$H, $^{13}$C{$^1$H}) and C/H/N microanalyses, as summarized in the experimental section. For adducts with =CHCO$_2$R''' moieties, the $^1$H NMR signal for the *E* C=C isomer was always downfield of the *Z*. Otherwise, all NMR features were routine. Four of the *t*-butyl cyanoacetate substrates were also new compounds (**5f**,**g**,**h**,**k**), and were prepared by standard procedures (usually alkylation) as described in the experimental section.

### 3.2.3. Probes of mechanism.

One fundamental question concerns the interaction of the reaction components with the catalyst Δ-(*S*,*S*)-**2**$^{3+}$ 2Cl$^{-}$B(C$_6$F$_5$)$_4^{-}$. The chiral cobalt trication has idealized $D_3$ symmetry, which means a principal $C_3$ axis that defines two "$C_3$ faces" and three $C_2$ axes in a perpendicular plane that define three "$C_2$ faces". These are illustrated in Figure 3.4,[7a] although it merits note that the idealized symmetry is never found crystallographically. For each $NH_2$ group, one proton is associated with a $C_3$ face, and the other (diastereotopic) with a $C_2$ face.

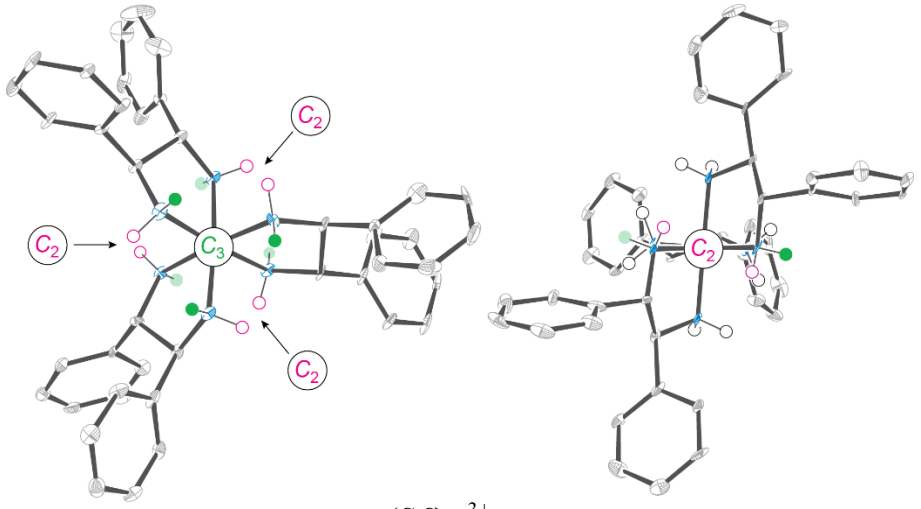


**Figure 3.4.** Representations of the trication Δ-(*S*,*S*)-**2**$^{3+}$; left, view down the idealized $C_3$ axis; right, view down one of three idealized $C_2$ axes.*

Previous studies, especially with the diastereomeric BAr$_f^{-}$ salt Λ-(*S*,*S*)-**2**$^{3+}$ 2Cl$^{-}$ BAr$_f^{-}$, have established significant hydrogen bonding between the two chloride anions and the two $C_3$ faces.[7a,21] Each face offers three roughly synperiplanar NH protons, which are depicted in green in Figure 3.4. Hence, the $^1$H NMR chemical shifts of these six NH protons are significantly downfield of the other six. The $C_2$ faces feature two roughly synperiplanar NH protons, which are depicted in magenta.

Thus, 10.0 equiv of dimethyl acetylenedicarboxylate (**4a**), ethyl

phenylcyanoacetate (**5a**), and pyridine were separately titrated into a sample of $CD_2Cl_2$ and the catalyst Δ-(*S*,*S*)-$\mathbf{2}^{3+}$ $2Cl^{-}B(C_6F_5)_4^{-}$. The amounts of the catalyst and solvent were identical to those used in Table 3.1, and thus the catalyst was only partially soluble until ca. 4 equiv of the additive was present. This renders the spectra with 1.0-3.0 equiv of additive less rigorously comparable to the others. In any case, the initial chemical shift difference between the diastereotopic protons associated with the $C_3$ and $C_2$ faces is ca. 2.1 ppm (the former signal is obscured by the phenyl protons of the catalyst).

As shown in Figure 3.5a (top), the successive addition of **4a** led to a slight downfield shift of the $C_2$ NH signal (δ 5.12 to 5.27 ppm; Δδ 0.15 ppm). Any shift of the obscured $C_3$ NH signal could be bounded as less than Δδ 0.01 ppm (upfield). For reference, the signal of the aliphatic CH groups, which always neighbor a $NH_2$ group, shifted less than the $C_2$ NH signal (δ 4.21 to 4.26 ppm; Δδ 0.05 ppm).

As shown in Figure 3.5b (middle), the successive addition of **5a** led to a more pronounced downfield shift of the $C_2$ NH signal (δ 5.12 to 5.42 ppm; Δδ 0.30 ppm). The $C_3$ NH signal was obscured by the phenyl protons of the catalyst and **5a**, and the aliphatic CH signal was obscured by the methylene protons of **5a**.

As shown in Figure 3.5c (bottom), the successive addition of pyridine led to a pronounced downfield shift of the $C_2$ NH signal (δ 5.12 to 6.12 ppm; Δδ 1.00 ppm). The $C_3$ NH signal was obscured by the aromatic protons of the catalyst and pyridine. The aliphatic CH signal shifted much less than the $C_2$ NH signal (δ 4.21 to 4.42 ppm; Δδ 0.21 ppm).

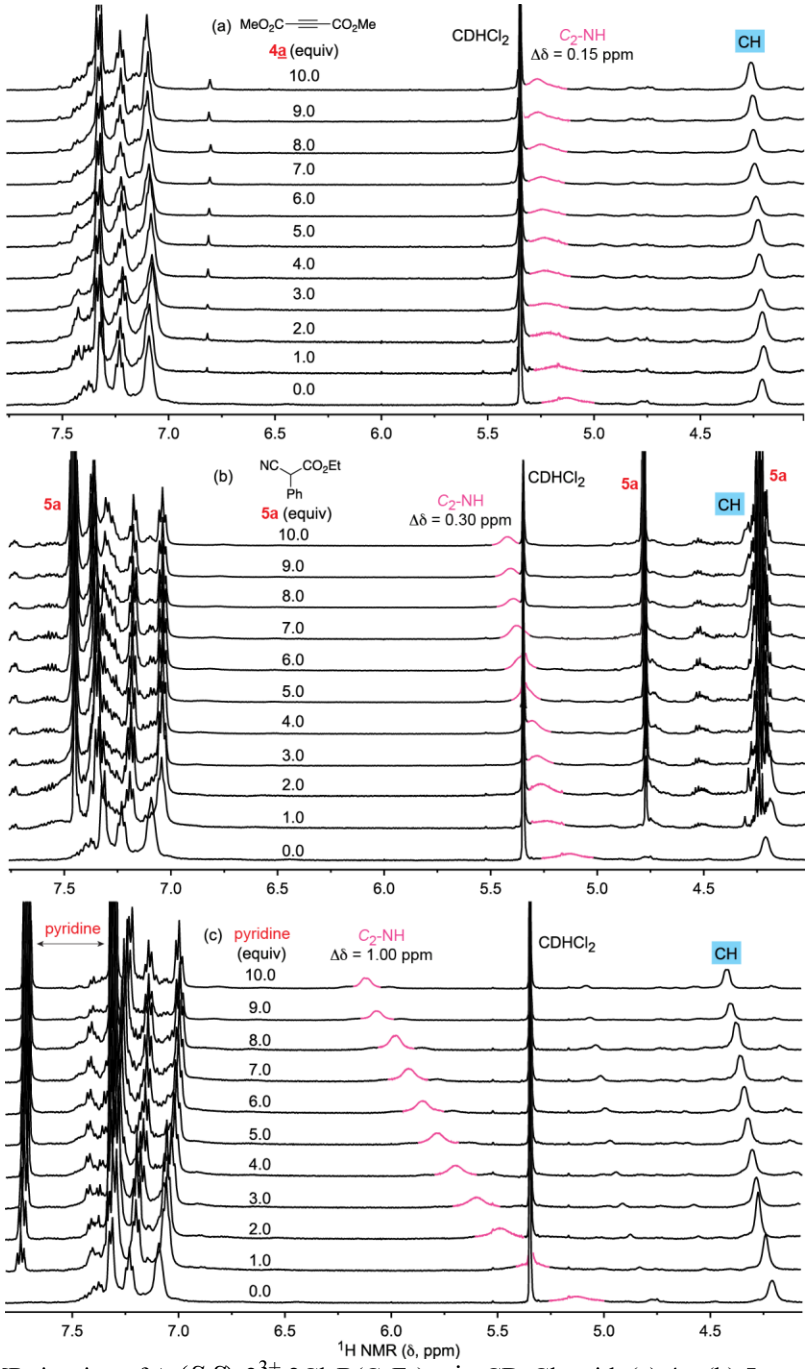


**Figure 3.5.** NMR titration of Δ-(*S*,*S*)-**2**$^{3+}$ $2Cl^{-}B(C_6F_5)_4^{-}$ in $CD_2Cl_2$ with (a) **4a**, (b) **5a**, and (c) pyridine.*

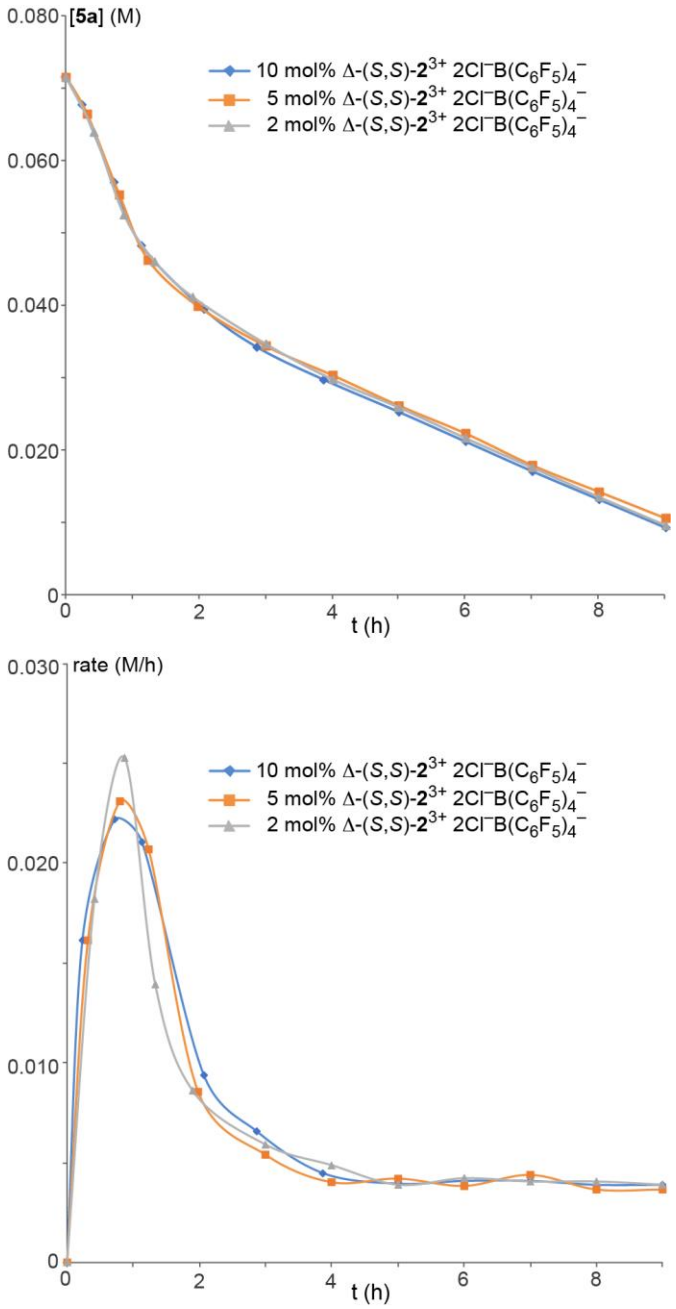


**Figure 3.6.** Application of the reaction progress kinetic analysis method[25] to a reaction similar to entry 22 of Table 3.1 (further details: see text). Top: plot of the concentration of **5a** versus time. Bottom: plot of Δ([**5a**])/Δt versus time.*

In a quest for further insight, reaction orders were sought. For this purpose, the recently popularized reaction progress kinetic analysis method was applied.[25] Accordingly, **4a**, **5a**, pyridine, Δ-(*S*,*S*)-$\mathbf{2}^{3+}$ $2Cl^{-}B(C_6F_5)_4^{-}$, and $CD_2Cl_2$ were combined in

a NMR tube in a manner similar to that in Table 3.1. but in the presence of the internal standard $Ph_2SiMe_2$. The reaction was monitored by $^1$H NMR at –36 °C. The concentration of **5a** and the rate (Δ([**5a**])/Δt) were then plotted against the reaction time as shown in Figure 6 for three experiments with 2.0, 5.0, and 10 mol% catalyst loadings.

Concentration and rate data for **4a** were similarly treated (Figure B-18, appendix B). Analyses established positive orders for **4a** and **5a** during the first hour after mixing. These then transitioned to zero order, which was maintained until the reaction was complete. The same data set was used for probing the order in catalyst. In an application of the time normalization method,[26] the concentration of **5a** was plotted against the normalized time (see experimental section) at different orders *n* as shown in Figure B-19 (appendix B). The best fit was obtained for $n = 0$, indicating a rate zero order in Δ-(*S*,*S*)-$\mathbf{2}^{3+}$ $2Cl^-B(C_6F_5)_4^-$. These data are further interpreted in the discussion section.

**3.3. Discussion**

As summarized in Figure 3.3, the cobalt complex Δ-(*S*,*S*)-$\mathbf{2}^{3+}$ $2Cl^-B(C_6F_5)_4^-$ and the base pyridine represent the best available catalyst system for enantioselective additions of substituted cyanoacetate esters to acetylenic esters, a powerful route to quaternary carbon stereocenters. The products are amenable to a number of subsequent functionalization protocols,[3] rendering them versatile synthetic building blocks. Furthermore, the reactions may be conducted in air, and the cobalt catalyst is commercially available.[27]

The objective of Figure 3.3 is to present the substrate scope in its entirety, with full representation of strengths and weaknesses. In some of the products with lower ee values, it is a simple matter of introducing a bulkier ester alkyl group on the cyanoacetate to obtain much higher ee values (e.g., ethyl vs. *t*-butyl as in **6ab and 6ac**). However, replacing the methyl or ethyl groups of the acetylene dicarboxylate diester with *t*-butyl groups kills all

reactivity (e.g., **6<u>a</u>c** or **6<u>b</u>c** vs. **6<u>d</u>c**). In any case, considering only the optimum ester alkyl groups (R', R'''), the ee values range from 70 to 98% with an average of 86%.

It would be premature to read too much significance into the poorer performing catalysts in Table 3.1. For example, bifunctional organocatalysts often give superior enantioselectivities.[4d,e] Indeed, Λ-(*S*)-**4**$^{3+}$ 3BAr$_f^-$, which features a tertiary amine tethered by a $(CH_2)_3$ spacer, has proven to be a highly enantioselective catalyst for certain addition reactions that require a Brønsted base,[8] and was therefore available in quantity for this study. However, catalysts with other tether lengths have also been prepared (e.g., $(CH_2)_n$ with $n$ = 1-4), as have the corresponding Δ diastereomers, and these remain to be screened. In the same vein, the naphthyl substituted catalyst Λ-(*S*,*S*)-**3**$^{3+}$ 2Cl$^-$BAr$_f^-$ is not yet available as the Δ diastereomer or analogous 2Cl$^-$B$(C_6F_5)_4^-$ salt, two attributes of the best catalyst in Table 3.1.

My data also illustrate the versatility of the chiral solvating agent (CSA) Λ-(*S*,*S*)-**2**$^{3+}$ 2I$^-$BAr$_f^-$, which is easily prepared in one step from a commercial precursor, for determining the enantiomeric purities of analytes with Lewis basic functional groups.[24] For most of the products in Figure 3.3, only 10 mol% was required. It is not surprising that a class of complexes capable of highly sensitive chiral recognition also can effect highly enantioselective catalysis.

Finally, to round out the picture with respect to other chiral hydrogen bond donor catalysts, three protocols that give other types of addition products with quaternary carbon stereocenters are illustrated in Figure 3.7.[5,10e] All of these deliver excellent enantioselectivities. One, developed by Meggers, features an iridium containing catalyst with NH donor groups that promotes additions of indoles to trisubstituted nitroalkenes.[10e]

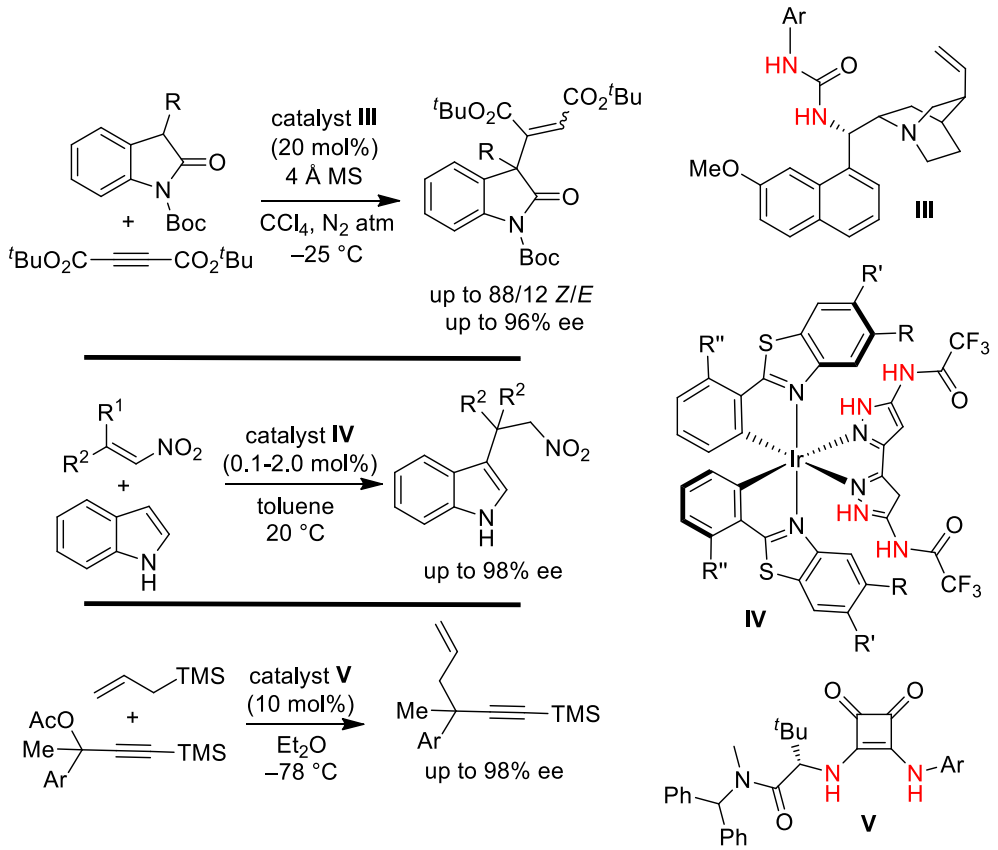


**Figure 3.7.** Enantioselective syntheses of compounds with quaternary stereocenters using other chiral hydrogen bond donor catalysts.*

Some headway has been made in computationally determining the mechanisms of enantioselective addition reactions catalyzed by metal containing hydrogen bond donors.[9c] However, these have involved ruthenium catalysts where the NH groups are remote from the metal and only three can simultaneously participate in the transition state. The situations with cobalt(III) catalysts of the types in Figure 3.2 are potentially much more complex. For example, it is clear from Figure 3.4 that 4-5 NH groups could potentially participate in a transition state assembly.

In any case, NMR data (Figure 3.5) establish that the $C_2$ site is capable of binding both types of substrates as well as the base pyridine. The greater downfield shifts observed with pyridine suggest a stronger binding constant. This could be a factor in the lower

enantioselectivities when pyridine is used in a tenfold molar excess of the catalyst as opposed to a 1:1 ratio (Table 3.1, entries 13 vs. 12). Similar NMR evidence has been obtained with related catalysts, such as the diastereomeric salt Λ-(*S*,*S*)-**2**$^{3+}$ 2Cl$^{-}$BAr$_f^{-}$, for substrate binding to the $C_2$ site.[7a,24]

However, there is also evidence that some level of access to the $C_3$ site can be required. Specifically, rates of additions of malonate esters to nitroalkenes become faster when the chloride ions of Λ-(*S*,*S*)-**2**$^{3+}$ 2Cl$^{-}$BAr$_f^{-}$ are replaced by more weakly hydrogen bonding anions such as $BF_4^{-}$ and $PF_6^{-}$.[7a] My own view is that a multitude of mechanistic pathways is available to this family of cobalt(III) complexes for catalyzing various addition reactions. For example, with some reactions Λ diastereomers of (*S*,*S*)-**2**$^{3+}$ 2X$^{-}$X'$^{-}$ provide higher enantioselectivities,[7a,7c] and with other reactions Δ diastereomers are more effective.[7b]

The reaction orders supplied by the data in Figures 3.6, B-18, and B-19 generate more questions than answers. The zero-order dependence upon the concentrations of the alkyne, cyanoacetate ester, and catalyst suggest a rest state and transition state of the same atomic compensation. A low energy ternary adduct is consistent with the enhanced solubility of Δ-(*S*,*S*)-**2**$^{3+}$ 2Cl$^{-}$B(C$_6$F$_5$)$_4^{-}$ in $CD_2Cl_2$ in the presence of the alkyne and cyanoacetate substrates. However, efforts to further define the mechanism have been hampered by problems with parallel experiments involving pyridine. For some reason, the data do not give interpretable plots. Despite the incomplete picture, it was felt best to share all data at this time.

In terms of reactions that can be effected with organocatalysts, zero order behavior with respect to one or both substrates is not unusual.[25,28] Initial regimes with positive order, as observed in Figures 3.6 and B-18, have been attributed to the interval required for accumulating both substrates on the catalyst to form the intermediate.[25,28b,c] Also,

reactions of metal containing catalysts that are zero order in catalyst have ample precedent.[29]

### 3.4. Conclusion

The study in chapter 3 has significantly expanded the scope of enantioselective reactions that can be catalyzed with chiral tris(1,2-diamine) cobalt(III) hydrogen bond donor catalysts of the types in Figure 3.2. Furthermore, it is the first that can be advertised as significantly improving upon existing literature catalysts, as opposed to being comparably effective (Figure 3.1).

### 3.5. Experimental

**General.** The complexes Λ-**1**$^{3+}$ 3BAr$_f^-$,[6] Λ-(*S*,*S*)-**2**$^{3+}$ 2Cl$^-$BAr$_f^-$,[21] Λ-(*S*,*S*)-**2**$^{3+}$ 2BF$_4^-$BAr$_f^-$,[21] Λ-(*S*,*S*)-**2**$^{3+}$ 2Cl$^-$B(C$_6$F$_5$)$_4^-$,[21] Δ-(*S*,*S*)-**2**$^{3+}$ 2Cl$^-$B(C$_6$F$_5$)$_4^-$,[21] Λ-(*S*,*S*)-**3**$^{3+}$ 2Cl$^-$BAr$_f^-$,[21] Λ-(*S*)-**4**$^{3+}$ 3BAr$_f^-$,[8] and Λ-(*S*,*S*)-**2**$^{3+}$ 2I$^-$BAr$_f^-$,[24] most of which are shown in Figure 3.2, were synthesized as reported earlier. Data on the known starting materials, solvents, and instrumentation are provided in appendix B. All reactions and workups were conducted in air.

**Catalyst screening (Tables 3.1).** A vial was charged with a stir bar, **4a** (0.0078 g, 0.055 mmol, 0.0068 mL), **5a** (0.0095 g, 0.0050 mmol, 0.0087 mL), and $CH_2Cl_2$ (0.50 mL). The sample was bought to the indicated temperature, and the catalyst (0.0050 mmol, 10 mol%) and base were added with stirring (100 mol% base: neat $Et_3N$ (0.0051 g, 0.050 mmol, 0.0070 mL) or pyridine (0.0040 g, 0.050 mmol, 0.0040 mL); 10 mol% base: 0.20 mL of a 0.025 M $CH_2Cl_2$ solution). The reaction was monitored by TLC (silica gel, 9:1 v/v hexanes/ethyl acetate). After the time indicated in Table 3.1, the vial was opened to air and (for low temperature runs) allowed to warm to room temperature. The solvent was removed by rotary evaporation, and $CDCl_3$ (0.70 mL) was added. The *Z*/*E* C=C ratio was assayed by $^1$H NMR (*Z*/*E* =CH: 5.88-5.89/7.07-7.08 ppm, s/s). The sample was

chromatographed (silica gel, 1 × 20 cm column, packed in and eluted with 9:1 v/v hexanes/ethyl acetate). The product containing fractions were combined and the solvents were removed by rotary evaporation to give **6aa**. Further data are provided below.

**Additions of cyanoacetate esters 5 to acetylenic esters 4 (Figure 3.3).** A vial was charged with a stir bar, an alkyne **4** (0.055 mmol), a cyanoacetate **5** (0.050 mmol), and $CH_2Cl_2$ (0.50 mL). Except for the last two systems in Figure 3.3, the sample was placed in a –36 °C freezer and stirred. After 10 min, Δ-(*S*,*S*)-$\mathbf{2}^{3+}$ $2Cl^{-}B(C_6F_5)_4^{-}\cdot 3H_2O$ (0.010 g, 0.0050 mmol, 10 mol%) and a $CH_2Cl_2$ solution of pyridine (0.025 M, 0.20 mL, 0.0050 mmol) were added. The reaction was monitored by TLC (silica gel, 9:1 v/v hexanes/ethyl acetate). After the specified time, the samples of **6** were transferred to a hood, opened to air, and worked up analogously to those in Table 3.1. Further data are provided below.

**Determination of ee values.**[24] An NMR tube was charged with $CDCl_3$ (0.30 mL), a product **6** (0.010 mmol), and a 0.0050 M $CDCl_3$ solution of the chiral solvating agent Λ-(*S*,*S*)-$\mathbf{2}^{3+}$ $2I^{-}BAr_f^{-}\cdot 0.5H_2O$ (0.20 mL, (0.0010 mmol, 10 mol%) for **6aa**-**6ae**, **6ah**, **6ai**, **6ak**, **6bc**, and **6cc**; 0.40 mL (0.0020 mmol, 20 mol%) for **6af** and **6ag**; 0.80 mL (0.0045 mmol, 45 mol%) for **6aj**).[24] A $^1$H NMR spectrum was acquired and selected signals of the enantiomers were integrated (see Figures B-5 to B-17, appendix B).

**NMR titration experiments (Figure 3.5)**. An NMR tube was charged with Δ-(*S*,*S*)-$\mathbf{2}^{3+}$ $2Cl^{-}B(C_6F_5)_4^{-}\cdot 3H_2O$ (0.010 g, 0.0050 mmol) and $CD_2Cl_2$ (0.70 mL). The catalyst was only partially soluble. A $^1$H NMR spectrum was recorded. A 1.0 M $CD_2Cl_2$ solution of pyridine was added in 0.0050 mL increments (0.0050 mmol). A $^1$H NMR spectrum was recorded after each addition. The experiment was repeated with solutions of **4a** and **5a**.

**Rate Experiments (Figure 3.6). A** (determination of the order in **4a** and **5a**). An

NMR tube was charged with a stir bar, **4a** (0.0078 g, 0.055 mmol, 0.0068 mL), **5a** (0.0095 g, 0.0050 mmol, 0.0087 mL), the internal standard $Ph_2SiMe_2$ (0.0021 g, 0.010 mmol, 0.0022 mL), and $CD_2Cl_2$ (0.50 mL). The sample was vigorously stirred. The resulting solution was cooled to –36 °C, the stir bar removed, and a $^1$H NMR spectrum recorded. The stir bar was reintroduced, the solution cooled to –36 °C, and Δ-(*S*,*S*)-$\mathbf{2}^{3+}$ $2Cl^-$ $B(C_6F_5)_4^-\cdot 3H_2O$ (0.010 g, 0.0050 mmol, 10 mol%), and a $CD_2Cl_2$ solution of pyridine (0.025 M, 0.20 mL, 0.0050 mmol) were added with stirring. $^1$H NMR spectra were recorded at t (min) = 5, 15, 30, 60, 90, 120, 180, 240, 300, 360, 420, 480, 540 (always temporarily removing the stir bar). The experiment was repeated with 5.0 and 2.0 mol% catalyst loadings. The reaction progress kinetic analysis method[25] was applied. The concentration of **5a** at each time point t was calculated from the relative integration of the standard and plotted versus t (Figure 3.6). The instantaneous rate (Δ([**5a**])/Δt) was similarly plotted and the same analysis was performed for **4a** (Figure B-18). **B** (determination of the order in catalyst). The time normalization method[26] was used. The concentration of **5a** from **A** was plotted against the normalized time t' for each catalyst loading. The order in catalyst *n* was varied until the data points for all catalyst loadings overlaid (Figure B-19, appendix B).[26]

$$t' = t \times [\Delta\text{-}(S,S)\text{-}\mathbf{2}^{3+}\ 2Cl^-B(C_6F_5)_4^-]^n$$

where [Δ-(*S*,*S*)-$\mathbf{2}^{3+}$ $2Cl^-B(C_6F_5)_4^-$] represents total concentration of the catalyst in the reaction (M) and *n* is the order in catalyst.

**Syntheses of *t*-butyl 2-cyanododec-11-enoate (5f), *t*-butyl 2-cyanohexadecanoate (5g), and *t*-butyl 2-cyano-3-(*p*-tolyl)propanoate (5k).** A round bottom flask was charged with a stir bar, potassium carbonate (0.660 g, 4.40 mmol, 1.10 equiv), *t*-butyl cyanoacetate (1.69 g, 12.0 mmol, 1.68 mL), and $CH_3CN$ (10.0 mL). The mixture was vigorously stirred at room temperature. After 1 h, an alkyl bromide (4.00

mmol) was added dropwise. After 5 h, water (5.0 mL) and diethyl ether (10.0 mL) were added. The organic phase was collected, and the aqueous phase was extracted with diethyl ether (2 × 5.0 mL). The organic phases were combined, washed with HCl (1.0 M, 5.0 mL), and dried ($Na_2SO_4$). The solvents were removed by rotary evaporation. The residue was chromatographed (silica gel, 3 × 40 cm column, packed and eluted with 9:1 v/v hexanes/ethyl acetate). The solvent was removed from the product containing fractions by rotary evaporation.

This procedure was carried out with 10-bromo-1-decene (0.878 g, 4.00 mmol, 0.804 mL), 1-bromotetradecane (1.11 g, 4.00 mmol, 1.19 mL), or 4-methylbenzyl bromide (0.740 g, 4.00 mmol). The new compounds **5f** (0.871 g, 3.12 mmol, 78%), **5g** (1.08 g, 3.20 mmol, 80%), or **5k** (0.863 g, 3.52 mmol, 88%) were obtained as colorless oils

Data for **5f**. NMR ($CDCl_3$, δ in ppm): $^1H$ (500 MHz) 5.81 (m, 1H, C**H**=$CH_2$), 4.97 (m, 2H, CH=C$\mathbf{H}_2$), 3.39 (dd, $^3J_{HH}$ = 7.3, 6.7 Hz, 1H, C**H**CN), 2.04 (m, 2H, C$\mathbf{H}_2$CH=$CH_2$), 1.90 (m, 2H, CHC**HH'**), 1.51 (s, 9H, C(C$\mathbf{H}_3$)$_3$), 1.65-1.25 (m, 12H, (C$\mathbf{H}_2$)$_6$); $^{13}C\{^1H\}$ (125 MHz) 165.2 (s, **C**$O_2$C($CH_3$)$_3$), 139.1 (s, **C**H=$CH_2$), 117.0 (s, CH**C**N), 114.2 (s, CH=**C**$H_2$), 83.8 (s, **C**($CH_3$)$_3$), 38.6 (s, **C**HCN), 27.8 (s, C(**C**$H_3$)$_3$), (**C**$H_2$)$_8$ at 33.6, 29.9, 29.3, 29.1, 29.0, 28.9, 28.8, 26.7 (8 × s). Anal. Calcd. for $C_{17}H_{29}NO_2$ (279.22): C 73.07, H 10.46, N 5.01; found C 72.86, H 10.45, N 5.02.

Data for **5g**. NMR ($CDCl_3$, δ in ppm): $^1H$ (500 MHz) 3.40 (m, 1H, C**H**CN), 1.91 (m, 2H, CHC**HH'**), 1.51 (s, 9H, C(C$\mathbf{H}_3$)$_3$), 1.45-1.25 (m, 24H, (C$\mathbf{H}_2$)$_{12}$), 0.88 (t, $^3J_{HH}$ = 7.1 Hz, 3H, ($CH_2$)$_{12}$C$\mathbf{H}_3$); $^{13}C\{^1H\}$ (125 MHz) 165.2 (s, **C**$O_2$C($CH_3$)$_3$), 117.0 (s, CH**C**N), 83.6 (s, **C**($CH_3$)$_3$), 38.6 (s, **C**HCN), 27.8 (s, C(**C**$H_3$)$_3$), (**C**$H_2$)$_{13}$**C**$H_3$ at 31.9, 29.9, 29.67, 29.65, 29.64, 29.62, 29.5, 29.44, 29.35, 29.2, 28.8, 26.7, 22.7, 14.1 (14 × s). Anal. Calcd. for $C_{21}H_{39}NO_2$ (337.30): C 74.72, H 11.65, N 4.15; found C 72.76, H 11.59, N 3.65.

Data for **5k**. NMR ($CDCl_3$, δ in ppm): $^1H$ (500 MHz) 7.20-7.13 (m, 4H, $C_6\mathbf{H}_4$), 3.61 (dd, $^3J_{HH}$ = 8.4, 5.9 Hz, 1H, C**H**CN), 3.29-3.05 (m, 2H, $C_6\mathbf{H}_4$C**HH'**), 2.35 (s, 3H, $C_6\mathbf{H}_4C\mathbf{H}_3$), 1.47 (s, 9H, $C(C\mathbf{H}_3)_3$); $^{13}C\{^1H\}$ (125 MHz) 164.5 (s, $\mathbf{C}O_2C(CH_3)_3$), 137.3 and 132.4 (2 × s, $\mathbf{C}_{(sub)}$ of $C_6H_4$), 129.4 and 128.9 (2 × s, **C**H of $C_6H_4$), 116.7 (s, CH**C**N), 84.2 (s, $\mathbf{C}(CH_3)_3$), 40.7 (s, **C**HCN), 35.4 (s, $C_6H_4\mathbf{C}H_2$), 27.8 (s, $C(\mathbf{C}H_3)_3$), 21.1 (s, $C_6H_4\mathbf{C}H_3$). Anal. Calcd. for $C_{15}H_{19}NO_2$ (245.14): C 73.44, H 7.81, N 5.71; found C 73.61, H 7.66, N 5.78.

**Synthesis of *t*-butyl 2-cyano-3-(naphthalen-1-yl)propanoate (5h).** In a procedure adapted from one for closely related compounds,[30] a vial was charged with a stir bar, 1-naphthaldehyde (0.469 g, 3.00 mmol, 0.408 mL), 4-dimethylaminopyridine (0.073 g, 0.60 mmol, 20 mol%), Hantzsch ester (0.750 g, 3.00 mmol, 1.00 equiv), *t*-butyl cyanoacetate (0.423 g, 3.00 mmol, 0.429 mL), and ethanol (6.0 mL), sealed with a Teflon cap, and placed in an 80 °C oil bath. The sample was vigorously stirred for 12 h. The vial was opened to the air and allowed to cool. The solvent was removed by rotary evaporation. The residue was chromatographed (silica gel, 3 × 40 cm column, packed and eluted with 9:1 v/v hexanes/ethyl acetate). The solvent was removed from the product containing fractions by rotary evaporation to give **5h** as a yellow oil (0.660 g, 2.35 mmol, 78%). Anal. Calcd. for $C_{18}H_{19}NO_2$ (281.14): C 76.84, H 6.81, N 4.98; found C 77.06, H 6.77, N 4.91.

NMR ($CDCl_3$, δ in ppm): $^1H$ (500 MHz) 7.97 (d, $^3J_{HH}$ = 8.6 Hz, 1H, $C_{10}\mathbf{H}_7$), 7.91 (d, $^3J_{HH}$ = 8.0 Hz, 1H, $C_{10}\mathbf{H}_7$), 7.83 (d, $^3J_{HH}$ = 8.0 Hz, 1H, $C_{10}\mathbf{H}_7$), 7.59 (m, 1H, $C_{10}\mathbf{H}_7$), 7.53 (m, 1H, $C_{10}\mathbf{H}_7$), 7.48 (m, 1H, $C_{10}\mathbf{H}_7$), 3.84 (m, 2H, $C_{10}H_7$C**HH'**), 3.52 (m, 1H, C**H**CN), 1.48 (s, 9H, $C(C\mathbf{H}_3)_3$); $^{13}C\{^1H\}$ (125 MHz) 164.7 (s, $\mathbf{C}O_2C(CH_3)_3$), 134.0, 131.5, 131.2, 129.2, 128.6, 127.9, 126.7, 125.9, and 125.5 (10 × s, $\mathbf{C}_{10}H_7$), 116.6 (s, CH**C**N), 84.4 (s, $\mathbf{C}(CH_3)_3$), 39.8 (s, **C**HCN), 33.2 (s, Ar$\mathbf{C}H_2$), 27.8 (s, $C(\mathbf{C}H_3)_3$).

**3-Ethyl 1,2-dimethyl 3-cyano-4-phenylprop-1-ene-1,2,3-tricarboxylate (6aa,**

**Figure 3.3).** This known compound[2b] was obtained by the general procedure for Figure 3.3 as a colorless oil (0.016 g, 0.048 mmol, 95%, 91:9 *Z*/*E*, 99% ee). $R_f$ = 0.25 (80:20 v/v hexanes/ethyl acetate).

Data for *Z*-**6aa**. NMR ($CDCl_3$, δ in ppm): $^1$H (500 MHz) 7.65-7.40 (m, 5H, **Ph**), 5.88 (s, 1H, C=C**H**), 4.40-4.20 (m, 2H, C**H**$_2$CH$_3$), 3.83 and 3.75 (2 × s, 2 × 3H, 2 × CO$_2$C**H**$_3$), 1.28 (t, $^3J_{HH}$ = 7.0 Hz, 3H, CH$_2$C**H**$_3$); $^{13}$C{$^1$H} (125 MHz) 165.4, 165.1, and 164.0 (3 × s, **C**O$_2$Et and 2 × **C**O$_2$Me), 138.3 (s, **C**=CH), 132.9 (s, *i*-**Ph**), 131.1 and 129.9 (2 × s, *o*- and *m*-**Ph**), 129.5 (C=**C**H), 127.7 (s, *p*-**Ph**), 116.1 (s, **C**N), 64.0 (s, **C**H$_2$CH$_3$), 56.4 (s, **C**CN), 53.0 and 52.4 (2 × s, 2 × CO$_2$**C**H$_3$), 13.7 (s, CH$_2$**C**H$_3$). The configuration (*R*) was assigned by comparison to an authentic sample obtained from a reported procedure.[2b]

Partial data for *E*-**6aa**. $^1$H NMR (500 MHz, $CDCl_3$, δ in ppm): 7.07 (s, 1H, C=C**H**), 4.26-4.11 (m, 2H, C**H**$_2$CH$_3$), 3.72 (s, 3H, CO$_2$C**H**$_3$), 1.22 (t, $^3J_{HH}$ = 7.1 Hz, 3H, CH$_2$C**H**$_3$).

**3-ethyl 1,2-dimethyl 3-cyano-4-phenylbut-1-ene-1,2,3-tricarboxylate (6ab, Figure 3.3).** This new compound was isolated as a colorless oil (0.018 g, 0.050 mmol, >99%, 99:1 *Z*/*E*,[31] 44% ee). $R_f$ = 0.21 (90:10 v/v hexanes/ethyl acetate). Anal. Calcd. for $C_{18}H_{19}NO_6$ (345.12): C 62.60, H 5.55, N 4.06; found C 62.47, H 5.64, N 4.01.

Data for *Z*-**6ab**. NMR ($CDCl_3$, δ in ppm): $^1$H (500 MHz) 7.35-7.30 (m, 5H, **Ph**), 6.22 (s, 1H, C=C**H**), 4.35-4.25 (m, 2H, C**H**$_2$CH$_3$), 3.89 and 3.77 (2 × s, 2 × 3H, 2 × CO$_2$C**H**$_3$), 3.53 (d, $^2J_{HH}$ = 13.7 Hz, 1H, PhC**H**H'), 3.43 (d, $^2J_{HH}$ = 13.7 Hz, 1H, PhCH**H**'), 1.27 (t, $^2J_{HH}$ = 7.1 Hz, 3H, CH$_2$C**H**$_3$); $^{13}$C{$^1$H} (125 MHz) 165.0, 164.7, and 164.1 (3 × s, **C**O$_2$Et and 2 × **C**O$_2$Me), 140.0 (s, **C**=CH), 132.7 (s, *i*-**Ph**), 130.7 and 128.4 (2 × s, *o*- and *m*-**Ph**), 128.2 (C=**C**H), 126.3 (s, *p*-**Ph**), 115.5 (s, **C**N), 64.0 (s, **C**H$_2$CH$_3$), 54.9 (s, **C**CN), 53.1 and 52.4 (2 × s, 2 × CO$_2$**C**H$_3$), 41.2 (s, Ph**C**H$_2$), 13.7 (s, CH$_2$**C**H$_3$).

Partial data for *E*-**6ab**. $^1$H NMR (500 MHz, $CDCl_3$, δ in ppm): 7.07 (s, 1H, C=C**H**), 3.78 and 3.72 (2 × s, 2 × 3H, 2 × $CO_2C\mathbf{H}_3$), 3.66 (d, $^2J_{HH}$ = 13.6 Hz, 1H, PhC**H**H'), 3.60 (d, $^2J_{HH}$ = 13.6 Hz, 1H, PhCH**H'**), 1.21 (t, $^2J_{HH}$ = 7.1 Hz, 3H, $CH_2C\mathbf{H}_3$).

**3-*t*-Butyl 1,2-dimethyl 3-cyano-4-phenylbut-1-ene-1,2,3-tricarboxylate (6ac, Figure 3.3).** This new compound was isolated as a colorless oil (0.019 g, 0.050 mmol, >99%, 99:1 *Z*/*E*,[31,32] 88% ee). $R_f$ = 0.27 (90:10 v/v hexanes/ethyl acetate). Anal. Calcd. for $C_{20}H_{23}NO_6$ (373.15): C 64.33, H 6.21, N 3.75; found C 64.37, H 6.27, N 3.78.

Data for *Z*-**6ac**. NMR ($CDCl_3$, δ in ppm): $^1$H (500 MHz) 7.37-7.28 (m, 5H, **Ph**), 6.20 (s, 1H, C=C**H**), 3.89 and 3.76 (2 × s, 2 × 3H, 2 × $CO_2C\mathbf{H}_3$), 3.53-3.36 (m, 2H, PhC**HH'**), 1.46 (s, 9H, $C(C\mathbf{H}_3)_3$); $^{13}C\{^1H\}$ (125 MHz) 165.1, 164.2, and 163.3 (3 × s, $\mathbf{C}O_2C(CH_3)_3$ and 2 × $\mathbf{C}O_2CH_3$), 140.8 (s, **C**=CH), 133.0 (s, *i*-**Ph**), 130.7 and 128.4 (2 × s, *o*- and *m*-**Ph**), 128.0 (C=**C**H), 125.7 (s, *p*-**Ph**), 115.9 (s, **C**N), 85.8 (s, $\mathbf{C}(CH_3)_3$), 55.7 (s, **C**CN), 53.0 and 52.4 (2 × s, 2 × $CO_2\mathbf{C}H_3$), 41.2 (s, Ph$\mathbf{C}H_2$), 27.5 (s, $C(\mathbf{C}H_3)_3$).

Partial data for *E*-**6ac**. $^1$H NMR (500 MHz, $CDCl_3$, δ in ppm): 7.04 (s, 1H, C=C**H**), 3.78 and 3.69 (2 × s, 2 × 3H, 2 × $CO_2C\mathbf{H}_3$), 1.44 (s, 9H, $C(C\mathbf{H}_3)_3$).

**3-*t*-Butyl 1,2-dimethyl 3-cyanohexa-1,5-diene-1,2,3-tricarboxylate (6ad, Figure 3.3).** This new compound was isolated as a colorless oil (0.016 g, 0.050 mmol, >99%, 99:1 *Z*/*E*,[31] 80% ee). $R_f$ = 0.31 (90:10 v/v hexanes/ethyl acetate). Anal. Calcd. for $C_{16}H_{21}NO_6$ (323.14): C 59.43, H 6.55, N 4.33; found C 59.58, H 6.69, N 4.40.

Data for *Z*-**6ad**. NMR ($CDCl_3$, δ in ppm): $^1$H (500 MHz) 6.44 (s, 1H, C=C**H**), 5.85-5.72 (m, 1H, C**H**=$CH_2$), 5.37-5.26 (m, 2H, CH=C$\mathbf{H}_2$), 3.84 and 3.79 (2 × s, 2 × 3H, 2 × $CO_2C\mathbf{H}_3$), 2.96-2.73 (m, 2H, C**HH'**CH=$CH_2$), 1.50 (s, 9H, $C(C\mathbf{H}_3)_3$); $^{13}C\{^1H\}$ (125 MHz) 164.8, 164.2, and 163.0 (3 × s, $\mathbf{C}O_2C(CH_3)_3$ and 2 × $\mathbf{C}O_2CH_3$), 141.1 (s, **C**=CH), 129.6 (s, **C**H=$CH_2$), 125.1 (s, C=**C**H), 122.1 (s, CH=$\mathbf{C}H_2$), 115.8 (s, **C**N), 85.8 (s, $\mathbf{C}(CH_3)_3$), 54.0 (s, **C**CN), 52.9 and 52.4 (2 × s, 2 × $CO_2\mathbf{C}H_3$), 39.4 (s, $\mathbf{C}H_2CH{=}CH_2$),

27.5 (s, C(**C**$H_3$)$_3$).

Partial data for *E*-**6ad**. $^1$H NMR (500 MHz, $CDCl_3$, δ in ppm): 7.02 (s, 1H, C=C**H**), 1.48 (s, 9H, C(C**H**$_3$)$_3$).

**3-*t*-Butyl 1,2-dimethyl 3-cyanohepta-1,6-diene-1,2,3-tricarboxylate (6ae, Figure 3.3).** This new compound was isolated as a colorless oil (0.017 g, 0.050 mmol, >99%, *Z*/*E* = 99/1,[31] 98% ee). $R_f$ = 0.27 (90:10 v/v hexanes/ethyl acetate). Anal. Calcd. for $C_{16}H_{21}NO_6$ (337.15): C 60.52, H 6.87, N 4.15; found C 60.24, H 6.89, N 4.18.

Data for *Z*-**6ae**. NMR ($CDCl_3$, δ in ppm): $^1$H (500 MHz) 6.48 (s, 1H, C=C**H**), 5.86-5.73 (m, 1H, C**H**=$CH_2$), 5.16-5.01 (m, 2H, CH=C**H**$_2$), 3.84 and 3.79 (2 × s, 2 × 3H, 2 × $CO_2$C**H**$_3$), 2.37-2.03 (m, 4H, (C**H**$_2$)$_2$CH=$CH_2$), 1.51 (s, 9H, C(C**H**$_3$)$_3$); $^{13}$C{$^1$H} (125 MHz) 164.8, 164.2, and 163.2 (3 × s, **C**$O_2$C($CH_3$)$_3$ and 2 × **C**$O_2$$CH_3$), 142.0 (s, **C**=CH), 135.6 (s, **C**H=$CH_2$), 124.6 (s, C=**C**H), 116.5 (s, CH=**C**H$_2$), 116.0 (s, **C**N), 85.7 (s, **C**($CH_3$)$_3$), 53.9 (s, **C**CN), 52.9 and 52.4 (2 × s, 2 × $CO_2$**C**$H_3$), 34.3 (s, **C**H$_2$CH=$CH_2$), 29.4 (s, **C**H$_2$CH$_2$CH=$CH_2$), 27.5 (s, C(**C**$H_3$)$_3$).

Partial data for *E*-**6ae**. $^1$H NMR (500 MHz, $CDCl_3$, δ in ppm): 7.06 (s, 1H, C=C**H**), 3.86 (s, 3H, $CO_2$C**H**$_3$), 1.49 (s, 9H, C(C**H**$_3$)$_3$).

**3-*t*-Butyl 1,2-dimethyl 3-cyanotrideca-1,12-diene-1,2,3-tricarboxylate (6af, Figure 3.3).** This new compound was isolated as a colorless viscous oil (0.020 g, 0.048 mmol, 96%, 98:2 *Z*/*E*,[31] 70% ee). $R_f$ = 0.45 (90:10 v/v hexanes/ethyl acetate). Anal. Calcd. for $C_{23}H_{35}NO_6$ (421.25): C 65.53, H 8.37, N 3.32; found C 65.61, H 8.21, N 3.32.

Data for *Z*-**6af**. NMR ($CDCl_3$, δ in ppm): $^1$H (500 MHz) 6.46 (s, 1H, C=C**H**), 5.84-5.73 (m, 1H, C**H**=$CH_2$), 5.03-4.92 (m, 2H, CH=C**H**$_2$), 3.83 and 3.79 (2 × s, 2 × 3H, 2 × $CO_2$C**H**$_3$), 2.14-1.94 (m, 4H, C**H**$_2$($CH_2$)$_6$C**H**$_2$CH=$CH_2$), 1.51 (s, 9H, C(C**H**$_3$)$_3$), 1.46-1.22 (m, 12H, (C**H**$_2$)$_6$$CH_2$CH=$CH_2$); $^{13}$C{$^1$H} (125 MHz) 164.9, 164.3, and 163.5 (3 × s, **C**$O_2$C($CH_3$)$_3$ and 2 × **C**$O_2$$CH_3$), 142.3 (s, **C**=CH), 139.1 (s, **C**H=$CH_2$), 124.3 (s, C=**C**H),

116.3 (s, **C**N), 114.2 (s, CH=**C**$H_2$), 85.5 (s, **C**$(CH_3)_3$), 54.3 (s, **C**CN), 52.9 and 52.4 (2 × s, 2 × $CO_2$**C**$H_3$), 35.1 (s, **C**$H_2$CH=$CH_2$), 33.8 (s, C**C**$H_2$), 27.5 (s, C(**C**$H_3)_3$), $CH_2$(**C**$H_2)_6$ at 29.3, 29.2, 29.1, 29.0, 28.8, 25.1 (6 × s).

Partial data for *E*-**6af**. $^1$H NMR (500 MHz, $CDCl_3$, δ in ppm): 7.02 (s, 1H, C=C**H**), 3.85 and 3.82 (2 × s, 2 × 3H, 2 × $CO_2$C**H**$_3$), 1.48 (s, 9H, C(C**H**$_3)_3$).

**3-*t*-Butyl 1,2-dimethyl 3-cyanoheptadec-1-ene-1,2,3-tricarboxylate (6ag, Figure 3.3).** This new compound was isolated as a yellow viscous oil (0.021 g, 0.044 mmol, 88%, 98:2 *Z*/*E*,[31] 80% ee). $R_f$ = 0.55 (90:10 v/v hexanes/ethyl acetate). Anal. Calcd. for $C_{27}H_{45}NO_6$ (479.32): C 67.61, H 9.46, N 2.92; found C 67.09, H 9.28, N 2.93.

Data for *Z*-**6ag**. NMR ($CDCl_3$, δ in ppm): $^1$H (500 MHz) 6.46 (s, 1H, C=C**H**), 3.83 and 3.79 (2 × s, 2 × 3H, 2 × $CO_2$C**H**$_3$), 2.15 (m, 1H, C**H**H'$(CH_2)_{12}CH_3$), 1.98 (m, 1H, CH**H'**$(CH_2)_{12}CH_3$), 1.51 (s, 9H, C(C**H**$_3)_3$), 1.40-1.20 (m, 24H, (C**H**$_2)_{12}CH_3$), 0.88 (t, $^3J_{HH}$ = 7.1 Hz, 3H, $(CH_2)_{12}$C**H**$_3$); $^{13}$C{$^1$H} (125 MHz) 164.9, 164.3, and 163.5 (3 × s, **C**$O_2C(CH_3)_3$ and 2 × **C**$O_2CH_3$), 142.3 (s, **C**=CH), 124.3 (s, C=**C**H), 116.3 (s, **C**N), 114.2 (s, CH=**C**$H_2$), 85.5 (s, **C**$(CH_3)_3$), 54.3 (s, **C**CN), 52.9 and 52.4 (2 × s, 2 × $CO_2$**C**$H_3$), 27.5 (s, C(**C**$H_3)_3$), (**C**$H_2)_{13}$**C**$H_3$ at 35.2, 31.9, 29.67, 29.66, 29.64, 29.61, 29.55, 29.5, 29.4, 29.2, 29.1, 25.1, 22.7, 14.1 (14 × s). Partial data for *E*-**6ag**. $^1$H NMR (500 MHz, $CDCl_3$, δ in ppm): 7.02 (s, 1H, C=C**H**), 3.85 and 3.83 (2 × s, 2 × 3H, 2 × $CO_2$C**H**$_3$), 1.48 (s, 9H, C(C**H**$_3)_3$).

**3-*t*-Butyl 1,2-dimethyl 3-cyano-4-(naphthalen-1-yl)but-1-ene-1,2,3-tricarboxylate (6ah, Figure 3.3).** This new compound was isolated as a yellow viscous oil (0.021 g, 0.049 mmol, 99%, >99:<1 *Z*/*E*,[31] 88% ee). $R_f$ = 0.25 (90:10 v/v hexanes/ethyl acetate). Anal. Calcd. for $C_{24}H_{25}NO_6$ (423.17): C 68.07, H 5.95, N 3.31; found C 68.15, H 6.05, N 3.38.

Data for *Z*-**6ah**. NMR ($CDCl_3$, δ in ppm): $^1$H (500 MHz) 8.13 (d, $^3J_{HH}$ = 8.5 Hz,

1H, $C_{10}\mathbf{H}_7$), 7.90-7.80 (m, 2H, $C_{10}\mathbf{H}_7$), 7.60-7.41 (m, 4H, $C_{10}\mathbf{H}_7$), 6.26 (s, 1H, C=C**H**), 4.19 (d, $^2J_{HH}$ = 14.6 Hz, 1H, ArC**H**H'), 3.91 and 3.74 (2 × s, 2 × 3H, 2 × $CO_2C\mathbf{H}_3$), 3.86 (d, $^2J_{HH}$ = 14.6 Hz, 1H, ArCH**H**'), 1.39 (s, 9H, $C(C\mathbf{H}_3)_3$); $^{13}C\{^1H\}$ (125 MHz) 165.3, 164.3, and 163.6 (3 × s, $\mathbf{C}O_2C(CH_3)_3$ and 2 × $\mathbf{C}O_2CH_3$), 140.4 (s, **C**=CH), 133.9, 132.5, 129.5, 129.1, 128.8, 128.7, 126.5, 126.2, 125.8, 125.0, and 124.0 (11 × s, naphthyl $\mathbf{C}_{10}H_7$ and C=**C**H), 116.3 (s, **C**N), 85.9 (s, $\mathbf{C}(CH_3)_3$), 55.0 (s, **C**CN), 53.0 and 52.4 (2 × s, 2 × $CO_2\mathbf{C}H_3$), 36.8 (s, Ar$\mathbf{C}H_2$), 27.4 (s, $C(\mathbf{C}H_3)_3$).

Partial data for *E*-**6<u>a</u>h**. $^1$H NMR (500 MHz, $CDCl_3$, δ in ppm): 6.94 (s, 1H, C=C**H**), 4.19 (d, $^2J_{HH}$ = 14.6 Hz, 1H, ArC**H**H'), 3.78 (s, 3H, $CO_2C\mathbf{H}_3$), 1.41 (s, 9H, $C(C\mathbf{H}_3)_3$).

**3-*t*-Butyl 1,2-dimethyl 3-cyano-4-(furan-2-yl)but-1-ene-1,2,3-tricarboxylate (6<u>a</u>i, Figure 3.3).** This new compound was isolated as a yellow oil (0.015 g, 0.040 mmol, 82%, >99:<1 *Z*/*E*,[31] 88% ee). $R_f$ = 0.22 (90:10 v/v hexanes/ethyl acetate). Anal. Calcd. for $C_{18}H_{21}NO_7$ (363.13): C 59.50, H 5.83, N 3.85; found C 58.72, H 5.81, N 3.83.

Data for *Z*-**6<u>a</u>i**. NMR ($CDCl_3$, δ in ppm): $^1$H (500 MHz) 7.38 (m, 1H, furanyl O–C**H**), 6.40 (s, 1H, C=C**H**), 6.33 (m, 2H, furanyl O–CH=C**H**–C**H**), 3.86 and 3.78 (2 × s, 2 × 3H, 2 × $CO_2C\mathbf{H}_3$), 3.64 (d, $^2J_{HH}$ = 15.1 Hz, 1H, ArC**H**H'), 3.43 (d, $^2J_{HH}$ = 15.1 Hz, 1H, ArCH**H**'), 1.49 (s, 9H, $C(C\mathbf{H}_3)_3$); $^{13}C\{^1H\}$ (125 MHz) 164.7, 164.3, and 162.8 (3 × s, $\mathbf{C}O_2C(CH_3)_3$ and 2 × $\mathbf{C}O_2CH_3$), 147.5 (s, furanyl O-**C**($CH_2$)=), 142.8 (s, furanyl O–**C**H=), 140.0 (s, **C**=CH), 126.1 (C=**C**H), 115.8 (s, **C**N), 110.6 and 110.1 (2 × s, furanyl **C**H–**C**H=CH), 85.9 (s, $\mathbf{C}(CH_3)_3$), 54.0 (s, **C**CN), 53.0 and 52.4 (2 × s, 2 × $CO_2\mathbf{C}H_3$), 34.4 (s, Ar$\mathbf{C}H_2$), 27.5 (s, $C(\mathbf{C}H_3)_3$).

Partial data for *E*-**6<u>a</u>i**. $^1$H NMR (500 MHz, $CDCl_3$, δ in ppm): 7.05 (s, 1H, C=C**H**), 3.81 and 3.77 (2 × s, 2 × 3H, 2 × $CO_2C\mathbf{H}_3$), 1.51 (s, 9H, $C(C\mathbf{H}_3)_3$).

**3-*t*-Butyl 1,2-dimethyl 4-(4-bromophenyl)-3-cyanobut-1-ene-1,2,3-tricarboxylate (6<u>a</u>j, Figure 3.3).** This new compound was isolated as a colorless viscous

oil (0.016 g, 0.035 mmol, 70% or 71-68%, six replicate experiments), 97-96:3-4 *Z*/*E* (97.5:2.5 average crude),[31] 85% ee. $R_f$ = 0.27 (90:10 v/v hexanes/ethyl acetate). Anal. Calcd. for $C_{20}H_{22}BrNO_6$ (451.06): C 53.11, H 4.90, N 3.10; found C 51.25, H 4.74, N 2.99.

Data for *Z*-**6aj**. NMR ($CDCl_3$, δ in ppm): $^1$H (500 MHz) 7.49-7.43 (m, 2H, $C_6$**H**$_4$), 7.25-7.21 (m, 2H, $C_6$**H**$_4$), 6.19 (s, 1H, C=C**H**), 3.88 and 3.77 (2 × s, 2 × 3H, 2 × $CO_2C$**H**$_3$), 3.46-3.33 (m, 2H, $C_6H_4C$**HH'**), 1.48 (s, 9H, C(C**H**$_3$)$_3$); $^{13}$C{$^1$H} (125 MHz) 165.0, 164.1, and 163.1 (3 × s, **C**$O_2C(CH_3)_3$ and 2 × **C**$O_2CH_3$), 140.4 (s, **C**=CH), 132.0 (s, **C**$_{(sub)}$ of $C_6H_4$), 132.4 and 131.5 (2 × s, **C**H of $C_6H_4$), 125.8 (C=**C**H), 122.3 (s, **C**$_{(sub)}$ of $C_6H_4$), 115.6 (s, **C**N), 86.1 (s, **C**$(CH_3)_3$), 55.5 (s, **C**CN), 53.0 and 52.5 (2 × s, 2 × $CO_2$**C**$H_3$), 40.3 (s, $C_6H_4$**C**$H_2$), 27.5 (s, C(**C**$H_3$)$_3$).

Partial data for *E*-**6aj**. $^1$H NMR (500 MHz, $CDCl_3$, δ in ppm): 7.04 (s, 1H, C=C**H**), 3.79 and 3.72 (2 × s, 2 × 3H, 2 × $CO_2C$**H**$_3$), 1.52 (s, 9H, C(C**H**$_3$)$_3$).

**3-*t*-Butyl 1,2-dimethyl 3-cyano-4-(*p*-tolyl)-but-1-ene-1,2,3-tricarboxylate (6ak, Figure 3.3).** This new compound was isolated as a colorless viscous oil (0.017 g, 0.045 mmol, 90%, 98:2 *Z*/*E*,[31] 91% ee). $R_f$ = 0.38 (90:10 v/v hexanes/ethyl acetate). Anal. Calcd. for $C_{12}H_{25}NO_6$ (387.17): C 65.10, H 6.50, N 3.62; found C 63.75, H 6.26, N 3.62.

Data for *Z*-**6ak**. NMR ($CDCl_3$, δ in ppm): $^1$H (500 MHz) 7.25-7.20 (m, 2H, $C_6$**H**$_4$), 7.14-7.09 (m, 2H, $C_6$**H**$_4$), 6.20 (s, 1H, C=C**H**), 3.88 and 3.77 (2 × s, 2 × 3H, 2 × $CO_2C$**H**$_3$), 3.46 (d, $^2J_{HH}$ = 13.8 Hz, 1H, $C_6H_4C$**H**H'), 3.34 (d, $^2J_{HH}$ = 13.8 Hz, 1H, $C_6H_4CH$**H'**), 2.33 (s, 3H, $C_6H_4C$**H**$_3$), 1.46 (s, 9H, C(C**H**$_3$)$_3$); $^{13}$C{$^1$H} (125 MHz) 165.1, 164.2, and 163.4 (3 × s, **C**$O_2C(CH_3)_3$ and 2 × **C**$O_2CH_3$), 140.9 (s, **C**=CH), 137.7 (s, **C**$_{(sub)}$ of $C_6H_4$), 130.6 and 129.1 (2 × s, **C**H of $C_6H_4$), 130.0 (s, **C**$_{(sub)}$ of $C_6H_4$), 125.6 (C=**C**H), 115.9 (s, **C**N), 85.8 (s, **C**$(CH_3)_3$), 55.9 (s, **C**CN), 53.0 and 52.4 (2 × s, 2 × $CO_2$**C**$H_3$), 40.8 (s, $C_6H_4$**C**$H_2$), 27.5 (s, C(**C**$H_3$)$_3$), 21.1 (s, $C_6H_4$**C**$H_3$).

Partial data for *E*-**6ak**. $^1$H NMR (500 MHz, $CDCl_3$, δ in ppm): 7.02 (s, 1H, C=C**H**), 3.77 and 3.70 (2 × s, 2 × 3H, 2 × $CO_2C\mathbf{H}_3$), 1.44 (s, 9H, $C(C\mathbf{H}_3)_3$).

**3-*t*-Butyl 1,2-diethyl 3-cyano-4-phenylbut-1-ene-1,2,3-tricarboxylate (6bc, Figure 3.3).** This new compound was isolated as a colorless oil (0.020 g, 0.050 mmol, >99%, 99:1 *Z*/*E*,[31] 83% ee). $R_f$ = 0.25 (90:10 v/v hexanes/ethyl acetate). Anal. Calcd. for $C_{22}H_{27}NO_6$ (401.18): C 65.82, H 6.78, N 3.49; found C 66.43, H 7.03, N 3.64.

Data for *Z*-**6bc**. NMR ($CDCl_3$, δ in ppm): $^1$H (500 MHz) 7.37-7.30 (m, 5H, **Ph**), 6.20 (s, 1H, C=C**H**), 4.41-4.19 (m, 2H, $CO_2C\mathbf{H}_2CH_3$), 4.21 (q, $^3J_{HH}$ = 7.1 Hz, 2H, $CO_2C\mathbf{H}'_2CH'_3$), 3.52 (d, $^2J_{HH}$ = 13.7 Hz, 1H, PhC**H**H'), 3.39 (d, $^2J_{HH}$ = 13.7 Hz, 1H, PhCH**H'**), 1.46 (s, 9H, $C(C\mathbf{H}_3)_3$), 1.36 (t, $^3J_{HH}$ = 7.1 Hz, 3H, $CO_2CH_2C\mathbf{H}_3$), 1.29 (t, $^3J_{HH}$ = 7.1 Hz, 3H, $CO_2CH'_2C\mathbf{H}'_3$); $^{13}C\{^1H\}$ (125 MHz) 164.6, 163.8, and 163.4 (3 × s, $\mathbf{C}O_2C(CH_3)_3$ and 2 × $\mathbf{C}O_2CH_2CH_3$), 140.3 (s, **C**=CH), 133.2 (s, *i*-**Ph**), 130.7 and 128.4 (2 × s, *o*- and *m*-**Ph**), 128.0 (C=**C**H), 126.2 (s, *p*-**Ph**), 116.0 (s, **C**N), 85.7 (s, $\mathbf{C}(CH_3)_3$), 62.4 and 61.4 (2 × s, 2 × $CO_2\mathbf{C}H_2CH_3$), 55.7 (s, **C**CN), 41.2 (s, Ph$\mathbf{C}H_2$), 27.5 (s, $C(\mathbf{C}H_3)_3$), 14.0 and 13.8 (2 × s, 2 × $CO_2CH_2\mathbf{C}H_3$).

Partial data for *E*-**6bc**. $^1$H NMR (500 MHz, $CDCl_3$, δ in ppm): 7.03 (s, 1H, C=C**H**), 1.43 (s, 9H, $C(C\mathbf{H}_3)_3$).

**(*E*)-Di-*t*-butyl 3-cyano-4-phenylbut-1-ene-1,3-dicarboxylate (*E*-6cc, Figure 3.3),** This new compound was isolated as a colorless oil (0.0095 g, 0.027 mmol, 53%, <1/>99 *Z*/*E*,[33] 94% ee). $R_f$ = 0.24 (90:10 v/v hexanes/ethyl acetate). Anal. Calcd. for $C_{21}H_{27}NO_4$ (357.19): C 70.56, H 7.61, N 3.92; found C 69.82, H 7.67, N 3.81.

NMR ($CDCl_3$, δ in ppm): $^1$H (500 MHz) 7.37-7.28 (m, 5H, **Ph**), 6.86 (d, $^3J_{HH}$ = 15.6 Hz, 1H, C**H**=$CHCO_2C(CH_3)_3$), 6.19 (d, $^3J_{HH}$ = 15.6 Hz, 1H, CH=C**H**$CO_2C(CH_3)_3$), 3.36 (d, $^2J_{HH}$ = 13.6 Hz, 1H, PhC**H**H'), 3.10 (d, $^2J_{HH}$ = 13.6 Hz, 1H, PhCH**H'**), 1.50 and 1.39 (2 × s, 2 × 9H, 2 × $C(C\mathbf{H}_3)_3$); $^{13}C\{^1H\}$ (125 MHz) 164.6 and 164.1 (2 × s, 2 ×

**C**$O_2C(CH_3)_3$), 139.4 (s, **C**=CH), 133.2 (s, *i*-**Ph**), 130.3 and 128.5 (2 × s, *o*- and *m*-**Ph**), 128.1 (C=**C**H), 126.5 (s, *p*-**Ph**), 116.7 (s, **C**N), 85.4 and 81.5 (2 × s, 2 × **C**$(CH_3)_3$), 54.0 (s, **C**CN), 43.5 (s, Ph**C**$H_2$), 28.5 and 27.7 (2 × s, 2 × C(**C**$H_3)_3$).

### 3.6. References

(1) (a) Corey, E. J.; Guzman-Perez, A. The Catalytic Enantioselective Construction of Molecules with Quaternary Carbon Stereocenters. *Angew. Chem., Int. Ed.* **1998**, *37*, 388-401. Der katalytische enantioselektive Aufbau von Molekülen mit quartären Kohlenstoff-Stereozentren. *Angew. Chem.* **1998**, *110*, 402-415. (b) Christoffers, J.; Mann, A. Enantioselective Construction of Quaternary Stereocenters. *Angew. Chem., Int. Ed.* **2001**, *40*, 4591-4597. Enantioselektiver Aufbau quartärer Stereozentren. *Angew. Chem.* **2001**, *113*, 4725-4732. (c) Douglas, C. J.; Overman, L. E. Catalytic asymmetric synthesis of all-carbon quaternary stereocenters. *Proc. Natl. Acad. Sci. U. S. A.* **2004**, *101*, 5363-5367. (d) Christoffers, J.; Baro, A. Stereoselective Construction of Quaternary Stereocenters. *Adv. Synth. Catal.* **2005**, *347*, 1473-1482. (e) Trost, B. M.; Jiang, C. Catalytic Enantioselective Construction of All-Carbon Quaternary Stereocenters. *Synthesis* **2006**, 369-396. (f) Bella, M.; Gasperi, T. Organocatalytic Formation of Quaternary Stereocenters. *Synthesis* **2009**, *2009*, 1583-1614. (g) Hawner, C.; Alexakis, A. Metal-catalyzed asymmetric conjugate addition reaction: formation of quaternary stereocenters. *Chem. Commun.* **2010**, *46*, 7295-7306. (h) Wang, B.; Tu, Y. Q. Stereoselective Construction of Quaternary Carbon Stereocenters via a Semipinacol Rearrangement Strategy. *Acc. Chem. Res.* **2011**, *44*, 1207-1222. (i) Minko, Y.; Marek, I. Stereodefined acyclic trisubstituted metal enolates towards the asymmetric formation of quaternary carbon stereocentres. *Chem. Commun.* **2014**, *50*, 12597-12611. (j) Quasdorf, K. W.; Overman, L. E. Catalytic enantioselective synthesis of quaternary carbon stereocentres. *Nature* **2014**, *516*, 181-191. (k) Liu, Y.; Han, S.-J.; Liu, W.-B.; Stoltz, B. M. Catalytic Enantioselective Construction of Quaternary Stereocenters: Assembly of Key Building Blocks for the Synthesis of Biologically Active Molecules. *Acc. Chem. Res.* **2015**, *48*, 740-751. (l) Long, R.; Huang, J.; Gong, J.; Yang, Z. Direct construction of vicinal all-

carbon quaternary stereocenters in natural product synthesis. *Nat. Prod. Rep.* **2015**, *32*, 1584-1601. (m) Büschleb, M.; Dorich, S.; Hanessian, S.; Tao, D.; Schenthal, K. B.; Overman, L. E. Synthetic Strategies toward Natural Products Containing Contiguous Stereogenic Quaternary Carbon Atoms. *Angew. Chem., Int. Ed.* **2016**, *55*, 4156-4186. Strategien für die Synthese von Naturstoffen mit benachbarten stereogenen quartären Kohlenstoffatomen. *Angew. Chem.* **2016**, *128*, 4226-4258. (n) Feng, J.; Holmes, M.; Krische, M. J. Acyclic Quaternary Carbon Stereocenters via Enantioselective Transition Metal Catalysis. *Chem. Rev.* **2017**, *117*, 12564-12580. (o) Li, X.; Ragab, S. S.; Liu, G.; Tang, W. Enantioselective formation of quaternary carbon stereocenters in natural product synthesis: a recent update. *Nat. Prod. Rep.* **2020**, doi: 10.1039/C9NP00039A.

(2) (a) Wang, X.; Kitamura, M.; Maruoka, K. New, Chiral Phase Transfer Catalysts for Effecting Asymmetric Conjugate Additions of α-Alkyl- α-cyanoacetates to Acetylenic Esters. *J. Am. Chem. Soc.* **2007**, *129*, 1038-1039. (b) Hasegawa, Y.; Gridnev, D. I.; Ikariya, T. Enantioselective and *Z*/*E*-Selective Conjugate Addition of α-Sibstituted Cyanoacetates to Acetylenic Esters Catalyzed by Bifunctional Ruthenium and Iridium Complexes. *Angew. Chem., Int. Ed.* **2010**, *49*, 8157-8160. *Angew. Chem.* **2010**, *122*, 8333-8336.

(3) Some syntheses in which α-cyanocarbonyl intermediates are differentially functionalized: (a) Mermerian, A. H.; Fu, G. C. Nucleophile-Catalyzed Asymmetric Acylations of Silyl Ketene Imines: Application to the Enantioselective Synthesis of Verapamil. *Angew. Chem., Int. Ed.* **2005**, *44*, 949-952. *Angew. Chem.* **2005**, *117*, 971-974. (b) Levin, S.; Nani, R. R.; Reisman, S. E. Enantioselective Total Synthesis of (+)-Salvileucalin B. *J. Am. Chem. Soc.* **2011**, *133*, 774-776.

(4) For reviews, see (a) Taylor, M. S.; Jacobsen, E. N. Asymmetric Catalysis by Chiral Hydrogen-Bond Donors. *Angew. Chem., Int. Ed.* **2006**, *45,* 1520-1543;

Asymmetrische Katalyse durch chirale Wasserstoffbrückendonoren. *Angew. Chem.* **2006**, *118*, 1550-1573. (b) Doyle, A. G.; Jacobsen, E. N. Small-Molecule H-Bond Donors in Asymmetric Catalysis. *Chem. Rev.* **2007**, *107*, 5713-5743. (c) Yu, X.; Wang, W. Hydrogen-Bond-Mediated Asymmetric Catalysis. *Chem. Asian J.* **2008**, *3*, 516-532. (d) Miyabe, H.; Takemoto, Y. Discovery and Application of Asymmetric Reaction by Multi-Functional Thioureas. *Bull. Chem. Soc. Jpn.* **2008**, *81*, 785-795. (e) Held, F. E.; Tsogoeva, S. B. Asymmetric Cycloaddition Reactions Catalyzed by Bifunctional Thiourea and Squaramide Organocatalysts: Recent Advances. *Catal. Sci. Technol.* **2016**, *6*, 645-667.

(5) For some examples, see (a) Kang, G.; Wu, Q.; Liu, M.; Xu, Q.; Chen, Z.; Chen, W.; Luo, Y.; Ye, W.; Jiang, J.; Wu, H. Catalytic Stereoselective Conjugate Addition of Oxindole to Electron-Deficient Alkynes. *Adv. Synth. Catal.* **2013**, *355*, 315-320. (b) Wendlandt, A. E.; Vangal, P.; Jacobsen, E. N. Quaternary stereocentres via an enantioconvergent catalytic $S_N1$ reaction. *Nature* **2018**, *556*, 447-451.

(6) (a) Ganzmann, C.; Gladysz, J. A. Phase Transfer of Enantiopure Werner Cations into Organic Solvents: An Overlooked Family of Chiral Hydrogen Bond Donors for Enantioselective Catalysis. *Chem. Eur. J.* **2008**, *14*, 5397-5400. (b) Maximuck, W. J.; Ganzmann, C.; Alvi, S.; Hooda, K. R.; Gladysz, J. A. Rendering Classical Hydrophilic Enantiopure Werner Salts $[M(en)_3]^{n+}$ $nX^-$ Lipophilic (M/*n* = Cr/3, Co/3, Rh/3, Ir/3, Pt/4); New Chiral Hydrogen Bond Donor Catalysts and Enantioselectivities as a Function of Metal and Charge. *Dalton Trans*. **2020**, *49*, 3680-3691.

(7) (a) Lewis, K. G.; Ghosh, S. K.; Bhuvanesh, N.; Gladysz, J. A. Cobalt(III) Werner Complexes with 1,2-Diphenylethylenediamine Ligands: Readily Available, Inexpensive, and Modular Chiral Hydrogen Bond Donor Catalysts for Enantioselective Organic Synthesis. *ACS Cent. Sci.* **2015**, *1*, 50-56. (b) Kumar, A.; Ghosh, S. K.; Gladysz, J. A. Tris(1,2-diphenylethylenediamine)cobalt(III) Complexes: Chiral Hydrogen Bond

Donor Catalysts for Enantioselective α-Aminations of 1,3-Dicarbonyl Compounds. *Org. Lett.* **2016**, *18*, 760-763. (c) Joshi, H.; Ghosh, S. K.; Gladysz, J. A. Enantioselective Additions of Stabilized Carbanions to Imines Generated from α-Amido Sulfones By Using Lipophilic Salts of Chiral Tris(1,2-diphenylethylenediamine) Cobalt(III) Trications as Hydrogen Bond Donor Catalysts. *Synthesis* **2017**, *49*, 3905-3915. (d) Maximuck, W. J.; Gladysz, J. A. Lipophilic Chiral Cobalt(III) Complexes of Hexaamine Ligands; Efficacies as Enantioselective Hydrogen Bond Donor Catalysts. *Mol. Catal.* **2019**, *473*, 110360 (this journal has replaced conventional pagination by article numbers). (e) Kabes, C. Q.; Maximuck, W. J.; Ghosh, S. K.; Kumar, A.; Bhuvanesh, N.; Gladysz, J. A. Chiral Tricationic tris(1,2-diphenylethylenediamine) Cobalt(III) Hydrogen Bond Donor Catalysts with Defined Carbon/Metal Configurations; Matched/Mismatched Effects upon Enantioselectivities with Enantiomeric Chiral Counter Anions. *ACS Catal.* **2020**, *10*, 3249-3263.

(8) Ghosh, S. K.; Ganzmann, C.; Bhuvanesh, N.; Gladysz, J. A. Werner Complexes with ω-Dimethylaminoalkyl Substituted Ethylenediamine Ligands: Bifunctional Hydrogen-Bond-Donor Catalysts for Highly Enantioselective Michael Additions. *Angew. Chem., Int. Ed.* **2016**, *55*, 4356-4360; Werner-Komplexe mit ω-Dimethylaminoalkyl-substitutierten Ethylendiaminliganden: bifunktionale H-Brückendonor-Katalysatoren für hoch enantioselektive Michael-Additionen. *Angew. Chem.* **2016**, *128*, 4429-4433.

(9) (a) Scherer, A.; Mukherjee, T.; Hampel, F.; Gladysz, J. A. Metal Templated Hydrogen Bond Donors as 'Organocatalysts' for Carbon-Carbon Bond Forming Reactions: Syntheses, Structures, and Reactivities of 2-Guanidinobenzimidazole Cyclopentadienyl Ruthenium Complexes. *Organometallics* **2014**, *33*, 6709-6722. (b) Mukherjee, T.; Ganzmann, C.; Bhuvanesh, N.; Gladysz, J. A. Syntheses of Enantiopure Bifunctional 2-Guanidinobenzimidazole Cyclopentadienyl Ruthenium Complexes: Highly

Enantioselective Organometallic Hydrogen Bond Donor Catalysts for Carbon-Carbon Bond Forming Reactions. *Organometallics* **2014**, *33*, 6723-6737. (c) Wititsuwannakul, T.; Mukherjee, T.; Hall, M. B.; Gladysz, J. A. Computational Investigations of Enantioselection in Carbon-Carbon Bond Forming Reactions of Ruthenium Guanidino-benzimidazole Second Coordination Sphere Hydrogen Bond Donor Catalysts. *Organometallics* **2020**, *39*, 1149-1162. (d) Mukherjee, T.; Ghosh, S. K.; Wititsuwannakul, T.; Bhuvanesh, N.; Gladysz, J. A. A New Family of Chiral-at-Metal Ruthenium Complexes with Guanidinobenzimidazole and Pentaphenylcyclopentadienyl Ligands: Synthesis, Resolution, and Preliminary Screening as Enantioselective Second Coordination Sphere Hydrogen Bond Donor Catalysts. *Organometallics* **2020**, *39*, 1163-1175.

(10) (a) Chen, L.-A.; Tang, X.; Xi, J.; Xu, W.; Gong, L.; Meggers, E. Chiral-at-Metal Octahedral Iridium Catalyst for the Asymmetric Construction of an All-Carbon Quaternary Stereocenter. *Angew. Chem., Int. Ed.* **2013**, *52*, 14021-14025 and *Angew. Chem.* **2013**, *125*, 14271-14275. (b) Huo, H.; Fu, C.; Wang, C.; Harms, K.; Meggers, E. Metal-templated Enantioselective Enamine/H-bonding Dual Activation Catalysis. *Chem. Commun*. **2014**, *50*, 10409-10411. (c) Hu, Y.; Zhou, Z.; Gong, L.; Meggers, E. Asymmetric aza-Henry reaction to provide oxindoles with quaternary carbon stereocenter catalyzed by a metal-templated chiral Brønsted base. *Org. Chem. Front.* **2015**, *2*, 968-972. (d) Ding, X.; Lin, H.; Gong, L.; Meggers, E. Enantioselective Sulfa-Michael Addition to α,β-Unsaturated γ-Oxoesters Catalyzed by a Metal-Templated Chiral Brønsted Base. *Asian J. Org. Chem.* **2015**, *4*, 434-437. (e) Xu, W.; Shen, X.; Ma, Q.; Gong, L.; Meggers, E. Restricted Conformation of a Hydrogen Bond Mediated Catalyst Enables the Highly Efficient Enantioselective Construction of an All-Carbon Quaternary Stereocenter. *ACS Catal.* **2016**, *6*, 7641-7646. (f) Xu, W.; Arieno, M.; Löw, H.; Huang, K.; Xie, X.; Cruchter,

T.; Ma, Q.; Xi, J.; Huang, B.; Wiest, O.; Gong, L.; Meggers, E. Metal-Templated Design: Enantioselective Hydrogen-Bond-Driven Catalysis Requiring Only Parts-per-Million Catalyst Loading. *J. Am. Chem. Soc.* **2016,** *138*, 8774-8780. (g) Ding, X.; Tian, C.; Hu, Y.; Gong, L.; Meggers, E. Tuning the Basicity of a Metal-Templated Brønsted Base to Facilitate the Enantioselective Sulfa-Michael Addition of Aliphatic Thiols to α,β-Unsaturated *N*-Acylpyrazoles. *Eur. J. Org. Chem.* **2016**, *2016*, 887-890.

(11) (a) Belokon, Y. N.; Maleev, V. I.; North, M.; Larionov, V. A.; Savel'yeva, T. F.; Nijland, A.; Nelyubina, Y. V. Chiral Octahedral Complexes of $Co^{III}$ As a Family of Asymmetric Catalysts Operating under Phase Transfer Conditions. *ACS Catal.* **2013**, *3*, 1951-1955. (b) Maleev, V. I.; North, M.; Larionov, V. A.; Fedyanin, I. V.; Savel'yeva, T. F.; Moscalenko, M. A.; Smolyakov, A. F.; Belokon, Y. N. Chiral Octahedral Complexes of Cobalt(III) as "Organic Catalysts in Disguise" for the Asymmetric Addition of a Glycine Schiff Base Ester to Activated Olefins. *Adv. Synth. Catal.* **2014**, *356*, 1803-1810. (c) Larionov, V. A.; Markelova, E. P.; Smol'yakov, A. F.; Savel'yeva, T. F.; Maleev, V. I.; Belokon, Y. N. Chiral octahedral complexes of Co(III) as catalysts for asymmetric epoxidation of chalcones under phase transfer conditions. *RSC Adv.* **2015**, *5*, 72764-72771. (d) Rulev, Y. A.; Larionov, V. A.; Lokutova, A. V.; Moskalenko, M. A.; Lependina, O. L.; Maleev, V. I.; North, M.; Belokon, Y. N. Chiral Cobalt(III) Complexes as Bifunctional Brønsted Acid-Lewis Base Catalysts for the Preparation of Cyclic Organic Carbonate. *ChemSusChem* **2016**, *9*, 216-222.

(12) (a) Pardo, P.; Carmona, D.; Lamata, P.; Rodríguez, R.; Lahoz, F. J.; García-Orduña, P.; Oro, L. A. Reactivity of the Chiral Metallic Brønsted Acid [($\eta^6$-*p*-$MeC_6H_4$*i*Pr)Ru($\kappa^3$*P*,*O*,*O*′-POH)][$SbF_6$]$_2$ (POH = $S_{C1}$,$R_{C2}$)-$Ph_2PC(Ph)HC(OH)HCH_2$-OMe) toward Aldimines. *Organometallics* **2014**, *33*, 6927-6936. (b) Skubi, K. L.; Kidd, J. B.; Jung, H.; Guzei, I. A.; Baik, M.-H.; Yoon, T. P. Enantioselective Excited-State

Photoreactions Controlled by a Chiral Hydrogen-Bonding Iridium Sensitizer. *J. Am. Chem. Soc.* **2017**, *139*, 17186-17192.

(13) Morrison, C. N.; Prosser, K. E.; Stokes, R. W.; Cordes, A.; Metzler-Nolte, N.; Cohen, S. M. Expanding medicinal chemistry into 3D space; metallofragments as 3D scaffolds for fragment-based drug discovery. *Chem. Sci.* **2020**, *11*, 1216-1225.

(14) (a) Werner, A. Zur Kenntnis des asymmetrischen Kobaltatoms. I. *Ber. Dtsch. Chem. Ges.* **1911**, *44*, 1887-1898. King, V. L. is listed as an author for the experimental section. (b) Werner, A. Zur Kenntnis des asymmetrischen Kobaltatoms. II. *Ber. Dtsch. Chem. Ges.* **1911**, *44*, 2445-2455. (c) Werner, A. Zur Kenntnis des asymmetrischen Kobaltatoms. III. *Ber. Dtsch. Chem. Ges.* **1911**, *44*, 3272-3278. (d) Werner, A. Zur Kenntnis des asymmetrischen Kobaltatoms. IV. *Ber. Dtsch. Chem. Ges.* **1911**, *44*, 3279-3284. (e) Werner, A. Zur Kenntnis des asymmetrischen Kobaltatoms. V. *Ber. Dtsch. Chem. Ges.* **1912**, *45*, 121-130.

(15) (a) Morral, F. R. Alfred Werner and Cobalt Complexes. In *Werner Centennial*; Kauffman, G. B., Ed.; American Chemical Society: Washington, D. C., 1967; Vol. 62; pp. 70-77. (b) Kauffman, G. B. Alfred Werner's Research on Optically Active Coordination Compounds. *Coord. Chem. Rev.* **1974**, *12*, 105-149.

(16) Girolami, G. S.; Rauchfuss, T. B.; Angelici, R. J. *Synthesis and Technique in Inorganic Chemistry: A Laboratory Manual*, 3rd ed.; University Science Books: Sausalito, CA, 1999.

(17) Review of stereoisomerism in salts of the trication $[Co(en)_3]^{3+}$, and homologs with substituted 1,2-diamine ligands: Ehnbom, A.; Ghosh, S. K.; Lewis, K. G.; Gladysz, J. A. Octahedral Werner complexes with substituted ethylenediamine ligands: a stereochemical primer for a historic series of compounds now emerging as a modern family of catalysts. *Chem. Soc. Rev.* **2016**, *45*, 6799-6811.

(18) (a) Taube, H. Rates and Mechanisms of Substitution in Inorganic Complexes in Solution. *Chem. Rev*. **1952**, *50*, 69-126. (b) Data for $[Co(en)_3]^{3+}$: Friend, J. A.; Nunn, E. K. Substitution Reactions in the Trisethylenediaminecobalt(III) Ion. *J. Chem. Soc.* **1958**, 1567-1571. (c) For an entry level rationale, see *Selected Topics in Inorganic Chemistry*; Malik, W. U.; Tuli, G. D.; Madan, R. D.; S. Chand & Company: New Delhi, 2002. Chapter 14.

(19) (a) Sen, D.; Fernelius, W. C. Catalytic racemization of optically active complexes: Tris(ethylenediamine)cobalt(III), -platinum(IV), and -rhodium(III) halides. *J. Inorg. Nucl. Chem.* **1959**, *10*, 269-274. (b) Douglas, B. D. Racemization of Tris-(ethylenediamine)-cobalt(III) Ion in the Presence of Decolorizing Carbon. *J. Am. Chem. Soc.* **1954**, *76*, 1020-1021. (c) Harnung, S. E.; Kallesøe, S.; Sargeson, A. M.; Schäffer, C. E. The Tris[(±)-1,2-propanediamine]cobalt(III) System. *Acta Chem. Scand.* **1974**, *A28*, 385-398; see especially the final paragraph of the experimental section.

(20) Ghosh, S. K.; Ehnbom, A.; Lewis, K. G.; Gladysz, J. A. Hydrogen bonding motifs in structurally characterized salts of the tris(ethylenediamine) cobalt trication, $[Co(en)_3]^{3+}$; An interpretive review, including implications for catalysis. *Coord. Chem. Rev.* **2017**, *350*, 30-48. See also chapter 2, Figure 2.10 in this dissertation.

(21) Ghosh, S. K.; Lewis, K. G.; Kumar, A.; Gladysz, J. A. Syntheses of Families of Enantiopure and Diastereopure Cobalt Catalysts Derived from Trications of the Formula $[Co(NH_2CHArCHArNH_2)_3]^{3+}$. *Inorg. Chem.* **2017**, 56, 2304-2320.

(22) Wititsuwannakul, T.; Hall, M. B.; Gladysz, J. A. A Computational Study of Hydrogen Bonding Motifs in Halide, Tetrafluoroborate, Hexafluorophosphate, and Tetraarylborate Salts of Chiral Cationic Ruthenium and Cobalt Guanidinobenzimidazole Hydrogen Bond Donor Catalysts. *Polyhedron* **2020**, in press. DOI: 10.1016/j.poly.2020.114618.

(23) The best prices in effect as of the submission date of this manuscript are from Oakwood Chemical (http://www.oakwoodchemical.com) (*R*,*R*-dpen; $359/100 g) and Ark Pharm (http://www.arkpharminc.com) (*S*,*S*-dpen; $420/100 g). Accessed May 2, 2020.

(24) (a) Luu, Q. H.; Lewis, K. G.; Banerjee, A.; Bhuvanesh, N.; Gladysz, J. A. The robust, readily available cobalt(III) trication $[Co(NH_2CHPhCHPhNH_2)]^{3+}$ is a progenitor of broadly applicable chirality and prochirality sensing agents. *Chem. Sci.* **2018**, *9*, 5087-5099. (b) Alimohammadi, M.; Hasaninejad, A.; Luu, Q. H.; Gladysz, J. A. "Λ-[Co((*S*,*S*)-$NH_2CHPhCHPhNH_2)_3]^{3+}$ $2I^-B(C_6F_5)_4^-$: A Superior, Air- and Water-Stable Chiral Solvating Agent for Chirality Sensing", in preparation.

(25) Blackmond, D. G. Kinetic Profiling of Catalytic Organic Reactions as a Mechanistic Tool. *J. Am. Chem. Soc.* **2015**, *137*, 10852-10866. *J. Am. Chem. Soc.* **2016**, *138*, 460.

(26) Burés, J. A Simple Graphical Method to Determine the Order in Catalyst. *Angew. Chem., Int. Ed.* **2016**, *55*, 2028-2031. *Angew. Chem.* **2016**, *128*, 2068-2071.

(27) https://secure.strem.com/catalog/v/27-4011/16/cobalt_1867120-15-7 (accessed May 2, 2020).

(28) (a) Burés, J.; Armstrong, A.; Blackmond, D. G. Mechanistic Rationalization of Organocatalyzed Conjugate Addition of Linear Aldehydes to Nitro-olefins. *J. Am. Chem. Soc.* **2011**, *133*, 8822-8825. (b) Burés, J.; Armstrong, A.; Blackmond, D. G. Curtin-Hammett Paradigm for Stereocontrol in Organocatalysis by Diarylprolinol Ether Catalysts. *J. Am. Chem. Soc.* **2012**, *134*, 6741-6750. *J. Am. Chem. Soc.* **2012**, *134*, 14264. (c) Burés, J.; Dingwall, P.; Armstrong, A.; Blackmond, D. G. Rationalization of an Unusual Solvent-Induced Inversion of Enantiomeric Excess in Organocatalytic Selenylation of Aldehydes. *Angew. Chem., Int. Ed.* **2014**, *53*, 8700-8704. *Angew. Chem.*

**2014**, *126*, 8844-8848.

(29) Walsh, D. J.; Lau, S. H.; Hyatt, M. G.; Guironnet, D. Kinetic Study of Living Ring-Opening Metathesis Polymerization with Third Generation Grubbs Catalysts. *J. Am. Chem. Soc.* **2017**, *139*, 13644-13647.

(30) Ramachary, D. B.; Kishor, M.; Reddy, Y. V. Development of Pharmaceutical Drugs, Drug Intermediates and Ingredients by Using Direct Organo-Click Reactions. *Eur. J. Org. Chem.* **2008**, *2008*, 975-993.

(31) The more upfield C=C**H** $^{1}$H NMR signal was assigned to the *Z* C=C isomer.[2] See also Jackman, L. M.; Wiley, R. H. Studies in Nuclear Magnetic Resonance. Part II. Application to Geometric Isomerism about the Ethylenic Double Bond. *J. Chem. Soc.* **1960**, 2881-2886.

(32) The *Z* C=C configuration was further substantiated by $^{13}$C NMR spectra (no $\{^{1}H\}$) in which vicinal coupling could be observed between the bold (*E*) nuclei $CH_3O_2$**C**C=C**H** ($^{3}J_{CH}$ = 11.4 Hz). See von Philipsborn, W.; Vogeli, U. Vicinal C,H Spin Coupling in Substituted Alkenes. Stereochemical Significance and Structural Effects. *Org. Mag. Res.* **1975**, *7*, 617-627.

(33) The *E* configuration was assigned from the magnitude of the vicinal C**H**=C**H** coupling constant ($^{3}J_{HH}$). See Karplus, M. Vicinal Proton Coupling in Nuclear Magnetic Resonance. *J. Am. Chem. Soc.* **1963**, *85*, 2870-2871.

# 4. WERNER COMPLEXES AS HYDROGEN BOND DONOR CATALYSTS FOR THE ENANTIOSELECTIVE FORMATION OF CARBON-HETEROATOM BONDS AND HETEROCYCLES

## 4.1. Introduction

The last two decades have seen an impressive growth of hydrogen bond donors in asymmetric catalysis.[1] These catalysts heavily relied on carbon stereocenters. Recently, another approach has been introduced, in which metal based chirality is used.[2-8] The hydrogen bonding activity comes from the ligands and the metal centers do not activate reactants. The Gladysz group's interest has started and continuously developed in parallel with this field.[2-5]

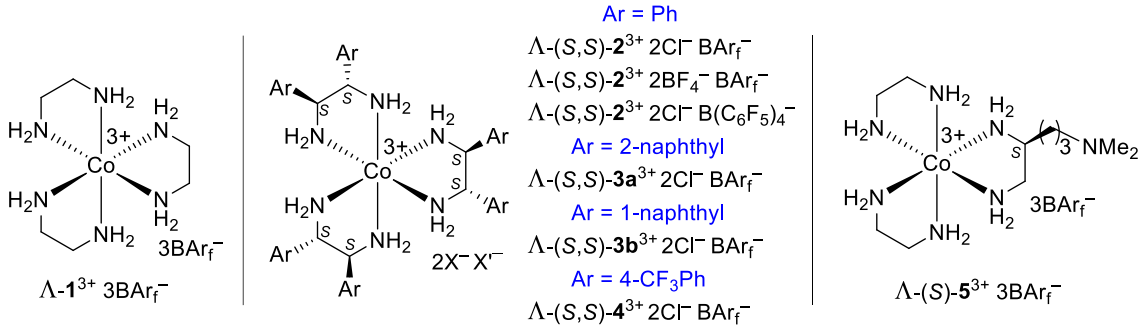


**Figure 4.1.** Representatives of Werner catalysts reported by the Gladysz group.

Representatives of the catalysts reported by the Gladysz group are illustrated in Figure 4.1. The absolute configurations at the chiral cobalt center are usually designated Λ and Δ. In most cases, the catalysts have extra stereocenters in the di- or triamine ligands and thus can exist as diastereomers (Figure 4.1, middle and right). Especially the diastereomeric mixed salts Λ- and Δ-(*S*,*S*)-**2**$^{3+}$ 2X$^{-}$X'$^{-}$ have been quite effective in a number of enantioselective transformations.[3] However, these reactions mainly focus on the formation of carbon-carbon bonds. Therefore, expanding the applicability of these new hydrogen bond donors to constructing carbon-heteroatom bonds has been one of my

priorities. In this chapter, I turn my interests to the synthesis of fluorinated compounds[9] as well as azirines[10] and tetrahydroquinolines[11] due to their vital roles in pharmaceuticals and agricultural chemistry.

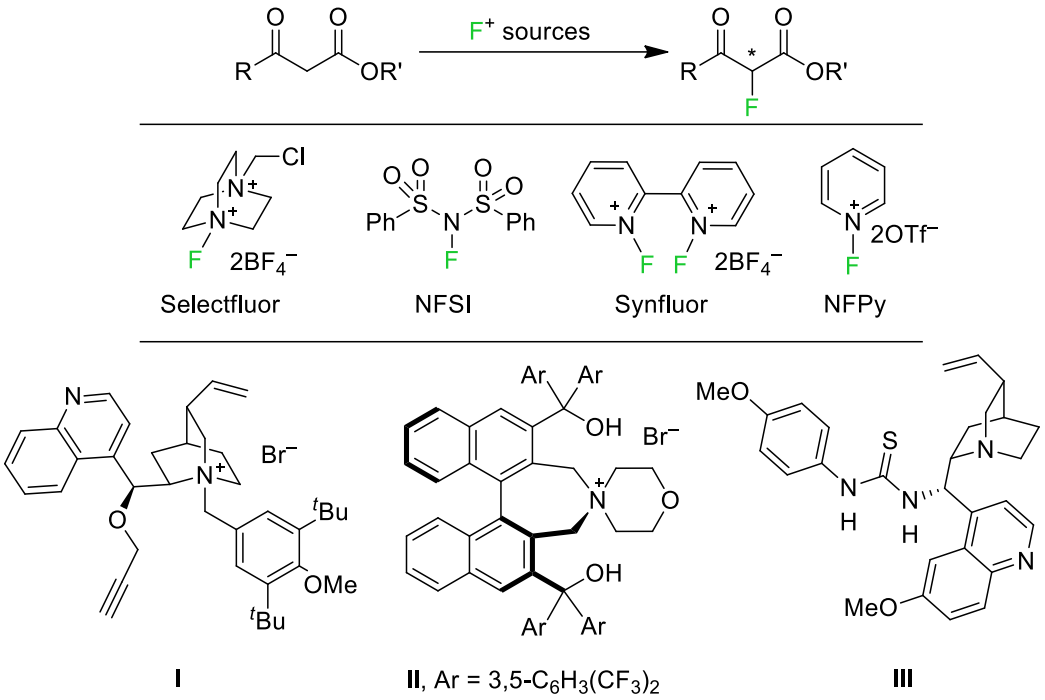


**Figure 4.2.** Examples of fluorination of β-keto esters (top), electrophilic fluorinating agents (middle), and organocatalysts in asymmetric fluorination of β-keto esters (bottom)

Catalytic asymmetric fluorination of organic substrates has been well studied,[12] especially the fluorination of β-keto esters (Figure 4.2, top).[13,14] These protocols usually use a chiral catalyst coupled with an electrophilic fluorinating agent (Figure 4.2, middle).[15] The most commonly used reagent is *N*-fluorobenzenesulfonimide (NFSI, Figure 4.2, middle)[12] owing to its commercial availability at a low price.[16] Some of the catalysts used in asymmetric fluorination of β-keto esters are organocatalysts (**I-III** in Figure 4.2, bottom).[14] Two of them are hydrogen bond donors (**II** and **III**).[14b,14c] I see this as an opportunity to apply the catalysts in Figure 4.1 to the asymmetric fluorination of β-keto esters.

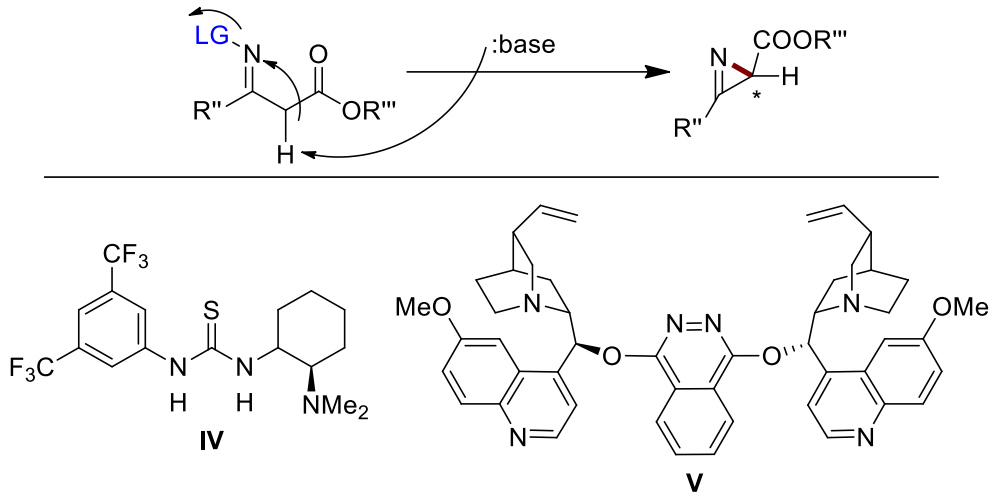


**Figure 4.3.** Example of the Neber reaction (top), and previously reported catalysts used in the Neber reactions (bottom).

Similarly, I sought to use the catalysts in Figure 4.1 to achieve enantioselectivity in the Neber reaction (Figure 4.3, top).[17] Asymmetric syntheses of azirines via the Neber reaction have been described before.[18] Two of those reports used organocatalysts (**IV** and **V** in Figure 4.3, bottom). Catalyst **IV** (often called Takemoto catalyst) is a hydrogen bond donor.[18a]

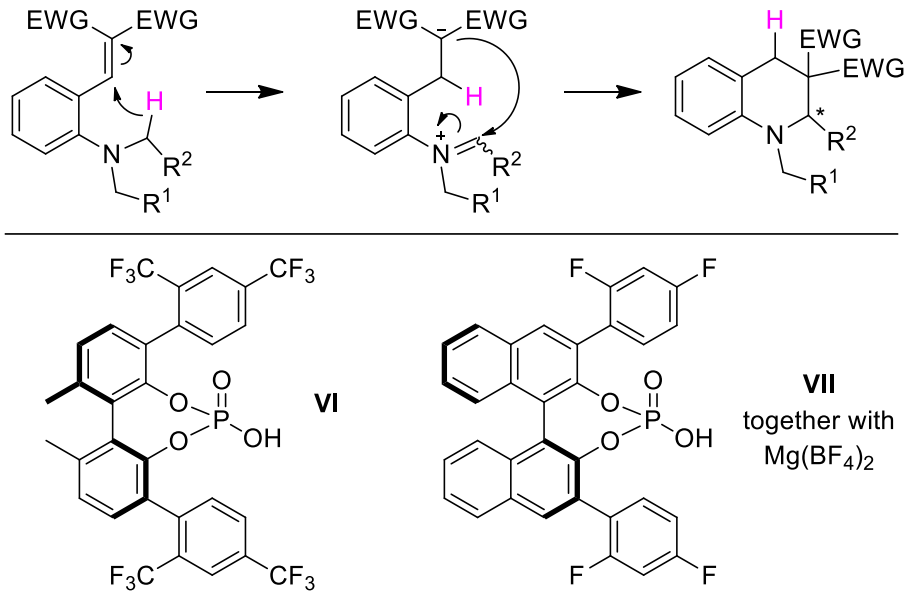


**Figure 4.4.** Examples of intramolecular hydride transfer reaction (top), and previously reported catalysts used (bottom).

The syntheses of tetrahydroquinolines[19] and tetrahydroisoquinolines[20] using chiral rhenium complexes have been reported by the Gladysz group. An intramolecular hydride transfer sequence (Figure 4.4, top) has also been used for the synthesis of tetrahydroquinoline.[21] Many Brønsted acids were used as the catalysts for this reaction.[21b] Two chiral phosphoric acids are shown in Figure 4.4 (bottom).[22] In this chapter, I applied the catalysts in Figure 4.1 to the reaction of Figure 4.4 (top) to synthesize tetrahydroquinolines.

**4.2. Results**

The enantiopure salt Λ-**1**$^{3+}$ 3BAr$_f^-$ (Figure 4.1) was obtained by a literature procedure.[2] Other catalysts incorporating other ligands of the type (*S*,*S*)-$NH_2CHArCHArNH_2$ and a bifunctional catalyst Λ-(*S*)-**5**$^{3+}$ 3BAr$_f^-$ were synthesized as previously reported.[4,23]

**4.2.1. Enantioselective fluorination of β-keto esters**

Attempts to achieve enantioselective fluorination of β-keto esters are summarized in Table 4.1. Commercial methyl cyclopentanone-2-carboxylate (**6**) and the fluorinating agent NFSI (Figure 4.2, middle) was combined in a 1:1 molar ratio in $CH_2Cl_2$ in the presence of 10 mol% of one of the catalysts in Figure 4.1 and at a temperature specified in Table 4.1. $K_2CO_3$ was then added with stirring. After the reaction was complete as indicated by TLC, aqueous and chromatographic workups (see experimental section for details) gave **7** in 82 to >99% yields. The ee values were determined by $^{19}$F NMR using the chiral solvating agent Λ-(*S*,*S*)-**2**$^{3+}$ 2I$^-$BAr$_f^-$.[24] All reactions and workups in this section were carried out in air.

**Table 4.1.** Catalyst screening for the fluorination of methyl 2-oxocyclopentanecarboxylate (**6**) by NFSI.[a]

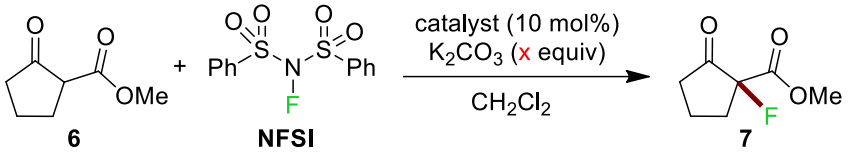


| Entry | Catalyst | x (equiv) | Temp. (°C) | Time (h) | Yield (%)[b] | Ee (%)[c] |
|---|---|---|---|---|---|---|
| 1 | – | 2.0 | rt | 26 | >99 | 0 |
| 2 | Λ-**1**$^{3+}$ 3BAr$_f^-$ | 2.0 | rt | 12 | >99 | 0 |
| 3 | Λ-**1**$^{3+}$ 3BAr$_f^-$ | – | rt | 30 | 0 | – |
| 4 | Λ-(*S*,*S*)-**2**$^{3+}$ 2Cl$^-$BAr$_f^-$ | 2.0 | rt | 19 | 99 | 13 (*S*) |
| 5 | Λ-(*S*,*S*)-**2**$^{3+}$ 2BF$_4^-$BAr$_f^-$ | 2.0 | rt | 19 | 96 | 10 (*S*) |
| 6 | Δ-(*S*,*S*)-**2**$^{3+}$ 2Cl$^-$B(C$_6$F$_5$)$_4^-$ | 2.0 | rt | 19 | >99 | 10 (*R*) |
| 7 | Δ-(*S*,*S*)-**2**$^{3+}$ 2Cl$^-$BAr$_f^-$ | 2.0 | rt | 19 | >99 | 7 (*R*) |
| 8 | Λ-(*S*,*S*)-**2**$^{3+}$ 2I$^-$BAr$_f^-$ | 2.0 | rt | 19 | 98 | 3 (*S*) |
| 9 | Λ-(*S*,*S*)-**2**$^{3+}$ 2I$^-$BAr$_f^-$ | 1.0 | 0 | 94 | 99 | 8 (*S*) |
| 10 | Λ-(*S*,*S*)-**2**$^{3+}$ 2I$^-$BAr$_f^-$ | 0.50 | 0 | 94 | 82 | 62 (*S*) |
| 11 | Λ-(*S*,*S*)-**2**$^{3+}$ 2Cl$^-$BAr$_f^-$ | 0.50 | 0 | 94 | >99 | 79 (*S*) |
| 12 | Λ-(*S*,*S*)-**2**$^{3+}$ 2Cl$^-$BAr$_f^-$ | 0.50 | –36 | 96 | 0 | – |
| 13 | Λ-(*S*,*S*)-**2**$^{3+}$ 2Cl$^-$BAr$_f^-$ | 0.50 | –78 | 96 | 0 | – |
| 14 | Λ-(*S*,*S*)-**3a**$^{3+}$ 2Cl$^-$BAr$_f^-$ | 0.50 | 0 | 120 | 99 | 50 (*S*) |
| 15 | Λ-(*S*)-**5**$^{3+}$ 3BAr$_f^-$ | – | 0 | 120 | 0 | – |

[a]A vial was charged with a stir bar, **6** (0.0071 g, 0.050 mmol, 0.0062 mL), NFSI (0.016 g, 0.050 mmol), a catalyst (10 mol%), and $CH_2Cl_2$. The sample was brought to the indicated temperature and $K_2CO_3$ was added with stirring. The reaction was monitored by TLC and worked up as described in the experimental section. [b]Isolated yields. [c]Determined by $^{19}$F NMR and HPLC (see experimental section for details).

The highest ee value (79%) was obtained when the catalyst Λ-(*S*,*S*)-$\mathbf{2}^{3+}$ $2Cl^{-}BAr_f^{-}$ (10 mol%) was used with 0.50 equiv of $K_2CO_3$ at 0 °C (entry 11). Further decreasing the temperature (entry 12 and 13) or using a bifunctional catalyst Λ-(*S*)-$\mathbf{5}^{3+}$ $3BAr_f^{-}$ (entry 15) resulted in no product formation. The catalyst Λ-(*S*,*S*)-$\mathbf{2}^{3+}$ $2I^{-}BAr_f^{-}$ also gave the product **7** in 82% yield and 62% ee (entry 10) under the reaction conditions in entry 11.

### 4.2.2. Neber synthesis of azirine

As summarized in Table 4.2, ethyl 3-((tosyloxy)imino)butanoate (**8**) was combined in dry $CH_2Cl_2$ with 10 mol% of a catalyst in Figure 4.1 at room temperature (except for entry 8 when the reaction was tested at –36 °C). A base was then added with stirring. After 48 h, unless noted, aqueous and chromatographic workups gave the product ethyl 3-methyl-2*H*-azirine-2-carboxylate (**9**) in 50 to >99 % yields. The ee values were determined by $^1$H NMR using the chiral solvating agent Λ-(*S*,*S*)-$\mathbf{2}^{3+}$ $2I^{-}BAr_f^{-}$.[24] All reactions and workups in this section were carried out in air.

When an inorganic base ($Na_2CO_3$) was used, an uncatalyzed reaction gave only a 40% yield of the product **9** after 72 h. In the presence of the catalyst Λ-(*S*,*S*)-$\mathbf{2}^{3+}$ $2Cl^{-}$ $BAr_f^{-}$ (10 mol%) and 2.0 equiv of $Na_2CO_3$, **9** was obtained in >99 % yield and 28% ee after 48 h (entry 2). The catalyst Λ-(*S*,*S*)-$\mathbf{2}^{3+}$ $2I^{-}BAr_f^{-}$ also gave **9** in >99 % yield but a lower 20% ee (entry 5). Decreasing the temperature (entry 8) resulted in a 50% yield and 56% ee. The highest enantioselectivity, 97% ee, was achieved when 10 mol% of Λ-(*S*,*S*)-$\mathbf{2}^{3+}$ $2Cl^{-}BAr_f^{-}$ and 2.0 equiv of $Et_3N$ were used at room temperature (entry 10). Additional approaches to enantioselective Neber reactions found in the literature are presented in the discussion section. The ee value in entry 10 is one of the highest obtained to date.

**Table 4.2.** Catalyst screening for the Neber synthesis of azirine **9**.[a]

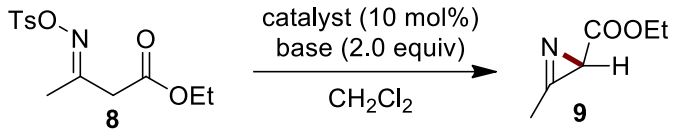


| Entry | Catalyst | Base | Temp. (°C) | Time (h) | Yield (%)[b] | Ee (%)[c] |
|---|---|---|---|---|---|---|
| 1 | – | $Na_2CO_3$ | rt | 72 | 40 | 0 |
| 2 | Λ-(*S*,*S*)-**2**$^{3+}$ 2Cl$^-$BAr$_f^-$ | $Na_2CO_3$ | rt | 48 | >99 | 28 (*S*) |
| 3 | Λ-(*S*,*S*)-**2**$^{3+}$ 2BF$_4^-$BAr$_f^-$ | $Na_2CO_3$ | rt | 48 | >99 | 12 (*S*) |
| 4 | Δ-(*S*,*S*)-**2**$^{3+}$ 2Cl$^-$B(C$_6$F$_5$)$_4^-$ | $Na_2CO_3$ | rt | 48 | >99 | 8 (*R*) |
| 5 | Λ-(*S*,*S*)-**2**$^{3+}$ 2I$^-$BAr$_f^-$ | $Na_2CO_3$ | rt | 48 | >99 | 20 (*S*) |
| 6 | Λ-(*S*,*S*)-**3a**$^{3+}$ 2Cl$^-$BAr$_f^-$ | $Na_2CO_3$ | rt | 72 | 99 | 30 (*S*) |
| 7 | Λ-(*S*,*S*)-**4**$^{3+}$ 2Cl$^-$BAr$_f^-$ | $Na_2CO_3$ | rt | 48 | 99 | 30 (*S*) |
| 8 | Λ-(*S*,*S*)-**2**$^{3+}$ 2I$^-$BAr$_f^-$ | $Na_2CO_3$ | –36 | 48 | 50 | 56 (*S*) |
| 9 | Λ-(*S*,*S*)-**2**$^{3+}$ 2Cl$^-$BAr$_f^-$ | $NaHCO_3$ | rt | 48 | 0 | – |
| 10 | Λ-(*S*,*S*)-**2**$^{3+}$ 2Cl$^-$BAr$_f^-$ | $Et_3N$ | rt | 48 | >99 | 97 (*S*) |
| 11 | Λ-(*S*,*S*)-**2**$^{3+}$ 2Cl$^-$BAr$_f^-$ | DABCO | rt | 48 | 0 | – |
| 12 | Λ-(*S*,*S*)-**2**$^{3+}$ 2Cl$^-$BAr$_f^-$ | pyridine | rt | 48 | >99 | 29 (*S*) |

[a]A vial was charged with a stir bar, **8** (0.0075 g, 0.025 mmol), a catalyst (10 mol%), and dry $CH_2Cl_2$. The sample was brought to the indicated temperature and a base was added with stirring. The reaction was monitored by TLC and worked up as described in the experimental section. [b]Isolated yields. [c]Determined by HPLC (see experimental section for details).

### 4.2.3. Tandem hydride transfer-cyclization

In initial screening reactions, 0.050 mmol of dimethyl 2-(2-(pyrrolidine-1-yl)benzylidene) malonate (**10a**) and 10 mol% of a catalyst from Figure 4.1 were combined

**Table 4.3.** Catalyst screening for the tandem hydride transfer-cyclization of dimethyl 2-(2-(pyrrolidin-1-yl)benzylidene) malonate (**10a**).[a]

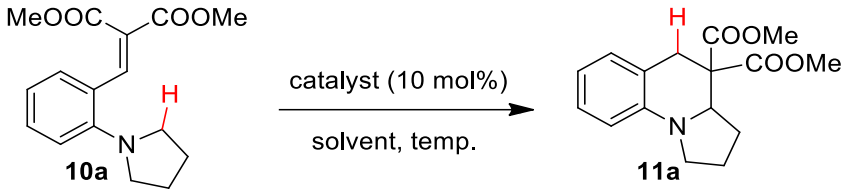


| Entry | Catalyst | Solvent | Temp (°C) | Time (h) | Yield (%)[b] | Ee (%)[c] |
|---|---|---|---|---|---|---|
| 1 | – | $CH_2Cl_2$ | rt | 168 | 0 | – |
| 2 | Λ-**1**$^{3+}$ 3BAr$_f^-$ | $CH_2Cl_2$ | rt | 17 | >99 | 1 (*S*) |
| 3 | Λ-(*S*,*S*)-**2**$^{3+}$ 2Cl$^-$BAr$_f^-$ | $CH_2Cl_2$ | rt | 168 | 17 | – |
| 4 | Λ-(*S*,*S*)-**2**$^{3+}$ 2Cl$^-$BAr$_f^-$ | $CH_2Cl_2$ | 50 | 48 | 30 | 24 (*S*) |
| 5 | Λ-(*S*,*S*)-**2**$^{3+}$ 2BF$_4^-$BAr$_f^-$ | $CH_2Cl_2$ | rt | 168 | 39 | 27 (*S*) |
| 6 | Λ-(*S*,*S*)-**2**$^{3+}$ 2BF$_4^-$BAr$_f^-$ | $CHCl_3$ | 50 | 120 | 99 | 27 (*S*) |
| 7 | Λ-(*S*,*S*)-**2**$^{3+}$ 2I$^-$BAr$_f^-$ | $CH_2Cl_2$ | 50 | 48 | >99 | 25 (*S*) |
| 8 | Λ-(*S*,*S*)-**2**$^{3+}$ 3BAr$_f^-$ | $CH_2Cl_2$ | rt | 1.5 | >99 | 10 (*S*) |
| 9 | Λ-(*S*,*S*)-**2**$^{3+}$ 3BAr$_f^-$ | $CH_2Cl_2$ | 0 | 24 | >99 | 8 (*S*) |
| 10 | Λ-(*S*,*S*)-**2**$^{3+}$ 3BAr$_f^-$ | $CH_2Cl_2$ | –36 | 168 | 0 | – |
| 11 | Λ-(*S*,*S*)-**2**$^{3+}$ 3BAr$_f^-$ | $CH_2Cl_2$ | 50 | 4 | 0 | – |
| 12 | Λ-(*S*,*S*)-**3b**$^{3+}$ 3BAr$_f^-$ | $CH_2Cl_2$ | rt | 4 | 90 | 24 (*S*) |
| 13 | Λ-(*S*,*S*)-**3b**$^{3+}$ 2Cl$^-$BAr$_f^-$ | $CH_2Cl_2$ | 50 | 24 | >99 | 35 (*S*) |
| 14 | Λ-(*S*,*S*)-**4**$^{3+}$ 2Cl$^-$BAr$_f^-$ | $CH_2Cl_2$ | 50 | 24 | 50 | 29 (*S*) |

[a]A vial was charged with a stir bar, **10a** (0.014 g, 0.050 mmol), a catalyst (10 mol%), and a solvent. The vial was sealed and the sample was brought to the indicated temperature. The reaction was stirred and monitored by TLC and worked up as described in the experimental section. [b]Isolated yields. [c]Determined by HPLC (see experimental section for details).

**Table 4.3.** Continued.[a]

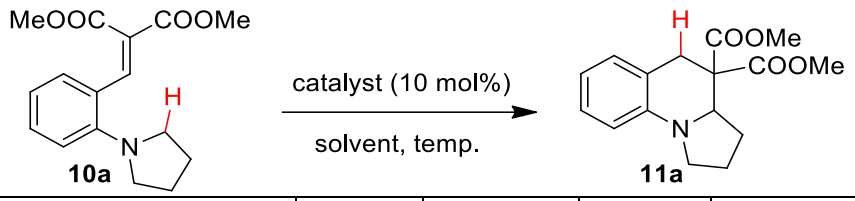


| Entry | Catalyst | Solvent | Temp (°C) | Time (h) | Yield (%)[b] | Ee (%)[c] |
|---|---|---|---|---|---|---|
| 15 | Λ-(*S*,*S*)-**3b**$^{3+}$ 2Cl$^-$BAr$_f^-$ | $CHCl_3$ | 50 | 24 | 50 | 43 (*S*) |
| 16 | Λ-(*S*,*S*)-**3b**$^{3+}$ 2Cl$^-$BAr$_f^-$ | toluene | 50 | 24 | >99 | 32 (*S*) |
| 17 | Λ-(*S*,*S*)-**3b**$^{3+}$ 2BF$_4^-$BAr$_f^-$ | $CHCl_3$ | 50 | 24 | 50 | 38 (*S*) |
| 18 | Λ-(*S*,*S*)-**3b**$^{3+}$ 2BF$_4^-$BAr$_f^-$ | $CH_2Cl_2$ | 50 | 24 | 60 | 31 (*S*) |
| 19 | Λ-(*S*,*S*)-**3a**$^{3+}$ 2BF$_4^-$BAr$_f^-$ | $CHCl_3$ | 50 | 96 | 50 | 11 (*S*) |
| 20 | Λ-(*S*,*S*)-**3a**$^{3+}$ 3BAr$_f^-$ | $CHCl_3$ | rt | 18 | 50 | 7 (*S*) |

[a]A vial was charged with a stir bar, **10a** (0.014 g, 0.050 mmol), a catalyst (10 mol%), and a solvent. The vial was sealed and the sample was brought to the indicated temperature. The reaction was stirred and monitored by TLC and worked up as described in the experimental section. [b]Isolated yields. [c]Determined by HPLC (see experimental section for details).

in a vial containing 2.00 mL of a solvent. The vial was sealed and the sample was brought to a temperature shown in Table 4.3. The mixture was stirred until TLC indicated that the reaction was complete. Chromatographic workups gave the cyclized product **11a**. The yields and ee values are summarized in Table 4.3.

The highest enantioselectivity (43% ee, Table 4.3, entry 15) was found when a more sterically demanding naphthyl substituted ethylenediamine ligand was used (Λ-(*S*,*S*)-**3b**$^{3+}$ 2Cl$^-$BAr$_f^-$ in Figure 4.1) at 50 °C (entry 15). All reactions at 50 °C in Table 4.3 (especially ones with the 3BAr$_f^-$ salts) showed noticeable decomposition of the catalysts. Solids with the characteristic green color of *trans*-[Co(NH$_2$CHArCHArNH$_2$)$_2$]Cl$_2$[3a,23] were observed.

The best performing conditions from Table 4.3 (entry 15) were then applied to several other substrates, as illustrated in Figure 4.5. A useful level of enantioselectivity was achieved only with **10b**, which has two *N*-benzyl substituents, and gave **11b** in 82% ee.

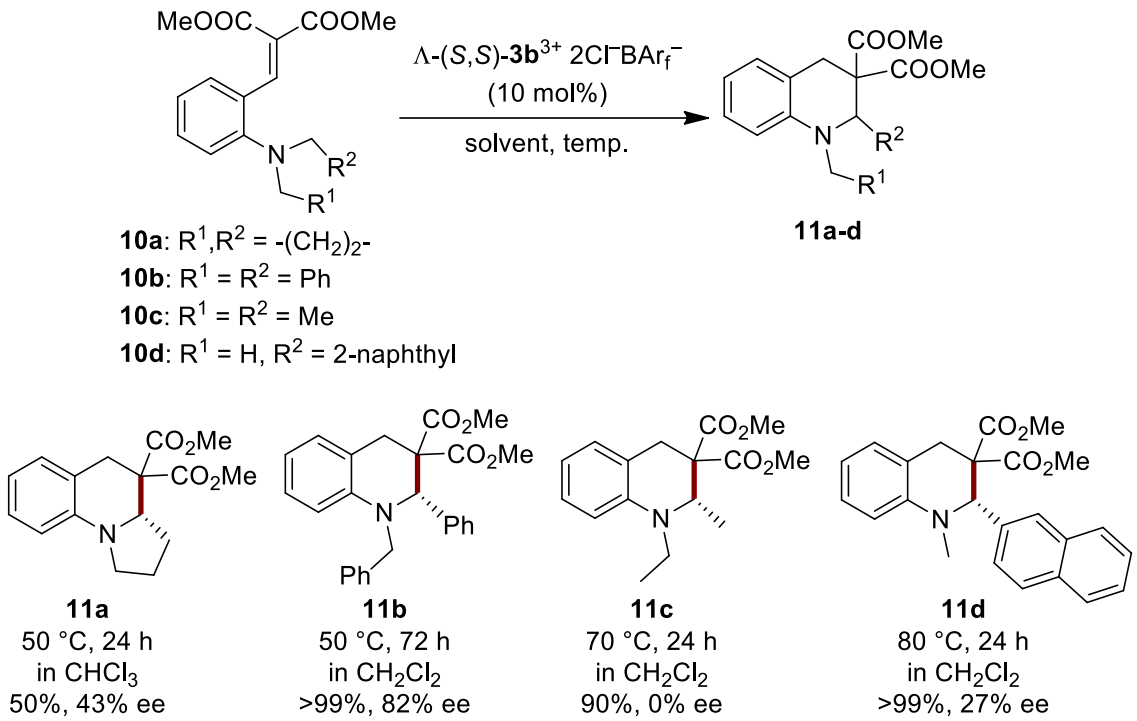


**Figure 4.5.** Substrate scope for the tandem hydride transfer-cyclization reaction. All yields are isolated yields and the ee was determined by HPLC (see experimental section and appendix C for details).

## 4.3. Discussion

### 4.3.1. Enantioselective fluorination of β-keto esters

The enantioselective fluorination of **6** (Table 4.1) has been previously studied with several other catalysts (Figure 4.6, top).[13c,d,14c] A quinine based thiourea hydrogen bond donor (**III**) gave the product **7** in 95% yield and 87% ee at –60 °C.[14c] A cobalt(II) salen complex **VIII** gave good enantioselectivity (90% ee) at –20 °C.[13d] A copper complex of a chiral sulfoximine ligand (**IX**) gave **7** in 74% ee.[13c] The highest ee obtained in Table 4.1 (79%) surpassed those obtained with catalyst **IX**.[13c] Although the catalyst Λ-(*S*,*S*)-**2**$^{3+}$

$2Cl^{-}BAr_f^{-}$ somewhat underperformed the hydrogen bond donor **III**, a fairer comparison will be made in future communications. Catalyst **III** is ineffective for a number of substrates (Figure 4.6, bottom). It is anticipated that the catalyst Λ-(*S*,*S*)-$\mathbf{2}^{3+}$ $2Cl^{-}BAr_f^{-}$ can improve the enantioselectivity in these cases. Future communications will also include comparison to the catalyst **II** (Figure 4.2), which was reported to give ee values of 85-98% for the products depicted in Figure 4.6 (bottom).

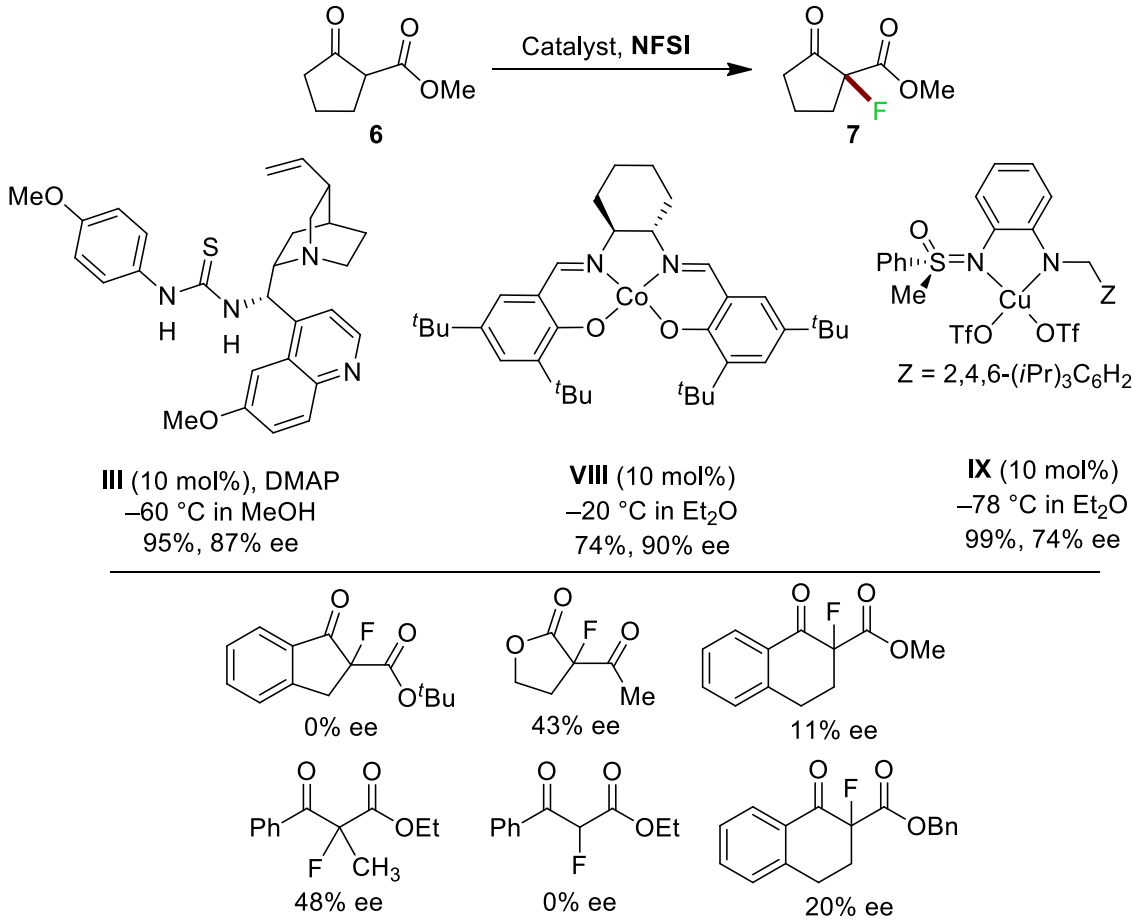


**Figure 4.6.** Previously reported catalysts for the enantioselective fluorination of β-keto ester **6** (top), and some systems that are not effective with the hydrogen bond donor **III** (bottom).

Two diastereomeric catalysts used in entries 4 and 7 of Table 4.1, Λ-(*S*,*S*)-$\mathbf{2}^{3+}$ $2Cl^{-}$ $BAr_f^{-}$ and Δ-(*S*,*S*)-$\mathbf{2}^{3+}$ $2Cl^{-}BAr_f^{-}$, showed some difference in enantioselectivity (13% vs. 7% ee, entry 4 vs. 7, Table 4.1). Among reported transformations catalyzed by the catalysts

in Figure 4.1, some worked best with the Λ diastereomer[3a,3c] while others gave better results with the Δ diastereomer.[3b,3f] Regardless, the cobalt configuration of the catalyst directed the configuration of the product **7**.

The failure with a bifunctional catalyst (entry 15, Table 4.1) could be due to the deactivation of the internal tertiary amine base by NFSI as reported before.[25] Switching between the lipophilic anions $BAr_f^-$ and $B(C_6F_5)_4^-$ also led to some degree of differences in enantioselectivity (entry 6 vs. 7, Table 4.1). Weaker but bulkier hydrogen bond accepting anions[26] such as $I^-$ and $BF_4^-$ also underperformed the stronger and less sterically demanding acceptor $Cl^-$.[26]

**4.3.2. Neber synthesis of azirine**

As shown in Table 4.2, all salts of the trication (*S*,*S*)-**2**$^{3+}$ and related species afford azirine **9** with significant enantioselectivity. However, the Δ diastereomers are always inferior to the Λ diastereomers (entry 3 vs. 4, Table 4.2). In contrast to what was observed in the fluorination of β-keto esters (section 4.2.1 and 4.3.1), increasing the bulkiness of the hydrogen bond donors brought about a small increase in the ee value (entries 6 and 7). However, due to the ease of access to Λ-(*S*,*S*)-**2**$^{3+}$ $2Cl^-BAr_f^-$ (commercially available),[27] further investigation was carried out with the benchmarked catalyst. The optimal enantioselectivity (97% ee, entry 10, Table 4.2) was obtained with 10 mol% of the catalyst Λ-(*S*,*S*)-**2**$^{3+}$ $2Cl^-BAr_f^-$, and 2.0 equiv of $Et_3N$ in $CH_2Cl_2$ at room temperature.

The effect of the halide anions in the catalysts ($Cl^-$ vs. $I^-$, entries 2 vs. 5) was smaller than that observed in the fluorination of β-keto esters (sections 4.2.1 and 4.3.1). On the other hand, the base used for the deprotonation of the α proton in **8** (Figure 4.3 and Table 4.2) seems to have a major effect on the enantioselectivity. For example, replacing the inorganic base $Na_2CO_3$ ($pK_a$ of $HCO_3^-$ = 10.3)[28] with an organic equivalent $Et_3N$ ($pK_a$ of $Et_3NH^+$ = 10.7)[29] resulted in a pronounced increase in the enantiomeric excess

(entries 2 vs. 10, $\Delta_{ee}$ = +69%). An opposite trend was found in the case of a bifunctional catalyst involving thiourea as the hydrogen bond donor (**IV** in Figure 4.7), in which $Na_2CO_3$ gave 64% ee of the product **9'** (Figure 4.7, top), and $Et_3N$ gave a 10% ee.[18a]

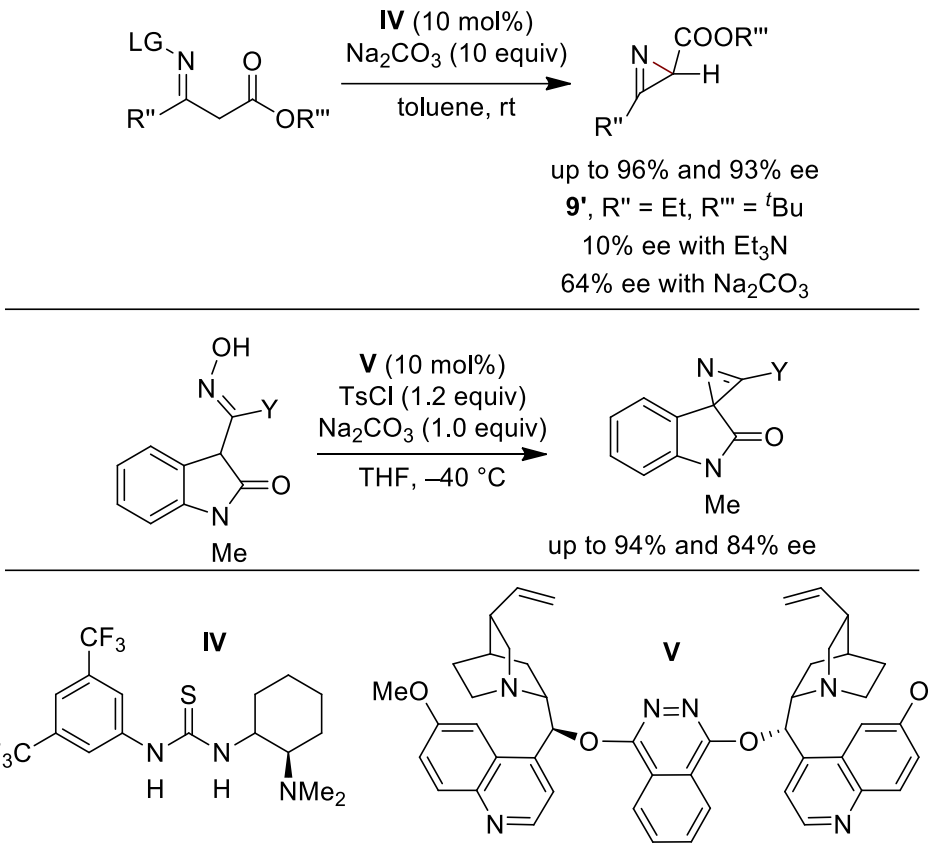


**Figure 4.7.** Enantiopure catalysts previously used in the Neber synthesis of azirines.

Under the ideal optimized conditions (Table 4.2, entry 10), the catalyst Λ-(*S*,*S*)-$\mathbf{2}^{3+}$ $2Cl^{-}BAr_f^{-}$ stands head and shoulders above other organocatalysts previously applied to the synthesis of azirines via the Neber method (Figure 4.7).[16a,16c] Given that the reactant **8** possesses one of the simplest combination of substituents found in the literature (R'' = Me and R''' = Et), expanding the substrate scope using these catalytic conditions is demanded and expected to bring a diversity of azirines with good to excellent enantiopurities. These data will be obtained and communicated in the future.

### 4.3.3. Tandem hydride transfer-cyclization

Figure 4.5 demonstrated the initial attempts in expanding the substrate scope of tetrahydroquinoline synthesis. When both $R^1$ and $R^2$ are phenyl groups (giving *N*-benzyl substituents as in **10b**), the product **11b** was obtained in >99% yield and 82% ee. However, when $R^1$ and $R^2$ were changed to other groups, the ee decreased (to 43% for **11a**, 0% for **11c**, and 27% for **11d**). Compound **11b** has been obtained before using a chiral phosphoric acid as the catalyst (**VI**, Figure 4.8, bottom) in 95% ee.[22a] A closely related compound (**11b'**, Figure 4.8) was also obtained in 85% ee using catalyst **VII**.[22b]

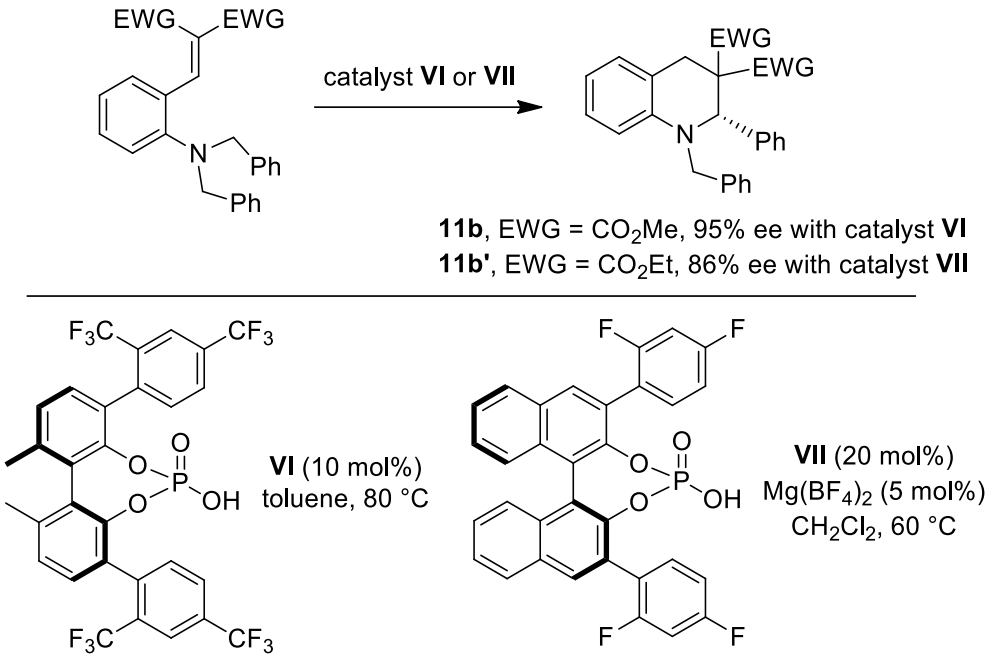


**Figure 4.8.** Catalysts previously used in the synthesis of **11b** and a closely related compound **11b'**.

The reasons for the decomposition of the catalysts under the reaction conditions are not clear since the catalysts described in this chapter have been established to be quite thermally stable.[3a,23] However, even more robust complexes are being searched for and investigated to minimize or avoid this problem.

## 4.4. Conclusion

This chapter reported three reactions catalyzed by Werner catalysts in addition to the one described in chapter 3. First, the fluorination of β-keto ester **6** using NFSI and the catalyst Λ-(*S*,*S*)-**2**$^{3+}$ 2Cl$^{-}$BAr$_f^{-}$ (10 mol%) gave the product **7** in 79% ee. Second, the Neber reaction using the catalyst Λ-(*S*,*S*)-**2**$^{3+}$ 2Cl$^{-}$BAr$_f^{-}$ (10 mol%) gave azirine **9** in >99% yield and 97% ee. Third, the intramolecular hydride transfer reaction using the catalyst Λ-(*S*,*S*)-**3b**$^{3+}$ 2Cl$^{-}$BAr$_f^{-}$ (10 mol%) gave tetrahydroquinoline **11b** in >99% yield and 82% ee.

It is anticipated that the substrate scope for the fluorination (section 4.2.1 and 4.3.1) and the Neber reaction (section 4.2.2 and 4.3.2) can be expanded in the future based on the promising results presented in this chapter. Exploration for other catalysts to synthesize tetrahydroquinoline (section 4.2.3 and 4.3.3) is being conducted in the Gladysz group.

The next chapter will introduce two more reactions using the catalyst Λ-(*S*,*S*)-**2**$^{3+}$ 2X$^{-}$X'$^{-}$, in which the anions X$^{-}$ and X'$^{-}$ participate in the reaction.

## 4.5. Experimental (see also appendix C)

**Catalyst screening for enantioselective fluorination of 6 (Table 4.1).** A vial was charged with a stir bar, **6** (0.0071 g, 0.050 mmol, 0.0062 mL), NFSI (0.016 g, 0.050 mmol), a catalyst (10 mol%), and $CH_2Cl_2$ (1.0 mL). The sample was brought to the indicated temperature and $K_2CO_3$ (0.0040-0.014 g, 0.025-0.10 mmol, 0.50-2.0 equiv) was added with stirring. The reaction was monitored by TLC (silica gel, 8:2 v/v hexanes/ethyl acetate). After the time indicated in Table 4.1, the vial was opened to air and (for low temperature runs) allowed to warm to room temperature. Water (3.0 mL) was added and the organic phase was collected and dried ($Na_2SO_4$). The solvent was removed by rotary evaporation and the residue was chromatographed (silica gel, 1 × 25 cm column, packed

in and eluted with 80:20 v/v hexanes/ethyl acetate). The product containing fractions were combined and the solvents were removed by rotary evaporation to give **7** (see appendix C for further data). An NMR tube was charged with a portion of **7** (0.0016 g, 0.010 mmol), $CDCl_3$ (0.30 mL), and a 0.0050 M $CDCl_3$ solution of the chiral solvating agent Λ-(*S*,*S*)-$\mathbf{2}^{3+}$ $2I^-BAr_f^-$ (0.20 mL, 0.0010 mmol, 10 mol%). A $^{19}F$ NMR spectrum was acquired and signals of the enantiomers were integrated (see Figure C-1 in appendix C). The dominant configuration was assigned by HPLC with a Chiralcel AD-H column, 98:2 hexane/isopropanol, 1.0 mL/min, 254 nm, $t_R$ = 31.4 min, $t_S$ = 33.5 min. The order of elution was established in an earlier study with an identical column.[14c]

**Catalyst screening for the Neber synthesis of the azirine 9 (Table 4.2).** A vial was charged with a stir bar, **8** (0.0075 g, 0.025 mmol), a catalyst (10 mol%), and 0.50 mL of dry $CH_2Cl_2$.[30] The sample was brought to the indicated temperature and a base (0.050 mmol, 2.0 equiv) was added with stirring. The reaction was monitored by TLC (silica gel, 75:25 v/v hexanes/ethyl acetate). After the time indicated in Table 4.2, the vial was opened to air and (for low temperature runs) allowed to warm to room temperature. For reactions using $Na_2CO_3$, water (3.0 mL) was added and the organic phase was collected and dried ($Na_2SO_4$). The solvent was removed by rotary evaporation and the residue was chromatographed (silica gel, 1 × 25 cm column, packed in and eluted with 80:20 v/v hexanes/ethyl acetate). For reactions with other bases, the solvent was removed by rotary evaporation and the residue was analogously chromatographed. The product containing fractions were combined and the solvents were removed by rotary evaporation to give **9** (see appendix C and Figure C-2 for further data). The ee value and the dominant configuration were determined by HPLC with a Chiralcel OD-H column, 98:2 hexane/isopropanol, 1.0 mL/min, 210 nm, $t_S$ = 7.55 min, $t_R$ = 11.77 min. The order of elution was established in an earlier study with an identical column.[31]

**Catalyst screening for the tandem hydride transfer-cyclization (Table 4.3 and Table C-1).** A vial was charged with a stir bar, **10a** (0.014 g, 0.050 mmol), a catalyst (10 mol%), and a solvent (2.00 mL). The vial was sealed and the sample was brought to the indicated temperature. The reaction was stirred and monitored by TLC (silica gel, 80:20 v/v hexanes/ethyl acetate). For the reactions at 50 °C, the sample was cooled to room temperature before each TLC run. After the time indicated in Table 4.3, the vial was opened to air and (for 50 °C runs) allowed to cool to room temperature. The reaction mixture was loaded directly onto a column (silica gel, 1 × 25 cm column) and that was eluted with hexanes and then 80:20 v/v hexanes/ethyl acetate. The product containing fractions were combined and the solvents were removed by rotary evaporation to give **11a** (see appendix C for further data). The ee value and the dominant configuration were determined by HPLC with a Chiralcel OJ-H column, 90:10 hexane/isopropanol, 1.0 mL/min, 254 nm, $t_R$ = 14.19 min, $t_S$ = 15.86 min. The order of elution was established in an earlier study with an identical column.[32]

**Substrate scope for the tandem hydride transfer-cyclization (Figure 4.5).** A vial was charged with a stir bar, **10** (0.050 mmol), the catalyst Λ-(*S*,*S*)-**3b**$^{3+}$ 2Cl$^{-}$BAr$_f^{-}$ ·2$H_2O$ (0.011 g, 0.0050 mmol, 10 mol%), and a solvent (2.00 mL). The vial was sealed and the sample was brought to the indicated temperature. The reaction was stirred and monitored by TLC (silica gel, 80:20 v/v hexanes/ethyl acetate). The sample was cooled to ambient temperature before each TLC run. After the time indicated in Figure 4.5, the vial was opened to air and allowed to cool to room temperature. The reaction mixture was loaded directly onto a column (silica gel, 1 × 25 cm column) and that was eluted with hexanes and then 80:20 v/v hexanes/ethyl acetate. The product containing fractions were combined and the solvents were removed by rotary evaporation to give **11** (see appendix C for further data). The ee values of **11** was determined by HPLC (see appendix C).

## 4.6. References

(1) For reviews, see (a) Taylor, M. S.; Jacobsen, E. N. Asymmetric Catalysis by Chiral Hydrogen-Bond Donors. *Angew. Chem., Int. Ed.* **2006***, 45,* 1520-1543; Asymmetrische Katalyse durch chirale Wasserstoffbrückendonoren. *Angew. Chem.* **2006**, *118*, 1550-1573. (b) Doyle, A. G.; Jacobsen, E. N. Small-Molecule H-Bond Donors in Asymmetric Catalysis. *Chem. Rev.* **2007**, *107*, 5713-5743. (c) Yu, X.; Wang, W. Hydrogen-Bond-Mediated Asymmetric Catalysis. *Chem. Asian J.* **2008**, *3*, 516-532. (d) Miyabe, H.; Takemoto, Y. Discovery and Application of Asymmetric Reaction by Multi-Functional Thioureas. *Bull. Chem. Soc. Jpn.* **2008**, *81*, 785-795. (e) Held, F. E.; Tsogoeva, S. B. Asymmetric Cycloaddition Reactions Catalyzed by Bifunctional Thiourea and Squaramide Organocatalysts: Recent Advances. *Catal. Sci. Technol.* **2016**, *6*, 645-667.

(2) (a) Ganzmann, C.; Gladysz, J. A. Phase Transfer of Enantiopure Werner Cations into Organic Solvents: An Overlooked Family of Chiral Hydrogen Bond Donors for Enantioselective Catalysis. *Chem. Eur. J.* **2008**, *14*, 5397-5400. (b) Maximuck, W. J.; Ganzmann, C.; Alvi, S.; Hooda, K. R.; Gladysz, J. A. Rendering Classical Hydrophilic Enantiopure Werner Salts $[M(en)_3]^{n+}$ $nX^-$ Lipophilic (M/*n* = Cr/3, Co/3, Rh/3, Ir/3, Pt/4); New Chiral Hydrogen Bond Donor Catalysts and Enantioselectivities as a Function of Metal and Charge. *Dalton Trans*. **2020**, *49*, 3680-3691.

(3) (a) Lewis, K. G.; Ghosh, S. K.; Bhuvanesh, N.; Gladysz, J. A. Cobalt(III) Werner Complexes with 1,2-Diphenylethylenediamine Ligands: Readily Available, Inexpensive, and Modular Chiral Hydrogen Bond Donor Catalysts for Enantioselective Organic Synthesis. *ACS Cent. Sci.* **2015**, *1*, 50-56. (b) Kumar, A.; Ghosh, S. K.; Gladysz, J. A. Tris(1,2-diphenylethylenediamine)cobalt(III) Complexes: Chiral Hydrogen Bond Donor Catalysts for Enantioselective *α*-Aminations of 1,3-Dicarbonyl Compounds. *Org. Lett.* **2016**, *18*, 760-763. (c) Joshi, H.; Ghosh, S. K.; Gladysz, J. A. Enantioselective

Additions of Stabilized Carbanions to Imines Generated from α-Amido Sulfones By Using Lipophilic Salts of Chiral Tris(1,2-diphenylethylenediamine) Cobalt(III) Trications as Hydrogen Bond Donor Catalysts. *Synthesis* **2017**, *49*, 3905-3915. (d) Maximuck, W. J.; Gladysz, J. A. Lipophilic Chiral Cobalt(III) Complexes of Hexaamine Ligands; Efficacies as Enantioselective Hydrogen Bond Donor Catalysts. *Mol. Catal.* **2019**, *473*, 110360 (this journal has replaced conventional pagination by article numbers). (e) Kabes, C. Q.; Maximuck, W. J.; Ghosh, S. K.; Kumar, A.; Bhuvanesh, N.; Gladysz, J. A. Chiral Tricationic tris(1,2-diphenylethylenediamine) Cobalt(III) Hydrogen Bond Donor Catalysts with Defined Carbon/Metal Configurations; Matched/Mismatched Effects upon Enantioselectivities with Enantiomeric Chiral Counter Anions. *ACS Catal.* **2020**, *10*, 3249-3263. (f) Luu, Q. H.; Gladysz, J. A. An Air and Water Stable Hydrogen Bond Donor Catalyst for the Enantioselective Generation of Quaternary Carbon Stereocenters by Additions of Substituted Cyanoacetate Esters to Acetylenic Esters. *Chem. Eur. J.* **2020**, *26*, accepted. DOI:10.1002/chem.202001639.

(4) Ghosh, S. K.; Ganzmann, C.; Bhuvanesh, N.; Gladysz, J. A. Werner Complexes with ω-Dimethylaminoalkyl Substituted Ethylenediamine Ligands: Bifunctional Hydrogen-Bond-Donor Catalysts for Highly Enantioselective Michael Additions. *Angew. Chem., Int. Ed.* **2016**, *55*, 4356-4360; Werner-Komplexe mit ω-Dimethylaminoalkyl-substitutierten Ethylendiaminliganden: bifunktionale H-Brückendonor-Katalysatoren für hoch enantioselektive Michael-Additionen. *Angew. Chem.* **2016**, *128*, 4429-4433.

(5) (a) Scherer, A.; Mukherjee, T.; Hampel, F.; Gladysz, J. A. Metal Templated Hydrogen Bond Donors as 'Organocatalysts' for Carbon-Carbon Bond Forming Reactions: Syntheses, Structures, and Reactivities of 2-Guanidinobenzimidazole Cyclopentadienyl Ruthenium Complexes. *Organometallics* **2014**, *33*, 6709-6722. (b) Mukherjee, T.; Ganzmann, C.; Bhuvanesh, N.; Gladysz, J. A. Syntheses of Enantiopure Bifunctional 2-

Guanidinobenzimidazole Cyclopentadienyl Ruthenium Complexes: Highly Enantioselective Organometallic Hydrogen Bond Donor Catalysts for Carbon-Carbon Bond Forming Reactions. *Organometallics* **2014**, *33*, 6723-6737. (c) Wititsuwannakul, T.; Mukherjee, T.; Hall, M. B.; Gladysz, J. A. Computational Investigations of Enantioselection in Carbon-Carbon Bond Forming Reactions of Ruthenium Guanidino-benzimidazole Second Coordination Sphere Hydrogen Bond Donor Catalysts. *Organometallics* **2020**, *39*, 1149-1162. (d) Mukherjee, T.; Ghosh, S. K.; Wititsuwannakul, T.; Bhuvanesh, N.; Gladysz, J. A. A New Family of Chiral-at-Metal Ruthenium Complexes with Guanidinobenzimidazole and Pentaphenylcyclopentadienyl Ligands: Synthesis, Resolution, and Preliminary Screening as Enantioselective Second Coordination Sphere Hydrogen Bond Donor Catalysts. *Organometallics* **2020**, *39*, 1163-1175.

(6) (a) Chen, L.-A.; Tang, X.; Xi, J.; Xu, W.; Gong, L.; Meggers, E. Chiral-at-Metal Octahedral Iridium Catalyst for the Asymmetric Construction of an All-Carbon Quaternary Stereocenter. *Angew. Chem., Int. Ed.* **2013**, *52*, 14021-14025 and *Angew. Chem.* **2013**, *125*, 14271-14275. (b) Huo, H.; Fu, C.; Wang, C.; Harms, K.; Meggers, E. Metal-templated Enantioselective Enamine/H-bonding Dual Activation Catalysis. *Chem. Commun*. **2014**, *50*, 10409-10411. (c) Hu, Y.; Zhou, Z.; Gong, L.; Meggers, E. Asymmetric aza-Henry reaction to provide oxindoles with quaternary carbon stereocenter catalyzed by a metal-templated chiral Brønsted base. *Org. Chem. Front.* **2015**, *2*, 968-972. (d) Ding, X.; Lin, H.; Gong, L.; Meggers, E. Enantioselective Sulfa-Michael Addition to α,β-Unsaturated γ-Oxoesters Catalyzed by a Metal-Templated Chiral Brønsted Base. *Asian J. Org. Chem.* **2015**, *4*, 434-437. (e) Xu, W.; Shen, X.; Ma, Q.; Gong, L.; Meggers, E. Restricted Conformation of a Hydrogen Bond Mediated Catalyst Enables the Highly Efficient Enantioselective Construction of an All-Carbon Quaternary Stereocenter. *ACS*

*Catal.* **2016**, *6*, 7641-7646. (f) Xu, W.; Arieno, M.; Löw, H.; Huang, K.; Xie, X.; Cruchter, T.; Ma, Q.; Xi, J.; Huang, B.; Wiest, O.; Gong, L.; Meggers, E. Metal-Templated Design: Enantioselective Hydrogen-Bond-Driven Catalysis Requiring Only Parts-per-Million Catalyst Loading. *J. Am. Chem. Soc.* **2016,** *138*, 8774-8780. (g) Ding, X.; Tian, C.; Hu, Y.; Gong, L.; Meggers, E. Tuning the Basicity of a Metal-Templated Brønsted Base to Facilitate the Enantioselective Sulfa-Michael Addition of Aliphatic Thiols to α,β-Unsaturated *N*-Acylpyrazoles. *Eur. J. Org. Chem.* **2016**, *2016*, 887-890.

(7) (a) Belokon, Y. N.; Maleev, V. I.; North, M.; Larionov, V. A.; Savel'yeva, T. F.; Nijland, A.; Nelyubina, Y. V. Chiral Octahedral Complexes of $Co^{III}$ As a Family of Asymmetric Catalysts Operating under Phase Transfer Conditions. *ACS Catal.* **2013**, *3*, 1951-1955. (b) Maleev, V. I.; North, M.; Larionov, V. A.; Fedyanin, I. V.; Savel'yeva, T. F.; Moscalenko, M. A.; Smolyakov, A. F.; Belokon, Y. N. Chiral Octahedral Complexes of Cobalt(III) as "Organic Catalysts in Disguise" for the Asymmetric Addition of a Glycine Schiff Base Ester to Activated Olefins. *Adv. Synth. Catal.* **2014**, *356*, 1803-1810. (c) Larionov, V. A.; Markelova, E. P.; Smol'yakov, A. F.; Savel'yeva, T. F.; Maleev, V. I.; Belokon, Y. N. Chiral octahedral complexes of Co(III) as catalysts for asymmetric epoxidation of chalcones under phase transfer conditions. *RSC Adv.* **2015**, *5*, 72764-72771. (d) Rulev, Y. A.; Larionov, V. A.; Lokutova, A. V.; Moskalenko, M. A.; Lependina, O. L.; Maleev, V. I.; North, M.; Belokon, Y. N. Chiral Cobalt(III) Complexes as Bifunctional Brønsted Acid-Lewis Base Catalysts for the Preparation of Cyclic Organic Carbonate. *ChemSusChem* **2016**, *9*, 216-222.

(8) (a) Pardo, P.; Carmona, D.; Lamata, P.; Rodríguez, R.; Lahoz, F. J.; García-Orduña, P.; Oro, L. A. Reactivity of the Chiral Metallic Brønsted Acid [($\eta^6$-*p*-$MeC_6H_4$*i*Pr)Ru($\kappa^3$*P*,*O*,*O'*-POH)]$[SbF_6]_2$ (POH = $S_{C1}$,$R_{C2}$)-$Ph_2PC(Ph)HC(OH)HCH_2$-OMe) toward Aldimines. *Organometallics* **2014**, *33*, 6927-6936. (b) Skubi, K. L.; Kidd,

J. B.; Jung, H.; Guzei, I. A.; Baik, M.-H.; Yoon, T. P. Enantioselective Excited-State Photoreactions Controlled by a Chiral Hydrogen-Bonding Iridium Sensitizer. *J. Am. Chem. Soc.* **2017**, *139*, 17186-17192.

(9) (a) Wang, J.; Sanchez-Rosello, M; Acena, J. L.; del Pozo, C.; Sorochinsky A. E.; Fustero, S.; Soloshonok, V. A.; Liu, H. Fluorine in Pharmaceutical Industry: Fluorine-Containing Drugs Introduced to the Market in the Last Decade (2001-2011). *Chem. Rev.* **2014**, *114*, 2432-2506. (b) Zhou, Y.; Wang, J.; Gu, Z.; Wang, S.; Zhu, W.; Acena, J. L.; Soloshonok, V. A.; Izawa, K.; Liu, H. Next Generation of Fluorine-Containing Pharmaceuticals, Compounds Currently in Phase II-III Clinical Trials of Major Pharmaceutical Companies: New Structural Trends and Therapeutic Areas. *Chem. Rev.* **2016**, *116*, 422-518.

(10) (a) Ogasawara, Y.; Liu, H. Biosynthetic Studies of Aziridine Formation in Azicemicins. *J. Am. Chem. Soc.* **2009**, *131*, 18066-18068. (b) Pitscheider, M.; Mausbacher, N.; Sieber, S. A. Antibiotic activity and target discovery of three-membered natural product-derived heterocycles in pathogenic bacteria. *Chem. Sci.* **2012**, *3*, 2035-2041.

(11) (a) Katritzky, A. R.; Rachwal, S.; Rachwal, B. Recent Progress in the Synthesis of 1,2,3,4-Tetrahydroquinolines. *Tetrahedron* **1996**, *52*, 15031-15070.

(12) (a) Ma, J.-A.; Cahard, D. Asymmetric Fluorination, Trifluoromethylation, and Perfluoroalkylation Reactions. *Chem. Rev.* **2008**, *108*, PR1-PR43. (b) Furuya, T.; Kamlet, A. S.; Ritter, T. Catalysis for fluorination and trifluoroethylation. *Nature* **2011**, *473*, 470-477. (c) Yang, X.; Wu, T.; Phipps, R. J.; Toste, F. D. Advances in Catalytic Enantioselective Fluorination, Mono-, Di-, and Trifluoromethylation, and Trifluoromethylthiolation Reactions. *Chem. Rev.* **2015**, *115*, 826-870.

(13) (a) Shibata, N.; Ishimaru, T.; Nagai, T.; Kohno, J.; Toru, T. First Enantio-Flexible Fluorination Reaction Using Metal-Bis(oxazoline) Complexes. *Synlett.* **2004**, *2004*, 1073-1076. (b) Suzuki, S.; Furuno, H.; Yokoyama, Y.; Inanaga, J. Asymmetric fluorination of β-keto esters catalyzed by chiral rare earth perfluorinated organophosphates. *Tetrahedron: Asymmetry* **2006**, *17*, 504-507. (c) Frings, M.; Bolm, C. Enantioselective Halogenation of β-Oxo Esters Catalyzed by a Chiral Sulfoximine-Copper Complex. *Eur. J. Org. Chem.* **2009**, *2009*, 4085-4090. (d) Kawatsura, M.; Hayashi, S.; Komatsu, Y.; Hayase, S.; Itoh, T. Enantioselective α-Fluorination and Chlorination of β-Ketoester by Cobalt Catalyst. *Chem. Lett.* **2010**, *39*, 466-467.

(14) (a) Kim, D. Y.; Park, E. J. Catalytic Enantioselective Fluorination of β-Keto Esters by Phase-Transfer Catalysis Using Chiral Quaternary Ammonium Salts. *Org. Lett.* **2002**, *4*, 545-547. (b) Wang, X.; Lan, Q.; Shirakawa, S.; Maruoka, K. Chiral bifunctional phase transfer catalyst for asymmetric fluorination of β-keto esters. *Chem. Commun.* **2010**, *46*, 321-323. (c) Xu, J.; Hu, Y.; Huang, D.; Wang, K.-H.; Xu, C.; Niu, T. Thiourea-Catalyzed Enantioselective Fluorination of Keto Esters. *Adv. Synth. Catal.* **2012**, *354*, 515-526.

(15) For lists of electrophilic fluorinating agents and their reactivities, see: (a) Lal, G. S.; Pez, G. P.; Syvret, R. G. Electrophylic NF Fluorinating Agents. *Chem. Rev.* **1996**, *96*, 1737-1755. (b) Rozatian, N.; Ashworth, I. W.; Sandford, G.; Hodgson, D. R. W. A quantitative reactivity scale for electrophilic fluorinating reagents. *Chem. Sci.* **2018**, *9*, 8692-8702.

(16) The best price found is $27.00 for 100 g of NFSI from www.arkpharminc.com. (access May 2, 2020).

(17) For a review see: Khlebnikov, A. F.; Novikov, M. S.; Rostovskii, N. V. Advances in 2*H*-azirine chemistry: A seven-year update. *Tetrahedron* **2019**, *75*, 2555-2624.

(18) (a) Sakamoto, S.; Inokuma, T.; Takemoto, Y. Organocatalytic Asymmetric Neber Reaction for the Synthesis of 2*H*-Azirine Carboxylic Esters. *Org. Lett.* **2011**, *13*, 6374-6377. (b) Cardoso, A. L.; Gimeno, L.; Lemos, A.; Palacios, F.; Pinho e Melo, T. M. V. D. The Neber Approach to 2-(Tetrazol-5-yl)-2*H*-Azirines. *J. Org. Chem.* **2013**, *78*, 6983-6991. (c) Zhao, J.-Q.; Yue, D.-F.; Zhang, X.-M; Xu, X.-Y.; Yuan, W.-C. The organocatalytic asymmetric Neber reaction for the enantioselective synthesis of spirooxindole 2*H*-azirines. *Org. Biomol. Chem.* **2016**, *14*, 10946-10952.

(19) Stark, G. A.; Arif, A. M.; Gladysz, J. A. Diastereoselective 1,2 Additions of Nucleophiles to Quinoline Complexes of the Chiral Rhenium Lewis Acid $[(\eta^5\text{-}C_5H_5)Re(NO)(PPh_3)]^+$. *Organometallics* **1994**, *13*, 4523-4530.

(20) (a) Stark, G. A.; Dewey, M. A.; Richter-Addo, G. B.; Knight, D. A.; Arif, A. M.; Gladysz, J. A. Diastereoselective Additions of Nucleophiles and Electrophiles to Isoquinoline and Quinoline Mediated by an Easily Resolved and Recycled Chiral Transition Metal Auxiliary; Enantioselective Syntheses of Alkyl, Dialkyl, and Trialkyl Hydroisoquinoline Derivatives. In *Stereoselective Reactions of Metal-Activated Molecules*; Werner, H.; Sundermeyer, J. Eds.; Vieweg-Verlag: Braunschweig, Germany, 1995; pp. 51-71. (b) Richter-Addo, G. B.; Knight, A. D.; Dewey, M. A.; Arif, A. M.; Gladysz, J. A. New Strategies for Enantioselective Syntheses of 1-Alkyl and 1,4-Dialkyl 1,2,3,4-Tetrahydroisoquinolines: Diastereoselective Additions of Nucleophiles and Electrophiles to Isoquinoline Mediated by an Easily Resolved and Recycled Chiral Transition Metal Auxiliary. *J. Am. Chem. Soc.* **1993**, *115*, 11863-11873.

(21) (a) Haibach, M. C.; Seidel, D. C-H Bond Functionalization through Intramolecular Hydride Transfer. *Angew. Chem., Int. Ed.* **2014**, *53*, 5010-5036. C-H-Funktionalisierung über intramolekularen Hydridtransfer. *Angew. Chem.* **2014**, *126*, 5110-5137. (b) Qin, Y.; Zhu, L.; Luo, S. Organocatalysis in Inert C-H Bond Functionalization. *Chem. Rev.* **2017**, *117*, 9433-9520.

(22) (a) Mori, K.; Ehara, K.; Kurihara, K.; Akiyama, T. Selective Activation of Enantiotopic C($sp^3$)–Hydrogen by Means of Chiral Phosphoric Acid: Asymmetric Synthesis of Tetrahydroquinoline Derivatives. *J. Am. Chem. Soc.* **2011**, *133*, 6166-6169. (b) Chen, L.; Zhang, L.; Lv, J.; Cheng, J.-P.; Luo, S. Catalytic Enantioselective *tert*-Aminocyclization by Asymmetric Binary Acid Catalysis (ABC): Stereospecific 1,5-Hydrogen Transfer. *Chem. Eur. J.* **2012**, *18*, 8891-8895.

(23) Ghosh, S. K.; Lewis, K. G.; Kumar, A.; Gladysz, J. A. Syntheses of Families of Enantiopure and Diastereopure Cobalt Catalysts Derived from Trications of the Formula $[Co(NH_2CHArCHArNH_2)_3]^{3+}$. *Inorg. Chem.* **2017**, 56, 2304-2320.

(24) Luu, Q. H.; Lewis, K. G.; Banerjee, A.; Bhuvanesh, N.; Gladysz, J. A. The robust, readily available cobalt(III) trication $[Co(NH_2CHPhCHPhNH_2)]^{3+}$ is a progenitor of broadly applicable chirality and prochirality sensing agents. *Chem. Sci.* **2018**, *9*, 5087-5099.

(25) Verniest, G.; Van Hende, E.; Surmont, R.; De Kimpe, N. Direct Electrophilic α-Fluorination of Imines: Efficient Synthesis of Mono- and Difluoroimines. *Org. Lett.* **2006**, *8*, 4767-4770.

(26) (a) Lungwitz, R.; Spange, S. A hydrogen bond accepting (HBA) scale for anions, including room temperature ionic liquids. *New. J. Chem.* **2008**, *32*, 392-394. (b) Claudio, A. F. M.; Swift, L.; Hallett, J. P.; Welton, T.; Coutinho, J. A. P.; Fleire, M. G.

Extended scale for hydrogen-bond basicity of ionic liquids. *Phys. Chem. Chem. Phys.* **2014**, *16*, 6593-6601.

(27) https://secure.strem.com/catalog/v/27-4010/16/cobalt_1542135-29-4 (accessed May 2, 2020).

(28) Perrin, D. D. Ionization Constants of Inorganic Acids and Bases in Aqueous Solution, 2 Ed; Pergamon, Oxford, 1982.

(29) Perrin, D. D.; Dempsey, B.; Serjeant, E. P. $pK_a$ Prediction for Organic Acids and Bases. Chapman and Hall, London, 1981.

(30) $CH_2Cl_2$ was dried and degassed described in appendix C.

(31) An, D.; Guan, X.; Guan, R.; Jin, L.; Zhang, G.; Zhang, S. Organocatalyzed nucleophilic addition of pyrazoles to 2*H*-azirines: asymmetric synthesis of 3,3-disubstituted aziridines and kinetic resolution of racemic 2*H*-azirines. *Chem. Commun.* **2016**, *52*, 11211-11214.

(32) Cao, W.; Liu, X.; Wang, W.; Lin, L.; Feng, X. Highly Enantioselective Synthesis of Tetrahydroquinolines via Cobalt(II)-Catalyzed Tandem 1,5-Hydride Transfer/Cyclization. *Org. Lett.* **2011**, *13*, 600-603.

# 5. WERNER COMPLEXES WITH NON-INNOCENT ANIONS IN ENANTIOSELECTIVE CATALYSIS

## 5.1. Introduction

Since the first report of lipophilic salts of enantiomers of the trication cobalt(III) tris(ethylenediamine) (Λ- and Δ-**1**$^{3+}$ in Figure 5.1),[1] many derivatives of this emerging class of chiral hydrogen bond donors have been described[2] exploiting both the ligand[2a] and metal center.[2b] Most effective in enantioselective catalysis are those containing the trication cobalt(III) tris((*S*,*S*)-diphenylethylenediamine) Λ- and Δ-(*S*,*S*)-**2**$^{3+}$ (Figure 5.1).[3]

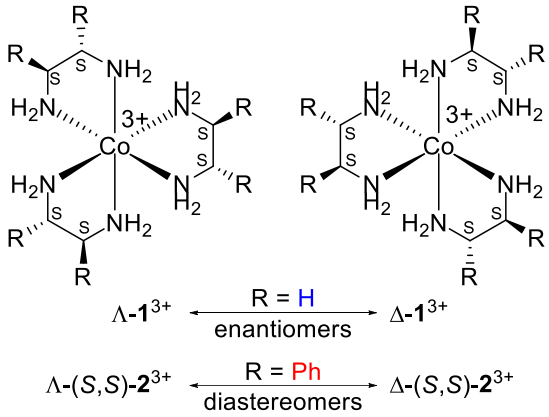


**Figure 5.1.** Representatives of the trications in Werner catalysts.

Multiple studies have established that organic substrates are activated by hydrogen bonding to the NH units that exist in abundance in these catalysts.[3a,3f,4] The number of Lewis basic functional groups that exhibit hydrogen bonding to Λ-(*S*,*S*)-**2**$^{3+}$ $2X^{-}X'^{-}$ also exceeds a dozen.[4] Naturally, exploratory chemistry involving Werner complexes has been centered around reactions where both the electrophiles and nucleophiles can bond to the trication (Figure 5.2 and chapter 4).[3]

Normally, three monoanions are present in the catalyst. One of those is usually a lipophilic non-coordinating tetraarylborate ($B(3,5\text{-}C_6H_3(CF_3)_2)_4^-$ = $BAr_f^-$ or $B(C_6F_5)_4^-$ ).[5] The enantioselectivity of the reactions in Figure 5.2 also showed some correlation to

the identity of these three anions.[3] Integrating chiral anions to the catalysts in fact resulted in a certain degree of match and mismatch phenomena in enantioselection.[3e] However direct participation of the anions in any reactions has not been evidenced.

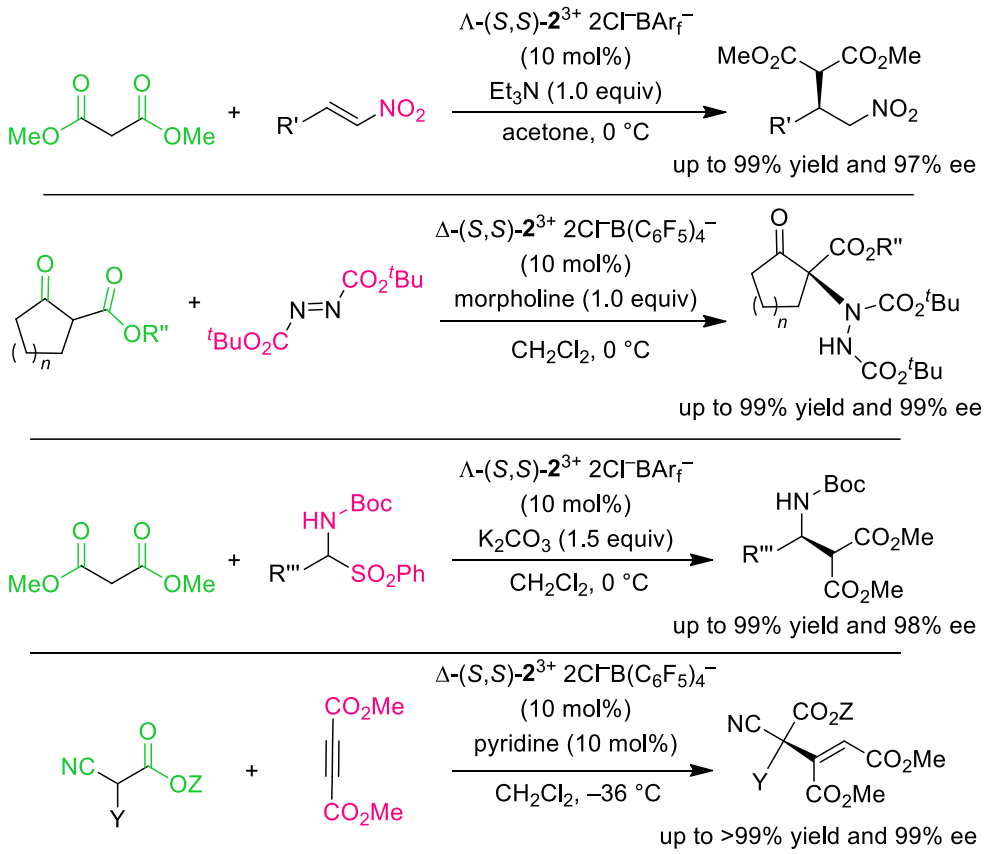


**Figure 5.2.** Highly enantioselective reactions catalyzed by Werner complexes. Color code: hydrogen bond acceptors in nucleophiles (green) and electrophiles (pink).

Motivated by the potentials of these underexplored species in my own catalysts, I set out to study several reactions, which require one or two anions to actively contribute as activators or catalysts themselves. To maximize the cooperation between the hydrogen bond donors and the anion, the reaction pools were simplified to those involving at least one reactant with a hydrogen bond accepting group. Two reactions that fit well into the category are presented in Figure 5.3. The former is known to be catalyzed by fluoride

anions,[6] and the latter operates via an iminium salt generated from the conjugate base of proline.[7]

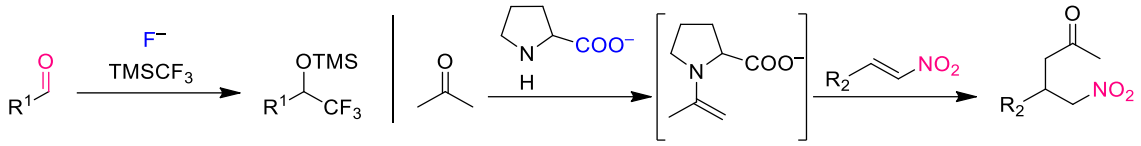


**Figure 5.3.** Reactions tested in this chapter: trifluoromethylations of aldehydes (left) and additions of enamines to C=C bonds (right).

## 5.2. Results

### 5.2.1. Syntheses of catalysts

Enantiopure Λ-**1**$^{3+}$ 3I$^-$, Λ-(*S*,*S*)-**2**$^{3+}$ 3Cl$^-$, and Δ-(*S*,*S*)-**2**$^{3+}$ 3Cl$^-$ were prepared as previously reported.[2] The complex Λ-**1**$^{3+}$ 3F$^-$ was synthesized following a procedure reported for the racemic salt **1**$^{3+}$ 3F$^-$.[8] The other catalysts containing fluoride anions investigated in Table 5.1 were synthesized as depicted in Scheme 5.1. Treating the chloride precursors with silver fluoride in water gave the tris(fluoride) salt of each cation in good yield. The salts Λ- and Δ-(*S*,*S*)-**2**$^{3+}$ 3F$^-$ are readily soluble in methanol but insoluble in other solvents such as $CH_2Cl_2$, $CHCl_3$, acetone, $CH_3CN$, and THF. Attempts to replace one fluoride anion by a $BAr_f^-$ anion with $Na^+$ $BAr_f^-$ for a more lipophilic salt were not successful. The salt Λ-(*S*,*S*)-**2**$^{3+}$ 3F$^-$ was characterized by $^1$H, $^{13}$C, $^{19}$F NMR. The purity and hydration level were confirmed by elemental analysis. The purity and hydration level of Δ-(*S*,*S*)-**2**$^{3+}$ 3F$^-$ will be reported in future communications.

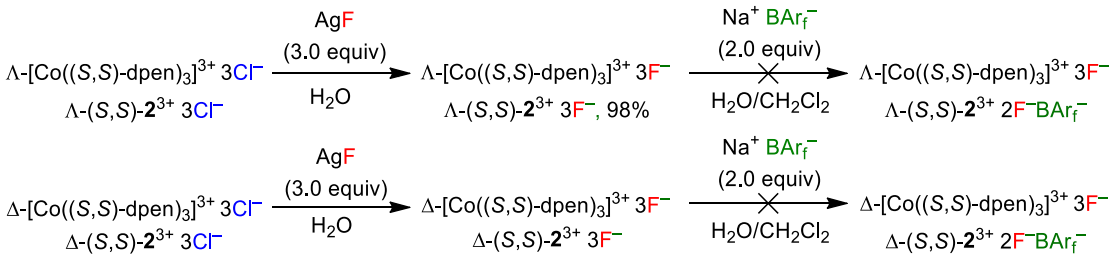


**Scheme 5.1.** Synthesis of the tris(fluoride) salts of the trications Λ- and Δ-(*S*,*S*)-**2**$^{3+}$.

### 5.2.2. Active fluoride anions in the enantioselective trifluoromethylation of aromatic aldehydes

Due to the low solubility in organic solvents of the fluoride salts of all cations investigated, reactions with neat benzaldehyde **3a** and trifluoromethyl trimethylsilane ($TMSCF_3$) were initially screened. As seen in Table 5.1, no background reaction was detected (entry 1). All "non-fluoride" salts of the trications Λ-$\mathbf{1}^{3+}$ and Λ-(*S*,*S*)-$\mathbf{2}^{3+}$ did not give catalytic activity (entry 2 and 3). The tris(fluoride) salt Λ-$\mathbf{1}^{3+}$ $3F^-$ gave a trace amount of the product 2,2,2-trifluoro-1-phenylethanol (**4a**, entry 4). The catalyst Δ-(*S*,*S*)-$\mathbf{2}^{3+}$ $3F^-$ gave **4a** in 90% ee and 76% yield as assayed by $^1$H NMR (66% after isolation, entry 5). Interestingly, the other diastereomer gave an excellent ee (99%) with the same dominant configuration of product (entry 6). Reducing the catalyst loading diminished yields and enantioselectivities (entry 7 and 8).

An identical series of reactions with the catalyst Λ-(*S*,*S*)-$\mathbf{2}^{3+}$ $3F^-$ was carried out in various solvents (0.10 mL, $CH_2Cl_2$, $CHCl_3$, acetone, $CH_3CN$, THF, DMSO, and DMF). Under these conditions, the catalyst Λ-(*S*,*S*)-$\mathbf{2}^{3+}$ $3F^-$ dissolved. However, benzaldehyde was fully recovered after column chromatography. When a 2:1 mixture of Λ-(*S*,*S*)-$\mathbf{2}^{3+}$ $3F^-$ (0.0085 g, 0.010 mmol) and Λ-(*S*,*S*)-$\mathbf{2}^{3+}$ $3BAr_f^-$ (0.030 g, 0.0050 mmol) was stirred vigorously in $CD_2Cl_2$, a clear solution was obtained. This had the potential to generate the mixed salt Λ-(*S*,*S*)-$\mathbf{2}^{3+}$ $2F^-BAr_f^-$. However, a reaction carried out in this solution gave 0% conversion of benzaldehyde as determined by $^1$H NMR.

**Table 5.1.** Catalyst screening for the trifluoromethylation of benzaldehyde.[a]

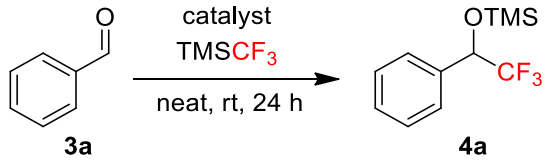


| Entry | Catalyst | Loading (mol%) | Yield (%)[b] | Ee (%)[c] |
|---|---|---|---|---|
| 1 | – | – | – | – |
| 2 | Λ-**1**$^{3+}$ 3I$^-$ | 10 | – | – |
| 3 | Λ-(*S*,*S*)-**2**$^{3+}$ 3Cl$^-$ | 10 | — | – |
| 4 | Λ-**1**$^{3+}$ 3F$^-$ | 10 | 3 | 0 |
| 5 | Δ-(*S*,*S*)-**2**$^{3+}$ 3F$^-$ | 10 | 76 (66) | 90 (*R*) |
| 6 | Λ-(*S*,*S*)-**2**$^{3+}$ 3F$^-$ | 10 | 78 (70) | 99 (*R*) |
| 7 | Λ-(*S*,*S*)-**2**$^{3+}$ 3F$^-$ | 5 | 50 (50) | 62 (*R*) |
| 8 | Λ-(*S*,*S*)-**2**$^{3+}$ 3F$^-$ | 1 | 5 | 0 |

[a]A vial was charged with benzaldehyde (0.055 g, 0.50 mmol, 0.050 mL), and a catalyst (1-10 mol%). $TMSCF_3$ (0.140 g, 1.00 mmol, 0.150 mL) was then added slowly over 30 min and the mixture was stirred for 24 h. [b]The reaction mixtures were dissolved in $CDCl_3$ and NMR yields were calculated from $^1$H NMR spectra using dimethyldiphenylsilane as the internal standard (see experimental section for details). Isolated yields are in parentheses. [c]Determined by HPLC (see experimental section for details).

The optimized conditions (Table 5.1, entry 6) were used for some other substrates. As summarized in Figure 5.4, substrates derived from benzaldehyde gave 99 to >99% ee (**4a**, and **4c**-**4e**). Substrates with naphthyl and thiophenyl substituents gave products with 84% and 54% ee respectively. Extensions to other aldehydes gave low yields and ee values. In all cases, the reaction turned black when $TMSCF_3$ was added to the reaction mixture.

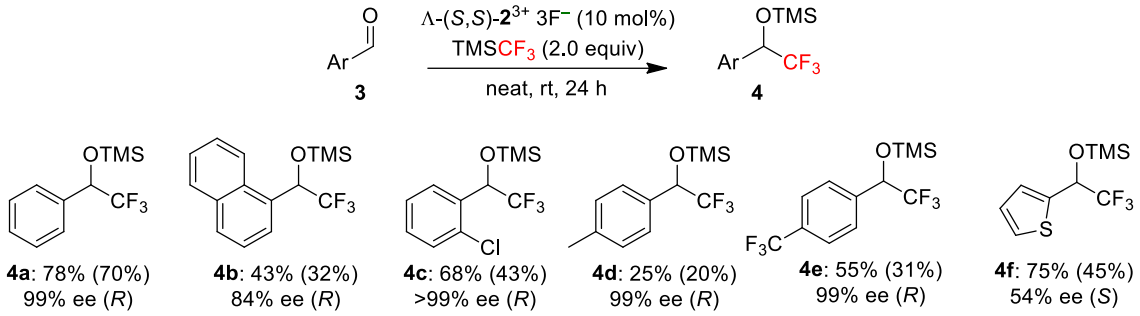


**Figure 5.4.** Substrate scope and $^1$H NMR yields for the enantioselective trifluoromethylation of aromatic aldehydes. Isolated yields are given in parentheses.

### 5.2.3. Active proline anions in the enantioselective condensation of ketones and *trans*-β-nitrostyrene

In initial screening reactions, acetone and trans-β-nitrostyrene (**5**) were combined in 10:1 mole ratio in $CH_2Cl_2$ in the presence of 10 mol% of a catalyst from Figure 5.1, $Na_2CO_3$ (40 mol%), and *D*- or *L*-proline (20 mol%). The results are summarized in Table 5.2. *D*-proline itself catalyzed the reaction and gave the product 5-nitro-4-phenylpentan-2-one (**6**) in 30 % yield and 15% ee (entry 1). The combination of *D* or *L*-proline and the catalyst Λ-**1**$^{3+}$ 3BAr$_f^-$ gave **6** in 17-25% ee (entries 3 to 6). The highest ee value (58%) was obtained when the catalyst Λ-(*S*,*S*)-**2**$^{3+}$ 2Cl$^-$BAr$_f^-$ (10 mol%) and *D*-proline (20 mol%) were used (entry 10).

**Table 5.2.** Catalyst screening for the addition of acetone to *trans*-β-nitrostyrene (**5**).[a]

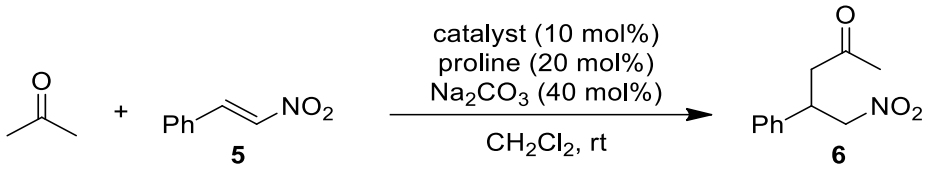


| Entry | Catalyst | Proline config. | Time (h) | Yield (%)[b] | Ee (%)[c] |
|---|---|---|---|---|---|
| 1 | – | *D* | 24 | 30 | 15 (*R*) |
| 2 | Λ-**1**$^{3+}$ 3BAr$_f^-$ | – | 29 | 10 | – |
| 3[d] | Λ-**1**$^{3+}$ 3BAr$_f^-$ | *D* | 72 | 50 | 17 (*R*) |
| 4[d] | Λ-**1**$^{3+}$ 3BAr$_f^-$ | *L* | 72 | 50 | 20 (*S*) |
| 5 | Λ-**1**$^{3+}$ 3BAr$_f^-$ | *D* | 20 | >99 | 20 (*R*) |
| 6 | Λ-**1**$^{3+}$ 3BAr$_f^-$ | *L* | 20 | >99 | 25 (*S*) |
| 7[d] | Λ-(*S*,*S*)-**2**$^{3+}$ 3BAr$_f^-$ | *D* | 24 | 0 | – |
| 8 | Λ-(*S*,*S*)-**2**$^{3+}$ 3BAr$_f^-$ | *D* | 20 | >99 | 22 (*R*) |
| 9 | Λ-(*S*,*S*)-**2**$^{3+}$ 3BAr$_f^-$ | *L* | 20 | >99 | 1 (*S*) |
| 10 | Λ-(*S*,*S*)-**2**$^{3+}$ 2Cl$^-$BAr$_f^-$ | *D* | 22 | 90 | 58 (*R*) |
| 11 | Λ-(*S*,*S*)-**2**$^{3+}$ 2Cl$^-$BAr$_f^-$ | *L* | 22 | 90 | 7 (*S*) |
| 12 | Δ-(*S*,*S*)-**2**$^{3+}$ 2Cl$^-$BAr$_f^-$ | *D* | 22 | 92 | 8 (*R*) |
| 13 | Δ-(*S*,*S*)-**2**$^{3+}$ 2Cl$^-$ BAr$_f^-$ | *L* | 20 | 90 | 18 (*S*) |

[a]A vial was charged with **5** (0.0075 g, 0.050 mmol), a catalyst (0.0050 mmol, 10 mol%), proline (0.0012 g, 0.010 mmol, 20 mol%), $Na_2CO_3$ (0.0022 g, 0.020 mmol, 40 mol%), and $CH_2Cl_2$ (0.50 mL). Acetone (0.036 mL, 0.50 mmol, 10 equiv) was then added with stirring. The reaction was monitored by TLC and worked up as described in the experimental section. [b]Isolated yields. [c]Determined by HPLC (see experimental section for details). [d]$Na_2CO_3$ was not added.

## 5.3. Discussion

### 5.3.1. Active fluoride anions in the enantioselective trifluoromethylation of aromatic aldehydes

All fluoride salts investigated in this reaction are hydrated. This is observed for many other fluoride salts, for example *t*-$Bu_4N^+$ $F^-$.[9] The best performing catalyst Λ-(*S*,*S*)-**2**$^{3+}$ 3$F^-$ under ideal conditions (neat, rt) gave 99% to >99% ee for substrates with a substituted phenyl ring (Figure 5.4). However, changing the aryl group to 1-naphthyl diminished the enantioselectivity (**4b**). A thiophene ring has similar effects. Attempts to expand the substrate scope were unsuccessful, especially for aliphatic aldehydes.

The enantioselective trifluoromethylation of aldehydes has been previously studied with other fluoride salts (Figure 5.5). The quinine based catalyst **I** gave the trifluoromethylated products in 11-58% ee (**4a** was not reported).[11c] A related species (**II** in Figure 5.5) gave the product **4a** in 46% ee.[11a] Catalyst **III** gave **4a** in 11% ee (other substrates were not reported for catalyst **III**).[11b] The ee values obtained for **4a**-**4e** in this chapter surpassed those obtained by all the catalysts in Figure 5.5.

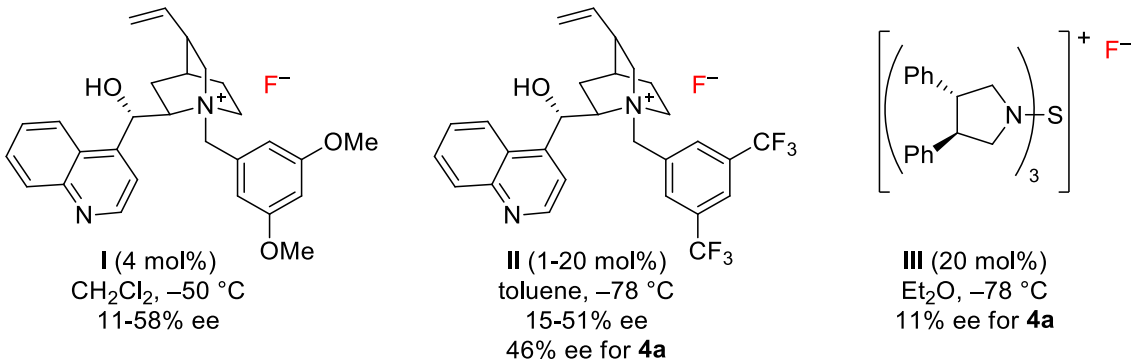


**Figure 5.5.** Previously reported catalysts for the enantioselective trifluoromethylation of aldehydes.

### 5.3.2. Active proline anions in the enantioselective condensation of ketones and *trans*-β-nitrostyrene

As summarized in Table 5.2, the combination of Werner catalysts and proline outperformed the individual catalysts in most cases. The absolute configuration of **6** depends on the configuration of proline. Some match and mismatch type phenomena[3e] was observed (entries 10 and 12). *D*-proline itself gave **6** in 15% ee (entry 1). When the catalysts Λ-(*S*,*S*)-$\mathbf{2}^{3+}$ $2Cl^{-}BAr_f^{-}$ and *D*-proline were used, **6** was obtained in 58% ee (entry 10). When the catalyst Δ-(*S*,*S*)-$\mathbf{2}^{3+}$ $2Cl^{-}BAr_f^{-}$ and *D*-proline were used, **6** was obtained in only 8% ee (entry 12).

The enantioselective condensation of ketones and nitrostyrenes has been previously studied with other hydrogen bond donors (Figure 5.6). A bifunctional thiourea catalyst (**IV** in Figure 5.6) gave **6** in 99% ee.[12] An ionic quinine based catalyst (**V**) containing the conjugate base of *L*-phenylglycine gave **6** in 95% ee.[7] Although the highest ee value (58%) obtained for **6** in this chapter is lower than those shown in Figure 5.6, an improvement in enantioselectivity is anticipated when anions of other amino acids are used (such as one in **V**). These studies are being conducted in the Gladysz group and will be communicated in the future.

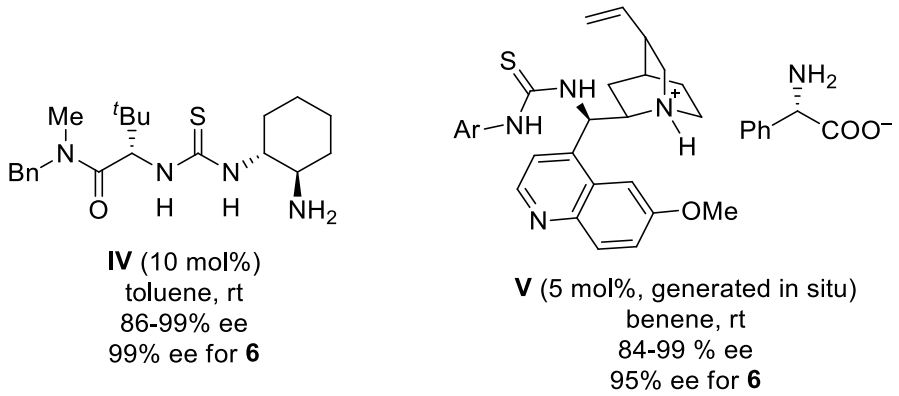


**Figure 5.6.** Previously reported hydrogen bond donor catalysts for the enantioselective condensation of ketones and nitrostyrenes.

## 5.4. Conclusion

This chapter reported two additional reactions catalyzed by Werner catalysts besides those described in chapters 3 and 4. First, the catalyst Λ-(*S*,*S*)-**2**$^{3+}$ 3F$^{-}$ was synthesized in 98% yield. Trifluoromethylation of aromatic aldehydes **3** using 10 mol% of Λ-(*S*,*S*)-**2**$^{3+}$ 3F$^{-}$ and $TMSCF_3$ gave **4** in 54% to >99% ee. These ee values are higher than those obtained from other fluoride containing catalysts previously studied. Second, condensation of acetone and trans-β-nitrostyrene using the catalyst Λ-(*S*,*S*)-**2**$^{3+}$ 2(*D*-proline)$^{-}$BAr$_f^{-}$ (generated in situ) gave the adduct **6** in 58% ee. Catalysts containing anions of other amino acids and an expansion of substrate scope for the condensation of ketones and nitrostyrenes will be communicated in the future.

## 5.5. Experimental (see also appendix D)

**Λ-(*S*,*S*)-2$^{3+}$ 3F$^{-}$.** A round bottom flask was charged with a suspension of Λ-(*S*,*S*)-**2**$^{3+}$ 3Cl$^{-}$·3$H_2O$ (0.170 g, 0.199 mmol) in water (30 mL) and anhydrous AgF (0.0762 g, 0.597 mmol) was added with vigorous stirring. A suspension of white particles in an orange solution formed. After 2 h, the mixture was filtered through a pad of Celite. Methanol (10 mL) was added to the filtrate and the solvents were removed by rotary evaporation and oil pump vacuum (20 h, rt) to give Λ-(*S*,*S*)-**2**$^{3+}$ 3F$^{-}$·4$H_2O$[13] (0.162 g, 0.195 mmol, 98%) as a brown solid, mp 112-115 °C dec (open capillary). Anal. Calcd. for $C_{42}H_{48}CoF_3N_6$·4$H_2O$ (824.86): C 61.16, H 6.84, N 10.19; found C 60.62, H 6.61, N 10.02.

Data: NMR (9:1 v/v $CD_2Cl_2$/$CD_3OD$, δ in ppm): $^1$H (500 MHz) 7.50-7.49 (m, 12H, *o*-Ph), 7.31-7.17 (m, 18H, *m*-, *p*-Ph), 6.41 (br s, 3H, N**H**H'), 6.25 (br s, 3H, NH**H'**), 4.51 (s, 6H, C**H**Ph), 2.98 (br s, 24H, $CD_3O$**H**/**H**$_2O$).[14] $^{13}$C{$^1$H} (125 MHz) 136.6 (s, *i*-Ph), 129.3 (s, *p*-Ph), 129.2 (s, *o*-Ph), 129.0 (*m*-Ph), 63.2 (s, **C**HPh). $^{19}$F (470 MHz) –102.4 (br s). IR (powder film, cm$^{-1}$): 3032 (m, $\nu_{NH}$), 1683 (m, $\delta_{NH}$), 1041 (vs, $\delta_{CCN}$).

**Δ-(*S*,*S*)-2$^{3+}$ 3F$^{-}$.** A round bottom flask was charged with a suspension of Δ-(*S*,*S*)-**2**$^{3+}$ 3Cl$^{-}$·3$H_2O$ (0.170 g, 0.199 mmol) in water (30 mL) and AgF (0.0762 g, 0.597 mmol) was added with vigorous stirring. A suspension of white particles in an orange solution formed. After 2 h, the mixture was filtered through a pad of Celite. Methanol (10 mL) was added to the filtrate and the solvents were removed by rotary evaporation and oil pump vacuum (20 h, rt) to give Δ-**2**$^{3+}$ 3F$^{-}$·$x$$H_2O$ (0.152 g) as a brown solid. $^{19}$F NMR (470 MHz, 9:1 v/v $CD_2Cl_2$/$CD_3OD$, δ in ppm): –102.4 (br s).

**Trifluoromethylation of aromatic aldehydes (Table 5.1 and Figure 5.4).** A vial was charged with an aldehyde **3** (0.50 mmol), and Λ-(*S*,*S*)-**2**$^{3+}$ 3F$^{-}$·4$H_2O$ (0.041 g, 0.050 mmol, 10 mol%). The mixture was vigorously stirred and $TMSCF_3$ (0.150 mL, 1.00 mmol, 2.0 equiv) was then added slowly over 30 min at room temperature. The reaction mixture turned black when $TMSCF_3$ was added. After 24 h, $Ph_2SiMe_2$ (0.011 mL, 0.050 mmol, 0.011 g) was added and the reaction was stirred for another 15 min. $CDCl_3$ (1.00 mL) was then added and the NMR yield was calculated from the $^1$H NMR spectrum using $Ph_2SiMe_2$ as the internal standard. The NMR sample was loaded directly on a silica gel column (2 × 25 cm) packed in and eluted with 90:10 v/v hexanes/ethyl acetate. The product containing fractions were combined and solvents were removed by rotary evaporation to give **4** (see appendix D for further details). Desilylated derivatives were better substrates for chiral HPLC analysis. Therefore, **4** was dissolved in ethyl acetate (2.0 mL). Concentrated HCl (0.1 mL, 36% w/w aq.) was added and the mixture was vigorously stirred at room temperature. After 6 h, water (10 mL) was added and the organic phase was collected. The aqueous phase was further extracted with ethyl acetate (2 × 10 mL). The organic phases were combined and dried ($Na_2SO_4$). Solvents were removed by rotary evaporation to give the desilylated derivative of **4**, which was analyzed as described in appendix D.

**Addition of acetone to nitrostyrene (Table 5.2).** A vial was charged with **5** (0.0075 g, 0.050 mmol), a catalyst (0.0050 mmol, 10 mol%), *D*- or *L*-proline (0.0012 g, 0.010 mmol, 20 mol%), $Na_2CO_3$ (0.0022 g, 0.020 mmol, 40 mol%), and $CH_2Cl_2$ (0.50 mL). The mixture was stirred for 10 min and then brought to the indicated temperature. Acetone (0.036 mL, 0.50 mmol, 10 equiv) was added with stirring. The mixture was monitored by TLC (silica gel, 3:1 v/v hexanes/ethyl acetate). When conversion was complete, the sample was loaded directly onto a prep TLC plate (silica gel) and eluted with 3:1 v/v hexanes/ethyl acetate. The product containing band ($R_f = 0.25$) was collected and **6** was extracted with 4:1 v/v $CH_2Cl_2$/MeOH. The solvent was removed by rotary evaporation to give **6** as a white solid (see appendix D for details). The ee value and the dominant configuration were determined by HPLC with a Chiralcel AS-H column, 60:40 hexane/isopropanol, 1.0 mL/min, 254 nm, $t_S$ = 8.84 min, $t_R$ = 10.77 min. The order of elution was established in an earlier study with an identical column.[12]

## 5.6. References

(1) Ganzmann, C.; Gladysz, J. A. Phase Transfer of Enantiopure Werner Cations into Organic Solvents: An Overlooked Family of Chiral Hydrogen Bond Donors for Enantioselective Catalysis. *Chem. Eur. J.* **2008**, *14*, 5397-5400.

(2) (a) Ghosh, S. K.; Lewis, K. G.; Kumar, A.; Gladysz, J. A. Syntheses of Families of Enantiopure and Diastereopure Cobalt Catalysts Derived from Trications of the Formula $[Co(NH_2CHArCHArNH_2)_3]^{3+}$. *Inorg. Chem.* **2017**, 56, 2304-2320. (b) Maximuck, W. J.; Ganzmann, C.; Alvi, S.; Hooda, K. R.; Gladysz, J. A. Rendering Classical Hydrophilic Enantiopure Werner Salts $[M(en)_3]^{n+}$ $nX^-$ Lipophilic (M/*n* = Cr/3, Co/3, Rh/3, Ir/3, Pt/4); New Chiral Hydrogen Bond Donor Catalysts and Enantioselectivities as a Function of Metal and Charge. *Dalton Trans*. **2020**, *49*, 3680-3691.

(3) (a) Lewis, K. G.; Ghosh, S. K.; Bhuvanesh, N.; Gladysz, J. A. Cobalt(III) Werner Complexes with 1,2-Diphenylethylenediamine Ligands: Readily Available, Inexpensive, and Modular Chiral Hydrogen Bond Donor Catalysts for Enantioselective Organic Synthesis. *ACS Cent. Sci.* **2015**, *1*, 50-56. (b) Kumar, A.; Ghosh, S. K.; Gladysz, J. A. Tris(1,2-diphenylethylenediamine)cobalt(III) Complexes: Chiral Hydrogen Bond Donor Catalysts for Enantioselective *α*-Aminations of 1,3-Dicarbonyl Compounds. *Org. Lett.* **2016**, *18*, 760-763. (c) Joshi, H.; Ghosh, S. K.; Gladysz, J. A. Enantioselective Additions of Stabilized Carbanions to Imines Generated from α-Amido Sulfones By Using Lipophilic Salts of Chiral Tris(1,2-diphenylethylenediamine) Cobalt(III) Trications as Hydrogen Bond Donor Catalysts. *Synthesis* **2017**, *49*, 3905-3915. (d) Maximuck, W. J.; Gladysz, J. A. Lipophilic Chiral Cobalt(III) Complexes of Hexaamine Ligands; Efficacies as Enantioselective Hydrogen Bond Donor Catalysts. *Mol. Catal.* **2019**, *473*, 110360 (this journal has replaced conventional pagination by article numbers). (e) Kabes, C. Q.;

Maximuck, W. J.; Ghosh, S. K.; Kumar, A.; Bhuvanesh, N.; Gladysz, J. A. Chiral Tricationic tris(1,2-diphenylethylenediamine) Cobalt(III) Hydrogen Bond Donor Catalysts with Defined Carbon/Metal Configurations; Matched/Mismatched Effects upon Enantioselectivities with Enantiomeric Chiral Counter Anions. *ACS Catal.* **2020**, *10*, 3249-3263. (f) Luu, Q. H.; Gladysz, J. A. An Air and Water Stable Hydrogen Bond Donor Catalyst for the Enantioselective Generation of Quaternary Carbon Stereocenters by Additions of Substituted Cyanoacetate Esters to Acetylenic Esters. *Chem. Eur. J.* **2020**, *26*, accepted. DOI:10.1002/chem.202001639.

(4) Luu, Q. H.; Lewis, K. G.; Banerjee, A.; Bhuvanesh, N.; Gladysz, J. A. The robust, readily available cobalt(III) trication $[Co(NH_2CHPhCHPhNH_2)]^{3+}$ is a progenitor of broadly applicable chirality and prochirality sensing agents. *Chem. Sci.* **2018**, *9*, 5087-5099.

(5) Wititsuwannakul, T.; Hall, M. B.; Gladysz, J. A. A Computational Study of Hydrogen Bonding Motifs in Halide, Tetrafluoroborate, Hexafluorophosphate, and Tetraarylborate Salts of Chiral Cationic Ruthenium and Cobalt Guanidinobenzimidazole Hydrogen Bond Donor Catalysts; Acceptor Properties of the "$BAr_f$" Anion. *Polyhedron* **2020**, in press. DOI: 10.1016/j.poly.2020.114618.

(6) (a) Ma, J.-A.; Cahard, D. Asymmetric Fluorination, Trifluoromethylation, and Perfluoroalkylation Reactions. *Chem. Rev.* **2008**, *108*, PR1-PR43. (b) Yang, X.; Wu, T.; Phipps, R. J.; Toste, F. D. Advances in Catalytic Enantioselective Fluorination, Mono-, Di-, and Trifluoromethylation, and Trifluoromethylthiolation Reactions. *Chem. Rev.* **2015**, *115*, 826-870.

(7) Mandal, T.; Zhao, C.-G. Modular Designed Organocatalytic Assemblies for Direct Nitro-Michael Addition Reactions. *Angew. Chem., Int. Ed.* **2008**, *47*, 7714-7717. *Angew. Chem.* **2008**, *120*, 7828-7831.

(8) Spinat, P. P; Whuler, A.; Brouty, C. Données cristallographiques des forms polymorphes du complexes racémique de fluorure de tris(éthylènediamine)cobalt(III). *J. Appl. Cryst.* **1981**, *14*, 211-212.

(9) (a) Sharma, R. K.; Fry, J. L. Instability of Anhydrous Tetra-*n*-alkylammonium Fluorides. *J. Org. Chem.* **1983**, *48*, 2112-2114. (b) Cox, D. P.; Terpinski, J.; Lawrynowicz, W. "Anhydrous" Tetrabutylammonium Fluoride: A Mild but Highly Efficient Source of Nucleophilic Fluoride Ion. *J Org. Chem.* **1984***,* 49*,* 3216-3219.

(10) All cobalt(III) complexes are isolated as hydrates, consistent with the appreciable hydrogen bond donor strengths of the NH groups. To aid readability, these are not specified in the formulae in the main text or graphics, but are given in the experimental section. The additional mass is taken into account in the stoichiometries and yield calculations. For additional related remarks, see reference 23 in reference 2a.

(11) (a) Iseki, K.; Nagai, T.; Kobayashi, Y. Asymmetric Trifluoromethylation of Aldehydes and Ketones with Trifluoromethyltrimethylsilane Catalyzed by Chiral Quaternary Ammonium Fluoride. *Tetrahedron Lett.* **1994**, *35*, 3137-3138. (b) Kuroki, Y.; Iseki, K. A chiral triaminosulfonium salt: design and application to catalytic asymmetric synthesis. *Tetrahedron Lett.* **1999**, *40*, 8231-8234. (c) Caron, S.; Do, N. M.; Arpin, P.; Lariveé, A. Enantioselective Addition of a Trifluoromethyl Anion to Aryl Ketones and Aldehydes. *Synthesis* **2003**, *11*, 1693-1698.

(12) Huang, H.; Jacobsen, E. N. Highly Enantioselective Direct Conjugate Addition of Ketones to Nitroalkenes Promoted by A Chiral Primary Amine-Thiourea Catalyst. *J. Am. Chem. Soc.* **2006**, *128*, 7170-7171.

(13) The hydration level was assigned based upon $^{1}$H NMR integrations and microanalyses. When these differ, the microanalytical values were given precedence, as the NMR integrations can be enhanced by protic impurities or NH/ND exchange.

(14) The increased integration of the OH signal over that derived from the microanalysis is believed to originate from protic impurities in the deuterated solvent.

# 6. SUMMARY AND CONCLUSION

The new cobalt-based CSAs described in chapter 2 can be applied to a wide variety of functional groups at significantly low loadings and in the presence of multiple analytes. The CSAs are stable to air and water, and readily available from inexpensive building blocks. Their success reflects the generality of second coordination sphere hydrogen bonding between the NH donor groups and Lewis basic functional groups in the analytes.

The study in chapter 3 has significantly expanded the scope of enantioselective reactions that can be catalyzed with hydrogen bond donor catalysts of the types $[Co((S,S)\text{-}NH_2CHPhCHPhNH_2)_3]^{3+}$ $2X^{-}X'^{-}$. Furthermore, it is the first that can be advertised as significantly improving upon existing literature catalysts, as opposed to being comparably effective.

Chapter 4 reported three reactions catalyzed by Werner catalysts in addition to the one described in chapter 3. It is anticipated that the substrate scope for the fluorination (section 4.2.1 and 4.3.1) and the Neber reaction (section 4.2.2 and 4.3.2) can be expanded in the future based on the promising results presented. Exploration for other catalysts to synthesize tetrahydroquinoline (section 4.2.3 and 4.3.3) will also be conducted in the Gladysz group.

Two additional reactions were reported in chapter 5. First, trifluoromethylation of aromatic aldehydes using 10 mol% of $\Lambda\text{-}[Co((S,S)\text{-}NH_2CHPhCHPhNH_2)_3]^{3+}$ $3F^{-}$ and $TMSCF_3$ gave 54% to >99% ee of trimethylsilyl-1-aryl-2,2,2-trifluoroethanols. Second, condensation of acetone and trans-β-nitrostyrene using the catalyst $\Lambda\text{-}[Co((S,S)\text{-}NH_2CHPhCHPhNH_2)_3]^{3+}$ $2(D\text{-prolinate})^{-}BAr_f^{-}$ (generated in situ) gave the adduct in 58% ee. Catalysts containing anions of other amino acids and an expansion of substrate scope for the condensation of ketones and nitrostyrenes will be communicated in the future.

APPENDIX A: THE ROBUST, AND READILY AVAILABLE COBALT (III) TRICATION $[Co(NH_2PhCHCHPhNH_2)_3]^{3+}$ IS A PROGENITOR OF BROADLY APPLICABLE CHIRALITY AND PROCHIRALITY SENSING AGENTS

**General data.** NMR spectra were recorded on a Varian NMRS 500 MHz spectrometer at ambient probe temperature. Chemical shifts (δ in ppm) were referenced to residual solvent signals ($^1$H: $CHCl_3$, 7.26; $CHD_2CN$, 1.94; DMSO-$d_5$, 2.50; $CHD_2OD$, 3.30; $CDHCl_2$, 5.32; acetone-$d_5$, 2.05; $^{13}$C: $CDCl_3$, 77.2; DMSO-$d_6$, 39.5; $CD_3OD$, 49.0; $CD_2Cl_2$, 54.0; acetone-$d_6$, 29.8) or external $C_6F_6$ ($^{19}$F, –164.9) or 85 wt% aqueous $H_3PO_4$ ($^{31}$P, 0.00). IR spectra were recorded on a Shimadzu IRAffinity-1 spectrometer (Pike MIRacle ATR system, diamond/ZnSe crystal). Melting points were determined using an OptiMelt MPA 100 instrument. Microanalyses were conducted by Atlantic Microlab. HPLC analyses were carried out with a Shimadzu instrument package (pump/autosampler/detector LC-20AD/SIL-20A/SPD-M20A).

NMR solvents (Cambridge Isotopes) were treated as follows: DMSO-$d_6$, distilled under vacuum and stored over molecular sieves; $CDCl_3$, $CD_2Cl_2$, acetone-$d_6$, $CD_3CN$, and $CD_3OD$, stored over molecular sieves. HPLC grade solvents (hexanes, Fischer; isopropanol (**38**), JT Baker) were degassed. The following materials were used as received: $CH_2Cl_2$ (EMD Chemicals, ACS grade), $CH_3OH$ (EMD, anhydrous, 99.8%), acetone (BDH, ACS grade), toluene (BDH, ACS grade), $Co(OAc)_2{\cdot}4H_2O$ (Alfa Aesar, 98%), (*S*,*S*)-dpen ($NH_2CHPhCHPhNH_2$; Oakwood or Combi blocks), activated charcoal (Acros, Norit SX 4), $Na^+$ $BAr_f^-$ ($BAr_f^-$ = $B(3,5\text{-}C_6H_3(CF_3)_2)_4^-$; Ark Pharm, 97%), aqueous HI (Aldrich, 57 wt%, 99.9%), $CoI_2$ (Aldrich, anhydrous, 99%), KI (Aldrich, anhydrous, 99%), NaI (EMD, >99.5%), silica gel (Silicycle SiliaFlash® F60), Celite 545 (Aldrich), (*S*)-1-phenethyl amine ((*S*)-**5**, TCI Chemicals, >98%, ee 97+%), 2-carbomethoxy cyclopentanone (**7**, TCI Chemicals, 97%), *D*- and *L*-proline (*R*- and *S*-**9**,

Acros Organics, 99%), (*S*)-1-phenylethanol ((*S*)-**10**; Alfa Aesar, 98+%), (*R*)-**10** (Alfa Aesar, 99%, ee 97+%), *DL*-lactide (**11**, Aldrich, 99%), *L*-lactide (*S*,*S*-**11**, Aldrich, 98%), (*S*)- and (*R*)-1,1'-bi-2-naphthol ((*S*)- and (*R*)-BINOL, Ark Pharm, >98%), δ-hexanolactone (**12**, Alfa Aesar, 98%), styrene oxide (**16**, Alfa Aesar, 98%), 1,2-propanediol (**21**, Aldrich, 99%), 1,2-butanediol (**22**, Aldrich, 98%), 2-carbomethoxy cycloheptanone (**23**, Aldrich, 99%), ethyl 2-methylacetoacetate (**24**, Alfa Aesar, 95%), 2-acetylcyclopentanone (**25**, TCI Chemicals, >95%), (*S*)-*tert*-butylsulfinamide ((*S*)-**26**, Ark Pharm, 98%), (*R*)-*tert*-butylsulfinamide ((*R*)-**26**, ACS Scientific, 98%), 2-methyltet-rahydofuran (**27**, Aldrich, >99%), 2-bromopropionamide (**30**, Aldrich, 99%), 2-carboethoxy cyclohexanone (**31**, Aldrich, 95%), cyclohexene oxide (**32**, TCI Chemicals, 98%), methyl ethyl ketone (**33**, Aldrich, 99%), chloroacetone (**34**, Acros Organics, 96%), DMSO (**35**, BDH, 99.9%), ethyl acetate (**36**, Aldrich, 99.8%), isopropylamine (**37**, Alfa Aesar, 99%), 1-methyl-2-oxindole (**39**, Aldrich, 97%), ethyl acetoacetate (**40**, Alfa Aesar, 99%), 2-bromoethyl acetate (**41**, TCI Chemicals, >98%), 3-pentanone (**42**, Aldrich, >99%), 2-bromoacetophenone (**43**, Alfa Aesar, 98%), ethyl chloroacetate (**44**, TCI Chemicals, 98%), benzyl carbamate (**45**, Alfa Aesar, 99%), ethyl cyanoacetate (**46**, TCI Chemicals, >98%), propionamide (**47**, TCI Chemicals, >98%), dimethyl malonates (Alfa Aesar, 98%), *sec*-butylbenzene (TCI Chemicals, >99%), nitroethane (Aldrich, >98%), 5-hydroxymethyl-2-pyrrolidinone (Chem-Impex International, 98.5%), propionitrile (Acros Organics, 99%), propionic acid (Alfa Aesar, 99%), methyl isovalerate (Aldrich, >98%), diethyl phosphite (Alfa Aesar, 96%), and tetrahydrofuran (Aldrich, >99%).

The following analytes were synthesized by literature procedures: (*S*)- and (*R*)-1-phenylethyl acetate ((*S*)- and (*R*)-**4**),[s1] 1-phenethyl amine (**5**),[s2] phenyl methyl sulfoxide (**6**),[s3] (*S*)- and (*R*)-Boc-BINOL ((*S*)- and (*R*)-**8**),[s1] (*S*)- and (*R*)-BINOL diacetate,[s1] 1-phenyl-1,2-ethanediol (**14**),[s4] 1-phenyl-2,2,2-trifluoroethanol (**15**),[s5] *N*-tosyl phenethyl

amine (**17**),[s6] *N*-acetyl phenethyl amine (**18**),[s2] hydroxyphenylmethyl diethyl phosphonate (**19**),[s7] hydroxyphenylmethyl dimethyl phosphonate (**20**),[s7] 2-phenyl-2-butanol (**28**),[s8] 1-phenyl-1-chloroethane.[s9] and methyl 2-bromopropionate (**29**).[s10] Ibuprofen (**13**) was isolated from commercially available tablets following a literature procedure.[s11]

**Extended Bibliography**. Additional literature that augments that given in the main text is supplied at the end of the references (other CSAs from 2014-present,[s12-s27] other NMR methods for prochirality sensing[s28-s33]).

**Table A-1.** Expansion of Table 2.1 showing the separation of all aliphatic $^1$H NMR signals (Δδ, ppm) of the enantiomers of racemic 1-phenylethyl acetate (**4**).

| Entry | CSA | Solvent | Δδ (ppm) PhC***H***(CH$_3$)O | Δδ (ppm) O(C=O)C***H***$_3$ | Δδ (ppm) PhCH(C***H***$_3$)O |
|---|---|---|---|---|---|
| 1 | Λ-**1**$^{3+}$ 3BAr$_f^-$ | $CD_2Cl_2$ | — | — | — |
| 2 | Λ-(*S*,*S*)-**2**$^{3+}$ 2Cl$^-$BAr$_f^-$ | $CD_2Cl_2$ | 1.32 | 0.50 | 0.28 |
| 3 | Δ-(*S*,*S*)-**2**$^{3+}$ 2Cl$^-$BAr$_f^-$ | $CD_2Cl_2$ | 0.15 | 0.02 | — |
| 4 | Λ-(*S*,*S*)-**2**$^{3+}$ 2Cl$^-$ | $CD_2Cl_2$ | 1.37 | 0.53 | 0.28 |
| 5 | Λ-(*S*,*S*)-**2**$^{3+}$ 3BAr$_f^-$ | $CD_2Cl_2$ | 0.34 | 0.15 | 0.08 |
| 6 | Λ-(*S*,*S*)-**2**$^{3+}$ 2I$^-$BAr$_f^-$ | $CD_2Cl_2$ | 1.30 | 0.52 | 0.25 |
| 7 | Λ-(*S*,*S*)-**2**$^{3+}$ 2I$^-$BAr$_f^-$ | $CDCl_3$ | 1.75 | 0.68 | 0.37 |
| 8 | Λ-(*S*,*S*)-**2**$^{3+}$ 2I$^-$BAr$_f^-$ | acetone-$d_6$ | — | — | — |
| 9 | Λ-(*S*,*S*)-**2**$^{3+}$ 2I$^-$BAr$_f^-$ | $CD_3CN$ | — | — | — |
| 10 | Λ-(*S*,*S*)-**2**$^{3+}$ 2I$^-$BAr$_f^-$ | DMSO-$d_6$ | — | — | — |
| 11 | Λ-(*S*,*S*)-**2**$^{3+}$ 2Cl$^-$BAr$_f^-$ | acetone-$d_6$ | — | — | — |
| 12 | Λ-(*S*,*S*)-**2**$^{3+}$ 2Cl$^-$BAr$_f^-$ | $CD_3CN$ | — | — | — |
| 13 | Λ-(*S*,*S*)-**2**$^{3+}$ 2Cl$^-$BAr$_f^-$ | DMSO-$d_6$ | — | — | — |

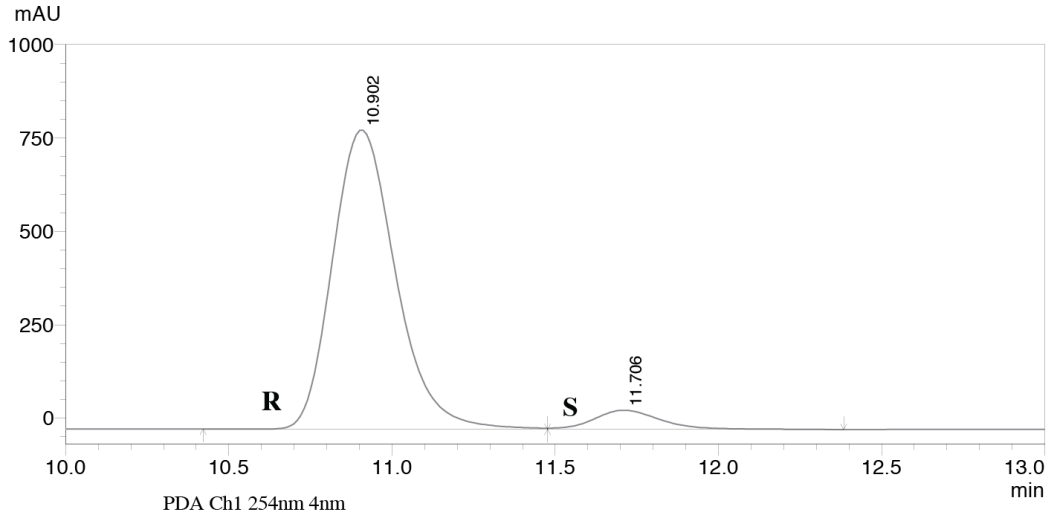


PDA Ch1 254nm 4nm

| Peak# | Ret. Time | Area | Height | Area % | Height % |
|---|---|---|---|---|---|
| 1 | 10.902 | 10801926 | 800685 | 93.679 | 93.979 |
| 2 | 11.706 | 728913 | 51298 | 6.321 | 6.021 |
| Total | | 11530838 | 851984 | 100.000 | 100.000 |

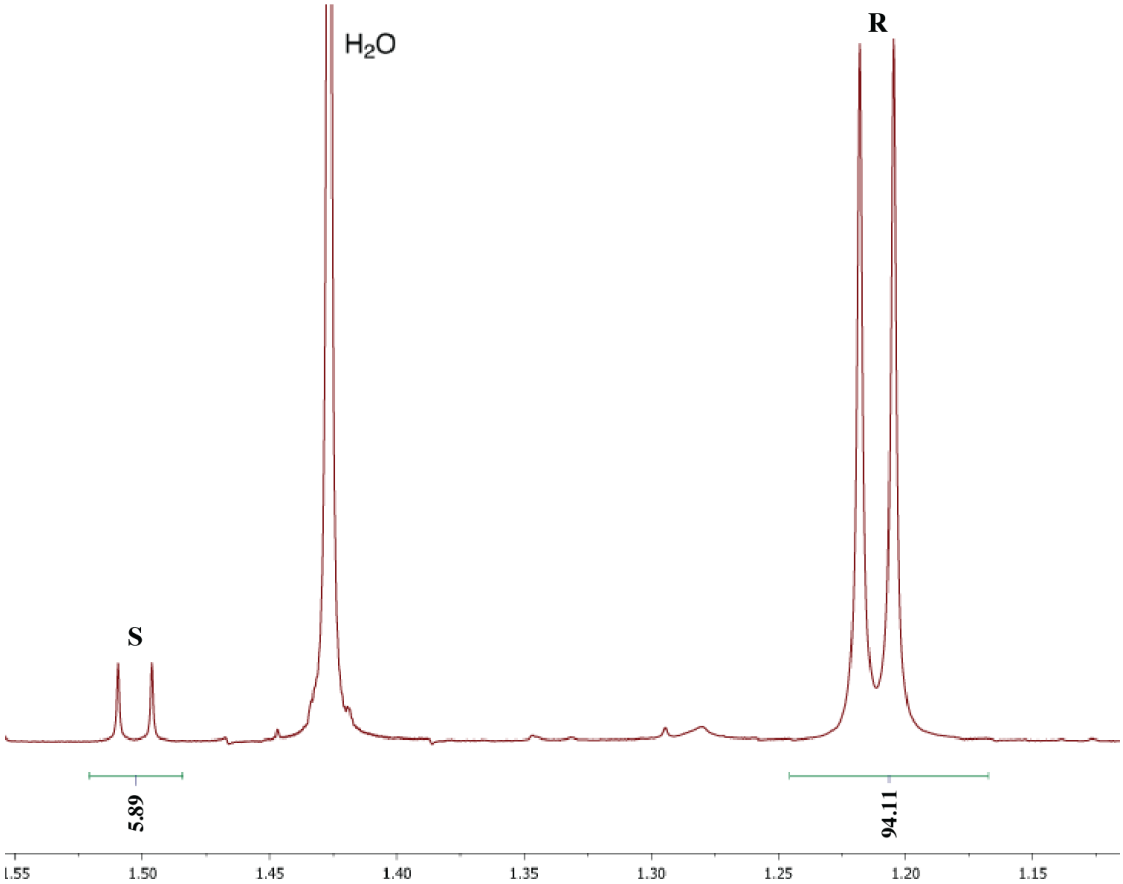


**Figure A-1.** HPLC trace (top) and $^{1}$H NMR spectrum (bottom) of **4** (88% ee) corresponding to the data in Table 2.3

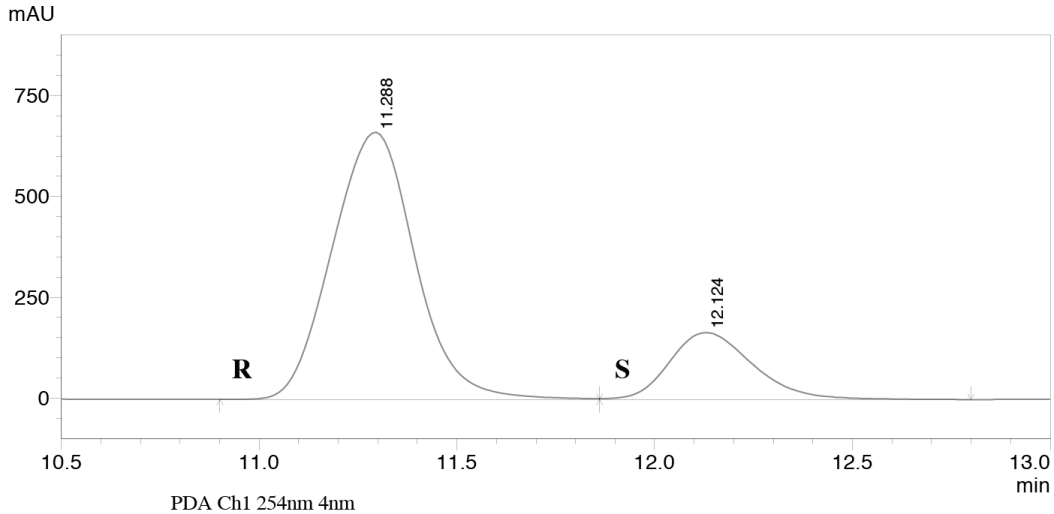


PDA Ch1 254nm 4nm

| Peak# | Ret. Time | Area | Height | Area % | Height % |
|---|---|---|---|---|---|
| 1 | 11.288 | 9643154 | 661589 | 79.945 | 79.961 |
| 2 | 12.124 | 2419045 | 165801 | 20.055 | 20.039 |
| Total | | 12062199 | 827390 | 100.000 | 100.000 |

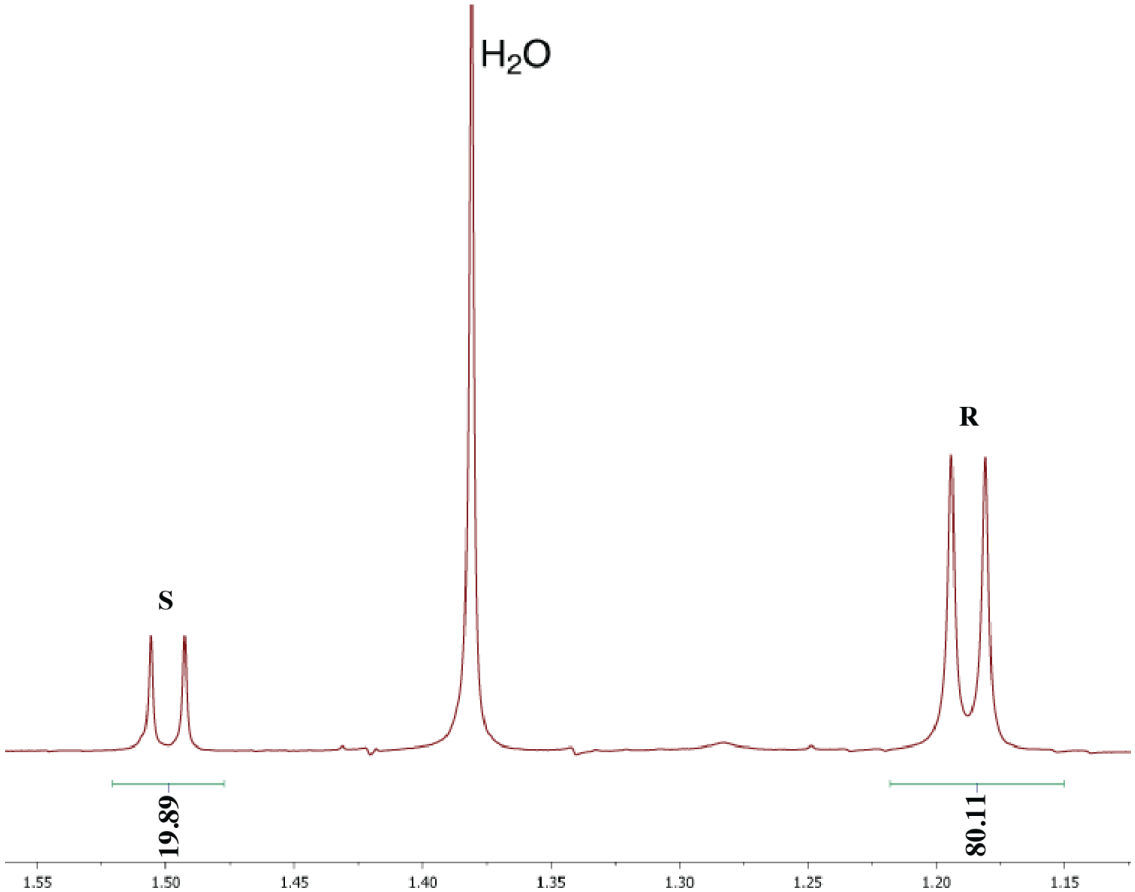


**Figure A-2.** HPLC trace (top) and $^{1}$H NMR spectrum (bottom) of **4** (60% ee) corresponding to the data in Table 2.3.

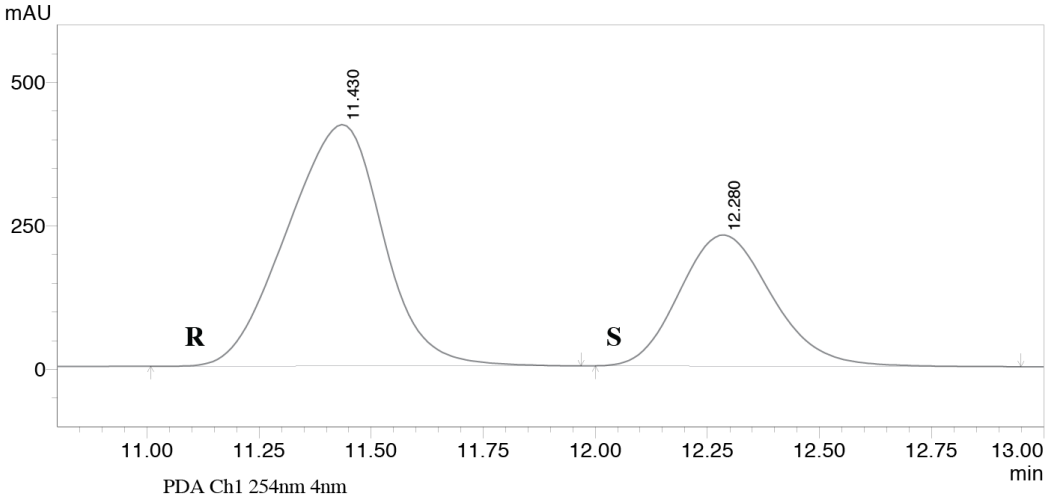


PDA Ch1 254nm 4nm

| Peak# | Ret. Time | Area | Height | Area % | Height % |
|---|---|---|---|---|---|
| 1 | 11.430 | 6300989 | 420643 | 65.750 | 64.822 |
| 2 | 12.280 | 3282337 | 228272 | 34.250 | 35.178 |
| Total | | 9583326 | 648915 | 100.000 | 100.000 |

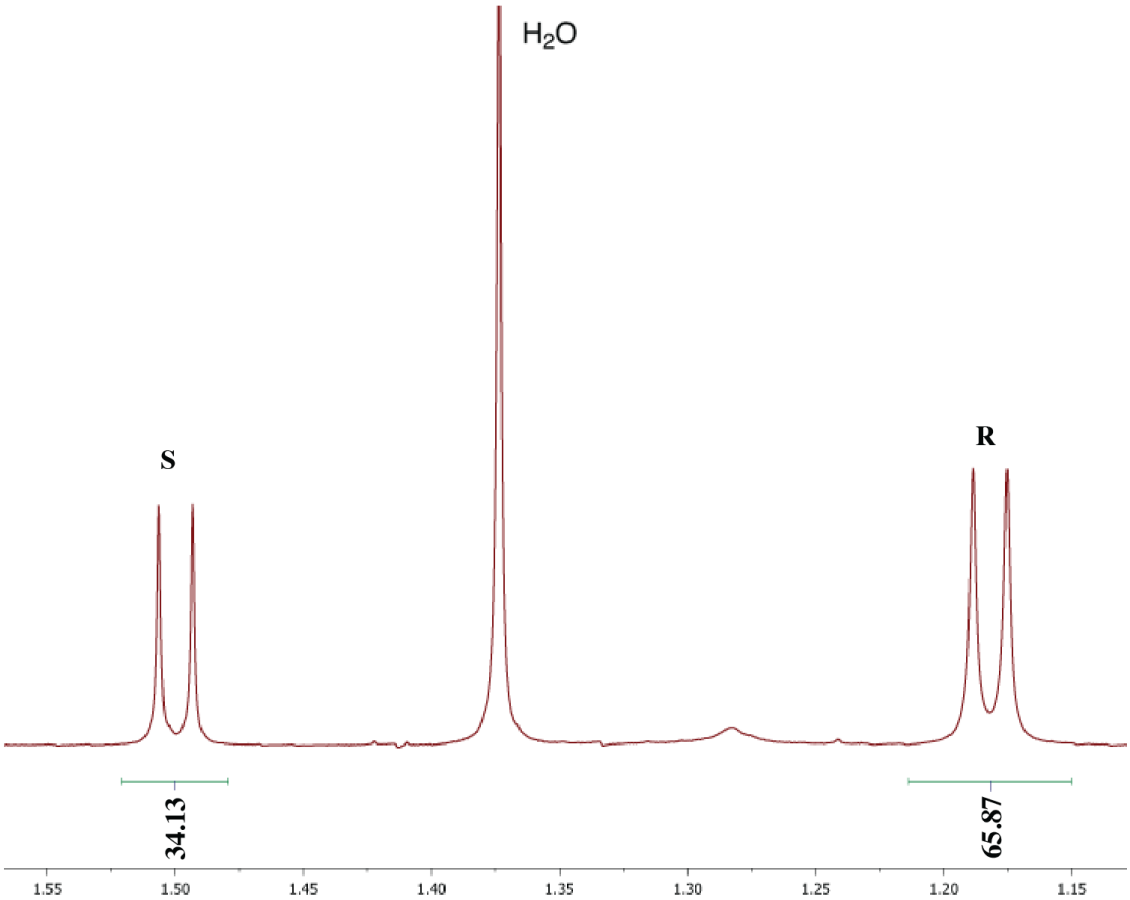


**Figure A-3.** HPLC trace (top) and $^{1}$H NMR spectrum (bottom) of **4** (32% ee) corresponding to the data in Table 2.3.

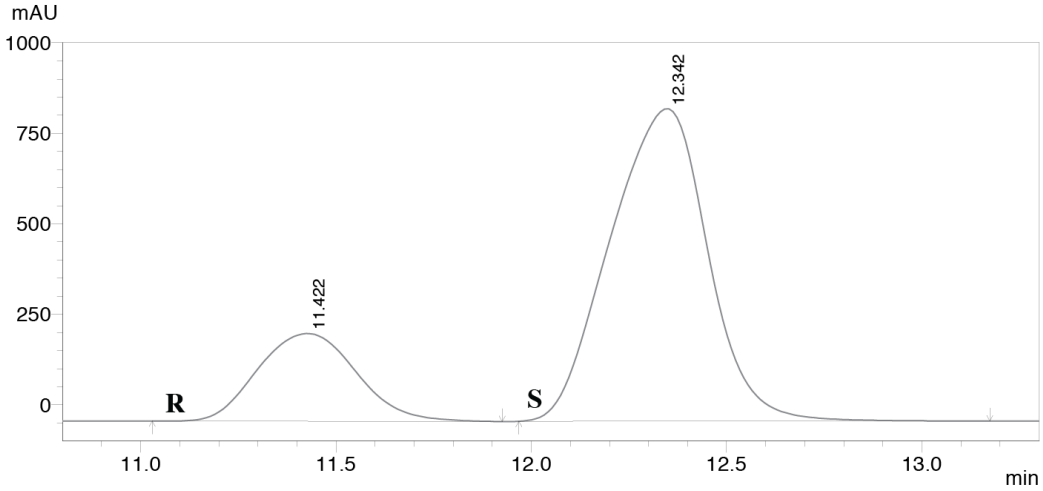


PDA Ch1 254nm 4nm

| Peak# | Ret. Time | Area | Height | Area % | Height % |
|---|---|---|---|---|---|
| 1 | 11.422 | 4252585 | 242308 | 22.088 | 21.927 |
| 2 | 12.342 | 14999902 | 862736 | 77.912 | 78.073 |
| Total | | 19252487 | 1105045 | 100.000 | 100.000 |

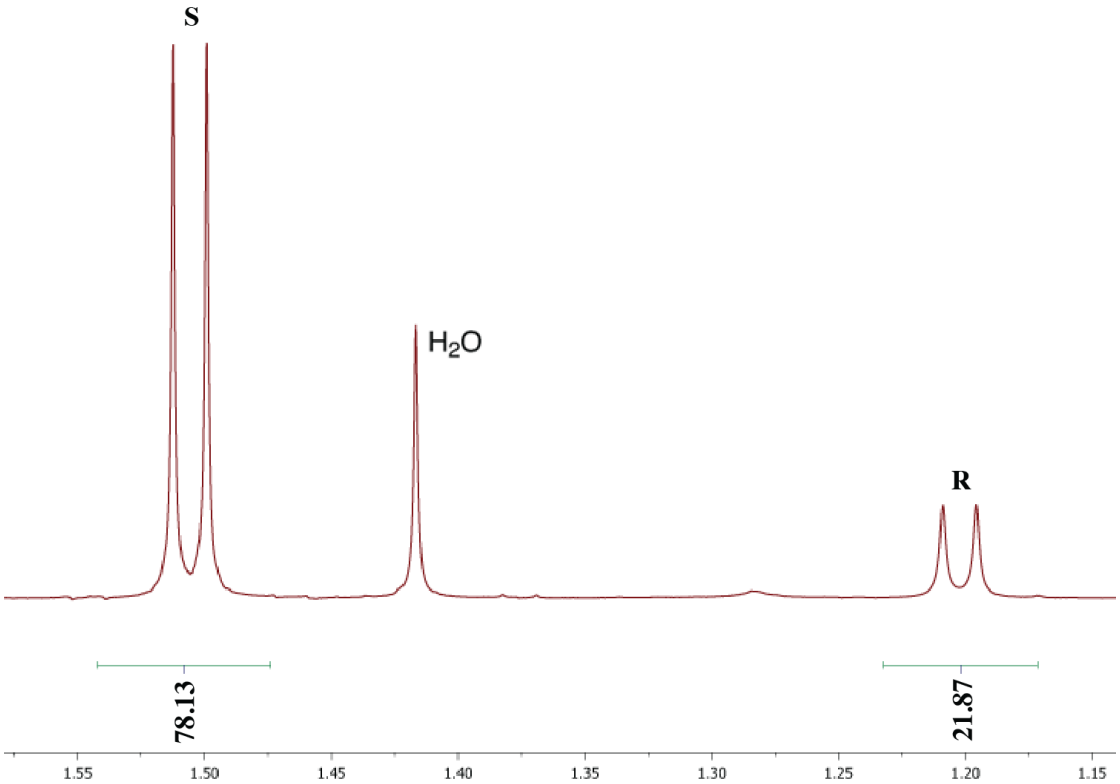


**Figure A-4.** HPLC trace (top) and $^{1}$H NMR spectrum (bottom) of **4** (–56% ee) corresponding to the data in Table 2.3.

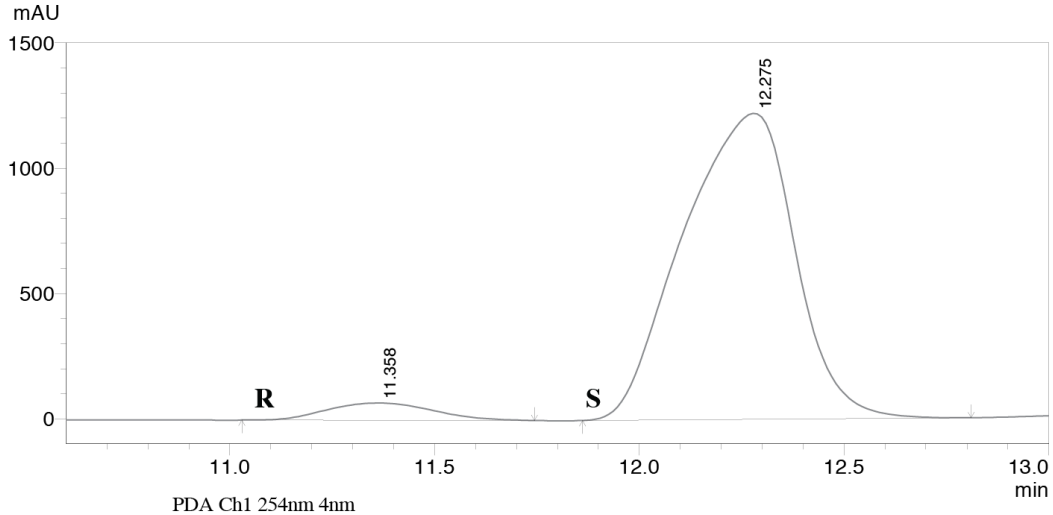


PDA Ch1 254nm 4nm

| Peak# | Ret. Time | Area | Height | Area % | Height % |
|---|---|---|---|---|---|
| 1 | 11.358 | 1239908 | 68869 | 5.066 | 5.336 |
| 2 | 12.275 | 23235959 | 1221729 | 94.934 | 94.664 |
| Total | | 24475867 | 1290599 | 100.000 | 100.000 |

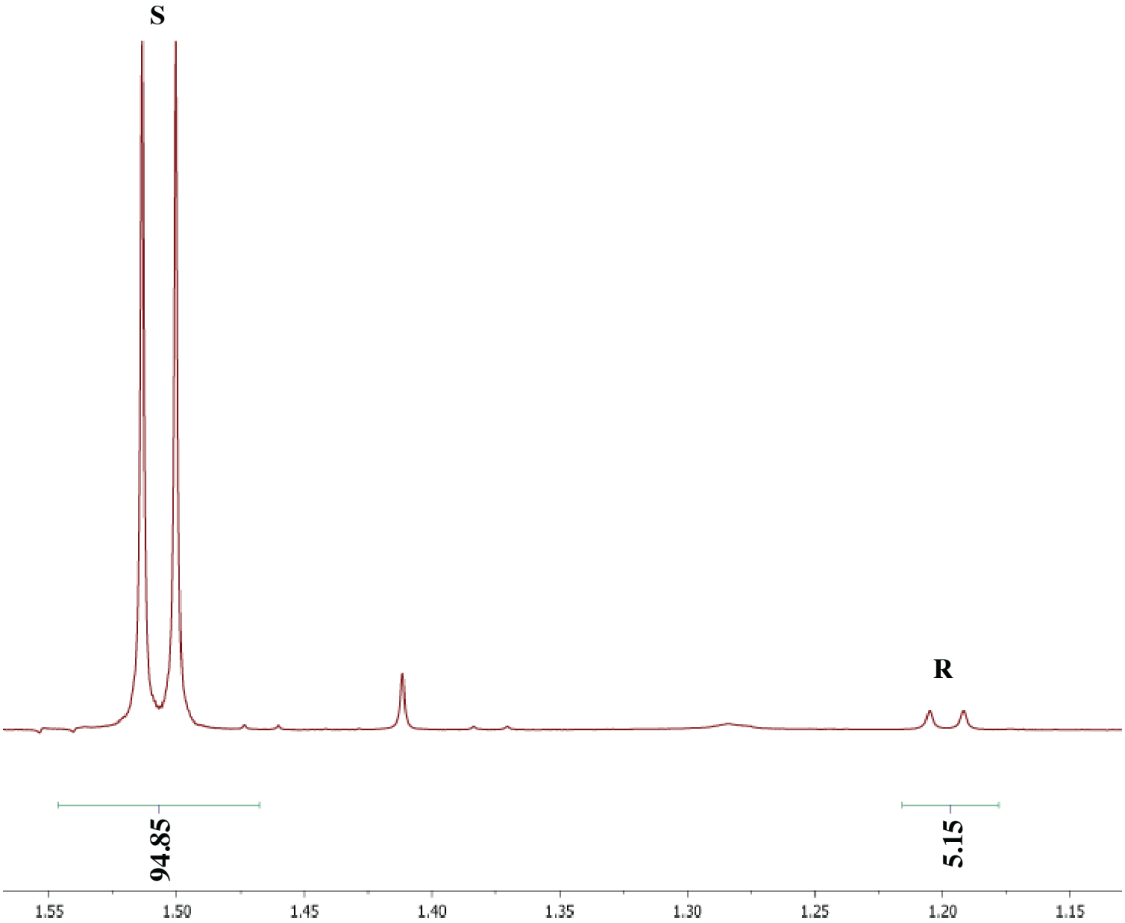


**Figure A-5.** HPLC trace (top) and $^{1}$H NMR spectrum (bottom) of **4** (–90% ee) corresponding to the data in Table 2.3.

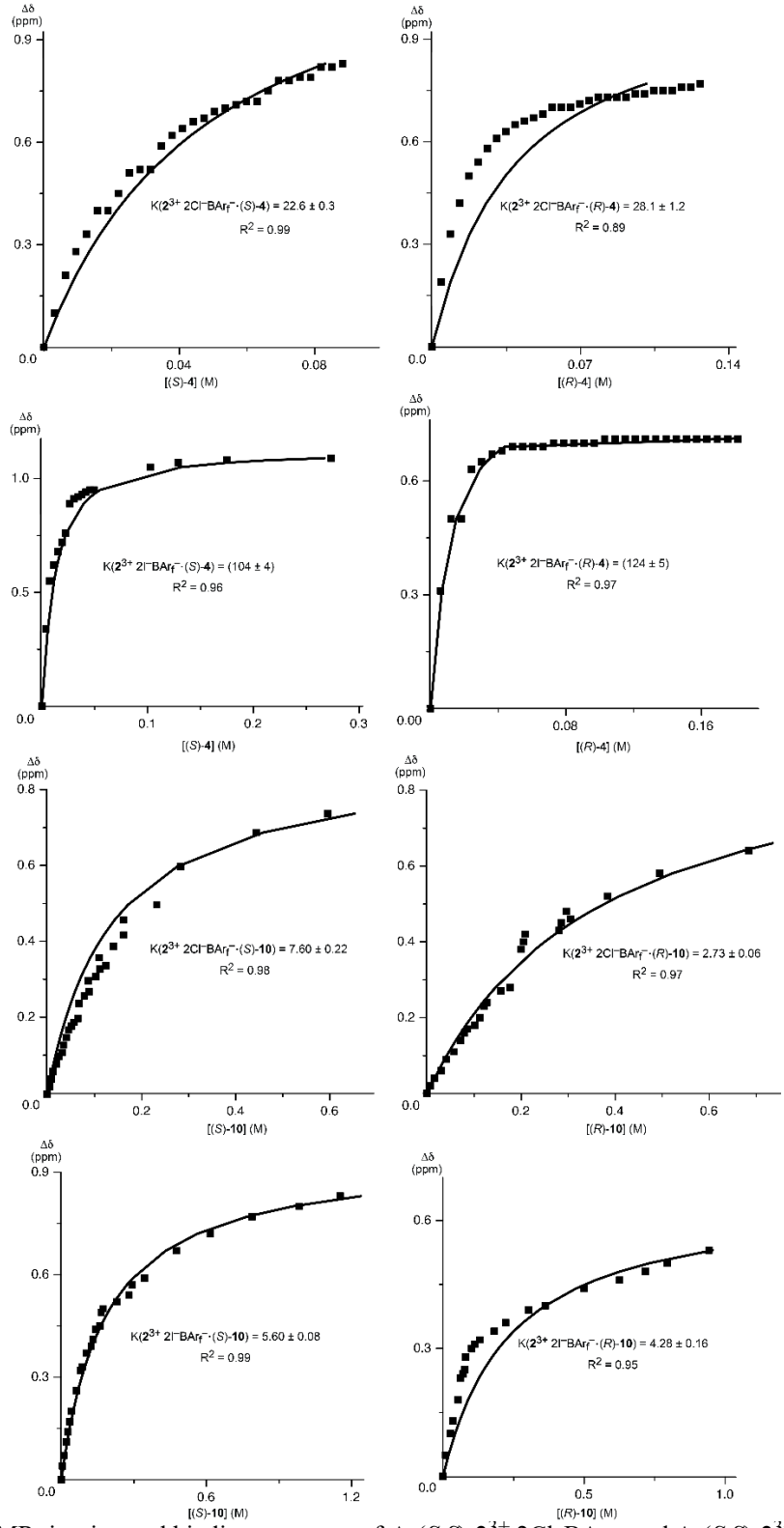


**Figure A-6.** NMR titration and binding constants of Λ-(*S*,*S*)-$\mathbf{2}^{3+}$ 2Cl⁻$BAr_f^-$ and Λ-(*S*,*S*)-$\mathbf{2}^{3+}$ 2I⁻$BAr_f^-$ with the analytes (*S*)-**4**, (*R*)-**4**, (*S*)-**10**, and (*R*)-**10**; raw data underlying Table 2.5.

**Table A-2.** Summary of crystallographic data for Λ-(*S*,*S*)-**2**$^{3+}$ 3I$^{-}$·6DMSO.[a]

| | |
|---|---|
| empirical formula | $C_{108}H_{168}Co_2I_6N_{12}O_{12}S_{12}$[a] |
| formula weight | 3080.44 |
| temperature of collection [K] | 110.0 |
| diffractometer | Bruker Quest |
| wavelength [Å] | 0.71073 |
| crystal system | monoclinic |
| space group | *P*2(1) |
| unit cell dimensions: | |
| *a* [Å] | 23.057(2) |
| *b* [Å] | 13.6098(12) |
| *c* [Å] | 23.378(2) |
| α [deg] | 90 |
| β [deg] | 110.977(2) |
| γ [deg] | 90 |
| V [Å$^3$] | 6849.8(10) |
| Z | 2[a] |
| $\rho_{calc}$ [Mg/m$^3$] | 1.494 |
| absorption coefficient [mm$^{-1}$] | 1.832 |
| F(000) | 3100 |
| Crystal size [mm$^3$] | 0.257 × 0.098 × 0.081 |
| Θ [deg] | 2.314 to 24.763 |
| range / indices (*h*, *k*, *l*) | –27,26; –16,15; –27,27 |
| reflections collected | 72270 |
| independent reflections | 22606 [R(int) = 0.0476] |
| completeness to Θ = 24.763° | 98.8% |
| absorption correction | semiempirical from equivalents |
| max. and min. transmission | 0.4283 and 0.3391 |
| refinement method | full-matrix least-squares on $F^2$ |
| data / restraints / parameters | 22606 / 2887 / 1441 |
| goodness-of-fit on $F^2$ | 1.214 |
| final R indices [I>2σ(I)] | *R*1 = 0.0820, w*R*2 = 0.1405 |
| R indices (all data) | *R*1 = 0.0993, w*R*2 = 0.1521 |
| absolute structure parameter | 0.08(3) |
| largest diff. peak and hole [e.Å$^{-3}$] | 4.180 / –1.492 |

[a]There are two independent molecules in the unit cell. Hence, there are two cobalt atoms in the empirical formula and the *Z* value represents the total number of dicobalt units.

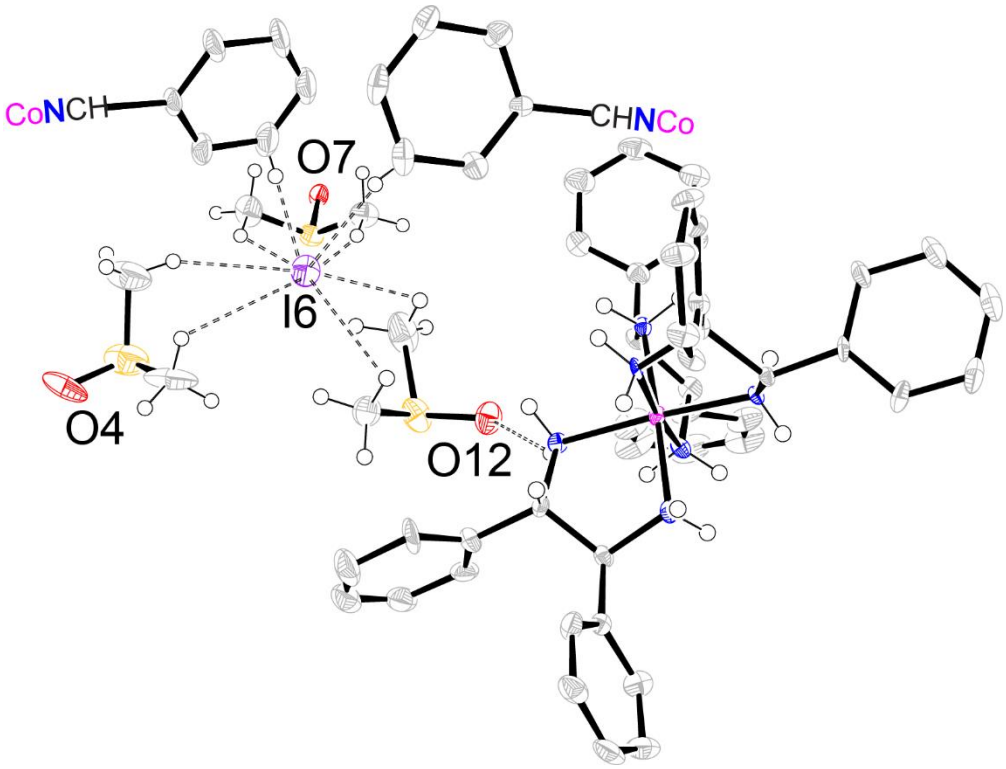


| I···HC (3 DMSO) | I···C (3 DMSO) |
|---|---|
| 4.043, 3.081, 3.083, 3.100, 3.321, 3.947 | 3.910, 3.938, 3.946, 3.992, 4.113, 4.294 |
| I···HC (2 Ph) | I···C (2 Ph) |
| 3.027, 3.285 | 3.921, 4.057 |

**Figure A-7.** Thermal ellipsoid diagram (50% probability level) showing the nearest contacts of the third iodide anion in Λ-(*S*,*S*)-**2**$^{3+}$ 3I$^{-}$·6DMSO (molecule 1) with neighboring atoms (CH of three DMSO molecules and two phenyl rings).

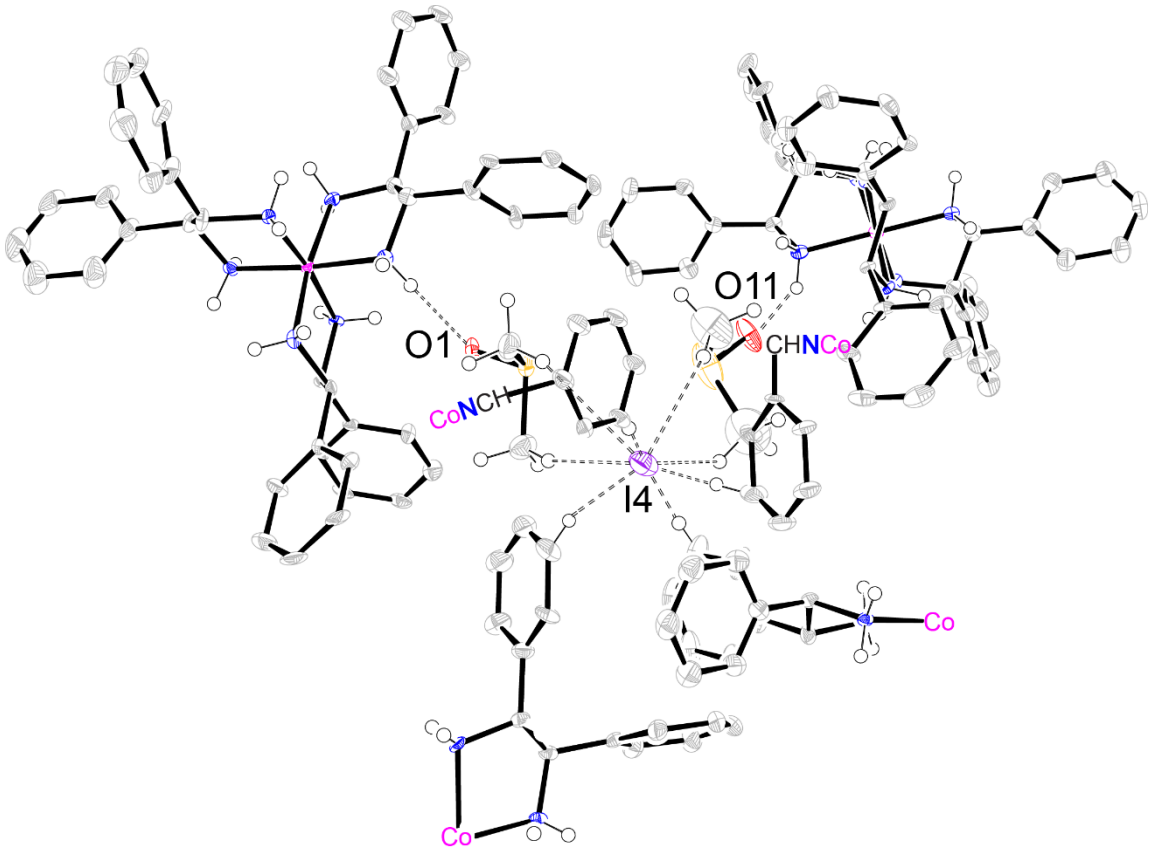


| I···HC (2 DMSO) | I···C (2 DMSO) |
|---|---|
| 2.996, 3.116, 3.120, 3.494 | 3.941, 4.028, 4.069, 4.165 |
| I···HC (4 Ph) | I···C (4 Ph) |
| 3.060, 3.082, 3.123, 3.151 | 3.848, 3.876, 4.039, 4.068 |

**Figure A-8.** Thermal ellipsoid diagram (50% probability level) showing the nearest contacts of the third iodide anion in Λ-(*S*,*S*)**2**$^{3+}$ 3I$^{-}$·6DMSO (molecule 2) with neighboring atoms (CH of two DMSO molecules and four phenyl rings).

**Table A-3.** Key interatomic distances (Å) and angles (°) in crystalline Λ-(*S*,*S*)-**2**$^{3+}$ 3I$^{-}$·6DMSO.

| molecule 1[a] | | molecule 2[a] | |
|---|---|---|---|
| Co(1)-N(1B) | 1.973(13) | Co(1D)-N(1D) | 1.958(12) |
| Co(1)-N(2B) | 1.986(13) | Co(1D)-N(2D) | 1.996(13) |
| Co(1)-N(3B) | 1.951(12) | Co(1D)-N(3D) | 1.977(12) |
| Co(1)-N(4B) | 1.944(12) | Co(1D)-N(4D) | 1.963(12) |
| Co(1)-N(5B) | 1.949(12) | Co(1D)-N(5D) | 1.952(13) |
| Co(1)-N(6B) | 1.971(12) | Co(1D)-N(6D) | 1.977(12) |
| N(1B)-C(1B) | 1.516(19) | N(1D)-C(1D) | 1.504(19) |
| N(2B)-C(8B) | 1.49(2) | N(2D)-C(8D) | 1.494(19) |
| N(3B)-C(6) | 1.509(19) | N(3D)-C(15D) | 1.490(18) |
| N(4B)-C(13) | 1.49(2) | N(4D)-C(22D) | 1.49(2) |
| N(5B)-C(1I) | 1.484(19) | N(5D)-C(36D) | 1.487(19) |
| N(6B)-C(1A) | 1.493(18) | N(6D)-C(29D) | 1.501(18) |
| I(2)···HN(2B) | 2.783 | I(1)···HN(1D) | 2.826 |
| I(2)···HN(4B) | 2.609 | I(1)···HN(3D) | 2.794 |
| I(2)···HN(6B) | 2.798 | I(1)···HN(5D) | 2.771 |
| I(5)···HN(1B) | 2.799 | I(3)···HN(2D) | 2.835 |
| I(5)···HN(3B) | 2.820 | I(3)···HN(4D) | 2.725 |
| I(5)···HN(5B) | 2.693 | I(3)···HN(6D) | 2.760 |
| I(6)···HC(2C) | 4.059 | I(4)···HC(1P) | 3.120 |
| I(6)···HC(1AA) | 3.081 | I(4)···HC(1Q) | 2.996 |
| I(2)···N(2B) | 3.652 | I(1)···N(1D) | 3.712 |
| I(2)···N(4B) | 3.506 | I(1)···N(3D) | 3.681 |
| I(2)···N(6B) | 3.672 | I(1)···N(5D) | 3.664 |
| I(5)···N(1B) | 3.675 | I(3)···N(2D) | 3.687 |
| I(5)···N(3B) | 3.700 | I(3)···N(4D) | 3.612 |
| I(5)···N(5B) | 3.585 | I(3)···N(6D) | 3.633 |
| I(6)···C(2C) | 4.294 | I(4)···C(1P) | 4.028 |
| I(6)···C(1AA) | 3.938 | I(4)···C(1Q) | 3.941 |
| O(7)···HN(3B) | 2.074 | O(1)···HN(1D) | 2.062 |
| O(8)···HN(2B) | 2.219 | O(2)···HN(6D) | 2.265 |
| O(9)···HN(4B) | 2.256 | O(3)···HN(4D) | 2.290 |
| O(10)···HN(6B) | 2.141 | O(4)···HN(5D) | 1.975 |
| O(11)···HN(1B) | 2.039 | O(5)···HN(3D) | 2.085 |
| O(12)···HN(5B) | 2.013 | O(6)···HN(2D) | 2.197 |
| O(7)···N(3B) | 2.897 | O(1)···N(1D) | 2.893 |
| O(8)···N(2B) | 2.969 | O(2)···N(6D) | 2.923 |

| | | | |
|---|---|---|---|
| O(9)···N(4B) | 3.011 | O(3)···N(4D) | 3.006 |
| O(10)···N(6B) | 2.965 | O(4)···N(5D) | 2.869 |
| O(11)···N(1B) | 2.882 | O(5)···N(3D) | 2.870 |
| O(12)···N(5B) | 2.859 | O(6)···N(2D) | 2.999 |
| N(1B)-Co(1)-N(2B) | 85.0(5) | N(1D)-Co(1D)-N(2D) | 84.7(5) |
| N(3B)-Co(1)-N(1B) | 92.8(5) | N(1D)-Co(1D)-N(3D) | 91.1(5) |
| N(3B)-Co(1)-N(2B) | 92.6(5) | N(1D)-Co(1D)-N(4D) | 174.6(5) |
| N(3B)-Co(1)-N(6B) | 172.5(5) | N(1D)-Co(1D)-N(6D) | 94.2(5) |
| N(4B)-Co(1)-N(1B) | 176.4(5) | N(3D)-Co(1D)-N(2D) | 93.3(5) |
| N(4B)-Co(1)-N(2B) | 92.8(5) | N(4D)-Co(1D)-N(2D) | 92.8(5) |
| N(4B)-Co(1)-N(3B) | 84.4(5) | N(4D)-Co(1D)-N(3D) | 84.1(5) |
| N(4B)-Co(1)-N(5B) | 93.1(5) | N(4D)-Co(1D)-N(6D) | 90.7(5) |
| N(4B)-Co(1)-N(6B) | 89.0(5) | N(5D)-Co(1D)-N(1D) | 88.7(5) |
| N(5B)-Co(1)-N(1B) | 89.3(5) | N(5D)-Co(1D)-N(2D) | 172.2(5) |
| N(5B)-Co(1)-N(2B) | 173.3(5) | N(5D)-Co(1D)-N(3D) | 91.0(5) |
| N(5B)-Co(1)-N(3B) | 91.4(5) | N(5D)-Co(1D)-N(4D) | 94.0(5) |
| N(5B)-Co(1)-N(6B) | 85.4(5) | N(5D)-Co(1D)-N(6D) | 84.5(5) |
| N(6B)-Co(1)-N(1B) | 93.9(5) | N(6D)-Co(1D)-N(2D) | 91.8(5) |
| N(6B)-Co(1)-N(2B) | 91.3(5) | N(6D)-Co(1D)-N(3D) | 172.9(5) |
| I(2)···H(2BA)-N(2B) | 160.5 | I(1)···H(1DA)-N(1D) | 164.7 |
| I(2)···H(4BA)-N(4B) | 168.6 | I(1)···H(3DA)-N(3D) | 165.2 |
| I(2)···H(6BA)-N(6B) | 161.5 | I(1)···H(5DA)-N(5D) | 167.3 |
| I(5)···H(1BA)-N(1B) | 161.7 | I(3)···H(2DA)-N(2D) | 156.4 |
| I(5)···H(3BA)-N(3B) | 163.0 | I(3)···H(4DA)-N(4D) | 165.5 |
| I(5)···H(5BA)-N(5B) | 166.6 | I(3)···H(6DA)-N(6D) | 161.3 |
| I(6)···H(2CA)-C(2C) | 97.2 | I(4)···H(1PB)-C(1P) | 154.7 |
| I(6)···H(1AB)-C(1AA) | 146.5 | I(4)···H(1QB)-C(1Q) | 162.6 |
| O(7)···H(3BB)-N(3B) | 149.8 | O(1)···H(1DB)-N(1D) | 159.1 |
| O(8)···H(2BB)-N(2B) | 139.2 | O(2)···H(6DB)-N(6D) | 147.6 |
| O(9)···H(4BB)-N(4B) | 140.1 | O(3)···H(4DB)-N(4D) | 135.5 |
| O(10)···H(6BB)-N(6B) | 150.2 | O(4)···H(5DB)-N(5D) | 167.0 |
| O(11)···H(1BB)-N(1B) | 153.6 | O(5)···H(3DB)-N(3D) | 143.9 |
| O(12)···H(5BB)-N(5B) | 154.1 | O(6)···H(2DB)-N(2D) | 146.7 |

[a]There are two independent molecules in the unit cell.

REFERENCES

(s1) Onishi, Y.; Nishimoto, Y.; Yasuda, M.; Baba, K. *Org. Lett.* **2014**, ***16***, 1176-1179.

(s2) Xu, F.; Wu, Q.; Chen, X.; Lin, X.; Wu, Q. *Eur. J. Org. Chem.* **2015**, *2015*, 5393-5401.

(s3) Kaczorowska, K.; Kolarska, Z.; Mitka, K.; Kowalski, P. *Tetrahedron* **2005**, *61*, 8315-8327.

(s4) Wang, Z.; Cui, Y.-T.; Xu, Z.-B.; Qu, J. *J. Org. Chem.* **2008**, *73*, 2270-2274.

(s5) Henderson, A. S.; Bower, J. F.; Galan, M. C. *Org. Biomol. Chem.* **2014**, *12*, 9180-9183.

(s6) Ankner, T.; Hilmersson, G. *Org. Lett.* **2009**, *11*, 503-506.

(s7) Tulsi, N. S.; Downey, A. M.; Cairo, C. W. *Bioorg. Med. Chem.* **2010**, *18*, 8679-8686.

(s8) Zong, H.; Huang, H.; Liu, J.; Bian, G.; Song, L. *J. Org. Chem.* **2012**, *77*, 4645-4652.

(s9) Jha, A. K.; Kishor, S.; Jain, N. *RSC Adv.* **2015**, *5*, 55218-55226.

(s10) Mei, Y.; Dissanayake, P.; Allen, M. J. *J. Am. Chem. Soc.* **2010**, *132*, 12871-12873

(s11) Chávez-Flores, D.; Salvador, J. M. *Biotechnol. J.* **2009**, ***4***, 1222-1224.

(s12) Zhou, E.; Zhang, J.; Lu, Y.; Dong, C. *ARKIVOC* **2014**, *2014*, 351-364.

(s13) Tanaka, K.; Iwashita, T.; Sasaki, C.; Takahashi, H. *Tetrahedron: Asymmetry* **2014**, *25*, 602-609.

(s14) Yuste, F.; Sánchez-Obregón, R.; Díaz, E.; García-Carrillo, M. A. *Tetrahedron: Asymmetry* **2014**, *25*, 224-228.

(s15) Wolf, C.; Cook, A. M.; Dannatt, J. E. *Tetrahedron: Asymmetry* **2014**, *25*, 163-169.

(s16) Borowiecki, P. *Tetrahedron: Asymmetry* **2015**, *26*, 16-23.

(s17) Jain, N.; Patel, R. B.; Bedekar, A. V. *RSC Adv.* **2015**, *5*, 45943-45955.

(s18) Kannappan, J.; Jain, N.; Bedekar, A. V. *Tetrahedron: Asymmetry* **2015**, *26*, 1102-1107.

(s19) Du, G.; Li, Y.; Ma, S.; Wang, R.; Li, B.; Guo, F.; Zhu, W.; Li, Y. *J. Nat. Prod.* **2015**, *78*, 2968-2974.

(s20) Silva, M. S.; Pietrobom, D. *New J. Chem.* **2015**, *39*, 8240-8244.

(s21) Pal, I.; Chaudhari, S. R.; Suryaprakash, N. R. *Magn. Reson. Chem.* **2015**, *53*, 142-146.

(s22) Laaksonen, T.; Heikkinen, S.; Wähälä, K. *Molecules* **2015**, *20*, 20873-20886.

(s23) Jung, S. H.; Kim, K. Y.; Ahn, A.; Lee, S. S.; Choi, M. Y.; Jaworski, J.; Jung, J. H. *New J. Chem.* **2016**, *40*, 7917-7922.

(s24) Li, G.; Cao, J.; Zong, W.; Lei, X.; Tan, R. *Org. Chem. Front.* **2016**, *3*, 96-102.

(s25) Dowey, A. E.; Puentes, C. M.; Carey-Hatch, M.; Sandridge, K. L.; Krishna, N. B.; Wenzel, T. J. *Chirality* **2016**, *28*, 299-305.

(s26) Uzarewicz-Baig, M.; Wilhelm, R. *Heteroat. Chem.* **2016**, *27*, 121-134.

(s27) Monteagudo, E.; March, P.; Álvarez-Larena, A.; Virgili, A. *ChemistrySelect* **2017**, *2*, 7362-7367.

(s28) Schurig, V. *Tetrahedron Lett.* **1976**, *17*, 1269-1272.

(s29) Magiera, D.; Szmigielska, A.; Pietrusiewicz, K. M.; Duddeck, H. *Chirality* **2004**, *16*, 57-64.

(s30) Naumann, C.; Kuchel, P. W. *J. Phys. Chem. A* **2008**, *112*, 8659-8664.

(s31) Naumann, C.; Kuchel, P. W. *Chem. Eur. J.* **2009**, *15*, 12189-12191.

(s32) Kuchel, P. W.; Naumann, C.; Chapman, B. E.; Shishmarev, D.; Håkansson, P.; Bacskay, G.; Hush, N. S. *J. Magn. Reson.* **2014**, *247*, 72-80.

(s33) Berdagué, P.; Herber-Pucheta, J.-E.; Jha, V.; Panossian, A.; Leroux, F. R.; Lesot, P. *New J. Chem.* **2015**, *39*, 9504-9517.

APPENDIX B: AN AIR AND WATER STABLE CATALYST FOR THE ENANTIOSELECTIVE GENERATION OF QUARTERNARY CARBON STEREOCENTERS BY ADDITION OF SUBSTITUTED CYANOACETATE ESTERS TO ACETYLENIC ESTERS

**General data.** NMR spectra were recorded on a Varian NMRS 500 MHz spectrometer at ambient probe temperature. Chemical shifts (δ in ppm) were referenced to residual solvent signals ($^1$H: $CHCl_3$, 7.26; $CDHCl_2$, 5.32; acetone-$d_5$, 2.05; $^{13}$C: $CDCl_3$, 77.2). Microanalyses (see the experimental section of chapter 3) were conducted by Atlantic Microlab. All reactions were carried out in air.

The following materials were used as received: NMR solvents (Cambridge Isotopes: $CDCl_3$, $CD_2Cl_2$, acetone-$d_6$), $CH_2Cl_2$ (EMD Chemicals, ACS grade), silica gel (Silicycle SiliaFlash® F60), TLC plates (silica gel, EMD Millipore), ethyl acetate (Sigma-Aldrich, ≥99.5%), hexanes (Sigma-Aldrich, ≥98.5%), $CH_3CN$ (anhydrous, BDH Chemicals, 99.5%), diethyl ether (Sigma-Aldrich, ≥99.0%), acetone (Sigma-Aldrich, 99.5%), toluene (Omnisolv, 99.9%), ethanol (Koptec, 200 proof), DMSO (BDH, 99.9%), conc. HCl (BDH Chemicals, 36.5-38% in water), sodium sulfate (anhydrous, EMD Millipore, 99.0%), dimethyl acetylenedicarboxylate (**4a**, Acros Organics, 98%), diethyl acetylenedicarboxylate (**4b**, Acros Organics, 97%), *t*-butyl propiolate (**4c**, Acros Organics, 98%), di(*t*-butyl) acetylenedicarboxylate (**4d**, eMolecules, 95%), ethyl phenylcyanoacetate (**5a**, Alfa Aesar, 98%), *t*-butyl cyanoacetate (TCI Chemicals, 97%), triethyl amine (Macron Fine Chemicals, 99.5%), pyridine (EMD Millipore, 99.0%), 2,6-lutidine (Acros Organics, 98%), 2,6-di(t-butyl)pyridine (Ambeed, 98%), *N*-methylimidazole (Acros Organics, 99%), morpholine (Alfa Aesar, 99%), 4-methylmorpholine (Alfa Aesar, 99%), potassium carbonate (anhydrous, Alfa Aesar, 99%), 10-bromo-1-decene (Sigma-Aldrich, 97%), 1-bromotetradecane (Alfa Aesar, 98%), 4-bromobenzyl bromide (Alfa Aesar, 97%), 4-methylbenzyl bromide (Alfa Aesar, 98%), 1-naphthaldehyde (TCI Chemicals, 95.0%), 4-dimethylaminopyridine (Sigma-Aldrich, 99%), Hantzsch ester (diethyl 1,4-dihydro-2,6-dimethyl-3,5-pyridinedicarboxylate, Matrix Scientific, 95%), $Ph_2SiMe_2$ (TCI Chemicals, 97.0%).

The following were synthesized by literature procedures: ethyl 2-cyano-3-phenylpropanoate (**5b**),[s1] *t*-butyl 2-cyano-3-phenylpropanoate (**5c**),[s2] *t*-butyl 2-cyanopent-4-enoate (**5d**),[s3] *t*-butyl 2-cyanohex-4-enoate (**5e**),[s3] *t*-butyl 2-cyano-3-(furan-2-yl)propanoate (**5i**),[s2] *t*-butyl 2-cyano-3-(4-bromophenyl)propanoate (**5j**),[s4] and Λ-(*S*,*S*)-$\mathbf{2}^{3+}$ $2I^{-}BAr_f^{-}$.[s5]

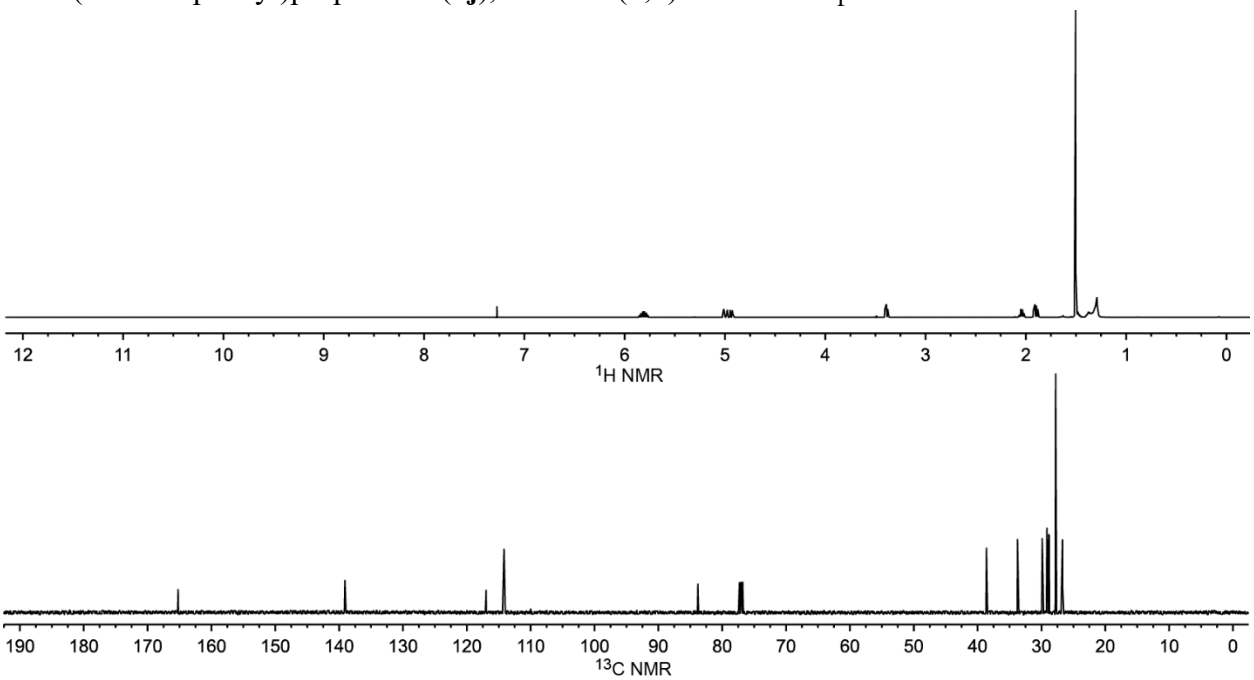


**Figure B-1.** $^1$H and $^{13}C\{^1H\}$ NMR spectra of **5f** in $CDCl_3$.

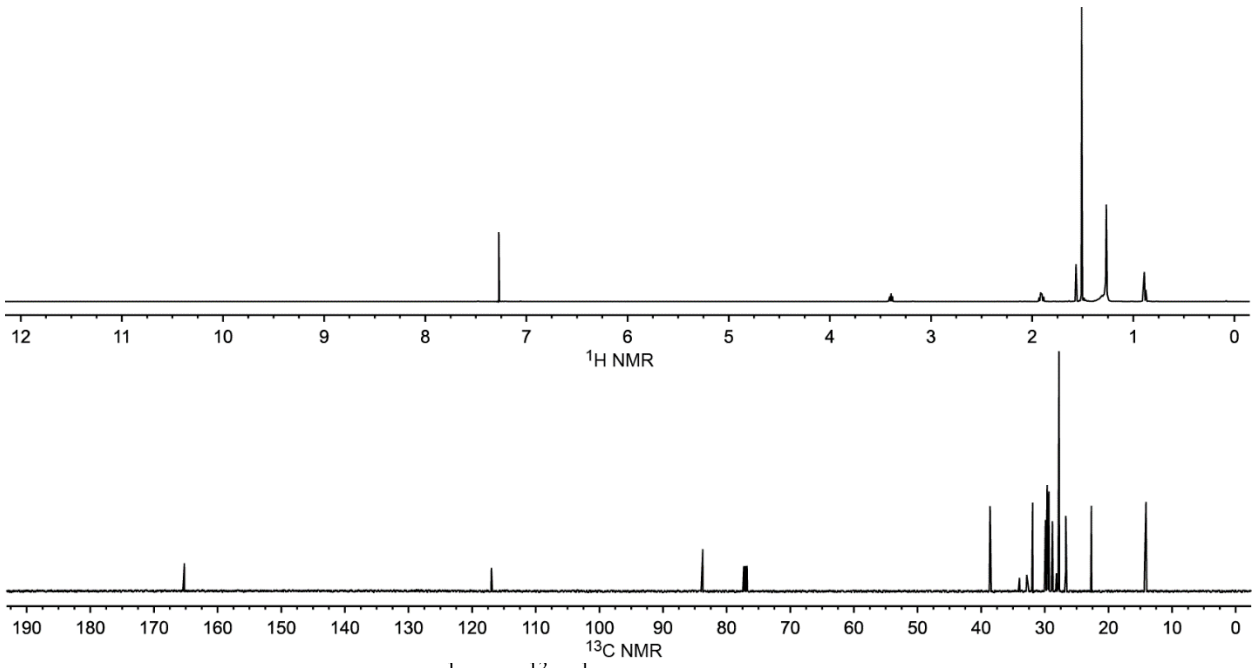


**Figure B-2.** $^{1}H$ and $^{13}C\{^{1}H\}$ NMR spectra of **5g** in $CDCl_3$.

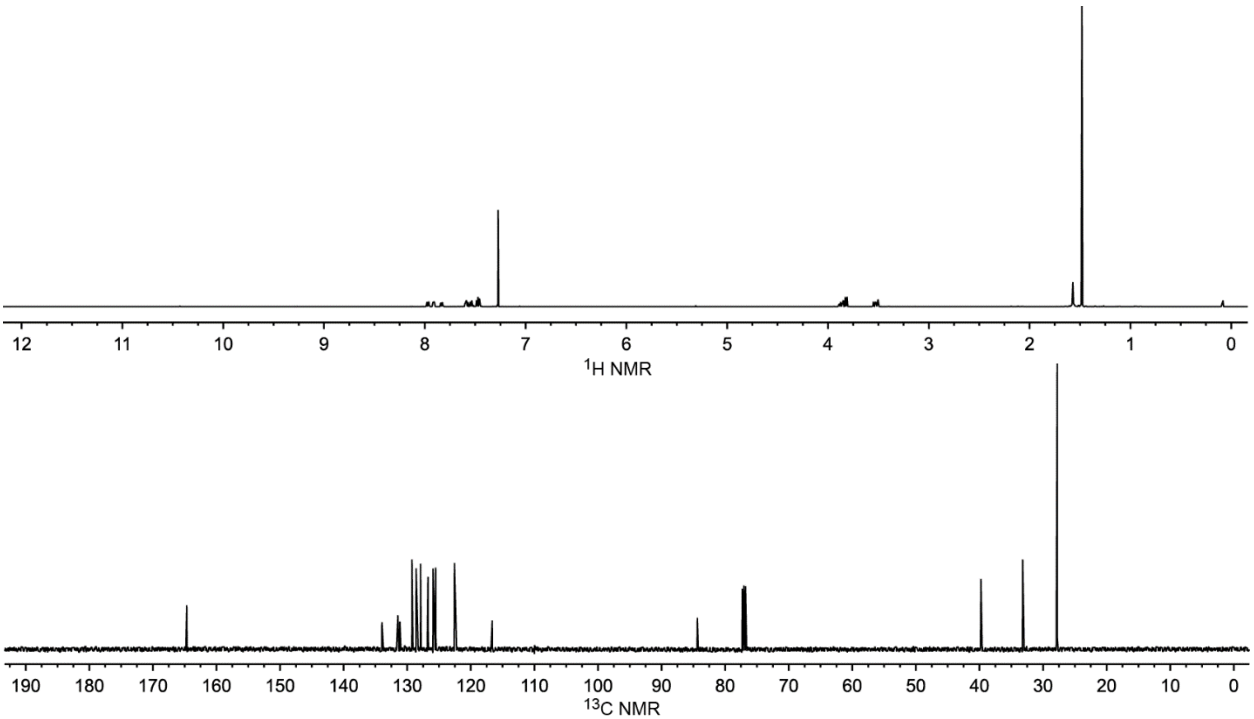


**Figure B-3.** $^{1}H$ and $^{13}C\{^{1}H\}$ NMR spectra of **5h** in $CDCl_3$.

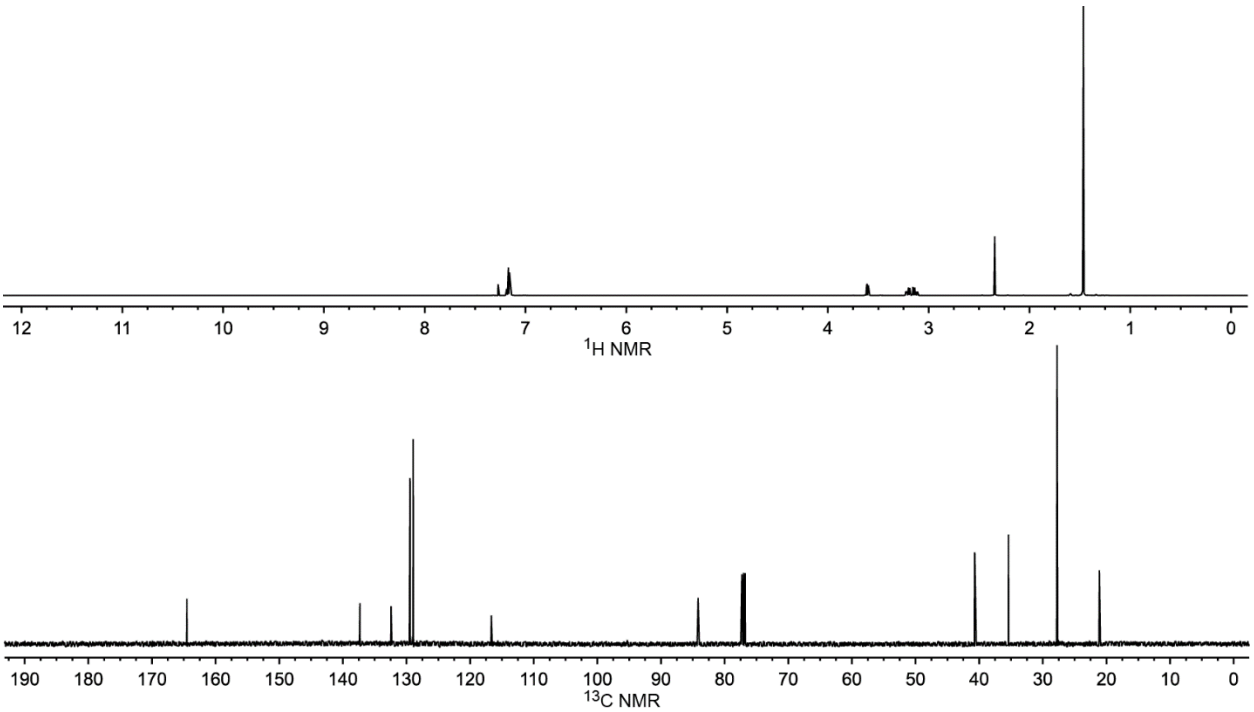


**Figure B-4.** $^{1}H$ and $^{13}C\{^{1}H\}$ NMR spectra of **5k** in $CDCl_3$.

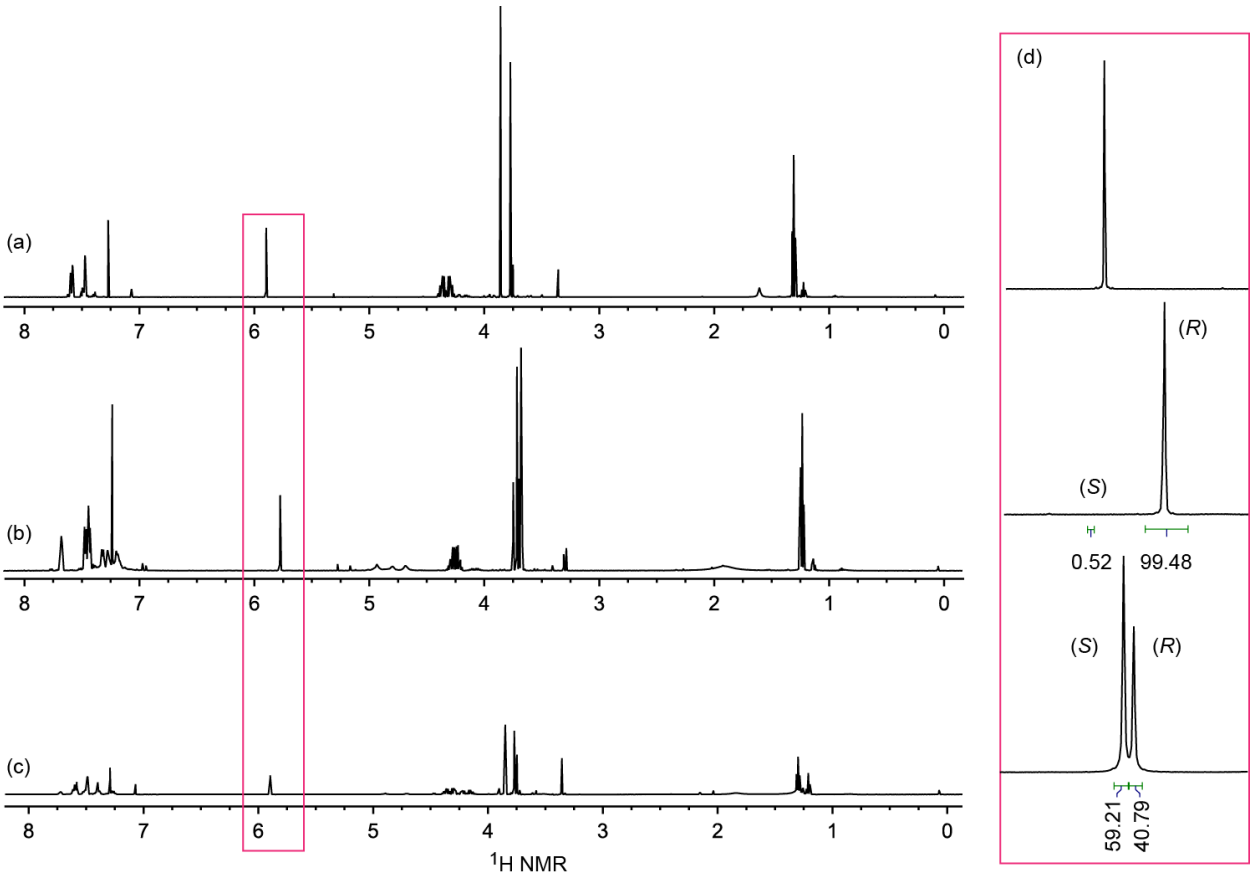


**Figure B-5.** Spectra of **6aa** in $CDCl_3$: (a) $^1$H NMR, (b) $^1$H NMR with 10 mol% Λ-(*S*,*S*)-**2**$^{3+}$ 2I$^-$BAr$_f^-$, (c) $^1$H NMR, independently prepared sample with 10 mol% Λ-(*S*,*S*)-**2**$^{3+}$ 2I$^-$BAr$_f^-$, and (d) expansion of δ 5.65-6.15 ppm region.

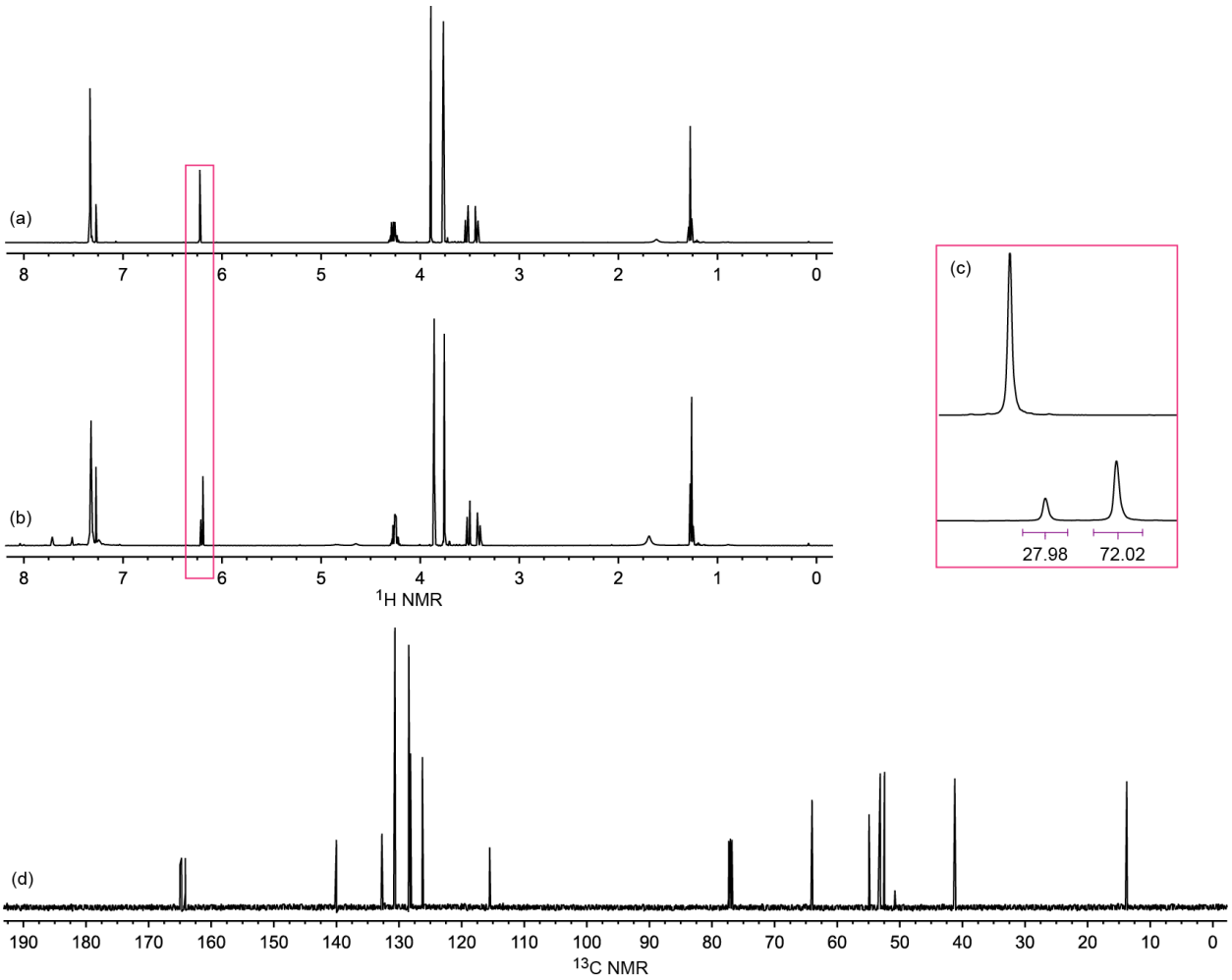


**Figure B-6.** Spectra of **6<u>a</u>b** in $CDCl_3$: (a) $^1$H NMR, (b) $^1$H NMR with 10 mol% Λ-(*S*,*S*)-**2**$^{3+}$ $2I^-BAr_f^-$, (c) expansion of δ 6.10-6.35 ppm region, and (d) $^{13}C\{^1H\}$ NMR.

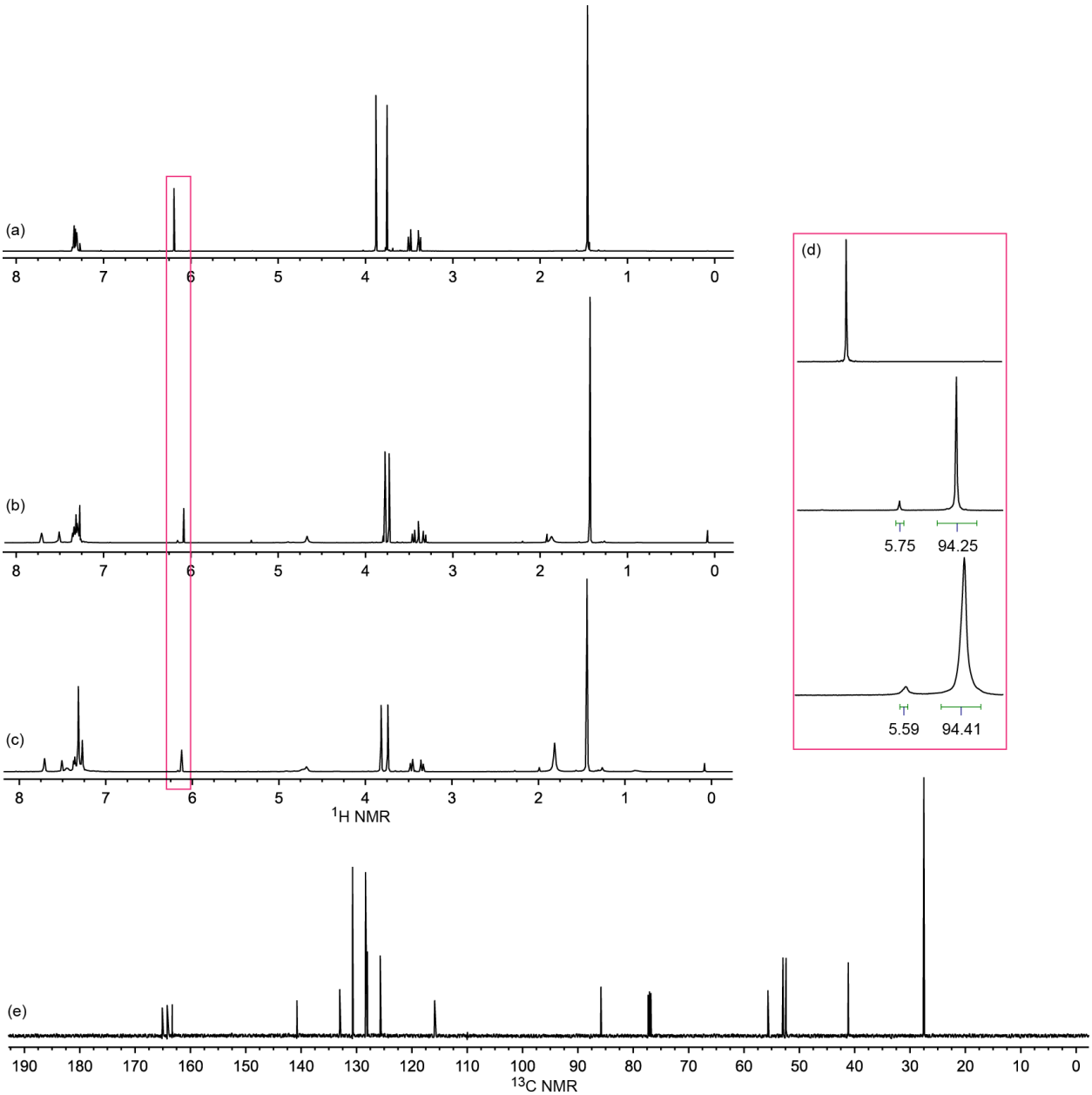


**Figure B-7.** Spectra of **6<u>a</u>c** in $CDCl_3$: (a) $^1$H NMR, (b) $^1$H NMR with 10 mol% Λ-(*S*,*S*)-**2**$^{3+}$ 2I$^-$BAr$_f^-$, (c) $^1$H NMR with 10 mol% Λ-(*S*,*S*)-**2**$^{3+}$ 2I$^-$BAr$_f^-$ of **6<u>a</u>c** from a reaction using 2,6-lutidine, (d) expansion of δ 6.00-6.25 ppm region, and (e) $^{13}$C{$^1$H} NMR.

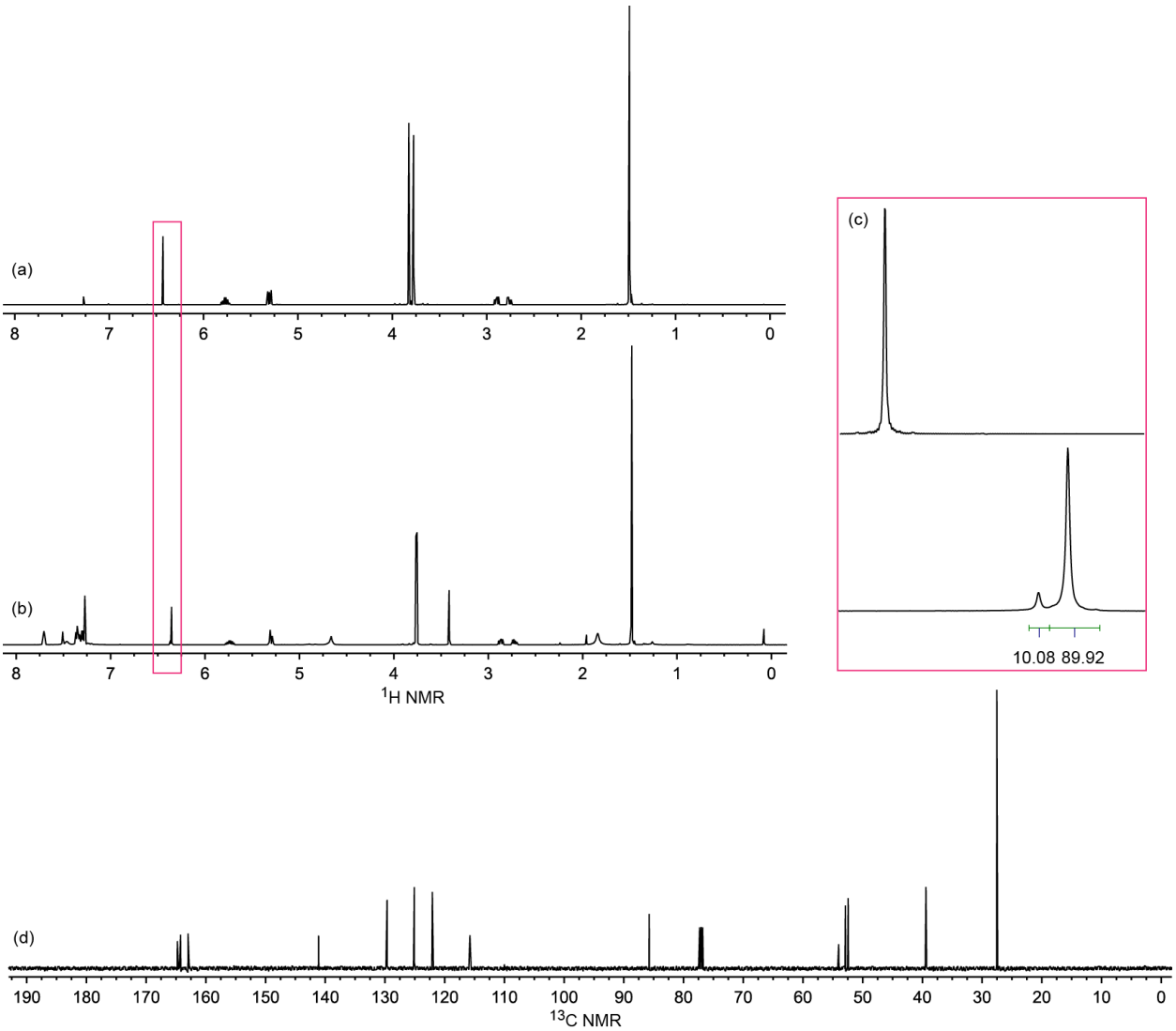


**Figure B-8.** Spectra of **6<u>a</u>d** in $CDCl_3$: (a) $^1$H NMR, (b) $^1$H NMR with 10 mol% Λ-(*S*,*S*)-**2**$^{3+}$ 2I$^-$BAr$_f^-$, (c) expansion of δ 6.25-6.50 ppm region, and (d) $^{13}$C{$^1$H} NMR.

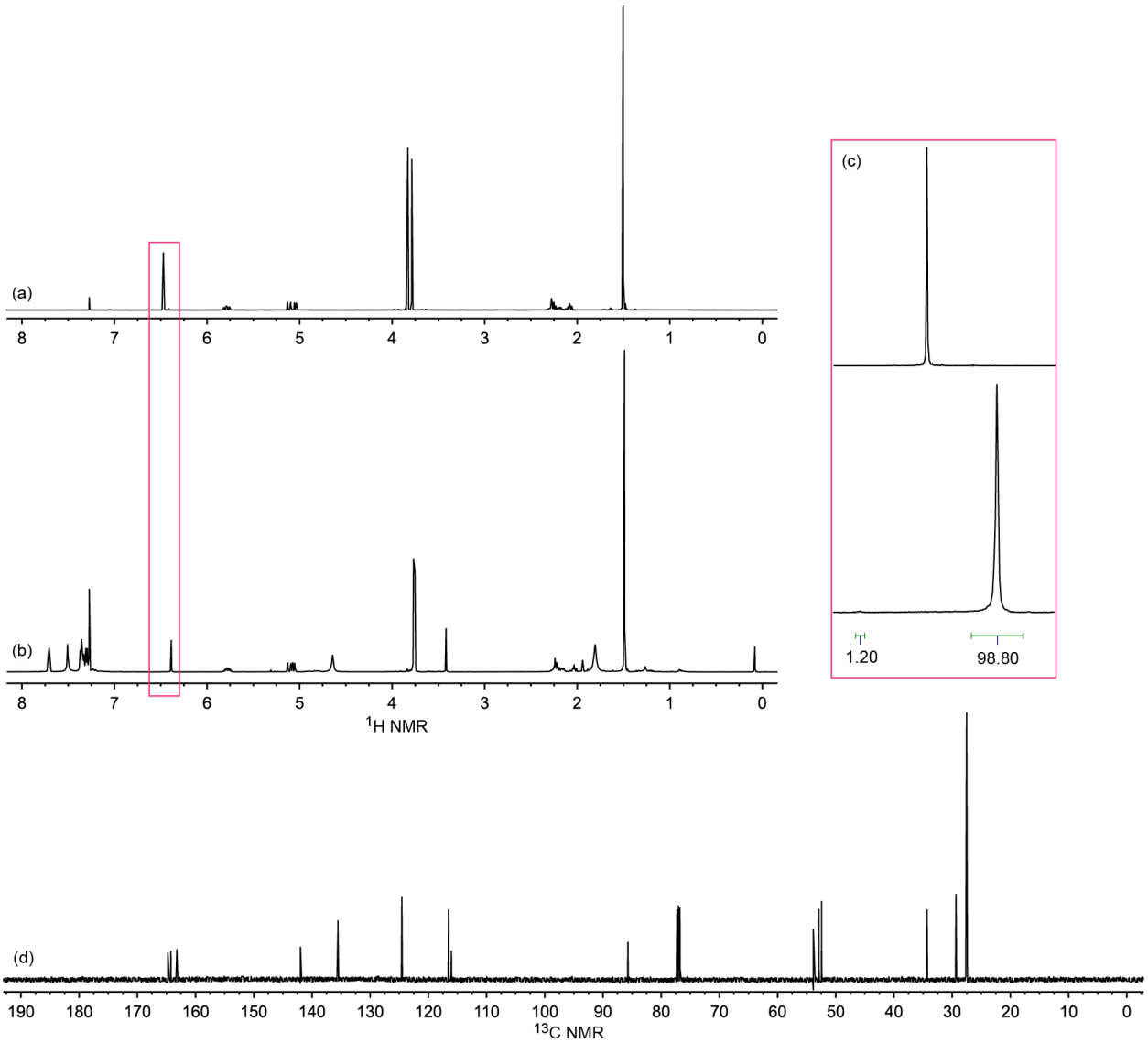


**Figure B-9.** Spectra of **6<u>a</u>e** in $CDCl_3$: (a) $^1$H NMR, (b) $^1$H NMR with 10 mol% Λ-(*S*,*S*)-**2**$^{3+}$ 2I$^-$BAr$_f^-$, (c) expansion of δ 6.35-6.60 ppm region, and (d) $^{13}$C{$^1$H} NMR.

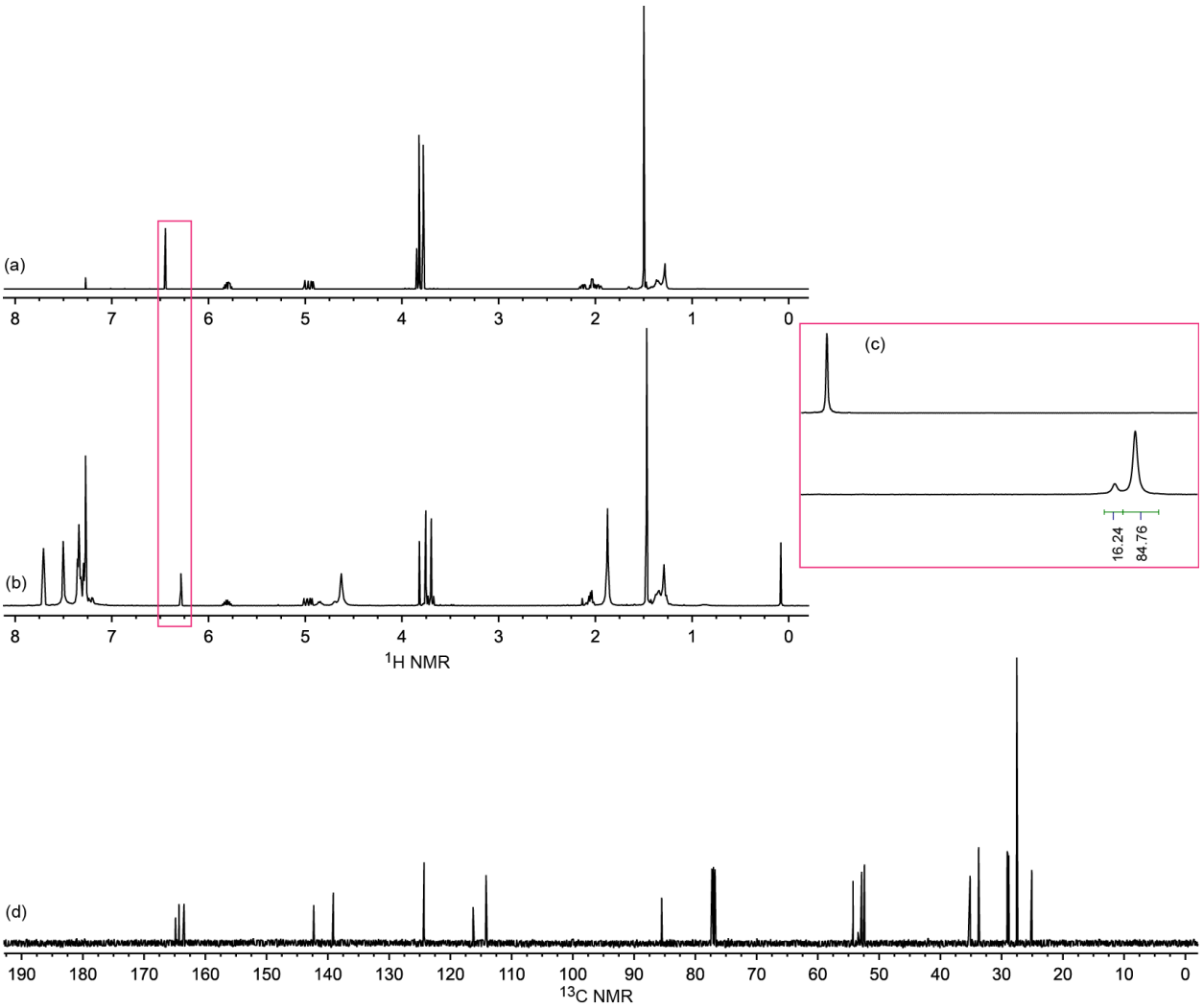


**Figure B-10.** Spectra of **6<u>a</u>f** in $CDCl_3$: (a) $^1$H NMR, (b) $^1$H NMR with 20 mol% Λ-(*S*,*S*)-**2**$^{3+}$ 2I$^-$BAr$_f^-$, (c) expansion of δ 6.20-6.50 ppm region, and (d) $^{13}$C{$^1$H} NMR.

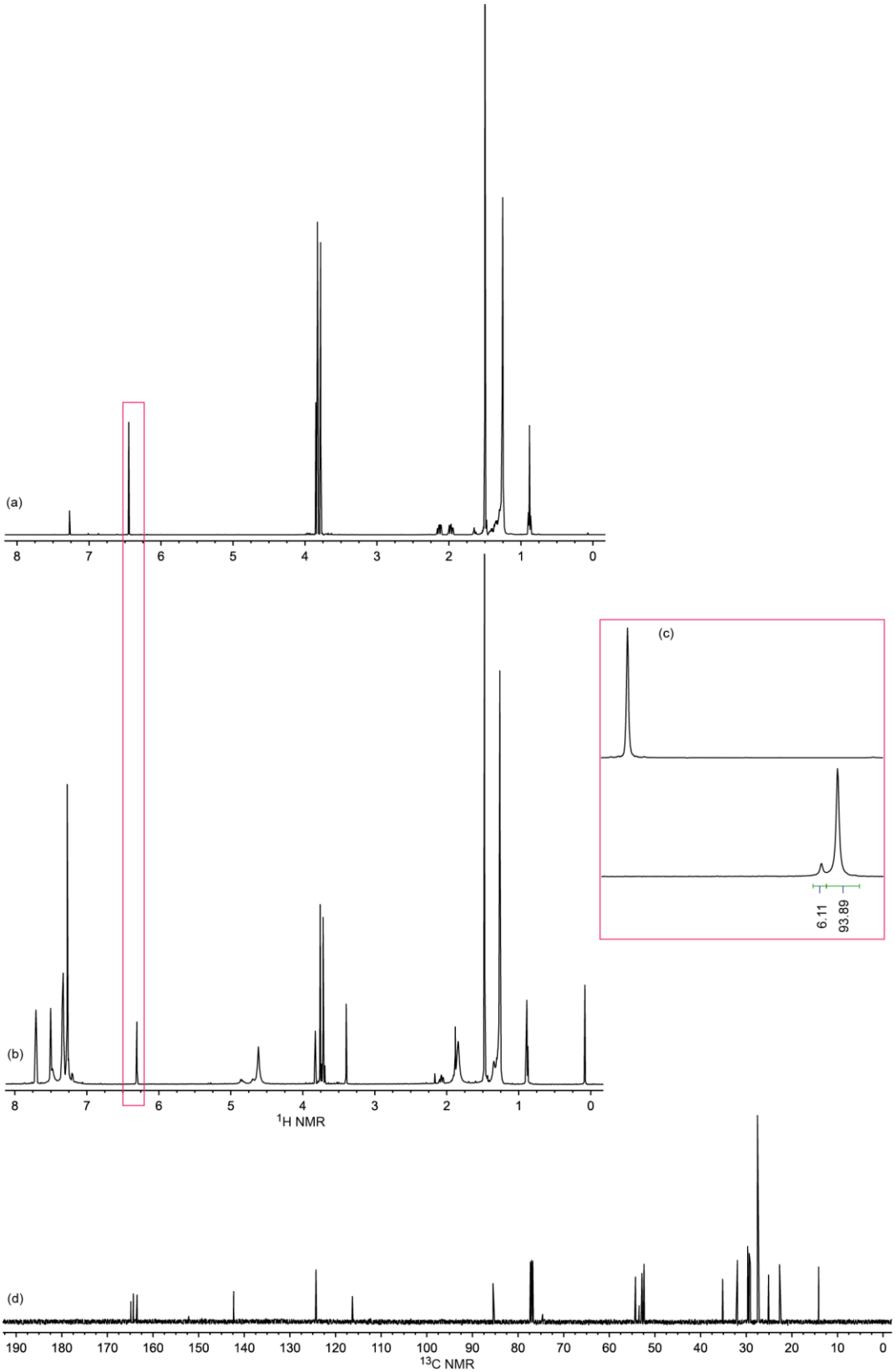


**Figure B-11.** Spectra of **6ag** in $CDCl_3$: (a) $^1$H NMR, (b) $^1$H NMR with 20 mol% Λ-(*S*,*S*)-**2**$^{3+}$ 2I$^-$BAr$_f^-$, (c) expansion of δ 6.20-6.50 ppm region, and (d) $^{13}$C{$^1$H} NMR.

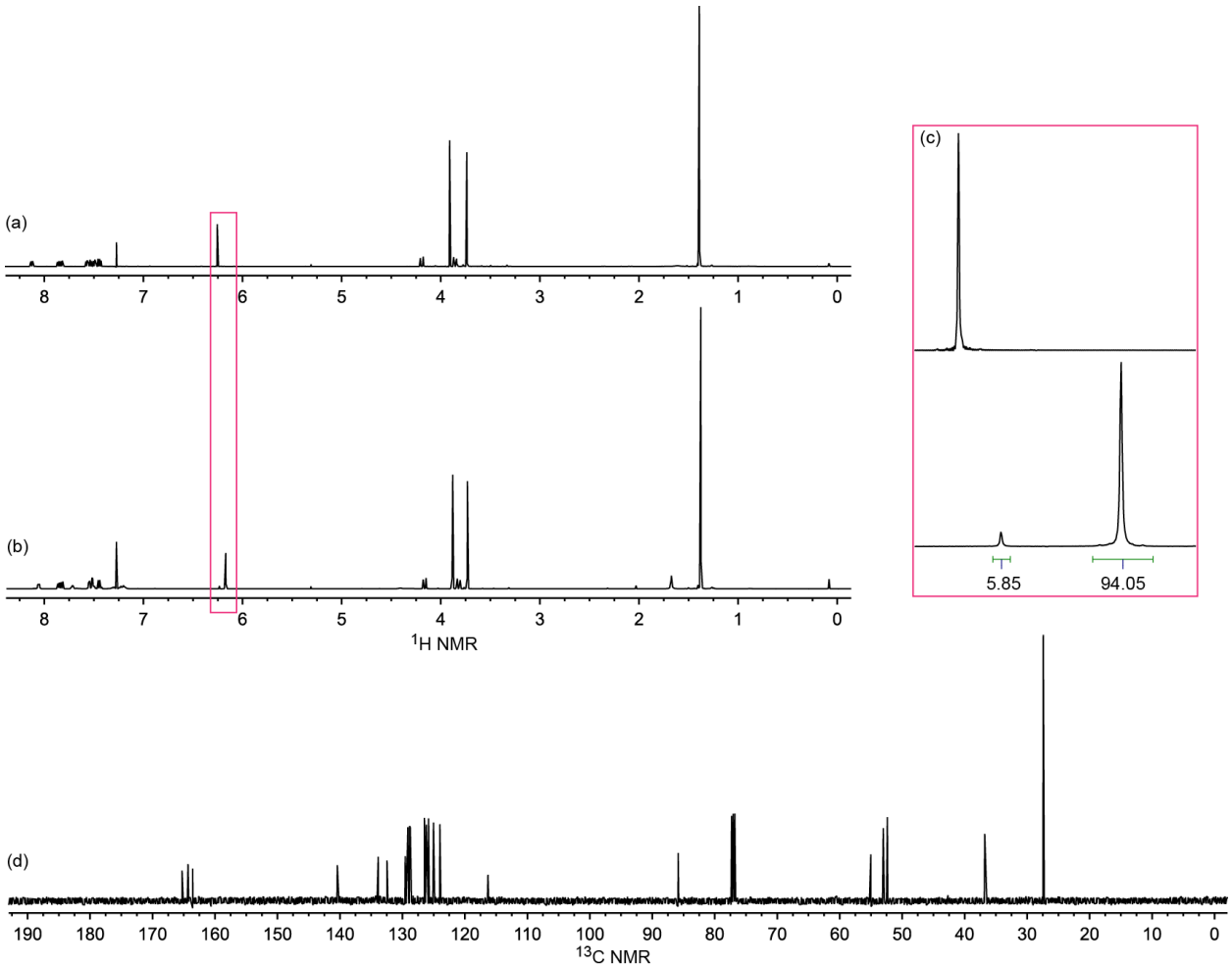


**Figure B-12.** Spectra of **6<u>a</u>h** in $CDCl_3$: (a) $^1$H NMR, (b) $^1$H NMR with 10 mol% Λ-(*S*,*S*)-**2**$^{3+}$ 2I$^-$BAr$_f^-$, (c) expansion of δ 6.10-6.30 ppm region, and (d) $^{13}$C{$^1$H} NMR.

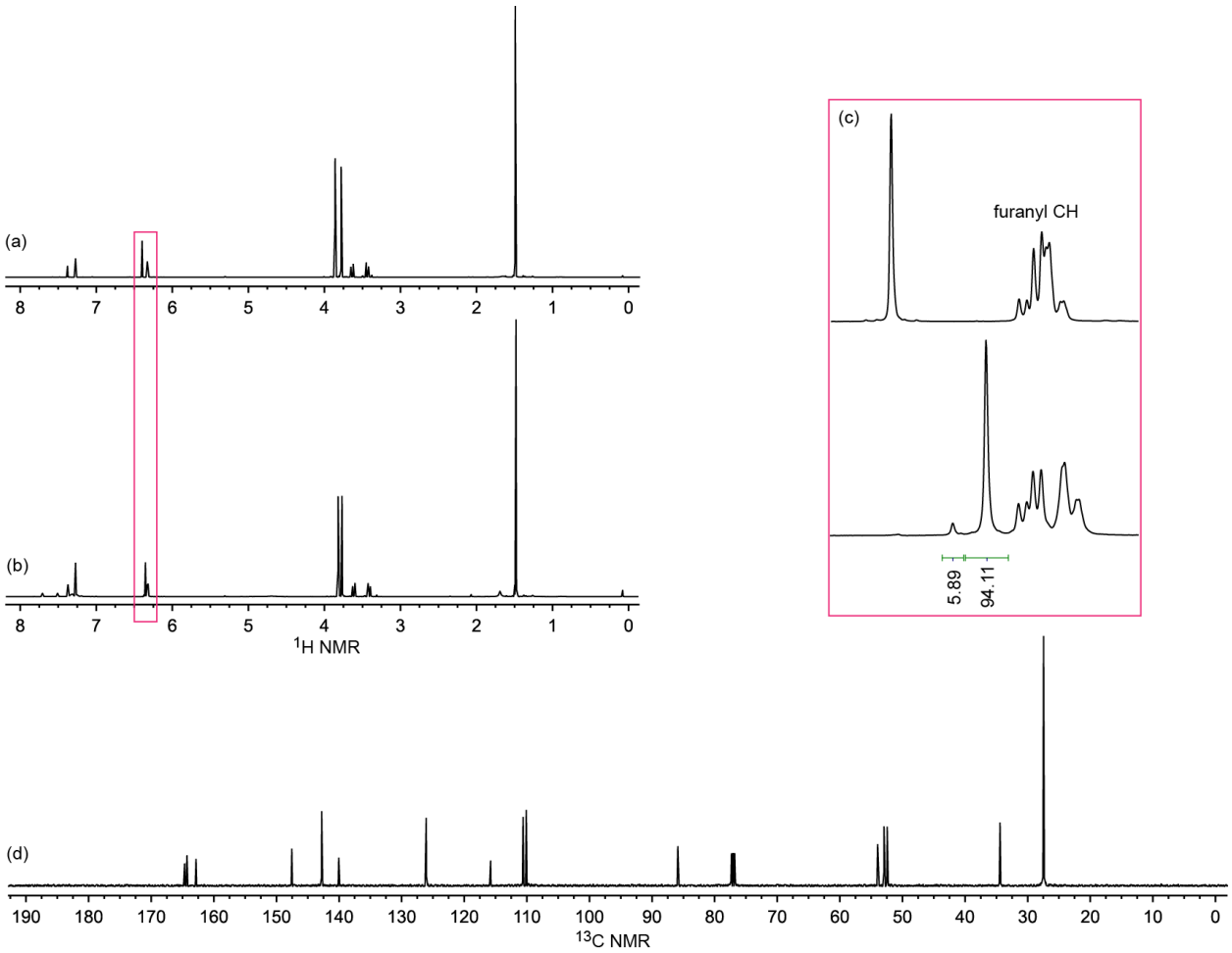


**Figure B-13.** Spectra of **6<u>a</u>i** in $CDCl_3$: (a) $^1$H NMR, (b) $^1$H NMR with 10 mol% Λ-(*S*,*S*)-**2**$^{3+}$ 2I$^-$BAr$_f^-$, (c) expansion of δ 6.20-6.50 ppm region, and (d) $^{13}$C{$^1$H} NMR.

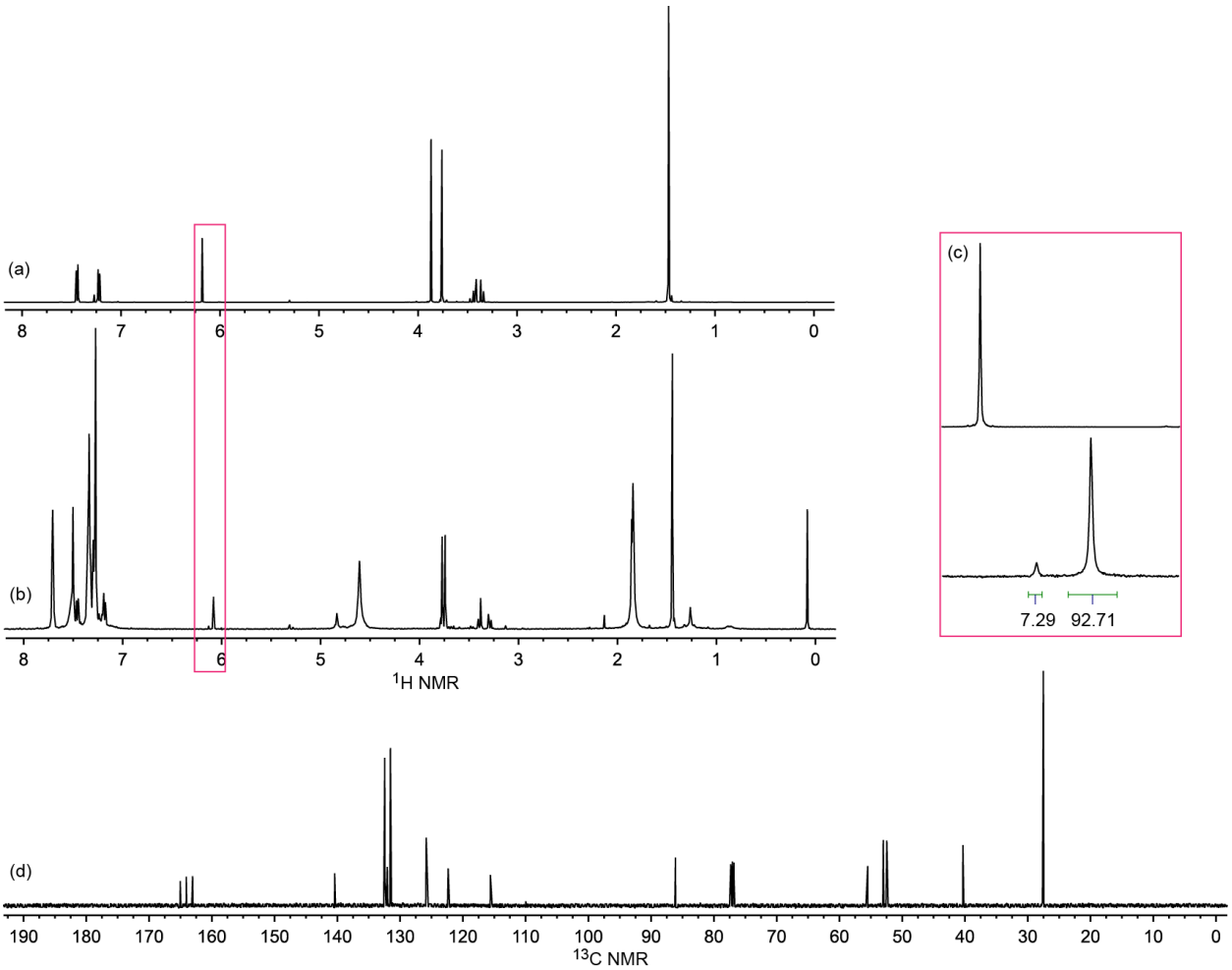


**Figure B-14.** Spectra of **6aj** in $CDCl_3$: (a) $^1$H NMR, (b) $^1$H NMR with 45 mol% Λ-(*S*,*S*)-**2**$^{3+}$ 2I$^-$BAr$_f^-$, (c) expansion of δ 5.95-6.25 ppm region, and (d) $^{13}$C{$^1$H} NMR.

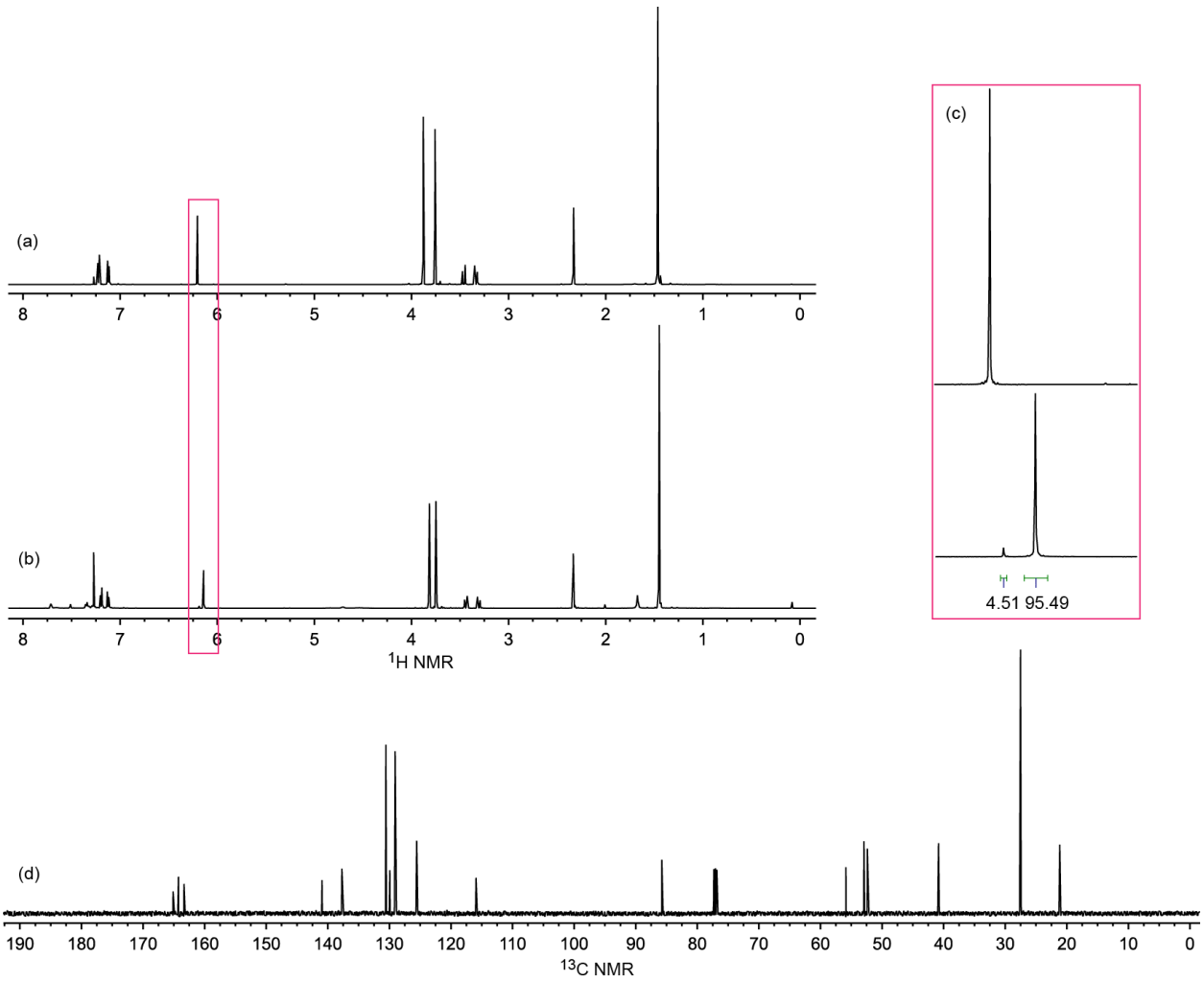


**Figure B-15.** Spectra of **6<u>a</u>k** in $CDCl_3$: (a) $^1$H NMR, (b) $^1$H NMR with 10 mol% Λ-(*S*,*S*)-**2**$^{3+}$ 2I$^-$BAr$_f^-$, (c) expansion of δ 6.00-6.25 ppm region, and (d) $^{13}$C{$^1$H} NMR.

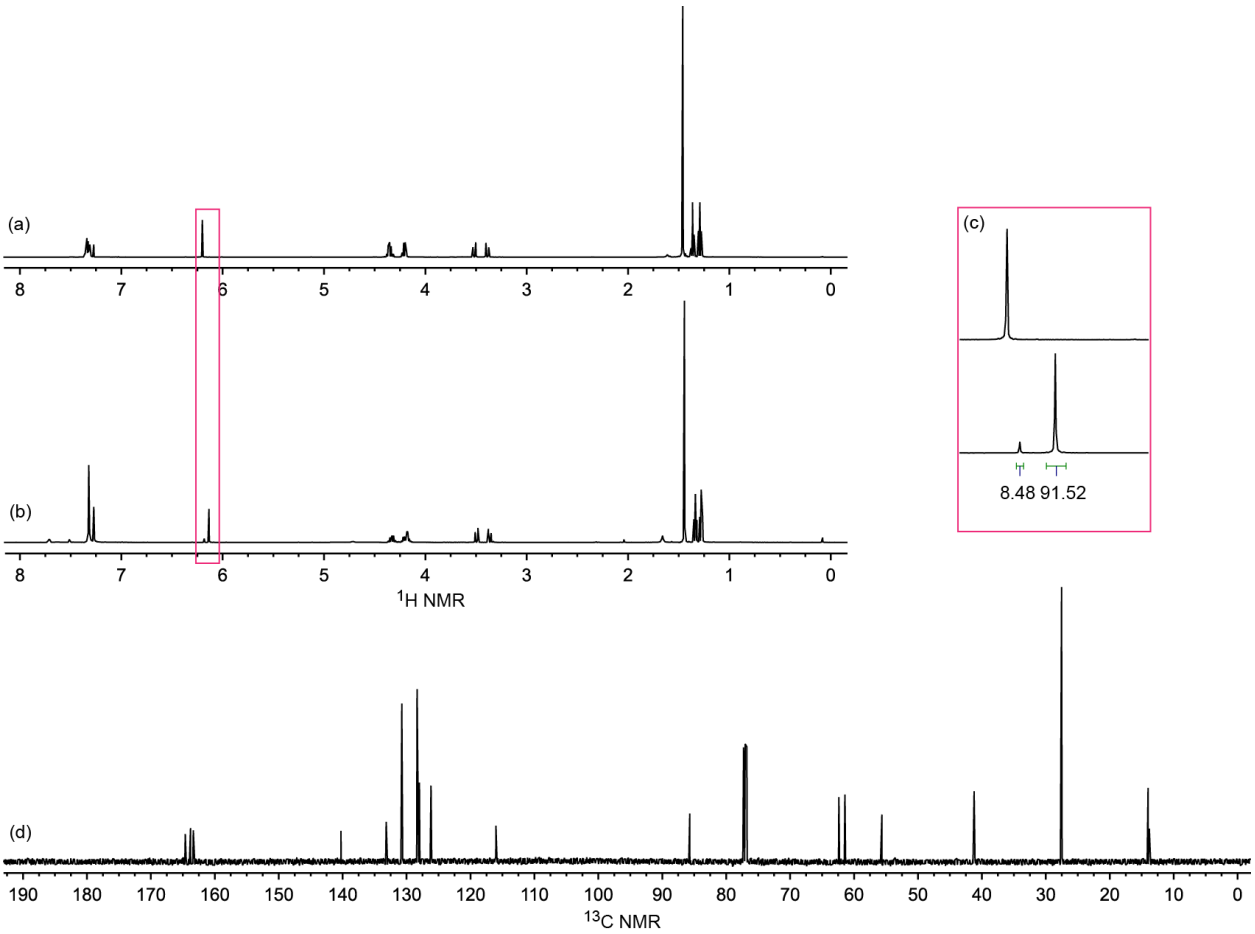


**Figure B-16.** Spectra of **6<u>b</u>c** in $CDCl_3$: (a) $^1$H NMR, (b) $^1$H NMR with 10 mol% Λ-(*S*,*S*)-**2**$^{3+}$ 2I$^-$BAr$_f^-$, (c) expansion of δ 6.00-6.25 ppm region, and (d) $^{13}$C{$^1$H} NMR.

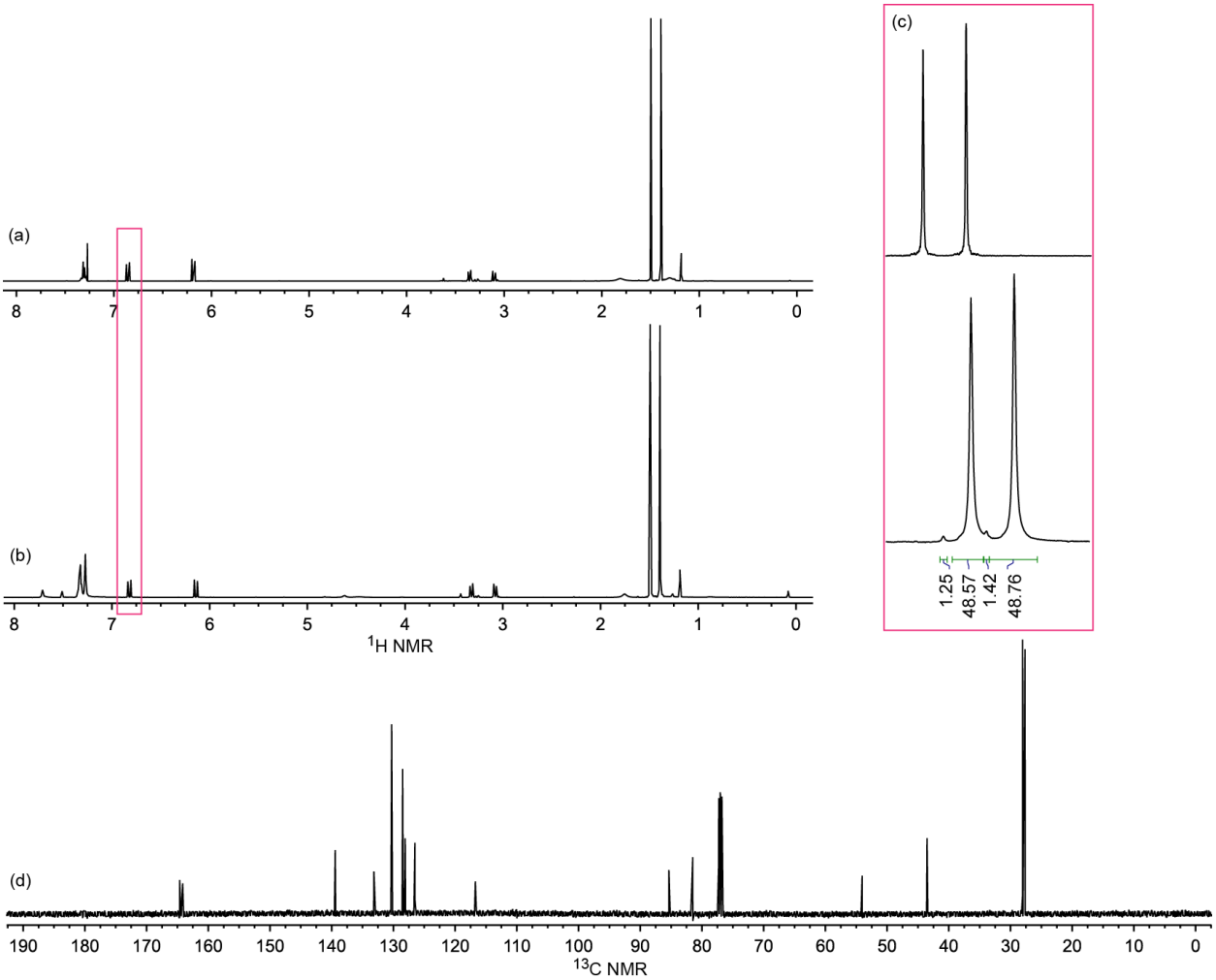


**Figure B-17.** Spectra of **6<u>c</u>c** in $CDCl_3$: (a) $^1$H NMR, (b) $^1$H NMR with 10 mol% Λ-(*S*,*S*)-**2**$^{3+}$ 2I$^-$BAr$_f^-$, (c) expansion of δ 6.70-6.95 ppm region, and (d) $^{13}$C{$^1$H} NMR.

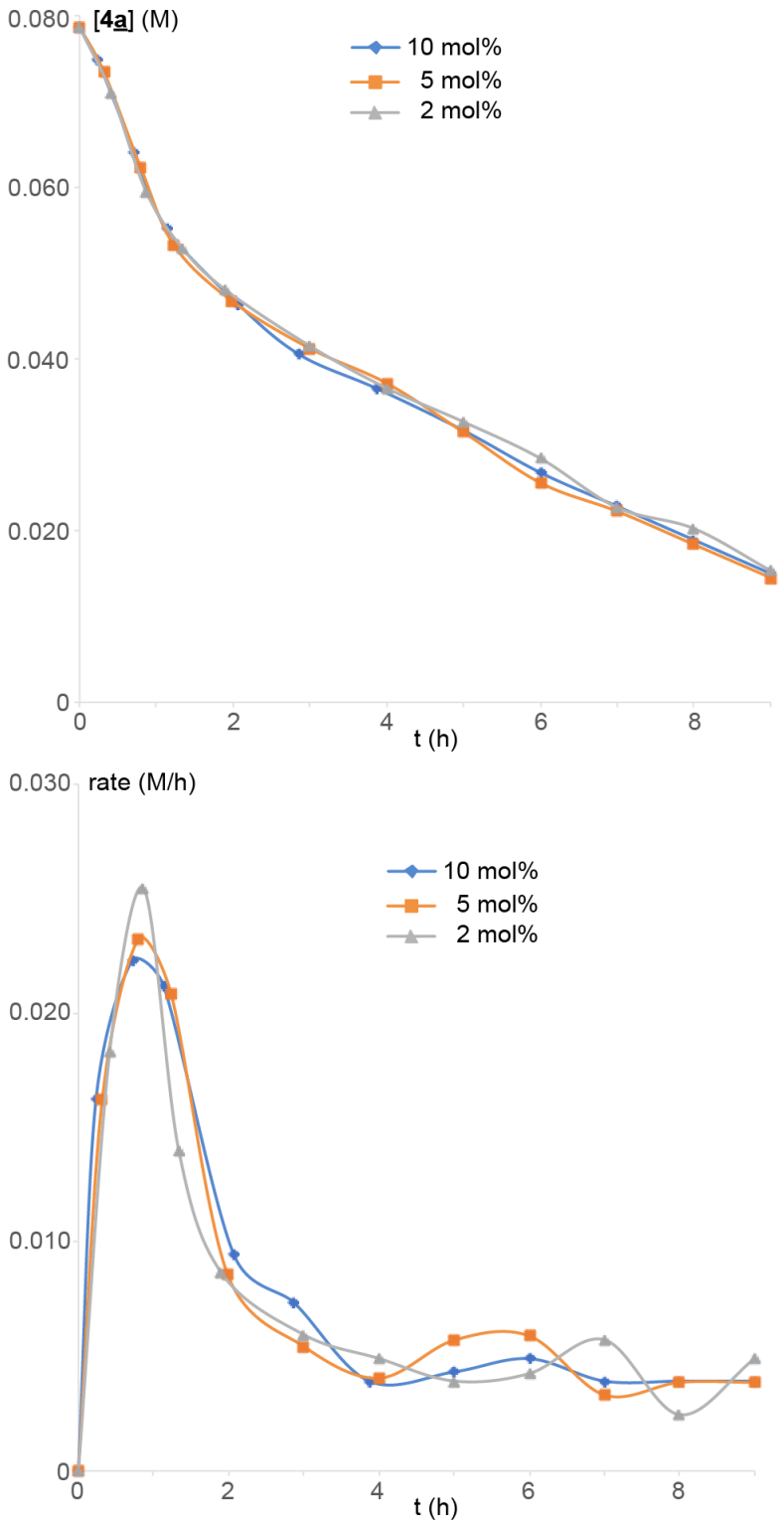


**Figure B-18.** Application of the reaction progress kinetic analysis method[s6] to a reaction similar to entry 22 of Table 3.1 (see text). Top: plot of the concentration of **4a** versus time. Bottom: plot of Δ([**4a**])/Δt versus time.

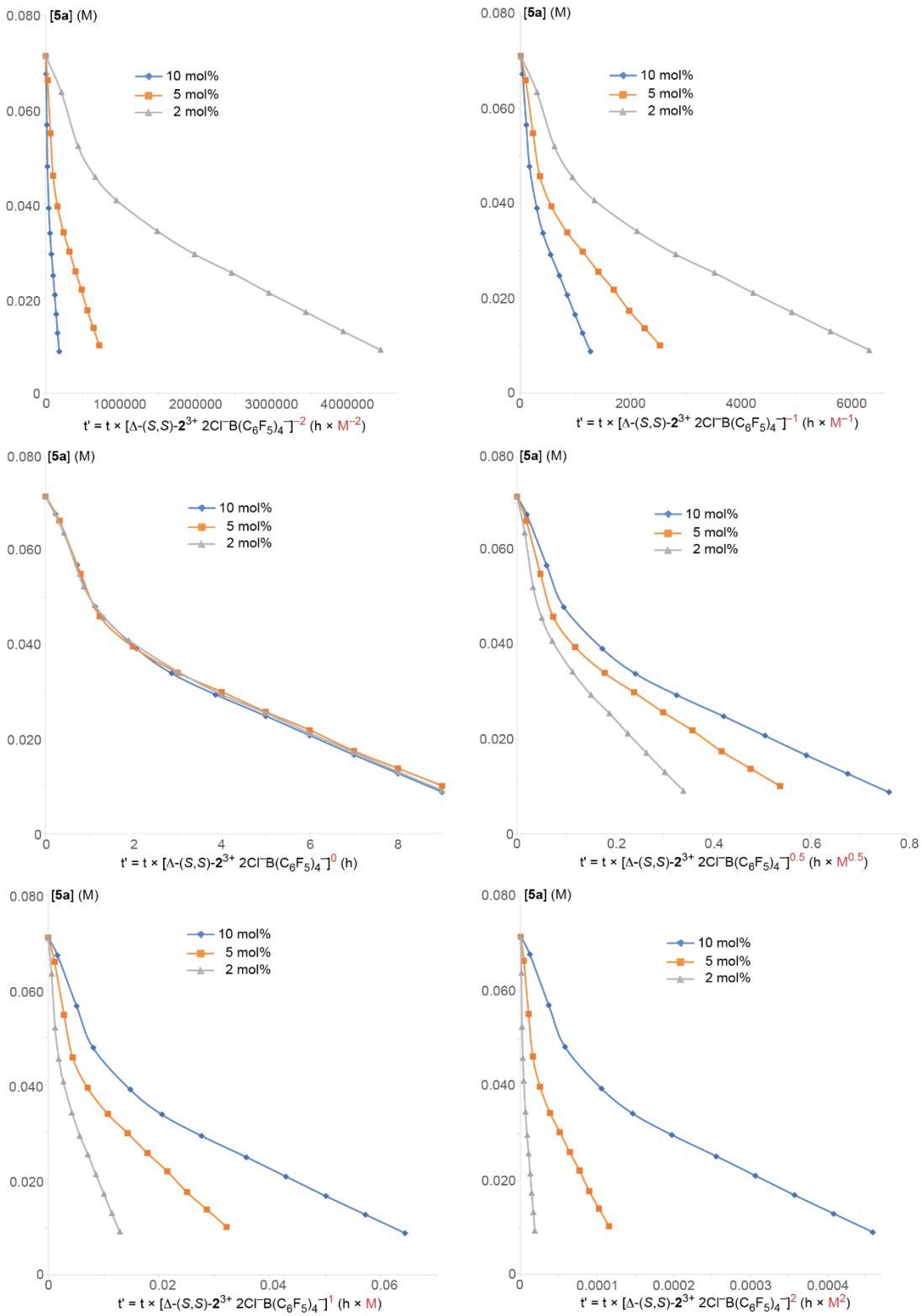


**Figure B-19.** Application of the time normalization method (see text)[S7] to the determination of the order in catalyst of a reaction similar to entry 12 of Table 3.1.

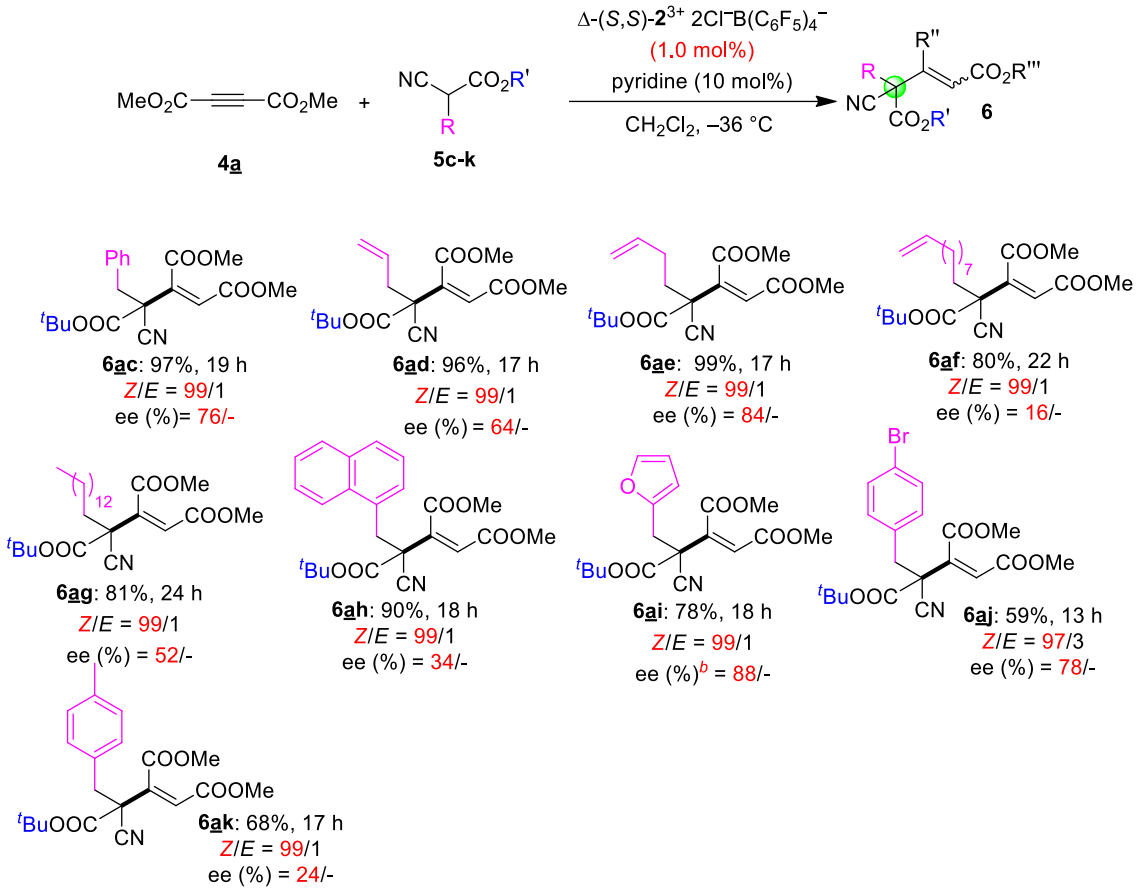


**Figure B-20.** Scope of enantioslectivities when 1.0 mol% catalyst was used.

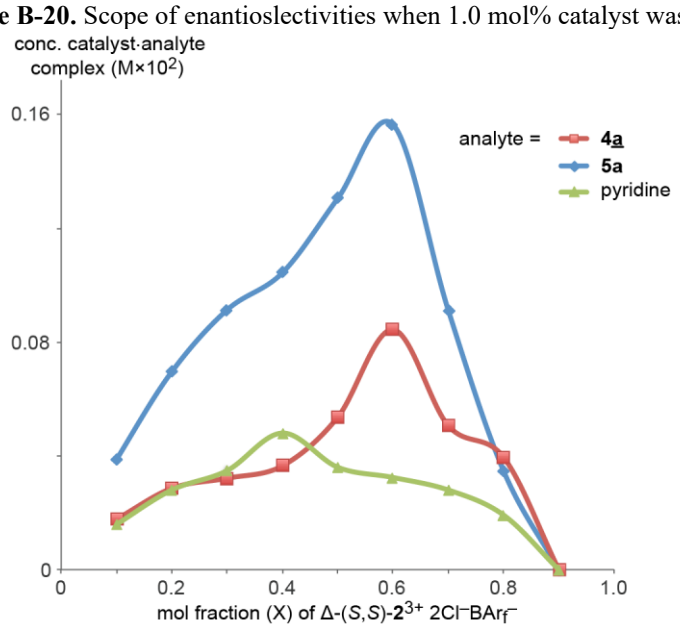


**Figure B-21.** Job plots for mixtures of Δ-(*S*,*S*)-**2**$^{3+}$ 2Cl$^-$BAr$_f^-$ and **4a**, **5a**, and pyridine in $CD_2Cl_2$ at ambient temperature.

REFERENCES

(s1) Tanimoto, H.; Shitaoka, T.; Yokoyama, K.; Morimoto, T.; Nishiyama, Y.; Kakiuchi, K. *J. Org. Chem.* **2016**, *81*, 8722-8735.

(s2) Grigg, R.; Lofberg, C.; Whitney, S.; Sridharan, V.; Keep, A.; Derrick A. *Tetrahedron* **2009**, *65*, 849-854.

(s3) Wang, X.; Kitamura, M.; Maruoka, K. *J. Am. Chem. Soc.* **2007**, *129*, 1038-1039.

(s4) Ramachary, D. B.; Kishor, M.; Reddy, Y. V. *Eur. J. Org. Chem.* **2008**, *2008*, 975-993.

(s5) Luu, Q. H.; Lewis, K. G.; Banerjee, A.; Bhuvanesh, N.; Gladysz, J. A. *Chem. Sci.* **2018**, *9*, 5087-5099.

(s6) Blackmond, D. G. *J. Am. Chem. Soc.* **2015**, *137*, 10852-10866. *J. Am. Chem. Soc.* **2016**, *138*, 460.

(s7) Burés, J. A. *Angew. Chem., Int. Ed.* **2016**, *55*, 2028-2031. *Angew. Chem.* **2016**, *128*, 2068-2071.

APPENDIX C: WERNER COMPLEXES AS HYDROGEN BOND DONOR CATALYSTS FOR THE ENANTIOSELECTIVE FORMATION OF CARBON-HETEROATOM BONDS AND HETEROCYCLES.

**General data.** NMR spectra were recorded on a Varian NMRS 500 MHz spectrometer at ambient probe temperature. Chemical shifts (δ in ppm) were referenced to residual solvent signals ($^{1}H$: $CHCl_3$, 7.26; $^{13}C$: $CDCl_3$, 77.2; or external $C_6F_6$ ($^{19}F$, –164.9). HPLC analyses were carried out with a Shimadzu instrument package (pump/autosampler/detector LC-20AD/SIL-20A/SPD-M20A). NMR solvent $CDCl_3$ (Cambridge Isotopes) stored over molecular sieves. HPLC grade solvents (hexanes, Fischer; isopropanol, JT Baker) were degassed. The $CH_2Cl_2$ (BDH Chemicals, ACS grade) was dried and degassed using a Glass Contour solvent purification system.

The following materials were used as received unless noted: silica gel (Silicycle SiliaFlash® F60), TLC plates (silica gel, EMD Millipore), ethyl acetate (Sigma-Aldrich, ≥99.5%), hexanes (Sigma-Aldrich, ≥98.5%), $CH_3CN$ (anhydrous, BDH Chemicals, 99.5%), acetone (Sigma-Aldrich, 99.5%), toluene (Omnisolv, 99.9%), $CH_2Cl_2$ (Sigma-Aldrich, >99.5%) $K_2CO_3$ (anhydrous, Alfa Aesar, 99%), 2-oxocyclopentanecarboxylate (**6**, TCI, >97%), *N*-fluorobenzenesulfonimide (NFSI, Arkpharm, 98%). $Na_2CO_3$ (anhydrous, Mallinckrodt, 99%), $NaHCO_3$ (anhydrous, Mallinckrodt, 99%), triethyl amine (Macron Fine Chemicals, 99.5%), pyridine (EMD Millipore, 99.0%), DABCO (Alfa Aesar, 98%), sodium sulfate (anhydrous, EMD Millipore, 99.0%).

The following were synthesized by literature procedures: ethyl 3-((tosyloxy)imino)butanoate (**8**),[s1] dimethyl 2-(2-(pyrrolidin-1-yl)benzylidene) malonate (**10a**),[s2] dimethyl 2-(2-(dibenzylamino)benzylidene) malonate (**10b**),[s3] dimethyl 2-(2-(diethylamino)benzylidene) malonate (**10c**),[s3] dimethyl 2-(2-(methyl(naphthalen-2-ylmethyl)amino)benzylidene) malonate (**10d**).[s2]

**Methyl 1-fluoro-2-oxocyclopentanecarboxylate (7).** This known compound[s4] was isolated as a yellow liquid (0.0079 g, 0.050 mmol, >99%, 79% ee). The ee value was determined by $^{19}$F NMR using the chiral solvating agent Λ-(*S*,*S*)-**2**$^{3+}$ 2I$^{-}$BAr$_f^{-}$ (Figure C-1). The dominant configuration was assigned by HPLC with a Chiralcel AD-H column, 98:2 hexane/isopropanol, 1.0 mL/min, 254 nm, $t_R$ = 31.4 min (minor), $t_S$ = 33.5 min (major). The order of elution was established in an earlier study with an identical column.[s4]

Data for **7**: NMR ($CDCl_3$, δ in ppm): $^1$H (500 MHz) 3.80 (s, 3H, $CO_2C\mathbf{H}_3$), cyclopentane ring -$(CH_2)_3$- at 2.62-2.40 (m, 3H), 2.23-2.36 (m, 1H), and 2.20-2.05 (m, 2H); $^{19}$F (470 MHz) –163.60 (t, $^3J_{FH}$ = 21.0 Hz).

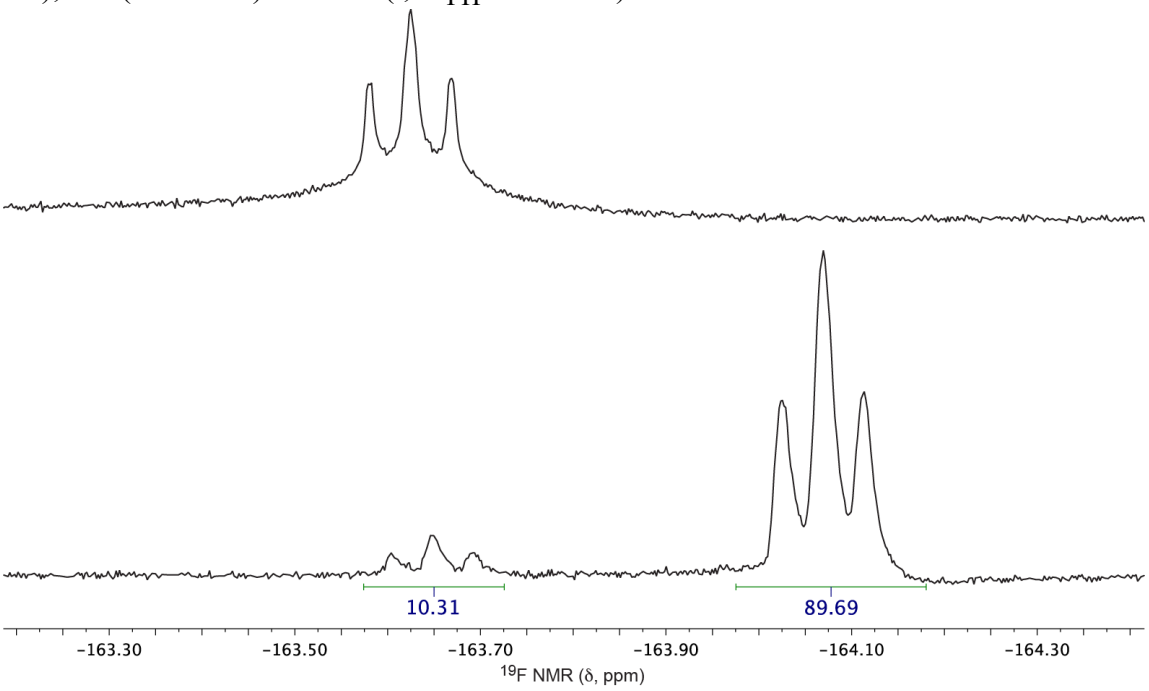


**Figure C-1.** Spectra of **7** in $CDCl_3$: (top) $^{19}$F NMR, and (bottom) $^{19}$F NMR with 10 mol% Λ-(*S*,*S*)-**2**$^{3+}$ 2I$^{-}$ BAr$_f^{-}$.

**Ethyl 3-methyl-2*H*-azirine-2-carboxylate (9).** This known compound[s1] was isolated as a colorless oil (0.0032 g, 0.025 mmol, >99%, 97% ee). The ee value and the dominant configuration were determined by HPLC with a Chiralcel OD-H column, 98:2

hexane/isopropanol, 1.0 mL/min, 210 nm, $t_S$ = 7.66 min (major), $t_R$ = 11.96 min (minor). The order of elution was established in an earlier study with an identical column.[s1]

$^1$H NMR (500 MHz, $CDCl_3$, δ in ppm) 4.43 (q, $^3J_{HH}$ = 7.1 Hz, 2H, $CO_2C\mathbf{H}_2CH_3$), 3.42 (s, 1H, C**H**$CO_2$Et), 2.74 (s, 3H, C$\mathbf{H}_3$C=N), 1.38 (t, $^3J_{HH}$ = 7.1 Hz, 3H, $CO_2CH_2C\mathbf{H}_3$).

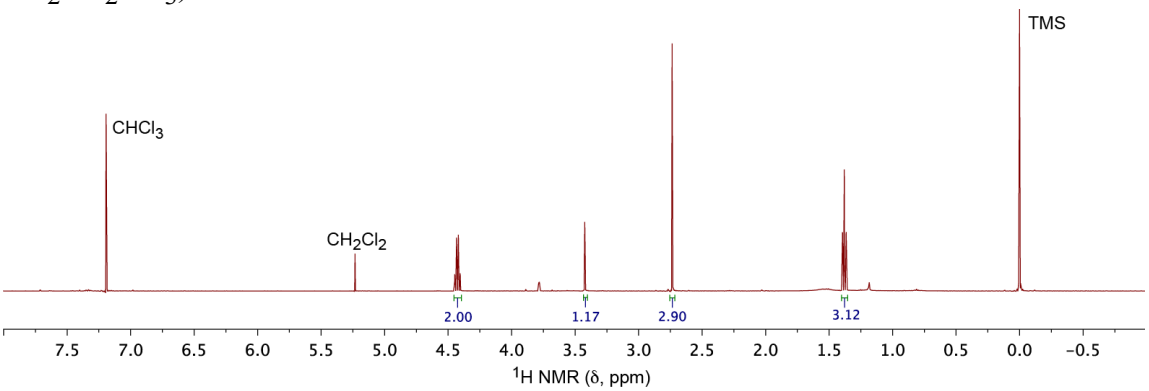


**Figure C-2.** $^1$H NMR Spectrum of **9** in $CDCl_3$.

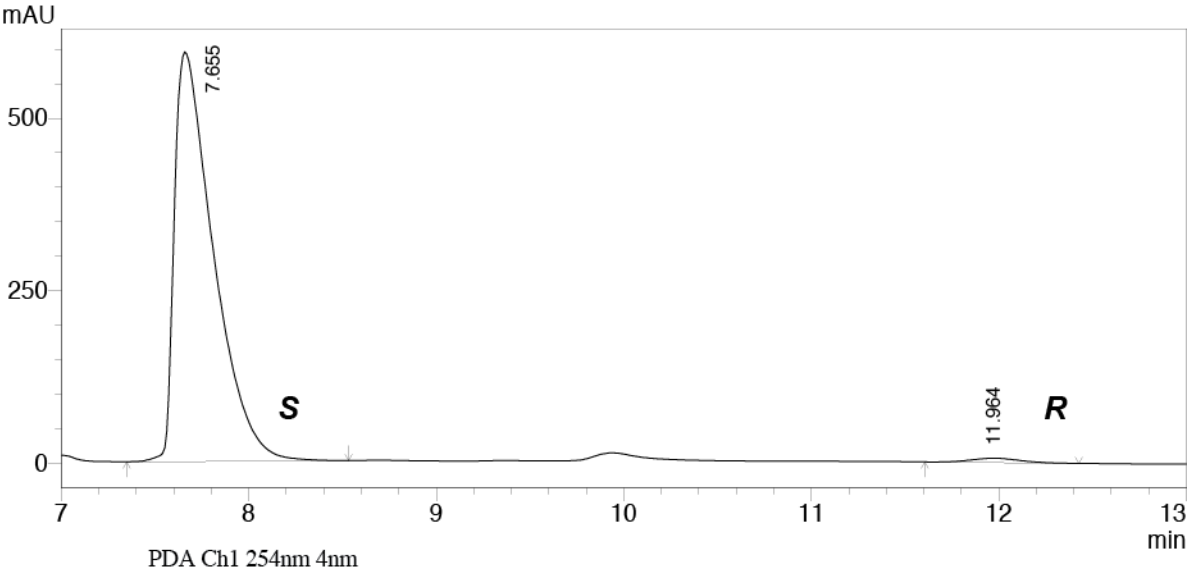


PDA Ch1 254nm 4nm

| Peak# | Ret. Time | Area | Height | Area % | Height % |
|---|---|---|---|---|---|
| 1 | 7.655 | 8605614 | 593743 | 98.663 | 98.933 |
| 2 | 11.964 | 116645 | 6403 | 1.337 | 1.067 |
| Total | | 8722259 | 600147 | 100.000 | 100.000 |

**Figure C-3.** HPLC trace of **9** (97% ee) corresponding to data in entry 10 of Table 4.2.

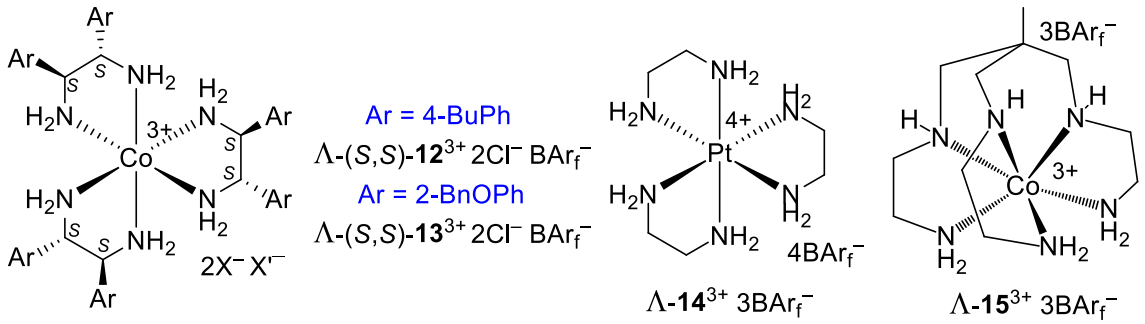


**Figure C-4.** Catalysts used in Table C-1 that were not included in Table 4.3.

**Table C-1.** Expansion of Table 4.3 in Chapter 4.[a]

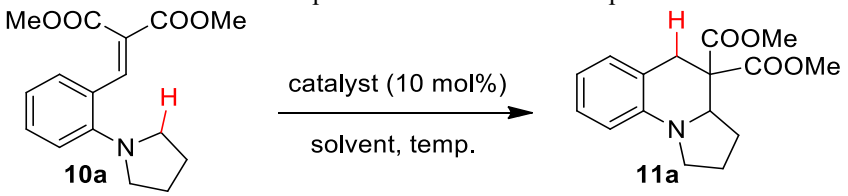


| Entry | Catalyst | Solvent | Temp (°C) | Time (h) | Yield (%)[b] | Ee (%)[c] |
|---|---|---|---|---|---|---|
| 1 | – | $CH_2Cl_2$ | rt | 168 | 0 | – |
| 2 | Λ-**1**$^{3+}$ 3BAr$_f^-$ | $CH_2Cl_2$ | rt | 17 | >99 | 1 (*S*) |
| 3 | Λ-(*S*,*S*)-**2**$^{3+}$ 2Cl$^-$BAr$_f^-$ | $CH_2Cl_2$ | rt | 168 | 17 | – |
| 4 | Λ-(*S*,*S*)-**2**$^{3+}$ 2Cl$^-$BAr$_f^-$ | $CH_2Cl_2$ | 50 | 48 | 30 | 24 (*S*) |
| 5 | Λ-(*S*,*S*)-**2**$^{3+}$ 2BF$_4^-$BAr$_f^-$ | $CH_2Cl_2$ | rt | 168 | 39 | 27 (*S*) |
| 6 | Λ-(*S*,*S*)-**2**$^{3+}$ 2BF$_4^-$BAr$_f^-$ | $CDCl_3$ | 50 | 120 | 99 | 27 (*S*) |
| 7 | Λ-(*S*,*S*)-**2**$^{3+}$ 2I$^-$BAr$_f^-$ | $CH_2Cl_2$ | 50 | 48 | >99 | 25 (*S*) |
| 8 | Λ-(*S*,*S*)-**2**$^{3+}$ 3BAr$_f^-$ | $CH_2Cl_2$ | rt | 1.5 | >99 | 10 (*S*) |
| 9 | Λ-(*S*,*S*)-**2**$^{3+}$ 3BAr$_f^-$ | $CH_2Cl_2$ | 0 | 24 | >99 | 8 (*S*) |
| 10 | Λ-(*S*,*S*)-**2**$^{3+}$ 3BAr$_f^-$ | $CH_2Cl_2$ | –36 | 168 | 0 | – |

[a]A vial was charged with a stir bar, **10a** (0.014 g, 0.050 mmol), a catalyst (10 mol%), and a solvent. The vial was sealed and the sample was brought to the indicated temperature. The reaction was stirred and monitored by TLC and was worked up as described in the experimental section. [b]Isolated yields. [c]Determined by HPLC (see experimental section for details).

**Table C-1.** Continued.[a]

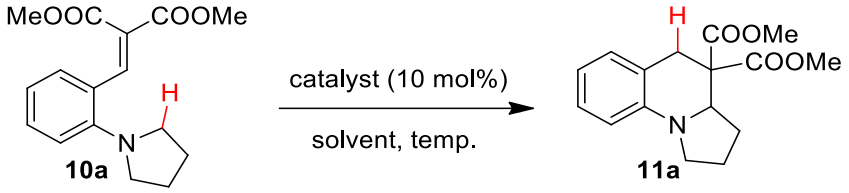


| Entry | Catalyst | Solvent | Temp (°C) | Time (h) | Yield (%)[b] | Ee (%)[c] |
|---|---|---|---|---|---|---|
| 11 | Λ-(*S*,*S*)-**2**$^{3+}$ 3BAr$_f^-$ | $CDCl_3$ | rt | 4 | >99 | 50 (*R*) |
| 12 | Λ-(*S*,*S*)-**2**$^{3+}$ 3BAr$_f^-$ | toluene | rt | 2 | >99 | 4 (*S*) |
| 13 | Λ-(*S*,*S*)-**2**$^{3+}$ 3BAr$_f^-$ | dioxane | rt | 4 | >99 | 6 (*R*) |
| 14 | Λ-(*S*,*S*)-**2**$^{3+}$ 3BAr$_f^-$ | THF | rt | 72 | 0 | – |
| 15 | Λ-(*S*,*S*)-**2**$^{3+}$ 3BAr$_f^-$ | $CH_3CN$ | rt | 72 | 10 | – |
| 16 | Λ-(*S*,*S*)-**2**$^{3+}$ 3BAr$_f^-$ | acetone | rt | 72 | 10 | – |
| 17 | Λ-(*S*,*S*)-**3a**$^{3+}$ 3BAr$_f^-$ | $CHCl_3$ | rt | 18 | 50 | 7 (*S*) |
| 18 | Δ-(*S*,*S*)-**12**$^{3+}$ 3BAr$_f^-$ | $CHCl_3$ | rt | 18 | 50 | 6 (*S*) |
| 19 | Λ-(*S*,*S*)-**3b**$^{3+}$ 3BAr$_f^-$ | $CH_2Cl_2$ | rt | 1.5 | >99 | 0 |
| 20 | Λ-(*S*,*S*)-**3b**$^{3+}$ 3BAr$_f^-$ | $CHCl_3$ | rt | 4 | 90 | 24 (*S*) |
| 21 | Λ-(*S*,*S*)-**3b**$^{3+}$ 2Cl$^-$BAr$_f^-$ | $CH_2Cl_2$ | 50 | 24 | >99 | 35 (*S*) |
| 22 | Λ-(*S*,*S*)-**4**$^{3+}$ 2Cl$^-$BAr$_f^-$ | $CH_2Cl_2$ | 50 | 24 | 50 | 29 (*S*) |
| 23 | Λ-(*S*,*S*)-**13**$^{3+}$ 2Cl$^-$BAr$_f^-$ | $CH_2Cl_2$ | 50 | 24 | >99 | 10 (*S*) |
| 24 | Λ-(*S*,*S*)-**13**$^{3+}$ 2Cl$^-$BAr$_f^-$ | $CH_2Cl_2$ | rt | 3 | >99 | 6 (*S*) |

[a]A vial was charged with a stir bar, **10a** (0.014 g, 0.050 mmol), a catalyst (10 mol%), and a solvent. The vial was sealed and the sample was brought to the indicated temperature. The reaction was stirred and monitored by TLC and was worked up as described in the experimental section. [b]Isolated yields. [c]Determined by HPLC (see experimental section for details).

**Table C-1.** Continued.[a]

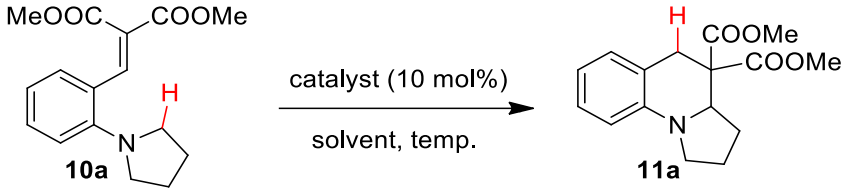


| Entry | Catalyst | Solvent | Temp (°C) | Time (h) | Yield (%)[b] | Ee (%)[c] |
|---|---|---|---|---|---|---|
| 25 | Λ-(*S*,*S*)-**14**$^{3+}$ 3BAr$_f^-$ | $CH_2Cl_2$ | rt | 2 | >99 | 0 |
| 26 | Λ-(*S*,*S*)-**14**$^{3+}$ 3BAr$_f^-$ | $CH_2Cl_2$ | rt | 120 | >99 | 0 |
| 27 | Λ-(*S*,*S*)-**2**$^{3+}$ 3I$^-$ | $CH_2Cl_2$ | 50 | 48 | 0 | – |
| 28 | Λ-(*S*,*S*)-**15**$^{3+}$ 3BAr$_f^-$ | $CH_2Cl_2$ | rt | 24 | >99 | 2 (*S*) |
| 29 | Λ-(*S*,*S*)-**15**$^{3+}$ 3BAr$_f^-$ | $CHCl_3$ | rt | 24 | >99 | 6 (*S*) |
| 30 | Λ-(*S*,*S*)-**3b**$^{3+}$ 2Cl$^-$BAr$_f^-$ | $CHCl_3$ | 50 | 24 | 50 | 43 (*S*) |
| 31 | Λ-(*S*,*S*)-**3b**$^{3+}$ 2Cl$^-$BAr$_f^-$ | toluene | 50 | 24 | >99 | 32 (*S*) |
| 32 | Λ-(*S*,*S*)-**3b**$^{3+}$ 2BF$_4^-$BAr$_f^-$ | $CHCl_3$ | 50 | 24 | 50 | 38 (*S*) |
| 33 | Λ-(*S*,*S*)-**3b**$^{3+}$ 2BF$_4^-$BAr$_f^-$ | $CH_2Cl_2$ | 50 | 24 | 60 | 31 (*S*) |
| 34 | Λ-(*S*,*S*)-**3a**$^{3+}$ 2BF$_4^-$BAr$_f^-$ | $CHCl_3$ | 50 | 96 | 50 | 11 (*S*) |

[a]A vial was charged with a stir bar, **10a** (0.014 g, 0.050 mmol), a catalyst (10 mol%), and a solvent. The vial was sealed and the sample was brought to the indicated temperature. The reaction was stirred and monitored by TLC and was worked up as described in the experimental section. [b]Isolated yields. [c]Determined by HPLC (see experimental section for details).

**Dimethyl 1,2,3,3a-tetrahydropyrrolo[1,2-a]quinoline-4,4(5H)-dicarboxylate (11a, Figure 4.5).** This known compound[s2] was isolated as a white solid (0.0070 g, 0.025 mmol, 50%, 43% ee). The ee value and the dominant configuration were determined by HPLC with a Chiralpak OJ-H column, 90:10 hexane/isopropanol, 1.0 mL/min, 254 nm, $t_R$

= 13.54 min (minor), $t_S$ = 15.05 min (major). The order of elution was established in an earlier study with an identical column.[s2]

$^1$H NMR (500 MHz, $CDCl_3$, δ in ppm) 7.08 (t, $^3J_{HH}$ = 7.8 Hz, 1H, Ar**H**), 7.01 (d, $^3J_{HH}$ = 7.2 Hz, 1H, Ar**H**), 6.62-6.57 ( m, 1H, Ar**H**), 6.46 (d, $^3J_{HH}$ = 7.8 Hz, 1H, Ar**H**), 3.79 (s, 3H, $CO_2$**Me**), 3.76 (dd, $^3J_{HH}$ = 9.0, 6.6 Hz, 1H, NC**H**$CH_2$), 3.57 (s, 3H, $CO_2$**Me**), 3.40-3.32 (m, 2H, ArC**HH'**), –(C**H**$_2$)$_3$– at: 3.32-3.27(m, 1H), 3.24 (d, $^3J_{HH}$ = 15.6 Hz, 1H), 2.46-2.37 (m, 1H), 2.18-2.03 (m, 2H), 1.98-1.88 (m, 1H).

**Dimethyl 1-benzyl-2-phenyl-1,2-dihydroquinoline-3,3(4H)-dicarboxylate (11b, Figure 4.5).** This known compound[s3] was isolated as a white solid (0.021 g, 0.050 mmol, >99%, 82% ee). The ee value and the dominant configuration were determined by HPLC with a Chiralpak AD-H column, 90:10 hexane/isopropanol, 0.5 mL/min, 254 nm, $t_S$ = 13.88 min (major), $t_R$ = 17.12 min (minor). The order of elution was established in an earlier study with an identical column.[s3]

$^1$H NMR (500 MHz, $CDCl_3$, δ in ppm) 7.32-7.10 (m, 12H, Ar**H**), 6.66 (d, $^3J_{HH}$ = 8.0 Hz, 1H, Ar**H**), 6.52 (d, $^3J_{HH}$ = 8.0 Hz, 1H, Ar**H**), 5.31 (s, 1H, NC**H**Ph), 4.48 (d, $^2J_{HH}$ = 17.2 Hz, 1H, NC**H**H'Ph), 4.32 (d, $^2J_{HH}$ = 17.2 Hz, 1H, NCH**H'**Ph), 3.65 (s, 3H, $CO_2$**Me**), 3.57 (s, 3H, $CO_2$**Me**), 3.40 (d, $^2J_{HH}$ = 16.0 Hz, 1H, ArCH**H'**), 3.32 (d, $^2J_{HH}$ = 16.0 Hz, 1H, ArC**H**H').

**Dimethyl 1-ethyl-2-methyl-1,2-dihydroquinoline-3,3(4H)-dicarboxylate (11c, Figure 4.5).** This known compound[s3] was isolated as a colorless oil (0.013 g, 0.045 mmol, 90%, 0% ee). The ee value was determined by HPLC with a Chiralpak AD-H column, 90:10 hexane/isopropanol, 0.5 mL/min, 254 nm, $t_S$ = 9.61 min, $t_R$ = 11.00 min.[s3]

$^1$H NMR (500 MHz, $CDCl_3$, δ in ppm) 7.10-7.02 (m, 2H, Ar**H**), 6.60 (d, $^3J_{HH}$ = 7.6 Hz, 1H, Ar**H**), 6.54 (d, $^3J_{HH}$ = 7.6 Hz, 1H, Ar**H**), 4.18 (q, $^3J_{HH}$ = 6.8 Hz, 1H, NC**H**$CH_3$), 3.77 (s, 3H, $CO_2$**Me**), 3.61 (s, 3H, $CO_2$**Me**), 3.50-3.35 (m, 2H, NC**H**$_2$$CH_3$),

3.32-3.20 (d, $^2J_{HH}$ = 17.2 Hz, 1H, ArC**H**H'), 3.20 (d, $^2J_{HH}$ = 17.2 Hz, 1H, ArCH**H**'), 1.20 (d, $^3J_{HH}$ = 6.8 Hz, 3H, NCHC$\mathbf{H}_3$), 1.05 (t, $^3J_{HH}$ = 6.8 Hz, 3H, $NCH_2C\mathbf{H}_3$).

**Dimethyl 1-methyl-2-(naphthalen-2-yl)-1,2-dihydroquinoline-3,3(4H)-dicarboxylate (11d, Figure 4.5).** This known compound[s2] was isolated as a colorless oil (0.020 g, 0.050 mmol, >99%, 27% ee). The ee value and the dominant configuration were determined by HPLC with a Chiralpak IC column, 90:10 hexane/isopropanol, 1.0 mL/min, 254 nm, $t_R$ = 7.00 min (minor), $t_S$ = 11.20 min (major). The order of elution was established in an earlier study with an identical column.[s2]

$^1$H NMR (500 MHz, $CDCl_3$, δ in ppm) 7.81-7.77 (m, 1H, Ar**H**), 7.75-7.12 (m, 2H, Ar**H**), 7.61 (s, 1H, Ar**H**), 7.45-7.44 (m, 2H, Ar**H**), 7.26-7.22 (m, 1H, Ar**H**), 7.19 (t, $^3J_{HH}$ = 7.5 Hz, 1H, Ar**H**), 7.07 (d, $^3J_{HH}$ = 7.2 Hz, 1H, Ar**H**), 6.67 (t, $^3J_{HH}$ = 7.5 Hz, 1H, Ar**H**), 6.65 (d, $^3J_{HH}$ = 8.4 Hz, 1H, Ar**H**), 5.29 (s, 1H, NC**H**$C_{10}H_7$), 3.62 (s, 3H, $CO_2$**Me**), 3.56 (s, 3H, $CO_2$**Me**), 3.37-3.23 (m, 2H, ArC**HH**'), 2.93 (s, 3H, NC$\mathbf{H}_3$).

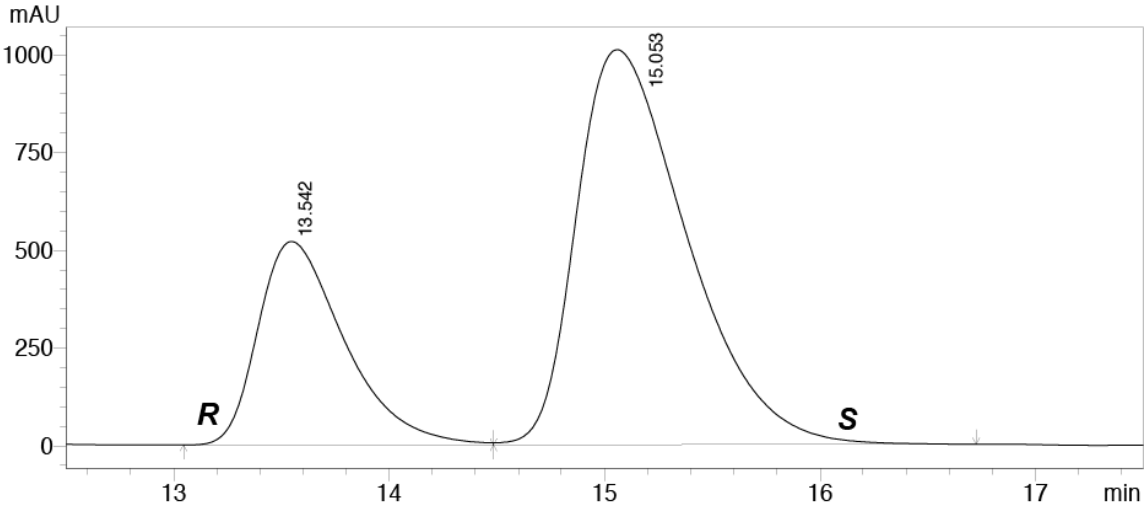


PDA Ch1 254nm 4nm

| Peak# | Ret. Time | Area | Height | Area % | Height % |
|---|---|---|---|---|---|
| 1 | 13.542 | 14497213 | 519965 | 28.674 | 33.989 |
| 2 | 15.053 | 36061085 | 1009860 | 71.326 | 66.011 |
| Total | | 50558297 | 1529825 | 100.000 | 100.000 |

**Figure C-4.** HPLC trace of **11a** (43% ee) corresponding to data in Figure 4.5.

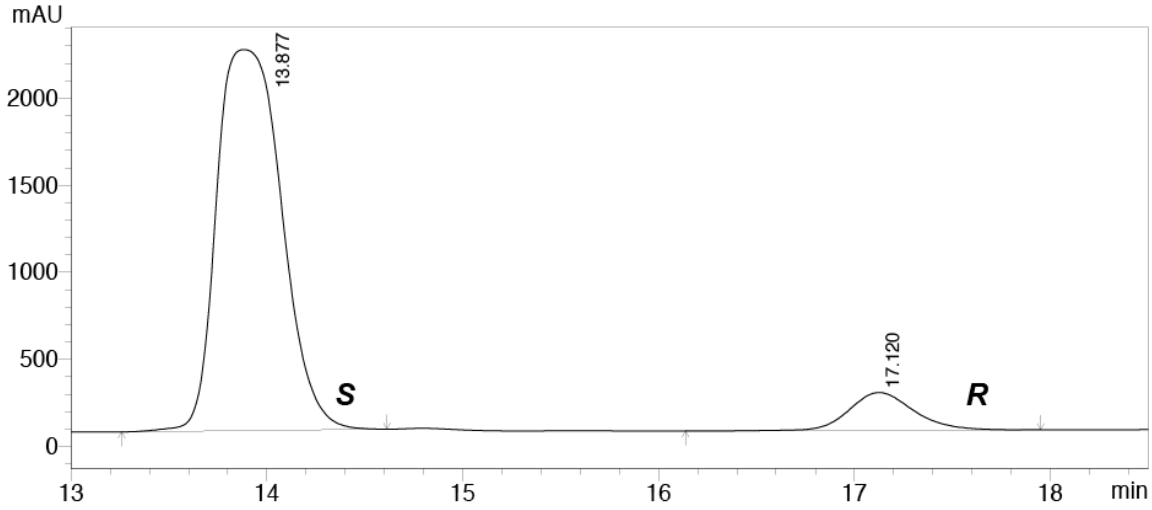


PDA Ch1 254nm 4nm

| Peak# | Ret. Time | Area | Height | Area % | Height % |
|---|---|---|---|---|---|
| 1 | 13.877 | 50454461 | 2186785 | 90.947 | 90.950 |
| 2 | 17.120 | 5022147 | 217590 | 9.053 | 9.050 |
| Total | | 55476609 | 2404374 | 100.000 | 100.000 |

**Figure C-5.** HPLC trace of **11b** (82% ee) corresponding to data in Figure 4.5.

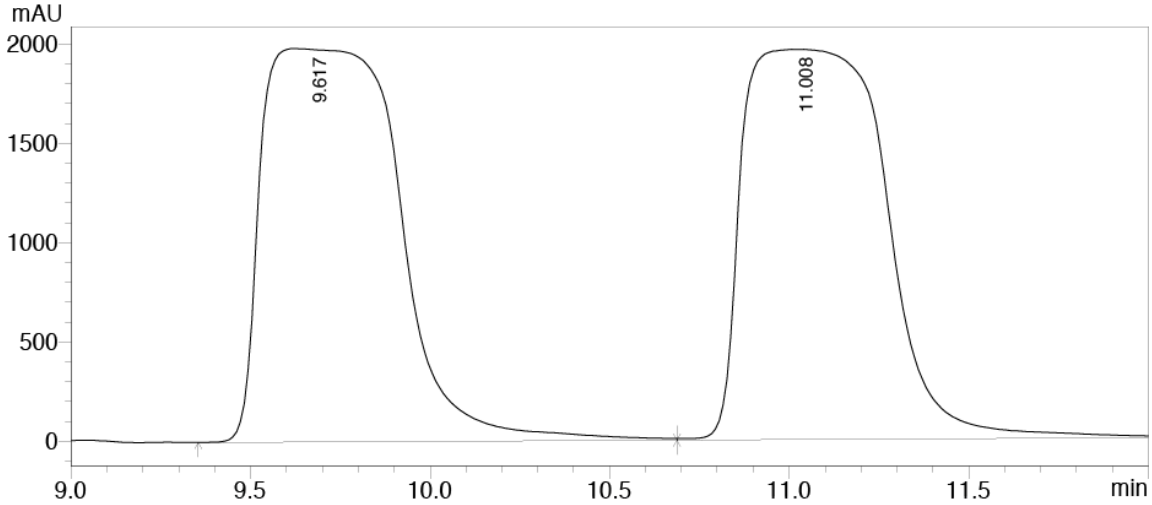


PDA Ch1 254nm 4nm

| Peak# | Ret. Time | Area | Height | Area % | Height % |
|---|---|---|---|---|---|
| 1 | 9.617 | 52149178 | 1980114 | 49.336 | 50.209 |
| 2 | 11.008 | 53552666 | 1963611 | 50.664 | 49.791 |
| Total | | 105701844 | 3943725 | 100.000 | 100.000 |

**Figure C-6.** HPLC trace of **11c** (0% ee) corresponding to data in Figure 4.5.

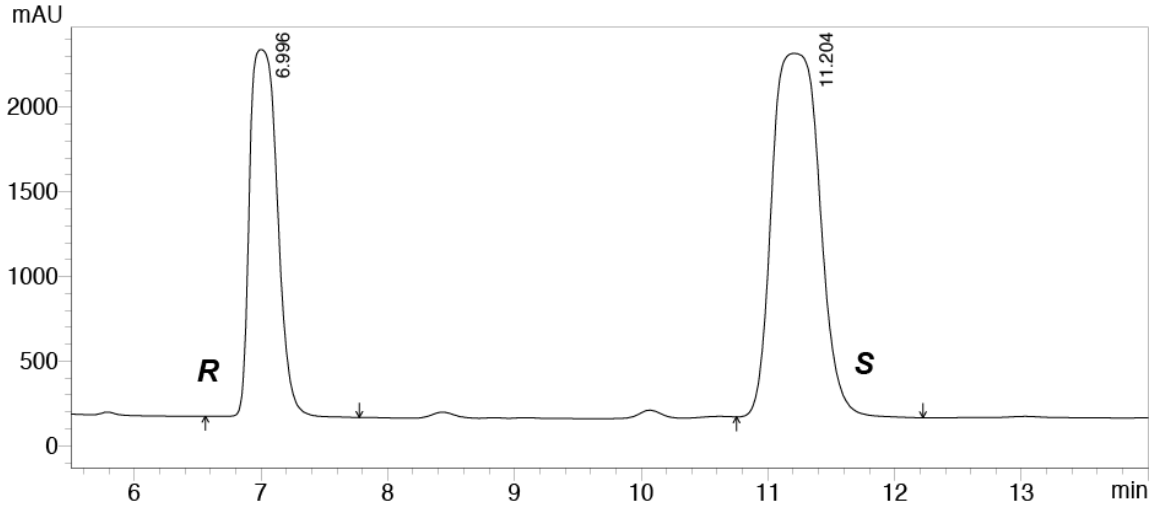


PDA Ch1 254nm 4nm

| Peak# | Ret. Time | Area | Height | Area % | Height % |
|---|---|---|---|---|---|
| 1 | 6.996 | 32790030 | 2167861 | 36.994 | 50.219 |
| 2 | 11.204 | 55845235 | 2148996 | 63.006 | 49.781 |
| Total | | 88635266 | 4316857 | 100.000 | 100.000 |

**Figure C-7.** HPLC trace of **11d** (27% ee) corresponding to data in Figure 4.5.

REFERENCES

(s1) An, D.; Guan, X.; Guan, R.; Jin, L.; Zhang, G.; Zhang, S. *Chem. Commun.* **2016**, *52*, 11211-11214.

(s2) Cao, W.; Liu, X.; Wang, W.; Lin, L.; Feng, X. *Org. Lett.* **2011**, *13*, 600-603.

(s3) Mori, K.; Ehara, K.; Kurihara, K.; Akiyama, T. *J. Am. Chem. Soc.* **2011**, *133*, 6166-6169.

(s4) Xu, J.; Hu, Y.; Huang, D.; Wang, K.-H.; Xu, C.; Niu, T. *Adv. Synth. Catal.* **2012**, *354*, 515-526..

APPENDIX D: WERNER COMPLEXES WITH NON-INNOCENT ANIONS IN ENANTIOSELECTIVE CATALYSIS.

**General data.** NMR spectra were recorded on a Varian NMRS 500 MHz spectrometer at ambient probe temperature. Chemical shifts (δ in ppm) were referenced to residual solvent signals ($^{1}H$: $CHCl_3$, 7.26; $CHD_2OD$, 3.30; $CDHCl_2$, 5.32; $^{13}C$: $CDCl_3$, 77.2; $CD_3OD$, 49.0; $CD_2Cl_2$, 54.0) or external $C_6F_6$ ($^{19}F$, –164.9). IR spectra were recorded on a Shimadzu IRAffinity-1 spectrometer (Pike MIRacle ATR system, diamond/ZnSe crystal). Melting points were determined using an OptiMelt MPA 100 instrument. Microanalyses were conducted by Atlantic Microlab. HPLC analyses were carried out with a Shimadzu instrument package (pump/autosampler/detector LC-20AD/SIL-20A/SPD-M20A).

NMR solvents (Cambridge Isotopes) were treated as follows: $CDCl_3$, $CD_2Cl_2$, and $CD_3OD$, stored over molecular sieves. HPLC grade solvents (hexanes, Fischer; isopropanol, JT Baker) were degassed. The following materials were used as received: $CH_2Cl_2$ (Sigma-Aldrich, >99.5%), $CH_3OH$ (Sigma-Aldrich, >99.8%), $CHCl_3$ (Macron Fine Chemicals, ACS grade), THF (Sigma-Aldrich, >99.9%), DMSO (BDH, ACS grade), DMF (Mallinckrodt Chemicals, ACS grade), hexanes (Sigma-Aldrich, >98.5%), ethyl acetate (Sigma-Aldrich, >99.5%), $Na^+$ $BAr_f^-$ ($BAr_f^-$ = $B(3,5\text{-}C_6H_3(CF_3)_2)_4^-$; Ark Pharm, 97%), AgF (anhydrous, Aldrich, 99%), silica gel (Silicycle SilicaFlash® F60), Celite 545 (Aldrich), $Na_2SO_4$ (EMD, anhydrous, >99%), $Ph_2SiMe_2$ (TCI Chemicals, 97.0%), trifluoromethyl trimethylsilane ($TMSCF_3$, Oakwood Chemical, 98%), concentrated HCl (BDH, ACS grade), benzaldehyde (**3a**, Alfa Aesar, >99%), 1-naphthaldehyde (**3b**, TCI, >95%), 2-chlorobenzaldehyde (**3c**, Aldrich, 99%), *p*-tolualdehyde (**3d**, Alfa Aesar, 98%), 4-(trifluoromethyl)benzaldehyde (**3e**, TCI, >95%), 2-thiophenecarboxaldehyde (**3f**, Alfa Aesar, >98%).

**Trimethylsilyl-1-phenyl-2,2,2-trifluoroethanol (4a, Figure 5.4).** This known compound[s1] was isolated as a colorless liquid (0.087 g, 0.35 mmol, 70%, 99% ee). NMR ($CDCl_3$, δ in ppm): $^1$H (500 MHz) 7.70-7.40 (m, 5H, Ph), 4.98 (q, $^3J_{FH}$ = 6.6 Hz, 1H, PhC**H**$CF_3$), 0.18 (s, 9H, Si(C**H**$_3$)$_3$); $^{19}$F (470 Hz) –78.3 (d, $^3J_{FH}$ = 6.6 Hz, 3F, C**F**$_3$). The ee value and the dominant configuration were determined by HPLC after conversion to the corresponding alcohol as described in the main text: Chiralcel OD-H column, 98:2 hexane:isopropanol, 1.0 mL/min, 254 nm, $t_R$ = 23.08 min (major), $t_S$ = 30.05 min (minor). The order of elution was established in an earlier study with an identical column.[s2]

**Trimethylsilyl-1-(1-naphthyl)-2,2,2-trifluoroethanol (4b, Figure 5.4).** This known compound[s3] was isolated as a yellow liquid (0.048 g, 0.16 mmol, 32%, 84% ee). NMR ($CDCl_3$, δ in ppm): $^1$H (500 MHz) 8.15 (d, $^3J_{HH}$ = 8.5 Hz, 1H, Ar**H**), 7.95-7.90 (m, 2H, Ar**H),** 7.88 (d, $^3J_{HH}$ = 7.2 Hz, 1H, Ar**H**), 7.62-7.52 (m, 3H, Ar**H),** 5.81 (q, $^3J_{FH}$ = 6.3 Hz, 1H, ArC**H**$CF_3$), 0.14 (s, 9H, Si(C**H**$_3$)$_3$); $^{19}$F (470 Hz) –77.3 (d, $^3J_{FH}$ = 6.3 Hz, 3F, C**F**$_3$). The ee value and the dominant configuration were determined by HPLC after conversion to the corresponding alcohol as described in the main text: Chiralcel AS-H column, 98:2 hexane/isopropanol, 1.0 mL/min, 254 nm, $t_R$ = 18.68 min (major), $t_S$ = 21.30 min (minor). The order of elution was established in an earlier study with an identical column.[s4]

**Trimethylsilyl-1-(2-chlorophenyl)-2,2,2-trifluoroethanol (4c, Figure 5.4).** This new compound was isolated as a colorless liquid (0.061 g, 0.22 mmol, 43%, >99% ee). NMR ($CDCl_3$, δ in ppm): $^1$H (500 MHz) 7.41-7.40 (m, 1H, Ar**H),** 7.39 (d, $^3J_{HH}$ = 1.9 Hz, 1H, Ar**H**), 7.35-7.31 (m, 2H, Ar**H),** 5.57 (q, $^3J_{FH}$ = 6.2 Hz, 1H, ArC**H**$CF_3$), 0.13 (s, 9H, Si(C**H**$_3$)$_3$); $^{19}$F (470 Hz) –78.2 (d, $^3J_{FH}$ = 6.3 Hz, 3F, C**F**$_3$). The ee value was determined by HPLC after conversion to the corresponding alcohol as described in the main text: Chiralcel OD-H column, 98:2 hexane/isopropanol, 1.0 mL/min, 254 nm, t = 33.11 min.

The dominant configuration was presumed to be analogous to those of **4a**,**b**,**d-f**.

**Trimethylsilyl-1-(4-methylphenyl)-2,2,2-trifluoroethanol (4d, Figure 5.4).** This known compound[s1] was isolated as a colorless liquid (0.026 g, 0.10 mmol, 20%, 99% ee). NMR ($CDCl_3$, δ in ppm): $^1$H (500 MHz) 7.39 (d, $^3J_{HH}$ = 8.5 Hz, 2H, Ar**H**), 7.20 (d, $^3J_{HH}$ = 8.5 Hz, 2H, Ar**H**), 4.95 (q, $^3J_{FH}$ = 6.6 Hz, 1H, ArC**H**$CF_3$), 2.37 (s, 3H, C$\mathbf{H}_3$Ar), 0.15 (s, 9H, Si(C$\mathbf{H}_3$)$_3$); $^{19}$F (470 Hz) –78.5 (d, $^3J_{FH}$ = 6.6 Hz, 3F, C$\mathbf{F}_3$). The ee value and the dominant configuration were determined by HPLC after conversion to the corresponding alcohol as described in the main text: Chiralcel OD-H column, 98:2 hexane/isopropanol, 1.0 mL/min, 254 nm, $t_R$ = 17.85 min (major), $t_S$ = 25.18 min (minor). The order of elution was established in an earlier study with an identical column.[s5]

**Trimethylsilyl-1-(4-trifluoromethylphenyl)-2,2,2-trifluoroethanol (4e, Figure 5.4).** This known compound[s6] was isolated as a yellow liquid in 31% yield (0.031 g, 0.15 mmol, 31%, 99% ee). NMR ($CDCl_3$, δ in ppm): $^1$H (500 MHz) 7.66 (d, $^3J_{HH}$ = 8.1 Hz, 2H, Ar**H**), 7.60 (d, $^3J_{HH}$ = 8.1 Hz, 2H, Ar**H**), 4.98 (q, $^3J_{FH}$ = 6.4 Hz, 1H, ArC**H**$CF_3$), 0.15 (s, 9H, Si(C$\mathbf{H}_3$)$_3$); $^{19}$F (470 Hz) –62.8 (s, 3F, Ar$CF_3$), –78.3 (d, $^3J_{FH}$ = 6.5 Hz, 3F, CHC$\mathbf{F}_3$). The ee value and the dominant configuration were determined by HPLC after conversion to the corresponding alcohol as described in the main text: Chiralcel OD column, 95:5 hexane/isopropanol, 1.0 mL/min, 254 nm, $t_R$ = 6.93 min (major), $t_S$ = 7.69 min (minor). The order of elution was established in an earlier study with an identical column.[s7]

**Trimethylsilyl-1-(2-thiophenyl)-2,2,2-trifluoroethanol (4f, Figure 5.4).** This known compound[s8] was isolated as a colorless liquid (0.057 g, 0.23 mmol, 45%, 54% ee). NMR ($CDCl_3$, δ in ppm): $^1$H (500 MHz) 7.36 (d, $^3J_{HH}$ = 5.1 Hz, 1H, Ar**H**), 7.16 (d, $^3J_{HH}$ = 3.5 Hz, 1H, Ar**H**), 7.04 (dd, $^3J_{HH}$ = 3.6, 5.0 Hz, 1H, Ar**H**), 5.26 (q, $^3J_{FH}$ = 6.3 Hz, 1H, ArC**H**$CF_3$), 0.15 (s, 9H, Si(C$\mathbf{H}_3$)$_3$); $^{19}$F (470 Hz) –79.5 (d, $^3J_{FH}$ = 6.3 Hz, 3F, CHC$\mathbf{F}_3$).

The ee value and the dominant configuration were determined by HPLC after conversion to the corresponding alcohol as described in the main text: Chiralcel OD column, 95:5 hexane/isopropanol, 0.8 mL/min, 254 nm, $t_S$ = 36.4 min (major), $t_R$ = 47.2 min (minor). The order of elution was established in an earlier study with an identical column.[s9]

**5-nitro-4-phenylpentane-2-one (6, Table 5.2, entry 10)**. This known compound[s10] was isolated as a white solid (0.011 g, 0.050 mmol, >99%, 58% ee). NMR ($CDCl_3$, δ in ppm): $^1$H (500 MHz) 7.35 (m, 2H, Ph**H**), 7.32 (m, 1H, Ph**H**), 7.22 (m, 2H, Ph**H**), PhC**H**C**H**$_2$NO$_2$ at: 4.71 (m, 1H), 4.62 (m, 1H), 4.04 (m, 1H), 2.93 (d, $^3J_{HH}$ = 7.3 Hz, 2H, CH$_3$C(O)C**H**$_2$), 2.12 (s, 3H, C**H**$_3$C(O)CH$_2$). The ee value and the dominant configuration were determined by HPLC with a Chiralcel AS-H column, 60:40 hexane/isopropanol, 1.0 mL/min, 254 nm, $t_S$ = 8.84 min (minor), $t_R$ = 10.77 min (major). The order of elution was established in an earlier study with an identical column.[s10]

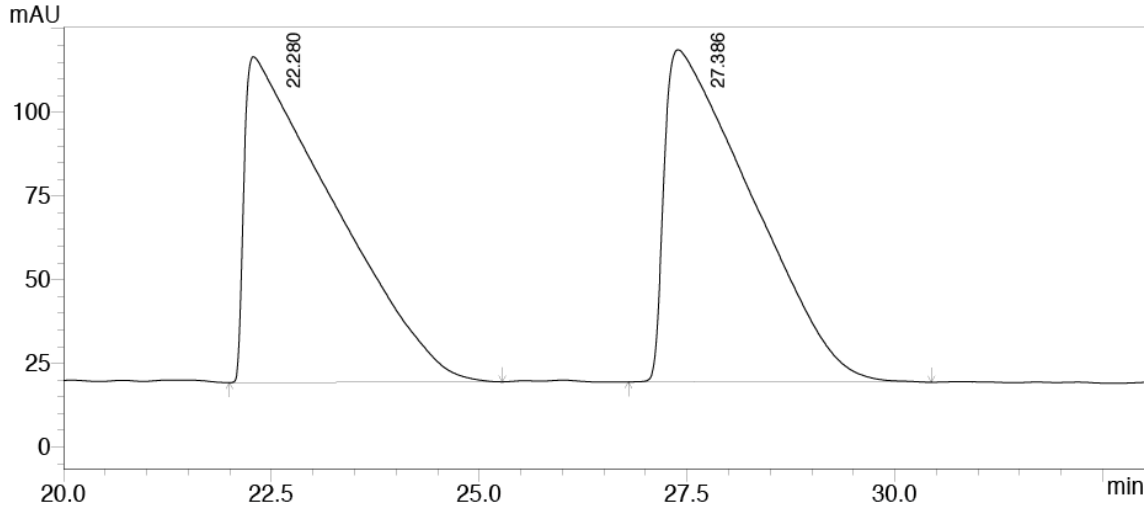


PDA Ch1 254nm 4nm

| Peak# | Ret. Time | Area | Height | Area % | Height % |
|---|---|---|---|---|---|
| 1 | 22.280 | 7300320 | 97349 | 50.174 | 49.513 |
| 2 | 27.386 | 7249551 | 99265 | 49.826 | 50.487 |
| Total | | 14549871 | 196614 | 100.000 | 100.000 |

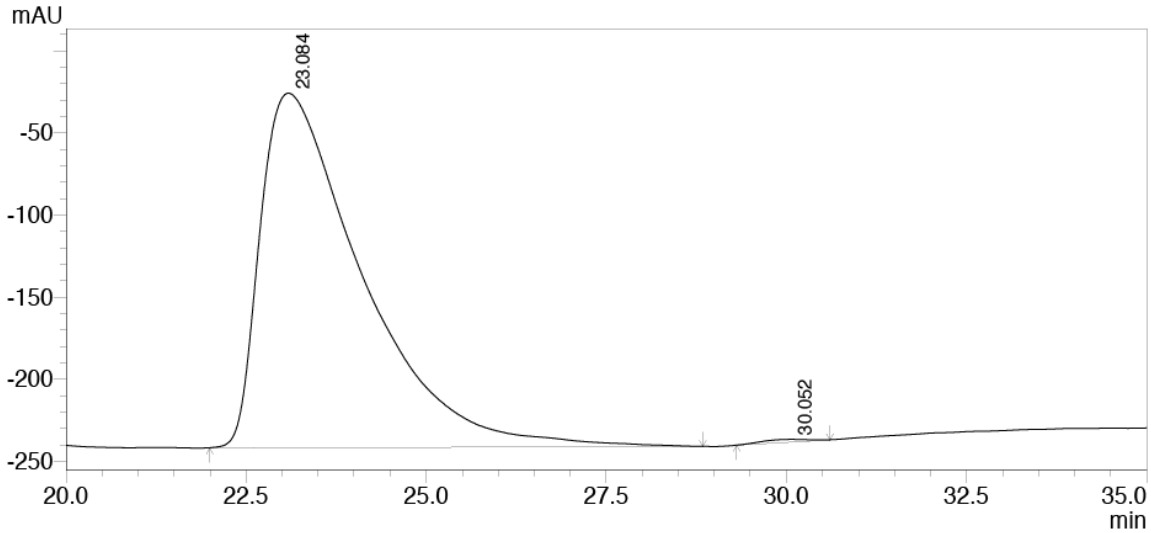


PDA Ch1 254nm 4nm

| Peak# | Ret. Time | Area | Height | Area % | Height % |
|---|---|---|---|---|---|
| 1 | 23.084 | 21327159 | 215935 | 99.643 | 99.257 |
| 2 | 30.052 | 76467 | 1616 | 0.357 | 0.743 |
| Total | | 21403626 | 217552 | 100.000 | 100.000 |

**Figure D-1.** HPLC trace of **4a**: racemic sample (top), and scalemic sample (99% ee, bottom) corresponding to data in Figure 5.4 and Table 5.1, entry 6.

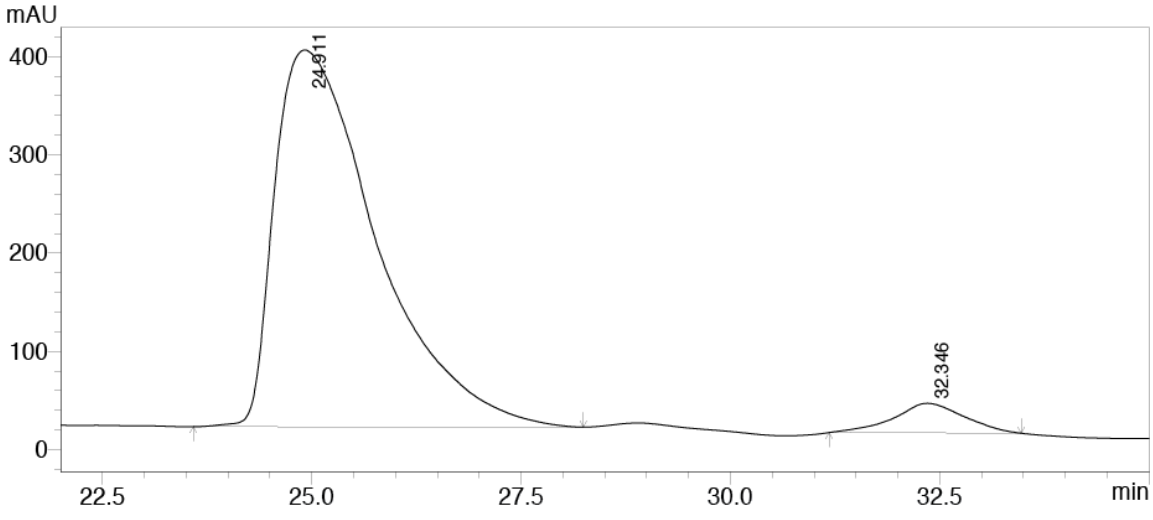


PDA Ch1 254nm 4nm

| Peak# | Ret. Time | Area | Height | Area % | Height % |
|---|---|---|---|---|---|
| 1 | 24.911 | 32423426 | 383447 | 94.845 | 92.717 |
| 2 | 32.346 | 1762423 | 30118 | 5.155 | 7.283 |
| Total | | 34185849 | 413565 | 100.000 | 100.000 |

**Figure D-2.** HPLC trace of **4a** (90% ee,) corresponding to data in Table 5.1, entry 5.

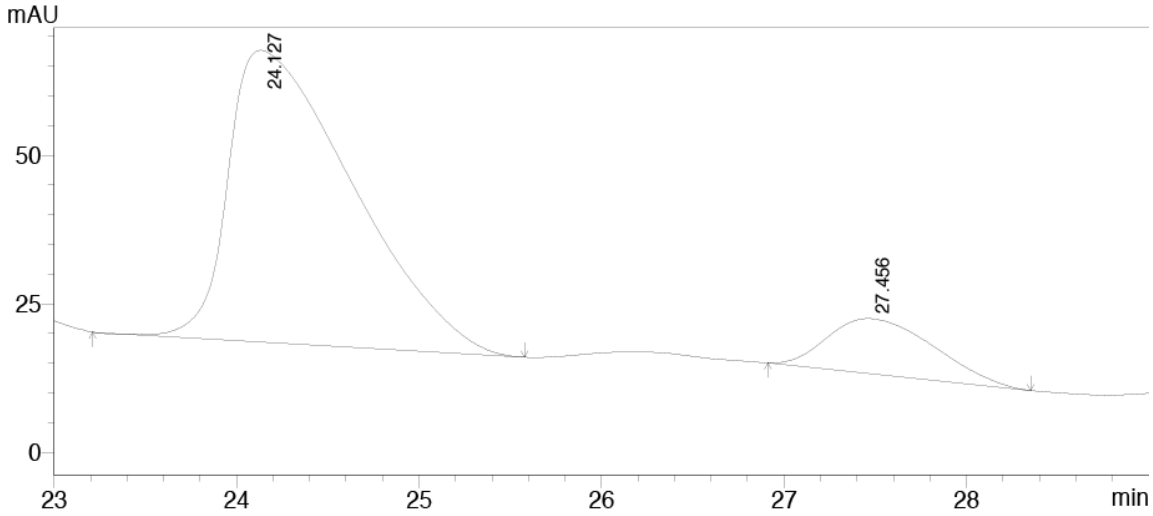


PDA Ch1 254nm 4nm

| Peak# | Ret. Time | Area | Height | Area % | Height % |
|---|---|---|---|---|---|
| 1 | 24.127 | 2329310 | 49079 | 86.040 | 84.187 |
| 2 | 27.456 | 377915 | 9219 | 13.960 | 15.813 |
| Total | | 2707226 | 58298 | 100.000 | 100.000 |

**Figure D-3.** HPLC trace of **4a** (62% ee) corresponding to data in Table 5.1, entry 7.

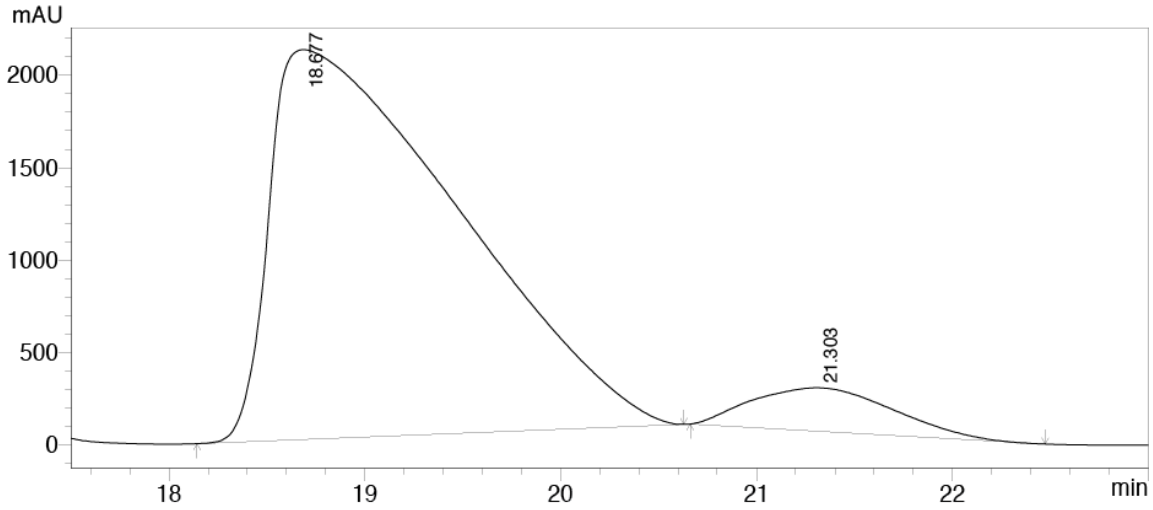


PDA Ch1 254nm 4nm

| Peak# | Ret. Time | Area | Height | Area % | Height % |
|---|---|---|---|---|---|
| 1 | 18.677 | 141087499 | 2107679 | 92.285 | 89.999 |
| 2 | 21.303 | 11795668 | 234218 | 7.715 | 10.001 |
| Total | | 152883167 | 2341897 | 100.000 | 100.000 |

**Figure D-4.** HPLC trace of **4b** (84% ee) corresponding to data in Figure 5.4.

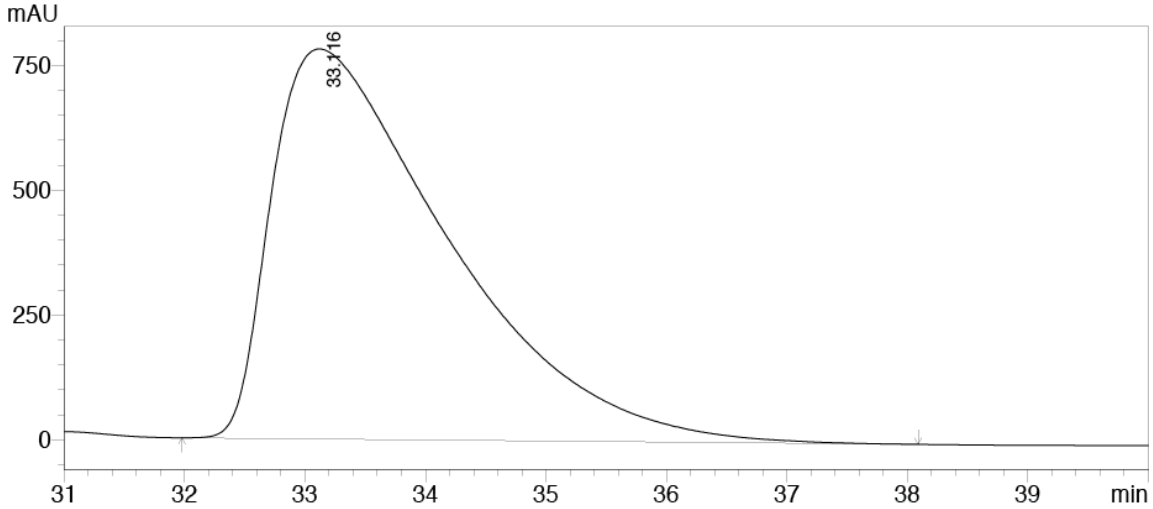


PDA Ch1 254nm 4nm

| Peak# | Ret. Time | Area | Height | Area % | Height % |
|---|---|---|---|---|---|
| 1 | 33.116 | 80086401 | 781339 | 100.000 | 100.000 |
| Total | | 80086401 | 781339 | 100.000 | 100.000 |

**Figure D-5.** HPLC trace of **4c** (>99% ee) corresponding to data in Figure 5.4.

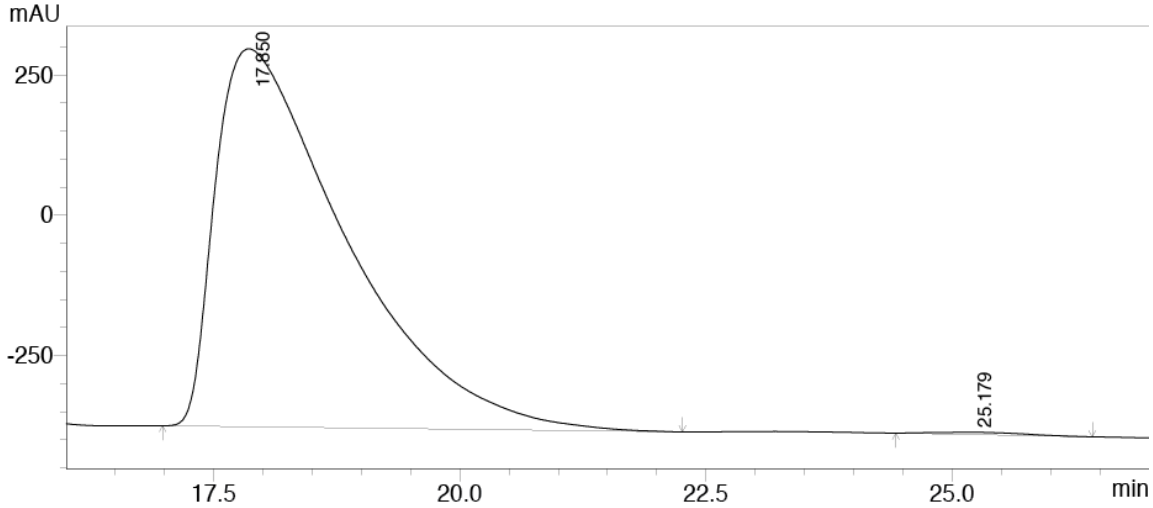


PDA Ch1 254nm 4nm

| Peak# | Ret. Time | Area | Height | Area % | Height % |
|---|---|---|---|---|---|
| 1 | 17.850 | 62256041 | 673207 | 99.591 | 99.410 |
| 2 | 25.179 | 255678 | 3997 | 0.409 | 0.590 |
| Total | | 62511719 | 677204 | 100.000 | 100.000 |

**Figure D-6.** HPLC trace of **4d** (99% ee) corresponding to data in Figure 5.4.

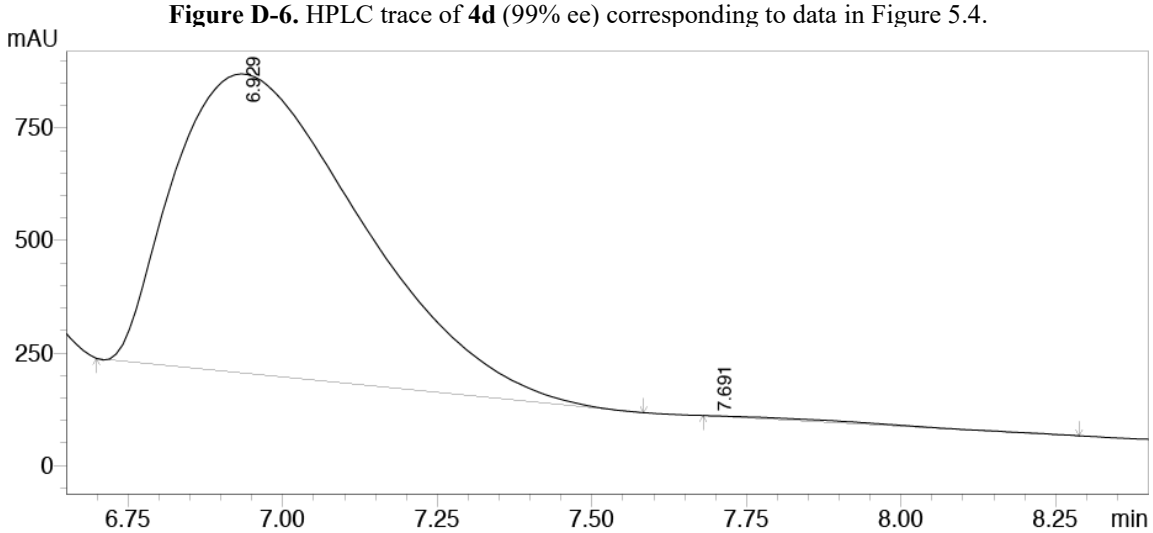


PDA Ch1 254nm 4nm

| Peak# | Ret. Time | Area | Height | Area % | Height % |
|---|---|---|---|---|---|
| 1 | 6.929 | 13936592 | 664155 | 99.649 | 99.945 |
| 2 | 7.691 | 49029 | 366 | 0.351 | 0.055 |
| Total | | 13985621 | 664521 | 100.000 | 100.000 |

**Figure D-7.** HPLC trace of **4e** (99% ee) corresponding to data in Figure 5.4.

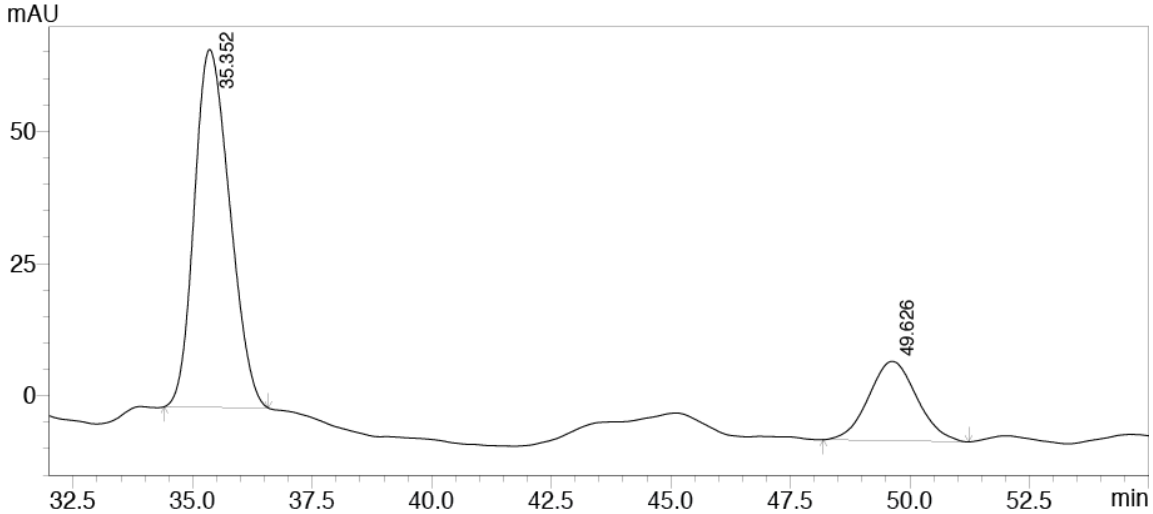


PDA Ch1 254nm 4nm

| Peak# | Ret. Time | Area | Height | Area % | Height % |
|---|---|---|---|---|---|
| 1 | 35.352 | 3493157 | 67622 | 76.872 | 81.839 |
| 2 | 49.626 | 1050992 | 15006 | 23.128 | 18.161 |
| Total | | 4544149 | 82628 | 100.000 | 100.000 |

**Figure D-8.** HPLC trace of **4f** (54% ee) corresponding to data in Figure 5.4.

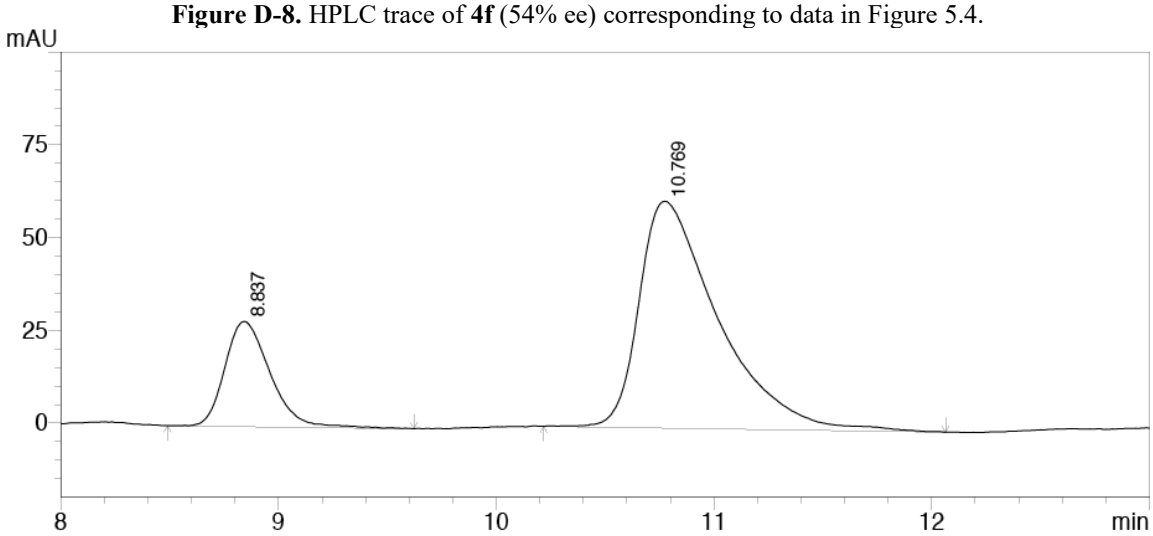


PDA Ch1 254nm 4nm

| Peak# | Ret. Time | Area | Height | Area % | Height % |
|---|---|---|---|---|---|
| 1 | 8.837 | 411495 | 28404 | 21.035 | 31.731 |
| 2 | 10.769 | 1544715 | 61112 | 78.965 | 68.269 |
| Total | | 1956210 | 89516 | 100.000 | 100.000 |

**Figure D-9.** HPLC trace of **6** (58% ee) corresponding to data in entry 10, Table 5.2.

REFRENCES

(s1) Prakash, G. K. S.; Panja, C.; Vaghoo, H.; Surampudi, V.; Kultyshev, R.; Mandal, M.; Rasul, G.; Mathew, T.; Olah, G. A. *J. Org. Chem.* **2006**, *71*, 6806-6813.

(s2) Aziziglu, M.; Erdogan, A.; Arslan, N.; Turgut, Y.; Hosgoren, H.; Pirinccioglu, N. *Tetrahedron: Asymmetry* **2016**, *27*, 614-622.

(s3) Cui, B.; Sun, H.; Xu, Y.; Duan, L.; Li, Y.-M. *Tetrahedron* **2017**, *73*, 6754-6762.

(s4) Wu, S.; Guo, J.; Sohail, M.; Cao, C.; Chen, F.-X. *J. Flourine Chem.* **2013**, *148*, 19-29.

(s5) Zhao, H.; Qin, B.; Liu, X.; Feng, X. *Tetrahedron* **2007**, *63*, 6822-6826.

(s6) Klein, J. E. M. N.; Rommel, S.; Plietker, B. *Organometallics* **2014**, *33*, 5802-5810.

(s7) Slungard, S. V.; Krakeli, T.-A.; Thvedt, T. H. K.; Fuglseth, E.; Sundby, E.; Hoff, B. H. *Tetrahedron* **2011**, *67*, 5642-5650.

(s8) Mizuta, S.; Shibata, N.; Ogawa, S.; Fujimoto, H.; Nakamura, S.; Toru, T. *Chem. Commun.* **2006**, *2006*, 2575-2677.

(s9) Contente, M. L.; Serra, I.; Molinari, F.; Gandolfi, R.; Pinto, A.; Romano, D. *Tetrahedron* **2016**, *72*, 3974-3979.

(s10) Huang, H.; Jacobsen, E. N. *J. Am. Chem. Soc.* **2006**, *128*, 7170-7171.